Glycosaminoglycan-Protein Interactions:

The Fibroblast Growth Factor Paradigm

by

Chi-Pong Kwan

Submitted to the Division of Bioengineering and Environmental Health
in Partial Fulfillment of the Requirements for the Degree of

Doctor of Philosophy

in

Molecular Biotechnology and Pharmacology

at the

MASSACHUSETTS INSTITUTE OF TECHNOLOGY

June 2002

Author _____
Biological Engineering Division
May 17, 2002

Certified by _____
Ram Sasisekharan
Associate Professor of Biological Engineering
Thesis Supervisor

Accepted by _____
Ram Sasisekharan
Associate Professor of Biological Engineering
Chairman of Graduate Students

Thesis Committee

Committee Chair

Professor Bevin P. Engelward

Assistant Professor

Biological Engineering Division, MIT

Committee Member

Professor Alan J. Grodzinsky

Biological Engineering Division, Department of Electrical Engineering and Computer Science and Department of Mechanical Engineering, MIT

Committee Member

Professor Matthew A. Nugent

Department of Ophthalmology and Department of Biochemistry, Boston University School of Medicine

Glycosaminoglycan-Protein Interactions: The Fibroblast Growth Factor Paradigm

by

Chi-Pong Kwan

Submitted to the Biological Engineering Division
on May 20, 2002 in Partial Fulfillment of the Requirements for
the Degree of Doctor of Philosophy in Molecular Biotechnology and Pharmacology

Abstract

Specific interactions between heparan sulfate glycosaminoglycans (HSGAGs) and proteins are central to a wide range of biological processes such as anticoagulation, angiogenesis and growth factor activation. The specificity involved in the HSGAG-protein interactions stems from the structural heterogeneity of HSGAGs, which are highly acidic biopolymers associated on the cell surface and in the extracellular matrix. It is believed that structural specificity in the HSGAG-protein interactions determines the biological functions mediated by HSGAG-binding proteins such as basic fibroblast growth factor (FGF2). A number of models have been proposed to account for the mode of FGF-FGFR interactions and the role of HSGAGs in modulating FGF2 signaling. It was hypothesized that one role played by HSGAGs was to stabilize FGF2 oligomers in a "side-by-side" or *cis* fashion for presentation to fibroblast growth factor receptor (FGFR). In this thesis research, we systematically examined different proposed modes of FGF2 dimerization and showed that extensive oligomerization of a FGF2 mutant protein could be achieved by oxidatively crosslinking. Heparin, a highly sulfated form of HSGAGs, was demonstrated to increase the extent of oligomerization. Therefore, the results reported here were consistent with the hypothesis that HSGAGs promoted FGF2 oligomerization in a "side-by-side" mode. The functional significance of a FGF2 dimer was tested using a genetically engineered dimeric FGF2 (dFGF2). Biochemical and biophysical properties of dFGF2, such as protein folding, heparin affinity and receptor

binding, were assayed. dFGF2 was found to exhibit higher activities in stimulating cell proliferation and cell survival *in vitro* compared with the monomeric wildtype. An *in vivo* rat cornea pocket model further corroborated the *in vitro* findings. The functional role of HSGAGs derived from the cell surface was studied here. It was found that distinct HSGAG fragments released by heparinase treatment were capable of modulating FGF2-stimulated cell proliferation depending on the expression of FGFR isoforms. This founding is consistent with the proposal that structural specificity of distinct HSGAG fragments dictated the interaction of HSGAGs with FGF and FGFR. The role of heparinase-generated HSGAG fragments in inhibiting cell proliferation was investigated. B16 melanoma cells treated with heparinase III were found to exhibit biochemical and morphological hallmarks of apoptosis. Conditioned medium derived from heparinase-treated cells was shown to be effective in suppressing cell growth. Gene array experiments and caspase activity assays further suggested that apoptotic cell death was mediated through a caspase 8-, death receptor-dependent pathway. Thus, the present study lends further credence to the proposal that cell surface HSGAGs plays a critical role in orchestrating cell phenotype. This thesis work provides the framework for understanding the molecular mechanism of growth factor activation and the structure-function relationship of HSGAG-mediated cell signaling. Results from this study may potentially be useful for therapeutic protein engineering and carbohydrate-based drug discovery.

Thesis Supervisor: Ram Sasisekharan

Title: Associate Professor of Biological Engineering

Acknowledgements

This thesis research would never come to completion without the support and encouragement from my thesis advisor Prof. Ram Sasisekharan. Over the years, I benefit a great deal from the intellectual exchange with my mentor and I truly enjoy the time working in his laboratory as a graduate student.

I am very fortunate to have the opportunity to be part of a highly dynamic research group. Every one in Ram's lab contributes to making it an excellent hub for learning and growth. Thanks to Dr. Ganesh Venkataraman, Dr. Ranga Godavarti, Dr. Barbara Natke, Dr. Yosuf El-shabrawi, Dr. James Myette, Dr. Mallik Sundaram, Dr. Shiladitya Sengupta, Dr. Yiwei Qi, Dr. Ganlin Zhao, Kris Holley, Dr. Steffen Ernst, Dr. Zachary Shriver, Joseph C. Davis, Dr. Dongfang Liu, Kevin Pojasek, Nishla Keiser, Rahul Raman, David Eavarone, Tanyel Kiziltepe, Vikas Prabhakar, David Berry and Cindy Ku. I would also like to thank the current and former administrative staffs from our lab—Ada Ziolkowski, Karie Ng and Diana Lewicki. The excellent administrative staffs in the Toxicology/Bioengineering and Environmental Health/Biological Engineering headquarter have made my life as a graduate student much easier. My thanks go to Dalia, Debra, Mariann, Kerry and Suzette. I am also grateful to the Essigmann Lab for allowing me to use the phosphorimaging system and to the Sinskey Lab for advice on microarray technology. People from the Varticovski Lab at St. Elizabeth Medical Center and Tufts University, where I worked for a year as a visiting scientist, have been so kind to me and I would like to thank Prof. Lyuba Varticovski, Dr. Rial Christensen, Dr. Isabel deAos Scherpenseel, Dr. Yihong Wang and Kahlil Mitchell.

Many people have helped enrich my experience at MIT to a new level that I would never have imagined. Among them are Richard Shyduroff and Prof. Barry Unger (E-club, MIT enterprise forum), Shirley Shepard, Scott Bankstein, David Manoni and David Chan (MIT $50K organizing team), and many others.

I am indebted to Ada Sung for her many years of excellent IT support and care. Last but not the least, I am grateful to my family members from Hong Kong, who have been extraordinarily supportive and understanding. In closing, I thank every one who has made me a better person in every sense during the course of my graduate study at MIT.

Short Table of Contents:

Detailed Table of Contents: Page

List of Figures

Page

Chapter 1 Motivation and Background

Chapter 2 Probing Protein-Protein Interaction in FGF2 Dimerization

Chapter 3 Protein Engineering of Dimeric Fibroblast Growth Factor

List of Tables

PART I: INTRODUCTION

Chapter 1: Motivation and Background

1.1 Motivation

In multi-cellular organisms, one of the mechanisms by which cells signal involves diffusible signaling molecules, cell surface receptors and complex carbohydrates such as heparan sulfate glycosaminoglycans (HSGAGs). All three components act cooperatively in a temporal and spatial manner. In the case of fibroblast growth factor (FGF) signaling, the three components (FGF, FGF receptor and HSGAGs) are localized in defined extracellular compartments and their expressions are tightly regulated. Specific interaction among these macromolecules forms the basis of cell signaling. Aberrant expression in any of these FGF signaling components often results in abnormal development, tumorigenesis or lethality.

Ubiquitous in the extracellular matrix (ECM) and on the cell surface, HSGAGs are structurally heterogeneous biopolymers consisting of differentially modified disaccharide building units (Section 1.4.4). HSGAGs interact with specific binding sites on both FGF and FGF receptor (FGFR) to form a multimeric signaling complex on the cell surface. In addition, distinct HSGAG sequences are believed to dictate the specificity of FGF-FGFR interactions and to modulate FGF-mediated signaling. Several models have been proposed to explain the role of HSGAGs in FGF signaling. One of the models, depicted in **Figure 1.1**, proposed that HSGAGs serve to induce FGF dimerization for enhancing receptor dimerization and subsequently activating an intracellular signaling cascade. As such, it is conceivable that cells are capable of not only responding to a given extracellular signal, but also fine-tuning their responsiveness to external stimuli by varying HSGAG sequences. This mechanism of modulating growth factor signaling through a specific glycosaminoglycan-protein interaction is believed to be important in normal cellular responses such as morphogenesis as well as in disease conditions such as tumor angiogenesis.

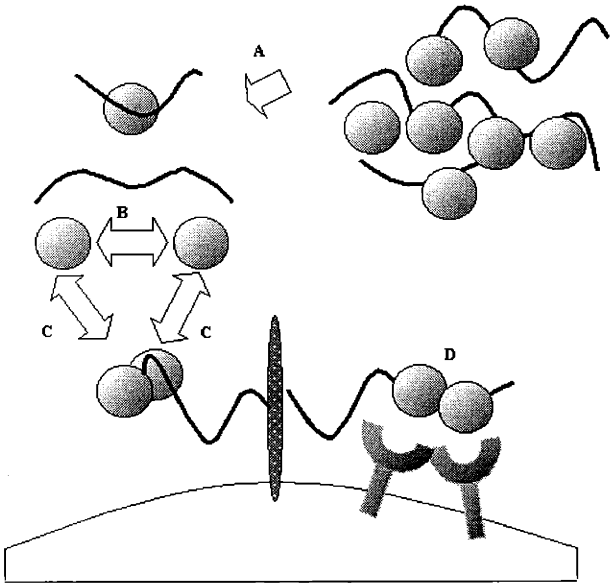

Figure 1.1: Working model of FGF signaling. FGF molecules are sequestered in the ECM by binding to HSGAGs. Upon degradation of the ECM, the FGF-HSGAG complex is released and diffuses to the cell surface (A). Free FGF molecules self-associate to form dimer or oligomer in the presence or absence of HSGAGs (B). Free HSGAG fragments or cell surface HSGAGs associated with the core protein of proteoglycan facilitate FGF dimerization (C) and present the FGF-HSGAG complex to FGFR. As a result of FGF-HSGAG binding to FGFR, receptor dimerization is triggered (D), leading to activation of an intracellular signaling cascade.

Motivation and objectives

This thesis work is motivated by the potential therapeutic applications of HSGAG-binding growth factors. By dissecting the role of HSGAGs in modulating cell signaling, it is anticipated to achieve the long-term goals of engineering growth factors with higher therapeutic value and isolating specific HSGAG fragments that modulate biological activities. Accordingly, the overall goal of this thesis research is to

> ***- develop a molecular understanding of the roles played by HSGAGs in cell signaling through FGF-dependent and FGF-independent mechanisms.***

The remainder of this Chapter provides an overview of what is currently known about HSGAG-mediated FGF signaling, leading to formulation of the specific objective of the thesis (Section 1.7).

1.2 Properties of Cell Signaling

Cells in a multi-cellular organism exchange chemical signals with one another in order to precisely coordinate their functions for the benefit of the organism as a unity. All biological processes are essentially driven by cell-cell communication, or cell signaling. The process of converting an extracellular signal to an intracellular response is known as signal transduction. From controlling cell division to determining cell fate, signal transduction plays an important role in orchestrating a variety of cellular functions in a temporally and spatially specific fashion. Malfunction in any of the signal transduction components could lead to catastrophic consequences such as abnormal development or uncontrolled growth, compromising the viability of the organism. Therefore, understanding the basic principles of signal transduction is critical to the characterization of any biological phenomena. In this section, an overview of the molecular events accompanying the transduction of extracellular signals into intracellular responses is provided. Although the discussion is focused on FGF signaling, most of the characteristics also apply to other signal transduction pathways.

1.2.1 Basic principles of cell signaling

One of the mechanisms by which cells communicate locally within a microenvironment involves specific interactions between secreted signaling molecules and cell surface receptors. Cells are constantly exposed to an enormous amount of extracellular information encoded in the form of signaling molecules such as proteins, lipids and dissolved gases. The landscape of signal transduction consists of three distinct compartments, namely the ECM, the cell surface and the intracellular space (**Figure 1.2**). The signaling molecules are released from a signaling cell into the ECM, where the signals can be sequestered temporarily or they can diffuse to the vicinity of a target cell.

Upon approaching the cell surface of the target cell, the signals may interact with various macromolecules such as proteoglycans and glycosaminoglycans (Section 1.4). Binding of the signals to the corresponding receptors initiates a cascade of events at the cell surface and in the intracellular space. As a result, a biological response is initiated and subsequently the signaling complexes are internalized for degradation by endocytosis.

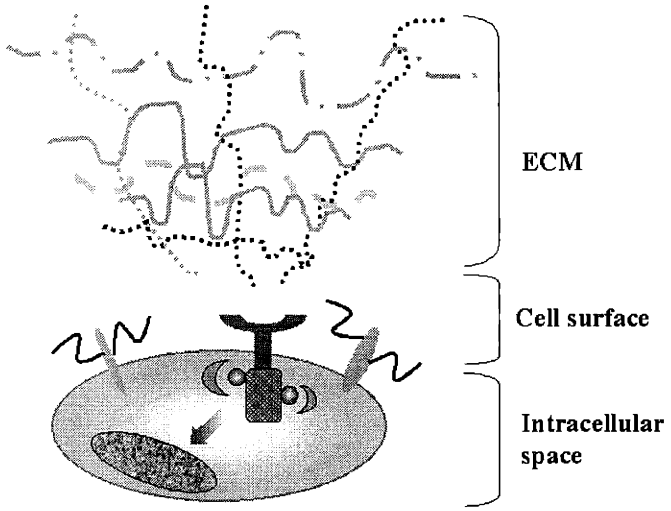

Figure 1.2: The landscape of signal transduction. Chemical signals released from a signaling cell first encounter various resident macromolecules in the extracellular matrix (ECM). As the signals traverse the ECM and reach the cell surface, they can interact with glycoproteins and receptors. Upon receptor binding and dimerization, the signals initiate a cascade of intracellular events and ultimately lead to gene transcription or repression within the nucleus.

In the case of growth factor signaling, the signaling molecule is a protein released from the signaling cell and the receptor is a single-pass transmembrane polypeptide consisting of an extracellular binding domain and two cytoplasmic tyrosine kinase domains. Binding of the growth factor to the extracellular domain of the receptor induces receptor dimerization (**Figure 1.3**), which brings the cytoplasmic tyrosine kinase domains of the two receptors into juxtaposition for autophosphorylation (Heldin, 1995). These phosphorylated tyrosine residues serve as docking sites for the cytoplasmic proteins containing the Src-homology (SH2) domains. Once phosphorylated, these SH2-containing proteins may serve as adaptors for recruiting other cytoplasmic proteins, or

they may become substrates for yet other kinases to phosphorylate. Therefore, as a result of receptor dimerization, a cascade of intracellular signaling events is activated. Other growth factors that bind to cell surface receptors with tyrosine kinase activity include platelet-derived growth factor (PDGF), epidermal growth factor (EGF) and vascular endothelial growth factor (VEGF).

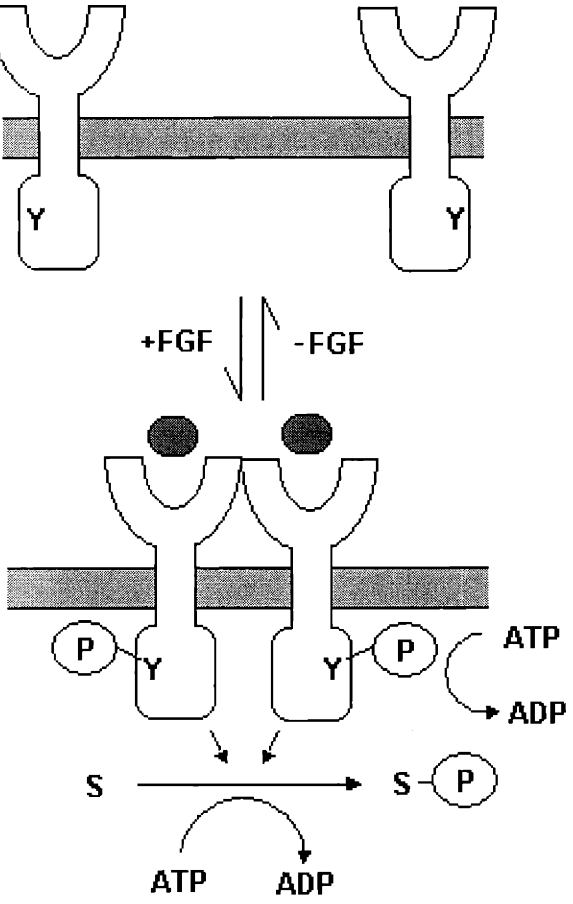

Figure 1.3: Activation of receptor tyrosine kinase by ligand binding. Top: In the absence of ligand binding, cell surface receptors are far apart from each other. No intracellular signaling is initiated. Bottom: Binding of the appropriate ligands induces non-covalent association of the receptors and the cytoplasmic domains are brought into close proximity with each other. As a result, specific tyrosine residues (Y) are auto-phosphorylated. Phosphorylated tyrosines in turn trigger phosphorylation of other intracellular substrates (S).

1.2.2 Receptor dimerization

Receptor dimerization can be achieved by a number of mechanisms. First, binding of growth factor (herein referred to as ligand) can bring receptors into close proximity for dimerization to occur. There are at least two means of ligand-induced receptor dimerization. A single ligand can bind two receptors through two independent receptor-binding sites, as in the cases of human growth hormones (de Vos, *et al.*, 1992) and erythropoietin (Watowich, *et al.*, 1994). Alternatively, two ligands can bind two receptors independently and the bound receptors are then associated. Second, receptor dimerization can also be achieved by a ligand-independent mechanism. Intermolecular disulfide bridges can force two receptors to form a covalent receptor dimer in the absence of ligand binding. This is the case for a subset of human inherited skeletal disorders, in which point mutations found in FGFR are believed to cause constitutive receptor dimerization through a disulfide linkage (Section 1.3.4). In addition to receptor dimerization, another key feature of growth factor signaling is the presence of specific tyrosine residues in the cytoplasmic domain of the receptor. Cells with mutations in the tyrosine residues fail to signal despite retaining the ability to bind growth factor.

Signal transduction exhibits several properties that are key to growth factor signaling. First, the signal can be amplified several-fold through activating the intracellular signaling cascade, thereby allowing a low concentration of chemical signals to sufficiently initiate a sustained biological response. Second, signals can be directed from a signaling cell to the target cell in a paracrine fashion, or from a signaling cell back to itself in an autocrine fashion. The latter is particularly evident in tumor growth, in which tumor cells over-produce large quantities of growth factors that subsequently stimulate their own growth. Third, the biological responses of some cell signaling pathways can be promoted or inhibited by other macromolecules synthesized by cells. Modulating cell signaling provides a mechanism by which cells can fine-tune their responses to a given signal. This also raises the interesting observation that cells are capable of making an extracellular environment that may in turn regulates cellular behavior.

Summary

Cell signaling is critical to many biological processes in normal development and disease progression. One of the mechanisms of signal transduction involves specific interaction between secreted chemical signals and cell surface receptors. As the signals traverse from the extracellular to the intracellular space, distinct molecular events occur including receptor dimerization, and auto-phosphorylation of receptor tyrosine kinase domains. Three characteristics of signal transduction (amplification, directionality and signal modulation) are important to the understanding of FGF signaling.

1.3 Fibroblast Growth Factor Signaling

The biological activity of FGFs is mediated through a dual-receptor system consisting of one of five high-affinity (K_d ~10^{-11} M) FGFRs (Section 1.3.4) (Kan, *et al.*, 1993), and low-affinity (K_d ~10^{-8} M) HSGAGs located at the cell surface and in the ECM (Section 1.4.4) (Faham, *et al.*, 1996; Ornitz, *et al.*, 1995). Specific interactions among these three components dictate the specificity and the intensity of FGF signaling. This section provides an overview of the diverse biological functions mediated by FGF signaling in physiological and pathological situations. The structural properties of FGF2 are thoroughly examined in Section 1.3.3. The current status of some of the clinical applications involving FGFs is also discussed. Further information on FGF signaling can be obtained from the review articles (Friesel and Maciag, 1995; Gospodarowicz, *et al.*, 1987; Nugent and Iozzo, 2000; Ornitz, 2000; Powers, *et al.*, 2000).

1.3.1 Early work on fibroblast growth factors

FGFs were first described in the literature in the early 1970s, when the two prototypic members of FGFs, FGF1 (acidic FGF with pI~5.6) and 2 (basic FGF with pI ~9.6), were isolated from bovine pituitary extracts as growth promotion factors based on their abilities to stimulate the proliferation of NIH3T3 cells (Armelin, 1973;

Gospodarowicz, 1974). FGF1 was later identified as a myoblast differentiation factor (Gospodarowicz, *et al.*, 1975). It was soon realized that FGF was also active in a wide variety of cell types, including neuronal cells, chondrocytes, osteoblasts, vascular smooth muscle cells and endothelial cells. The finding that FGF was mitogenic for endothelial cells *in vitro* (Gospodarowicz, *et al.*, 1976; Gospodarowicz, *et al.*, 1978) and *in vivo* (Gospodarowicz, *et al.*, 1979) subsequently led to the proposal that FGFs might play a role in tumor angiogenesis (Maciag, 1984). In fact, some FGF members (such as FGF3, 4, 5 and 6) were isolated as oncogenes from human tumor tissues or cell lines (Marics, *et al.*, 1989; Moore, *et al.*, 1986; Yoshida, *et al.*, 1987; Zhan, *et al.*, 1988). In 1984, a heparin affinity chromatography approach was adopted to purify FGFs to homogeneity. Since then, this strategy has greatly enhanced the isolation of FGFs from normal and pathological tissues (Gospodarowicz, *et al.*, 1984; Lobb and Fett, 1984; Shing, *et al.*, 1984). To date, the FGF family of growth factors consists of at least 23 members. It is important to note that the defining classification of FGF relies strictly on protein structural homology rather than the target sites of the growth-promoting activity. Although most FGF members are mitogens for fibroblasts (as the name of the growth factors implied), a few do not exhibit mitogenic activity in fibroblasts at all. A good example is the keratinocyte growth factor (KGF or FGF7), which is only active in epithelial cells expressing a specific receptor isoform (Gospodarowicz, *et al.*, 1987).

1.3.2 Biological properties of FGFs

FGFs are secreted signaling molecules that act primarily in the extracellular environment. Unlike most FGF members, FGF1, 2 and 9 lack the classical N-terminal leader sequences for secretion. This raises the intriguing question of whether FGF1 and 2 are only released passively upon disintegration of the plasma membrane in the event of cell lysis, or other novel secretory mechanism is involved in exporting FGF out of the cells. One possibility of FGF export is through binding to a carrier protein such as synaptotagmin, whose expression is believed to be required for FGF1 release (Carreira, *et al.*, 1998; LaVallee, *et al.*, 1998; Tarantini, *et al.*, 1998).

Upon binding to FGFRs, FGFs induce receptor dimerization and auto-phosphorylation of the tyrosine kinase domains. The phosphorylated tyrosine residues

serve to recruit specific cytoplasmic proteins and modify their activities by phosphorylation. As a result of protein phosphorylation, a cascade of intracellular signals is activated. Some of the signaling pathways activated by FGFs include the phospholipase C-γ, the mitogen activated protein kinase and the phosphatidylinositol 3-kinase pathways (Mason, 1994; Mohammadi, *et al.*, 1991; Powers, *et al.*, 2000). As a result of the "cross-talks" between different activated signaling pathways, FGFs are capable of mediating a multitude of cellular responses. The exact mechanism of the FGF-mediated "cross-talks" has yet to be characterized.

FGFs play a key role in a wide range of biological functions such as cell proliferation, differentiation, senescence and angiogenesis (Bikfalvi, *et al.*, 1997; Gospodarowicz, *et al.*, 1987; Hanahan and Folkman, 1996; Ornitz, 2000; Taipale and Keski-Oja, 1997). The biological significance of FGFs in development is implicated from several genetic studies. Gene inactivation experiments using knockout mice have indicated that FGFs orchestrate various crucial developmental processes within the nervous and vascular systems (Raballo, *et al.*, 2000). In another study, however, mice carrying targeted *FGF2* null mutation were morphologically normal except displaying impaired vascular smooth muscle contractility (Zhou, *et al.*, 1998). Over-expression of FGF1 in arteries by gene transfer induces intimal hyperplasia and exaggerated angiogenesis in the arterial wall *in vivo* (Nabel, *et al.*, 1993). Specific biological functions mediated by FGFs are highlighted below.

Cell proliferation

FGF1 and 2 are potent mitogens for many cell types, including fibroblasts, myoblasts, chrondrocysts, osteoblasts, endothelial cells, smooth muscle cells, neurons and epithelial cells (Gospodarowicz, *et al.*, 1987). Unlike FGF1 and 2, the activity of FGF7 (commonly known as keratinocyte growth factor or KGF) is restricted to epithelial cells expressing a splice variant of FGFR2. The potency exhibited by FGF2 to stimulate cell proliferation is estimated to be about 20- to 60-fold higher than transforming growth factor, epidermal growth factor and platelet-derived growth factor (Gospodarowicz, *et al.*,

1987). In the presence of heparin, half-maximal proliferation can be achieved by just 0.5 ng/ml FGF2 (Padera, *et al.*, 1999).

Cell survival

Maintaining cell survival, independent of cell proliferation, is critical in normal tissues, including the vascular endothelium whose turnover rate is exceedingly low (Folkman, 1995b). FGFs were shown to play an important role in maintaining the survival of endothelial cells, by protecting them from programmed cell death triggered by serum starvation (Araki, *et al.*, 1990; Karsan, *et al.*, 1997; Kuzuya, *et al.*, 1999) or by ionizing irradiation (Fuks, *et al.*, 1994). FGF2 also acts as a survival factor in 3T3 fibroblasts (Tamm, *et al.*, 1991), hippocampal neurons (Walicke, *et al.*, 1986), intestinal stem cells (Houchen, *et al.*, 1999), and injured neural tissues (Anderson, *et al.*, 1988). The intracellular signaling of cell survival is believed to be mediated through the phosphatidylinositol 3-kinase (PI3-kinase) pathway. Upon FGF binding and receptor dimerization, the assembly and cross-phosphorylation of multiple cytoplasmic docking proteins occur, which leads to the recruitment and activation of PI3-kinase (Ong, *et al.*, 2001).

Angiogenesis

Among the most characterized FGF-mediated biological functions is the ability to induce angiogenesis, or new blood vessel growth. FGF1 and FGF2 are potent mitogens for smooth muscle cells and endothelial cells (Desai and Libutti, 1999; Slavin, 1995), both of which are the major components of the vascular network. During embryonic development and adult female reproductive cycles, sprouting of new blood vessels from the existing vasculature takes place under a tight regulatory control. However, unregulated angiogenesis is believed to be a prerequisite in several pathological situations such as tumor metastasis, atherosclerosis and retinopathy (Folkman, 1995a; Hanahan and Folkman, 1996). FGF expression has been shown to be up-regulated in many types of cancer, including colon (Shin, *et al.*, 2000), breast (Smith, *et al.*, 1999), brain (Schmidt, *et*

al., 1999), head and neck (Dellacono, *et al.*, 1997), and lung (Berger, *et al.*, 1999). A more detailed discussion on various aspects of angiogenesis is provided in Chapter 4.

1.3.3 Structural properties of FGFs

All the members in the FGF family are believed to share a common structure consisting of 12 anti-parallel β–sheets folded into a barrel shape known as β–trefoil (Murzin, *et al.*, 1992). This structural foil can be subdivided into three motifs each consisting of four anti-parallel β–sheets, which are superimposable upon one another. The structural foil, which exhibits an approximate three-fold symmetry (**Figure 1.4**), is essentially similar to that of interleukin (IL)-1α and IL-1β (Zhang, *et al.*, 1991; Zhu, *et al.*, 1991).

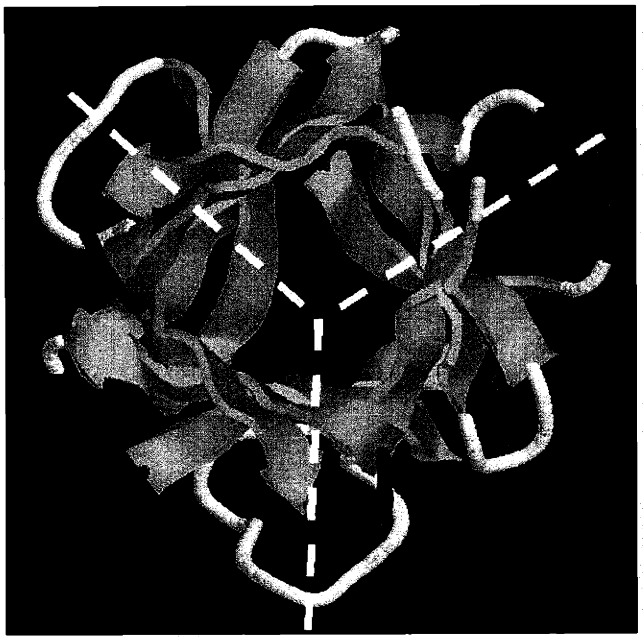

Figure 1.4: Structural fold of FGF2. A three-dimensional model of FGF2 is created using RasMol software based on the crystallographic coordinates (PDB code: 1BFC) of Faham et al (Faham, *et al.*, 1996). The structure consists of 12 β–sheets (yellow arrows) and a number of conformationally flexible loops (white and blue wires). The β-sheets are wrapped around an axis of symmetry perpendicular to the plane of the paper, creating an

opened barrel structure. An approximate three-fold symmetry of the structure is indicated with the white dashed lines.

Primary and secondary sites for receptor binding

Our laboratory and others have studied the receptor binding sites on FGF2 through a variety of techniques (Baird, *et al.*, 1988; Springer, *et al.*, 1994; Venkataraman, *et al.*, 1999a). These studies point to two sets of FGFR binding sites, namely the primary and the secondary receptor binding sites (**Figure 1.5**). The primary site consists of seven surface-exposed residues that are highly conserved in the FGF family (Venkataraman, *et al.*, 1999a). These residues form a contiguous surface on all FGF proteins and they are expected to interact with the immunoglobulin-like III (IgIII) domain of FGFR. The secondary site is made up of three residues that are not conserved in the FGF family. These residues are expected to bind to the IgII domain of FGFR. The divergent sequence and topological position of the secondary site in the FGF family is believed to form the basis of ligand-receptor specificity (Venkataraman, *et al.*, 1999a).

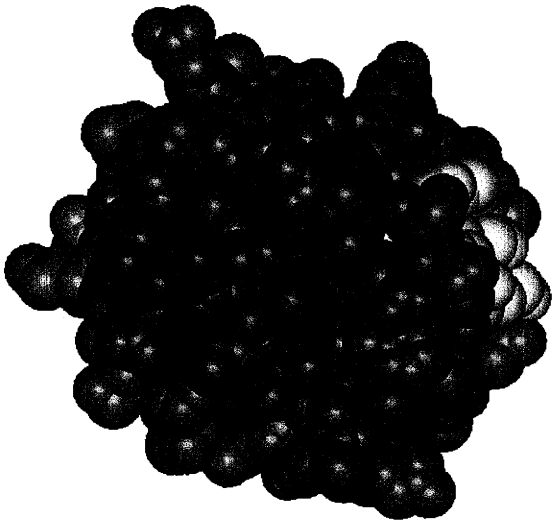

Figure 1.5: Topological mapping of the primary and secondary receptor binding sites in FGF2. Space-filled model of an FGF2 molecule (Zhu, *et al.*, 1991) (PDB code: 1BAS) is shown. The primary and the secondary receptor binding sites (Venkataraman, *et al.*, 1999a) are colored in blue and yellow, respectively. Note that these two sites are

roughly orthogonal to each other on the protein surface. The primary receptor binding site consists of Y24, E96, N101, Y103, L140 and M142. The secondary receptor binding site includes K110, Y111 and W114.

HSGAG-binding site

A striking feature of the FGF2 structure is the presence of a cluster of basic residues (arginine and lysine) on the protein surface (Faham, *et al.*, 1996; Zhang, *et al.*, 1991). As illustrated in **Figure 1.6**, this cluster of basic residues forms an almost continuous surface on one side of the FGF2 protein. It is generally believed that these basic residues provide the necessary charge complementarity and hydrogen bonding interactions with the sulfate groups of a HSGAG chain. The significance of the spatial distribution of these residues within the HSGAG-binding sites of FGF1, 2 and 7 is explored in detail in Appendix 2.

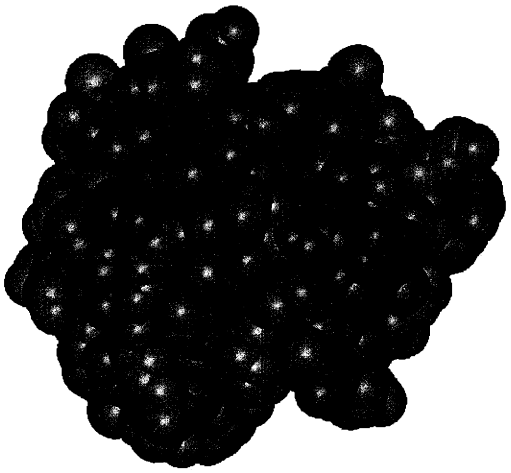

Figure 1.6: HSGAG-binding site on FGF2. Space filling model of a FGF2 molecule (Zhu, *et al.*, 1991) (PDB code: 1BAS) is shown. The residues implicated in HSGAG-binding are colored in red. In most cases, the side chains of these residues interact with specific groups on the HSGAG chain. Note that all these residues are clustered on a single protein surface. Residues at the HSGAG-binding site of FGF2 are K27, N28, N102, R121, K126, Q135, K136 and A137.

1.3.4 Fibroblast growth factor receptors

FGFRs are members of the transmembrane receptor tyrosine kinase superfamily which relays the external FGF signal to the inside of cell (Givol and Yayon, 1992; Jaye, *et al.*, 1992). Five different genes of FGFR (FGFR1-5) have been cloned (Chellaiah, *et al.*, 1994; Dell and Williams, 1992; Kim, *et al.*, 2001; Mansukhani, *et al.*, 1992; Ornitz and Leder, 1992; Sleeman, *et al.*, 2001; Wang, *et al.*, 1994; Werner, *et al.*, 1992; Yayon, *et al.*, 1991). All FGFRs share a basic structural organization: an extracellular domain composing of two or three Ig-like loops, a transmembrane domain of 13 amino acids, and a cytoplasmic domain composing of the tyrosine kinases (**Figure 1.7**).

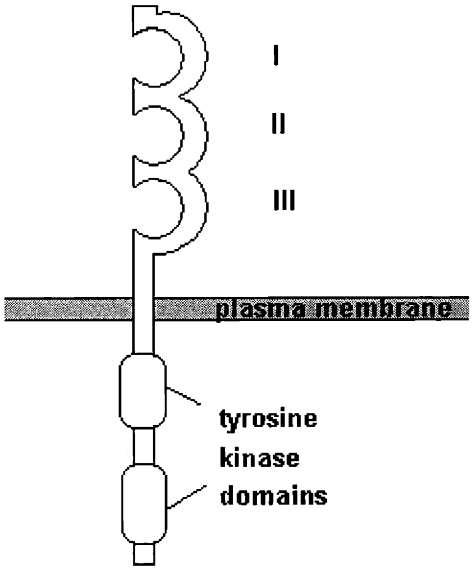

Figure 1.7: Schematic drawing of the fibroblast growth factor receptor. FGFR consists of two or three Ig-like loops (I-III), a transmembrane domain and two tyrosine kinase domains.

Only the IgII- and IgIII-like domains are involved in ligand binding while the N-terminal IgI-like domain is dispensable (Johnson, *et al.*, 1990). Alternative splicing of the gene encoding the Ig-like domains creates different isoforms of FGFR. One of the alternatively splicing events involves the three exons ("a", "b" and "c") within domain III of FGFR1-3. The FGFR encompassing the IIIb splice variant contains exons "a" and "b" whereas the IIIc contains exons "a" and "c." As a result, two isoforms are generated for

each of the mRNA encoding FGFR1-3. Sequence variation among different splice variants of FGFRs forms the primary basis of receptor binding specificity in FGF signaling.

As demonstrated by Ornitz *et al* (Ornitz, *et al.*, 1996), the receptor binding specificity differs markedly among different FGF members (**Table 1.1**). For example, FGF1 exhibits the broadest receptor specificity whereas FGF7 interacts exclusively with FGFR2b.

Relative FGF mitogenic activities (%)

	FGF1	FGF2	FGF3	FGF4	FGF5	FGF6	FGF7	FGF8	FGF9
FGFR1b	100	60	34	16	4	5	6	4	4
FGFR1c	100	104	0	102	59	55	0	1	21
FGFR2b	100	9	45	15	5	5	81	4	7
FGFR2c	100	64	4	94	25	61	3	16	90
FGFG3b	100	1	2	1	1	1	1	1	42
FGFR3c	100	107	1	69	12	9	1	41	96
FGFR4	100	113	6	108	7	79	2	77	75

Table 1.1: FGF-FGFR specificity. Relative mitogenic activities as measured by [^{3}H] tritium incorporation stimulated by FGF1-9 on engineered cells transfected with various FGFR isoforms. Modified from Ornitz *et al* (Ornitz, *et al.*, 1996).

Cells can selectively respond to a given FGF by regulating the types of FGFR expressed on the cell surface. Differential expression of FGFRs during the course of development and disease progression enables cells to directly regulate their responsiveness to external signals. In the developing mouse embryo, all FGFRs are expressed in various locations and at different stages (Chen, *et al.*, 2000). For example, in the smooth muscle cells isolated from rats, FGFR1 gene is expressed at a higher level in adult, whereas FGFR3 expression is higher in newborn animals. FGFR1-4 are differentially expressed during various growth phases of lung development in rats (Powell, *et al.*, 1998). In the atherosclerotic arteries, distinct patterns of FGFR expression were observed (Brogi, *et al.*, 1993). In prostate epithelial cells, the progression from a benign to a malignant state is correlated with a switch from FGFR2b to FGFR2c expression (Yan, *et al.*, 1993). Aberrant expression of FGFR is believed to contribute to the pathogenesis of many diseases. In a highly-malignant human breast

cancer cell line, FGFR2 transcript is about 40-fold over-expressed (Tannheimer, *et al.*, 2000). In human gastric cancer, the transcripts of FGFR1, FGFR2 and FGFR4 are up-regulated in cancerous tissues compared to their normal counterparts (Shin, *et al.*, 2000). A dominant negative form of FGFR1c is believed to impair pancreatic β-cell functions, contributing to type-2 diabetes (Hart, *et al.*, 2000).

A number of inherited disorders are associated with FGFRs (Kannan and Givol, 2000; Naski and Ornitz, 1998). Somatic mutations in FGFR1, 2 and 3 have been shown to markedly affect skeletal development in humans. Three broad classes of point mutations in FGFRs can be categorized. First, point mutations that disrupt the formation of intramolecular disulfide bonds could lead to ligand-independent receptor dimerization through intermolecular disulfide bond formation (Robertson, *et al.*, 1998). Representative diseases from this class include dwarfing chondrodyplasia. Constitutive FGFR activation appears to be the underlying cause of the diseases. Second, another class of mutations, found within the highly-conserved linker region between IgII and IgIII (Nagendra, *et al.*, 2001), is believed to alter FGF ligand specificity. Diseases resulted from this class of mutation include Apert syndrome, characterized by fusion of digits of the hands and feet. Third, point mutations found in the transmembrane domain of FGFR3 are implicated in achondroplasia, a condition of dwarfing (Rousseau, *et al.*, 1994; Shiang, *et al.*, 1994). All somatic mutations in FGFR are heterozygous and it appears that homozygosity is lethal by birth.

1.3.5 Clinical applications of FGFs

The potent mitogenicity of the FGF family of growth factors has prompted many investigators to evaluate FGFs as therapeutic proteins for a number of clinical applications. FGFs have been considered for treating a number of disorders including cardiovascular diseases. Both direct delivery and gene therapy approaches are being evaluated in various phases of preclincal and clinical testing. It is important to emphasize that, prior to clinical testing, a lot of research has been performed to improve protein stability and activity. In addition, the clinical application of FGFs would not been possible without the development of biomaterials that support sustained drug delivery.

The following discussion highlights some of the key aspects of applying FGFs in treating human diseases.

Protein stabilization and formulation

One of the most challenging problems in the delivery of therapeutic proteins is the preservation of protein stability at the target site. FGFs have a propensity to aggregate under oxidative conditions by intermolecular crosslinking through surface-exposed cysteines. Protein engineering approach was used to convert cysteines to other residues by site-directed mutagenesis (Arakawa, *et al.*, 1989; Fox, *et al.*, 1988). In the absence of a carrier, FGFs tend to adsorb to surfaces leading to a substantial loss of protein activity (Edelman, *et al.*, 1991). A number of carrier systems have been developed to stabilize protein and avoid absorption to surfaces. Bovine serum albumin and heparin are among the most commonly used carriers in FGF formulation. Bos *et al* developed an FGF2-loaded albumin-heparin biomaterials where endothelial cell proliferation occurred more readily *in vitro* (Bos, *et al.*, 1999). Edelman *et al* reported a method for incorporating FGF2 into microspheres encapsulated with heparin-sepharose beads, which supported the sustained release of FGF2 to cultured cells (Edelman, *et al.*, 1991). A heparin-like copolymer consisting of sulfated polysaccharides was developed by Taguchi *et al* as a biomaterial for stimulating cell proliferation (Taguchi, *et al.*, 1998). Radomsky *et al* observed accelerated bone fracture healing using a formulation of FGF2 combined with hyaluronic acid, a non-sulfated glycosaminoglycan (Radomsky, *et al.*, 1999). A biodegradable synthetic copolymer was synthesized by Bae *et al* for promoting skin wound healing (Bae, *et al.*, 2000). Gelatin hydrogel embedded with FGF2 was prepared by Yang *et al* for inducing new blood vessel growth in the rabbit cornea (Yang, *et al.*, 2000). Advances in biomaterial research are expected to greatly improve the stability and efficacy of FGFs for clinical applications.

Pharmacokinetics and toxicology

The pharmacokinetic and toxicological properties of FGF2 in experimental animal models have been reviewed by Goncalves (Goncalves, 1998) and are summarized below. After administrated to the systemic circulation, FGF2 is cleared rapidly from the bloodstream and is concentrated in the liver. The half-life of an intravenous bolus administration is approximately 2 minutes in rats and 1 hour in dogs. Intravenous administration of high doses of FGF2 to monkeys results in renal toxicity. Systemic administration in dogs over a prolonged period lowers blood cell production. The adverse effects discontinue after the treatment is suspended.

Pre-clincal and clinical testing

One of the most active areas of clinical research involving FGFs is in therapeutic angiogenesis, in which angiogenic factors are delivered to induce new collateral blood vessel growth in ischemic tissues such as myocardium and limb muscle (Freedman and Isner, 2001). Ischemia is a pathological condition characterized by inadequate blood flow and tissue oxygenation. Both FGF1 and 2 have been evaluated as therapeutic proteins for their abilities to induce new blood vessel growth and to improve blood flow into ischemic tissues. Lopez *et al* reported a significant increase in myocardial blood flow and cardiac function in a porcine model of myocardial ischemia following FGF1 delivery (Lopez, *et al.*, 1998). The safety and efficacy of using FGF2 to treat myocardial ischemia were demonstrated by Laham *et al* in a porcine model (Laham, *et al.*, 2000). In addition to the local delivery of FGFs, adenovirus-mediated FGF1 gene therapy was employed for targeted protein expression in non-ischemic tissues of rabbit and it was found to induce angiogenesis in the absence of ischemia (Safi, *et al.*, 1999). FGF2 was demonstrated to be safe and efficacious in reducing ischemic size in a randomized, double-blind clinical study involving twenty four patients (Laham, *et al.*, 1999). In addition to therapeutic angiogenesis, FGFs are also applied to accelerate wound healing. FGF1 incorporated into fibrin glue was demonstrated to partially restore hind limb function following spinal cord injury (Cheng, *et al.*, 1996). Also, bone fracture healing was shown to be promoted by grafting an FGF2-containing hydrogel (Radomsky, *et al.*,

1999). In several stroke animal models, intravenous administration of FGF2 has been demonstrated to enhance cerebral recovery by promoting neuronal cell survival (Ay, *et al.*, 1999; Kawamata, *et al.*, 1997; Sugimori, *et al.*, 2001).

Summary

FGF is a family of HSGAG-binding growth factors that play important roles in numerous biological functions including cell proliferation, survival, angiogenesis and morphogenesis. A landmark molecular feature of FGF is the presence of a cluster of basic residues exposed on the protein surface, which facilitates HSGAG-binding. Two orthogonally-positioned receptor-binding sites have been identified. Similar to most other growth factors and cytokines, high affinity interaction between FGF and FGFR initiates receptor dimerization followed by a cascade of intracellular phosphorylation events. In addition to the inherent FGF-FGFR specificity, it is believed that HSGAG may provide an additional level of control to dictate the specificity and thereby regulate the formation of signaling complex. Further investigation into how HSGAGs modulate FGF signaling may enable development of improved growth factors as therapeutic proteins.

1.3 Proteoglycans and Glycosaminoglycans

Carbohydrate is a major class of biological macromolecule found in most, if not all, organisms. It is perhaps the least understood macromolecule due to its enormous structural diversity and the lack of effective analytical tools to dissect this structure. Complex carbohydrates, such as HSGAGs found in proteoglycans, play an important role in a myriad of physiological and pathological processes. In this section, a general overview of proteoglycans and glycosaminoglycans is provided followed by a detailed discussion of the structural and biological properties of HSGAGs. General information on proteoglycans and glycosaminoglycans can be found in other review articles

(Gallagher, 1997; Perrimon and Bernfield, 2000; Sasisekharan and Venkataraman, 2000; Tumova, *et al.*, 2000; Turnbull, *et al.*, 2001).

1.4.1 Early work on glycosaminoglycans

The literature related to glycosaminoglycans dates back to more than a hundred years ago. Like many important classes of biopolymers such as nucleic acid and protein, glycosaminoglycans were not under active investigation until a biological function (e.g. anticoagulation in the case of heparin) was later demonstrated. Traditionally, the histological description of glycosaminoglycans (Junqueira, *et al.*, 1992) has been nothing more than a "ground substance" that serves to fill the space between cells and fibers of the connective tissue. A historical perspective of early glycosaminoglycan research is provided by Calabro *et al* (Calabro, *et al.*, 2000). In 1884, Kruenbergin described the first successful isolation of a glycosaminoglycan from hyaline cartilage using dilute alkaline extraction method. The chemical contents were deduced by Schmideberg in 1891 to include acetate, sulfate, glucuronic acid and hexosamine. The glycosaminoglycan preparation isolated from cartilage was later named "chondroitin sulfate."

The historical account of heparin is described by Roden (Roden, 1989) and is summarized as follows. In 1916, McLean unexpectedly discovered the anticoagulation property of heparin when he attempted to isolate the coagulation-promoting factor from ox heart. The newly discovered anticoagulant was named "heparin" in 1918 by Howell, McLean's mentor who was then inappropriately credited as the "father" of heparin. The cellular production and storage of heparin was found in 1936 to be within connective tissue type mast cell, the primary cellular mediator of inflammatory response. A second tissue type comprised of mucosal mast cell produces and stores chondroitin sulfate instead of heparin (Junqueira, *et al.*, 1992). In mid 1930s, clinical trials of heparin in treating postoperative thrombosis began in the United States, Canada and Europe. The clinical application of heparin has enabled many subsequent breakthroughs in cardiovascular surgery, including the use of heart-lung machine in open-heart surgery. In 1948, the first description of a less-sulfated form of heparin was provided by Jorpes and

Gardell. While heparin was found exclusively within the granules of mast cells, it was discovered in 1968 that a heparin-like polysaccharide was present in the ECM, on the cell surface and in the intracellular compartment of virtually all mammalian cells. This counterpart of heparin was then named "heparitin sulfate" and later renamed as "heparan sulfate." In 1981, it was found that heparan sulfate was linked to a protein core that was anchored on the plasma membrane. Remarkable progress in glycosaminoglycan research in the past two decades has not only advanced our understanding on the biopolymer itself, but also revised the traditional wisdom that glycosaminoglycans serve merely as a structural scaffold.

1.4.2 Proteoglycans

As suggested by the name, proteoglycans are composed of a protein core covalently attached to one or more glycosaminoglycan chains of the same or different types. Besides the glycosaminoglycan chains, the protein cores are also capable of interacting with growth factors for activity (Goretzki, *et al.*, 1999; Milev, *et al.*, 1998; Mongiat, *et al.*, 2000).

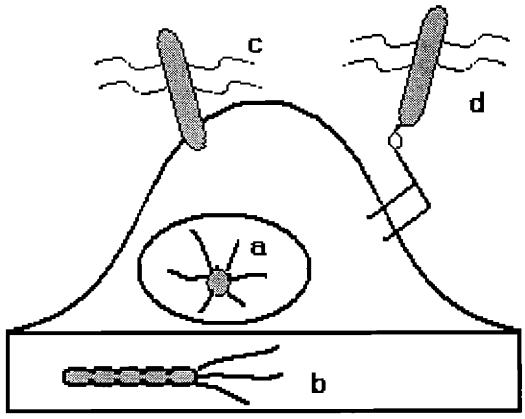

Figure 1.8: Morphological features of selected proteoglycans. Morphology of (a) serglycan, an intracellular proteoglycan located within an intracellular vesicle, (b) perlecan, a proteoglycan located within the basement membrane beneath a cell, (c) syndecan, an integral cell surface proteoglycan and (d) glypican, a GPI-anchored cell surface proteoglycan. Protruded from the core proteins (gray) are the glycosaminoglycan

chains. All structures are schematically depicted to illustrate their morphologies and ultra-structural distribution, and therefore are not drawn to scale.

Proteoglycans can be classified into three types according to their sub-cellular locations.

1. Intracellular proteoglycan

   This proteoglycan is found inside the storage granules of mast cells, basophilic leukocytes and the embryonic yolk sac. Serglycin, a representative intracellular proteoglycan, contains a small protein core with a stretch of serine-glycine dipeptide repeats (**Figure 1.8, a**). The glycosaminoglycan motif of serglycin in connective tissue type mast cells is heparin, which is detached from its core protein as free glycosaminoglycan chains upon extraction.

2. Extracellular proteoglycan

   Commonly found in bone, cartilage and skin tissues, extracellular proteoglycan is secreted by cells to their microenvironment. The protein core of extracellular proteoglycan often contains a few globular domains. Extracellular proteoglycans can be further divided into three subclasses according to their gross structures and functions.

   - Basement membrane proteoglycan, such as perlecan, is deposited to the basal side of epithelial and endothelial cells as well as to the basal lamina of muscle, nerve and fat cells. The core protein of perlecan comprises of five globular domains with structural homology to laminin and collagen, allowing the proteoglycan to interact with other basement membrane macromolecules (**Figure 1.8, b**). Blocking perlecan expression has been shown to inhibit tumor progression and angiogenesis *in vivo* (Sharma, *et al.*, 1998).

   - Large extracellular proteoglycans, such as aggrecan, form highly compressed aggregates and enable tissues to cushion excessive pressure

with minimal deformation. Found in cartilage, aggrecan contains a large protein core with three globular domains highly substituted with glycosaminoglycan chains. Of note is the finding that mutation in the aggrecan gene is associated with defective spinal cord development and dwarfism in mice (Watanabe, *et al.*, 1997).

- Small extracellular proteoglycans, such as biglycan and decorin, are ubiquitous in the ECM. Common structural features of small extracellular proteoglycans include a leucine-rich motif and intermolecular disulfide bridges. Biglycan and decorin are associated with various types of neurons.

3. Integral membrane proteoglycan

   Integral membrane proteoglycans are associated on the cell surface of most, if not all, mammalian cell types. The core protein is anchored on the plasma membrane by one of the two mechanisms.

   - Transmembrane intercalation

     Syndecan, a representative in this class of proteoglycan, is commonly found in epithelial cells. Its core protein contains a hydrophobic transmembrane domain for anchoring on the plasma membrane (**Figure 1.8, c**). Four members of syndecans (syndecan-1-4) have been described in vertebrates and a homologue is found in *Drosophila* and *C. elegans*. The glycosaminoglycan chains on syndecan bind growth factors as well as extracellular matrix proteins such as collagen, fibronectin and thrombospondin. Syndecan expression was found to be markedly elevated during tissue remodeling (Elenius, *et al.*, 1991; Gallo, *et al.*, 1996).

   - Glycosylphosphatidylinositol (GPI) linkage

     Glypican, a GPI-anchored proteoglycan, regulates the activity of various growth factors and morphogens (Baeg, *et al.*, 2001; De Cat and David,

2001; Lin and Perrimon, 1999). The core protein is posttranslationally "glypiated" in the endoplasmic reticulum by covalently attaching a GPI group to the C-terminus (**Figure 1.8, d**). Glypican can be released from the cell surface by treating with phospholipase C. Six glypicans have been identified in vertebrates. Of particular interest is the discovery that loss of glypican-3 expression contributes to a somatic overgrowth disorder called Simpson-Golabi-Behmel syndrome (Selleck, 1999). Recently, the HSGAG motif of glypican was shown to serve as a low-affinity receptor for endostatin, a pivotal anti-angiogenic protein derived from collagen (Karumanchi, *et al.*, 2001).

1.4.3 Molecular characteristics of glycosaminoglycans

Glycosaminoglycans (GAGs) are a family of linear biopolymers which include heparin, heparan sulfate, dermatan sulfate, chondroitin sulfate, keratan sulfate and hyaluronic acid. The GAG building block is a disaccharide repeat unit of an uronic acid (U) and a hexosamine (H). **Table 1.2** summarizes the structural features of the most common glycosaminoglycans.

Glycosaminoglycans	**U**	**H**	**Linkage**	**Modifications**
Hyaluronic acid	Glucuronic acid	Glucosamine	β1,3	none
Chondroitin 4 sulfate	Glucuronic acid	Galactosamine 4-SO_4	β1,3	O-sulfation
Chondroitin 6 sulfate	Glucuronic acid	Galactosamine 6-SO_4	β1,3	O-sulfation
Dermatan sulfate	Iduronic acid	Galactosamine 4-SO_4	β1,3	O-sulfation
Heparin / heparan sulfate	Iduronic acid / glucuronic acid	Glucosamine	β1,4	O-, N-sulfation C5-epimerization
Keratan sulfate	Galactose	Glucosamine	β1,3	O-sulfation

Table 1.2: Building blocks of selected glycosaminoglycans. Each glycosaminoglycan consists of an uronic acid (U) and a hexosamine (H). Linkage refers to the conformation of the glycosidic bond between adjacent U and H.

The tissue distribution of glycosaminoglycans have been described (Junqueira, *et al.*, 1992). Hyaluronic acid is rich in synovial fluid, vitreous of the eye and umbilical cord. It is the simplest form of glycosaminoglycan, which does not exhibit any chemical modification. Unlike other glycosaminoglycans, hyaluronic acid is synthesized on the plasma membrane rather than in the Golgi. Chondroitin sulfate and dermatan sulfate are derived from a common structure known as chondroitin. Chondroitin sulfate is found mainly in hyaline and elastic cartilages. Dermatan sulfate prevails in aorta, dermis, tendons, ligaments and fibrous cartilage. Keratin sulfate can be found in cartilage and cornea. Heparan sulfate is associated with reticular fiber and with the basement membrane.

1.4.4 Structure of Heparan sulfate glycosaminoglycans

Heparin and heparan sulfate, collectively known as heparan sulfate glycosaminoglycans (HSGAGs), are the most complex form of glycosaminoglycans. The structural complexity of HSGAGs stems from the combinatorial patterns of sulfation and the presence of conformationally flexible iduronic acid. Such intrinsic characteristics enable HSGAGs to display a diverse array of structural motifs for interaction with other macromolecules in modulating normal and pathological processes.

The primary structure of HSGAGs is remarkably complex due to the incomplete chemical modifications introduced during their biosynthesis. At a macroscopic level, HSGAG sequences can be categorized into two regions: "NS" blocks where sequences are highly sulfated with a mixture of iduronic and glucuronic acids, and "NAc" blocks where sequences are undersulfated with predominantly glucuronic acid (**Figure 1.9**). One distinction between heparin and heparan sulfate lies in the overall organization of the NS and NAc regions. Heparin contains densely sulfated NS regions whereas heparan sulfate contains mostly NAc regions with sporadic clusters of NS regions.

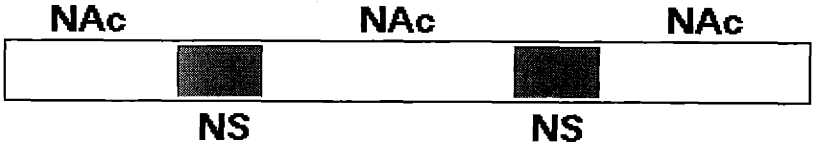

Figure 1.9: Organization of the primary structure of HSGAGs. Blocks of highly sulfated regions rich in N-sulfated groups (NS region) are separated by undersulfated regions rich in N-acetyl groups (NAc region). The length of the NS region is about 2-8 monosaccharide units whereas that of NAc region is about 20.

HSGAGs consist of about 20-100 disaccharide U-H repeats, where U can be a glucuronic acid or an iduronic acid and H is a glucosamine (**Figure 1.10**). Glycosidic linkage between U and H is β (1→4) whereas that between H and U is α (1→4). The epimeric state of the carboxylate group at the C5 position of the uronic acid determines whether it is a glucuronic acid or an iduronic acid. As discussed later in this Chapter, iduronic acid is unique in its highly flexible ring conformation which allows the iduronic acid containing glycosaminoglycan to interact more favorably with proteins.

The disaccharide building blocks of HSGAGs can be modified at four positions, namely the 3-O, 6-O and N positions in glucosamine, and the 2-O position in uronic acid. In addition, the uronic acid can exist in two epimeric forms: glucuronic acid and the conformationally flexible iduronic acid. Together, 32 possible chemical alphabets can be encoded in each disaccharide building block. Hence, the structural diversity of HSGAGs compounds exponentially as the chain length increases.

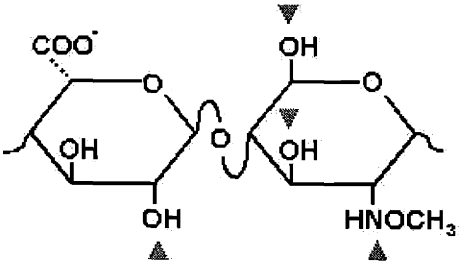

Figure 1.10: A disaccharide building block of HSGAGs. The pyranose ring on the left is an uronic acid and that on the right is a glucosamine. Note that carboxylate group at the C5 position of the uronic acid can be either in the axial or equatorial position (dash

line), resulting in two epimeric forms (iduronic acid and glucuronic acid). Each disaccharide repeat unit can be sulfated at 4 possible positions, as pointed by the triangles.

The overall conformation of a HSGAG chain resembles a right-handed helix[1], with the sulfate groups displayed orderly on the periphery (**Figure 1.11**). The helical structure of a heparin chain adopts a two-fold screw axis of symmetry such that the structure would superimpose upon itself when it rotates ~180° about a screw axis. The helical repeat distance was determined to be 16.8 Å for an iduronic acid-rich heparin chain (Atkins and Nieduszynski, 1976) and 19 Å for a glucuronic acid-rich heparan sulfate chain (Nieduszynski, 1985). It is important to consider both the primary sequence and the conformational feature of HSGAGs when studying FGF-HSGAG signaling complexes (Section 1.6). Further information on the secondary structure of HSGAGs can be found in a recent review (Mulloy and Forster, 2000).

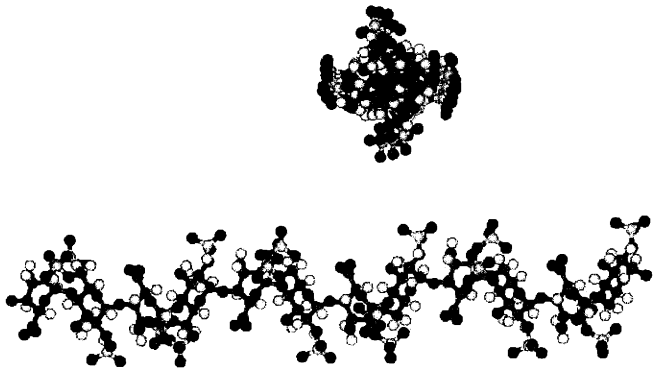

Figure 1.11: Conformation of a heparin fragment. Top, heparin (PDB code: 1HPN) is shown with its screw axis of symmetry pointing into the plane of the paper. Bottom, heparin is shown with its screw axis of symmetry pointing in parallel to the plane of the paper. Note that the orderly display of sulfate groups along the chain.

HSGAG sequences can differ substantially depending upon the cell types and the tissues (Lyon, *et al.*, 1994; Toida, *et al.*, 1997). Gross changes in HSGAGs are also found to accompany phenotypic changes in malignant transformation (Jayson, *et al.*,

[1] A right-handed helix means that the helical structure progresses in a counter-clockwise manner as it rises.

1998; Jayson, *et al.*, 1999), development (Brickman, *et al.*, 1998; Nurcombe, *et al.*, 1993) and aging (Feyzi, *et al.*, 1998). However, no evidence is currently available to demonstrate that a change in HSGAG sequence causes such phenotypic changes.

1.4.5 Biosynthesis and degradation of HSGAGs

The biosynthesis of HSGAGs has been reviewed earlier (Lindahl, *et al.*, 1998; Rosenberg, *et al.*, 1997; Salmivirta, *et al.*, 1996). The process can be divided into three steps: initiation, elongation and modification. In general, all the biosynthetic enzymes reside within the Golgi apparatus, possibly acting in concert within a multimeric biosynthetic complex.

- Initiation: The first step of HSGAG synthesis begins with the attachment of a tetrasaccharide spacer (xylose-galactose-galactose-glucuronic acid) to a serine residue at the protein core by glucuronyltransferase I (Kitagawa, *et al.*, 1998). This tetrasaccharide spacer is common to both HSGAGs and chondroitin sulfate.

- Elongation: An N-acetylglucosamine residue is added to the tetrasaccharide spacer by the glycosyltransferase encoded by the *EXTL2* gene (Kitagawa, *et al.*, 1999). Elongation of the nascent chain is performed by the alternate addition of glucuronic acid and glucosamine monosaccharide residues by HS copolymerase, EXT1 and EXT2 (McCormick, *et al.*, 2000; Senay, *et al.*, 2000; Wei, *et al.*, 2000). Mutations in the *EXT1/2* genes are linked to hereditary multiple exostoses, a genetic disease characterized by the formation of tumors at the growth plate of cartilage (Duncan, *et al.*, 2001).

- Modification: The nascent HSGAG chain is subject to a variety of chemical modifications catalyzed by different enzymes. N-deacetylase/N-sulfotransferase (NDST) replaces an acetyl group with a sulfate group in the glucosamine residues, creating a substrate for further modifications. C5 epimerase catalyses the conversion of a glucuronic acid to an iduronic acid. Sulfation at specific

positions on the HSGAG chain is mediated by different sulfotransferase isoforms. In each case, the sulfate donor is 3'-phosphoadenosine-5'-phosphosulfate (PAPS). 2-O-sulfotransferase adds a sulfate group to the 2-O position of an iduronic acid and rarely to a glucuronic acid. Similarly, 6-O and 3-O sulfotransferases transfer sulfate groups to the 6-O and 3-O positions of a glucosamine, respectively. It is important to emphasize that these enzymes do not modify all potential substrates to completion, resulting in a highly variable modification pattern on the HSGAG chain. Concerted action of these sulfotransferases and their respective isoforms are speculated to be the primary mediators of cell-ECM communication (Bowman and Bertozzi, 1999).

Unlike DNA and protein synthesis, HSGAGs are synthesized without a template. As a result, all the information embedded on HSGAG chains is driven by the concerted expression of the biosynthetic enzymes. An emerging area of research is to understand how HSGAG biosynthetic enzymes are regulated and how cells dynamically alter their expression to elicit different biological responses (Sasisekharan and Venkataraman, 2000; Turnbull, *et al.*, 2001). Aberrant expression of those enzymes is likely to alter HSGAG sequences and may impact the biological functions mediated by HSGAGs. With the aid of several recently developed analytical techniques (Turnbull, *et al.*, 1999; Venkataraman, *et al.*, 1999c; Vives, *et al.*, 1999), the fine structure of HSGAGs and their biological functions are beginning to be understood more in depth.

In mammalian cells, HSGAGs are internalized and degraded intracellularly by lysosomal enzymes such as glycosidase (which digests polysaccharide down to individual monosaccharides) and sulfatase (which removes sulfate groups by hydration). HSGAGs outside the cell can be degraded by heparanases, a secreted enzyme implicated in tumor metastasis (Hulett, *et al.*, 1999; Vlodavsky, *et al.*, 1999). All the mammalian HSGAG-degrading enzymes are hydrolases, which cleave the biopolymer by adding water molecules across the glycosidic bond. Heparinase, a lyase derived from the soil microbe *Flavobacterium heparinum*, is a distinct HSGAG-degrading enzyme which depolymerizes the biopolymer by β-elimination. Three distinct heparinases (hepI-III) have been cloned and sequenced from *F. heparinum* (Godavarti and Sasisekharan, 1996;

Sasisekharan, *et al.*, 1993; Su, *et al.*, 1996), each with distinct substrate specificities (Ernst, *et al.*, 1995) (**Figure 1.12**). HepI cleaves highly sulfated sequences found in the Ns region whereas hepIII cleaves undersulfated sequences primarily found in NAc region. HepII displays a mixed substrate specificity of hepI and hepIII, cleaving both highly sulfated and undersulfated sequences.

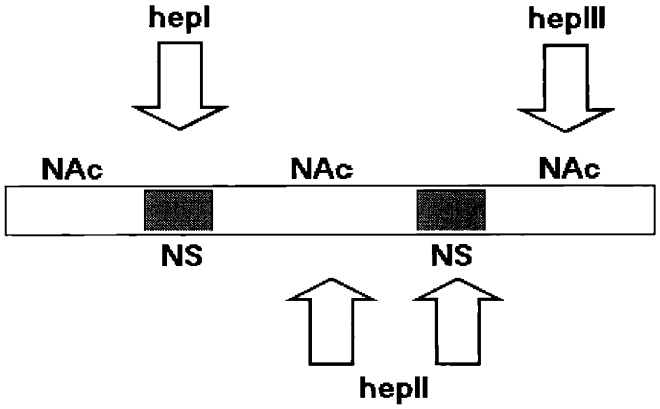

Figure 1.12: Substrate specificity of hepI, II and III. Highly sulfated domains are colored in gray while under-sulfated domains are uncolored. The arrows indicate the regions where the respective heparinases would digest.

Heparinases have been routinely used in our laboratory for sequencing HSGAGs (Shriver, *et al.*, 2000a; Shriver, *et al.*, 2000b; Venkataraman, *et al.*, 1999c) and for probing the role of HSGAGs in angiogenesis, tumorigenesis and development (Binari, *et al.*, 1997; Liu, *et al.*, 2002b). In addition, this panel of enzymes has been used as tools to manipulate cell surface HSGAGs for eliciting divergent biological responses (Chapter 5 and 6). The potential clinical applications of heparinases are diverse. Heparinase digestion of heparin is applied to produce low-molecular-weight heparin (Hedner, 2000; Weitz, 1997), which has fewer side effects than standard heparin (Young, *et al.*, 1994). Medical devices containing immobilized hepI are being tested for their safety and efficacy in controlling blood heparin levels (Ameer, *et al.*, 1999a; Ameer, *et al.*, 1999b; Ameer, *et al.*, 1999c). Administration of hepIII has been shown to suppress smooth muscle cell proliferation in rats following vascular injury (Silver, *et al.*, 1998).

1.4.6 Biological functions of HSGAGs

HSGAGs mediate a plethora of biological functions primarily through specific interaction with other macromolecules such as proteins, lipids and nucleic acids (Conrad, 1998). The number of HSGAG-binding macromolecules has increased to well over 100. A partial list of the HSGAG-binding macromolecules and the biological functions mediated by them is provided in **Table 1.3**.

Most of the cells within a given tissue are surrounded by an ECM meshwork, in which HSGAGs are a major component. Binding of FGF2 to the ECM HSGAG provides a reservoir of growth factors that can subsequently be mobilized to activate cell surface receptors (Vlodavsky, *et al.*, 1996; Vlodavsky, *et al.*, 1991). In addition, FGF2 binding to HSGAG protects the growth factors from inactivation (Gospodarowicz and Cheng, 1986) and proteolytic degradation (Sommer and Rifkin, 1989), thereby prolonging their biological activities. HSGAG binding also provides a mechanism to regulate the diffusion rate of FGF2 across the basement membrane and the ECM (Dowd, *et al.*, 1999; Flaumenhaft, *et al.*, 1990). The sequence information embedded within HSGAGs is believed to dictate the specificity of FGF2-FGFR binding through interactions with both FGF2 and FGFR (Guimond and Turnbull, 1999; Kan, *et al.*, 1999; Pye, *et al.*, 1998).

The interaction between HSGAGs and FGF2 within the ECM is remarkably dynamic. ECM proteolysis releases bound FGF2 and increases its bioavailability (Vlodavsky, *et al.*, 1991; Werb, 1997; Whitelock, *et al.*, 1996). FGF2 bound to HSGAGs can be released from the low-affinity sites by an excess of heparin. A number of experimental methods are developed to generate a soluble HSGAG-FGF2 complex that confers biological activity. Bound FGF2 can also be released from cell surface proteoglycans by either digesting the HSGAG chain with heparinase, or digesting the core protein with proteases such as plasmin, thrombin or collagenase (Whitelock, *et al.*, 1996). In the case of GPI-linked proteoglycan such as glypican, phospholipases can be applied to release FGF2 from the cell surface. In the following examples, specific biological functions mediated by HSGAGs are summarized.

Hemostasis	ATIII (Jin, *et al.*, 1997), plasminogen activator inhibitor type 1 (Ehrlich, *et al.*, 1991)
Mitogenesis	FGF (Gospodarowicz, *et al.*, 1986), hepatocyte growth factor (Lobb and Fett, 1984), Wnt/wg (Reichsman, *et al.*, 1996)
Lipoprotein clearance/localization	Lipoprotein lipase (Lookene, *et al.*, 1996), ApoE (Browning, *et al.*, 1994)
Adhesion	L–selectin (Giuffre, *et al.*, 1997), laminin (Beck, *et al.*, 1990), HIV (Tat protein) (Rusnati, *et al.*, 1999), herpes simplex virus (Feyzi, *et al.*, 1997; Shukla, *et al.*, 1999), malaria circumsporiozoite protein (Shakibaei and Frevert, 1996), human papillomavirus (Giroglou, *et al.*, 2001), *Helicobacter pylori* (Ascencio, *et al.*, 1993; Utt, *et al.*, 2001)
Enzymes	Elastase (Frommherz, *et al.*, 1991), hyaluronidase (Jones and Sawyer, 1989), mast cell protease (Hallgren, *et al.*, 2000), xanthine oxidase (Adachi, *et al.*, 1993), superoxide dismustase (Tibell, *et al.*, 1997)
Others	Prion (Gabizon, *et al.*, 1993), transcription factor (Dudas, *et al.*, 2000), β-amyloid (Lindahl, *et al.*, 1999)

Table 1.3: Selected examples of HSGAG-binding macromolecules.

Hemostasis

To maintain the hemodynamic state of blood in the vasculature, a complex system is in place to spontaneously arrest bleeding from the injured blood vessels. The normal state of the vasculature, or hemostasis, is tightly regulated by a host of proteases and their inhibitors. Hemostasis can be activated under pathological circumstances such as thrombosis. On the other hand, impaired hemostasis can lead to spontaneous bleeding or hemorrhage. HSGAGs play an important role in maintaining hemostasis by targeting multiple serine protease inhibitors, or serpins, of the blood coagulation cascade.

One of the most well-characterized targets is antithrombin III (ATIII), a member of the serpin family of serine protease inhibitors. ATIII is a N-linked glycosylated protein present at a concentration of ~2.5 μM in the serum (Murano, *et al.*, 1980). Binding of heparin to ATIII initiates a sequence of reactions. First, heparin induces a

conformational change in ATIII such that the carboxyl-terminal binding site is exposed for thrombin binding (Evans, *et al.*, 1992; Huntington and Gettins, 1998). Second, thrombin cleaves the reactive carboxyl-terminal loop of ATIII, abolishing its affinity for the bound heparin (Mourey, *et al.*, 1990; Pratt and Church, 1991). The cleaved ATIII fails to bind any target proteases. As a result of the cleavage, heparin is released in an unaltered form and is ready to react with other uncleaved ATIII. In this manner, heparin behaves as a catalyst for activating the inhibitory action of ATIII on thrombin by a factor of 100. Heparin also acts as a template by bringing ATIII and thrombin into close proximity for reaction. The minimal ATIII binding sequence is a pentasaccharide containing an unusual 3-O sulfate group, which is found approximately once in every three heparin chains (Lam, *et al.*, 1976). This specific pentasaccharide sequence is sufficient to induce a conformational change in ATIII, which in turns binds with an elevated affinity towards another serine protease called Factor Xa and inactivates its activity (**Figure 1.13, A**). While a specific pentasaccharide is sufficient to inhibit Factor Xa activity, a longer saccharide containing the pentasaccharide sequence is needed for inactivating thrombin activity. The extra saccharide sequence serves to provide thrombin with a binding site that is proximal to the pentasaccharide sequence (**Figure 1.13, B**).

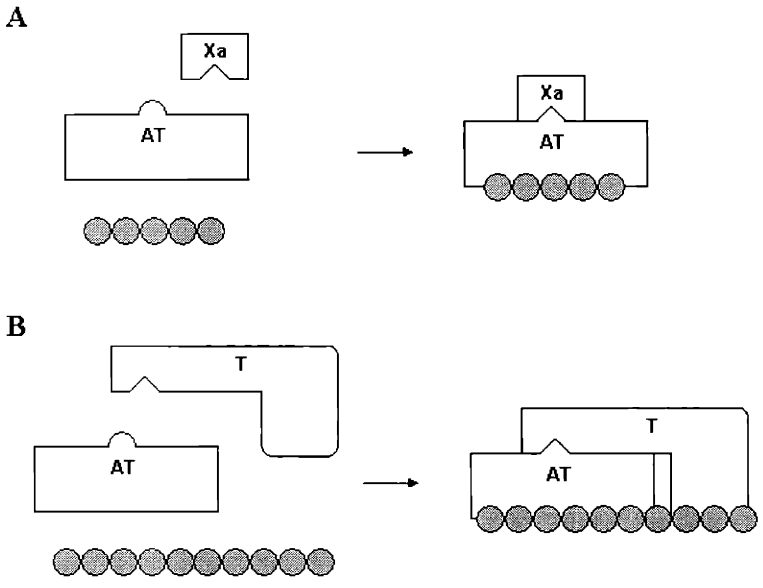

Figure 1.13: Inhibition of coagulation by HSGAGs. A: a specific pentasaccharide HSGAG chain (represented by a chain of circles) is necessary to inhibit Factor Xa

activity by binding to ATIII. B: a longer HSGAG chain containing the ATIII-specific pentasaccharide sequence is necessary for inhibiting thrombin activity.

Although heparin is widely used to suppress coagulation in clinical settings, it is not the physiologically relevant form of HSGAGs that mediates anticoagulation in the circulation. Rosenberg and co-workers demonstrated that cell surface HSGAGs found on the endothelium were in fact responsible for the antithrombin activity (Marcum and Rosenberg, 1984; Marcum and Rosenberg, 1985; Marcum, *et al.*, 1984). More recently, the cleaved conformation of ATIII (referred to as anti-angiogenic antithrombin, or aaAT) is shown to exhibit potent anti-angiogenic and anti-tumor activities in mouse models (O'Reilly, *et al.*, 1999). These findings suggest that the molecular players in the hemostatic system may contribute to the regulation of angiogenesis as well.

Morphogenesis

The role of HSGAGs in orchestrating body patterning *in vivo* is best illustrated by the genetic studies using *Drosophila* (Cumberledge and Reichsman, 1997; Perrimon and Bernfield, 2000). Genetic screens for mutations that disrupt normal morphogenesis uncovered a number of genes involved in various steps of HSGAG biosynthesis (**Table 1.4**).

Drosophila genes	Mammalian homolog	Phenotype	Reference
sugarless, kiwi, ska	UDP-glucose dehydrogenase	Defective Wg, FGF and Dpp signaling	(Binari, *et al.*, 1997; Hacker, *et al.*, 1997; Haerry, *et al.*, 1997)
sulfateless	NDST	Defective Wg, FGF and Hh signaling	(Lin and Perrimon, 1999)
tout-velu	HS copolymerase	Hh signaling	(Bellaiche, *et al.*, 1998; The, *et al.*, 1999)
pipe	2-O-sulfotransferase	Doral-ventral patterning	(Sen, *et al.*, 1998)

Table 1.4: A list of mutations implicated in HSGAG biosynthesis. Wg, Wingless; Dpp, Decapentaplegic; Hh, Hedgehog.

These mutants exhibit aberrant body patterning phenotypes with striking resemblance to the mutants defective in one or multiple signal transduction pathways, such as Wingless (Wg), Decapentaplegic (Dpp), Hedgehog (Hh) and FGF signaling. In

all cases, normal phenotypes can be restored by ectopic expression of the wildtype alleles. These genetic analyses indicate that impaired HSGAG biosynthesis compromises morphogenesis and therefore provide convincing evidence that HSGAGs are critical to growth factor signaling *in vivo*. In addition to the genetic studies, biochemical and cell biology studies also suggest that HSGAGs are involved in modulating signal transduction. Wg/Wnt-1, a secreted growth factor in Wg signaling, is shown to bind tightly to the cell surface and the ECM (Papkoff and Schryver, 1990). The binding can be reversed by adding exogenous heparin (Papkoff and Schryver, 1990; Reichsman, *et al.*, 1996). Experimental conditions that deplete HSGAGs, such as heparinase digestion or sodium chlorate treatment, also inhibit Wg signaling (Reichsman, *et al.*, 1996).

Tumor progression and metastasis

HSGAGs have been implicated to play a fundamental role in regulating the proliferative and metastatic phenotype of tumor cells (Sanderson, 2001). Given the roles of HSGAGs played in mediating the cell-cell and cell-ECM interactions, it was proposed that the metastatic potential of tumors might be related to their capacity to degrade HSGAGs (Nakajima, *et al.*, 1983). Under normal circumstances, HSGAGs could serve as a physical blockage to prevent tumor cells from infiltrating into normal tissues. Upon malignant transformation, cells tend to lose cell-cell contact with one another and with the ECM. This is believed to be caused in part by a loss of cell surface HSGAGs. Consistent with this idea is the general observation that diminished level of cell surface HSGAGs in tumor cells correlated with a higher metastatic potential. Removal of HSGAGs from the cell surface may be mediated by the activity of heparanase, a mammalian HSGAG-degrading enzyme over-expressed in many tumors (Hulett, *et al.*, 1999; Vlodavsky, *et al.*, 1999). The level of heparanase activity appears to correlate with the metastatic potential of a number of tumors (Nakajima, *et al.*, 1983; Vlodavsky, *et al.*, 1983). Furthermore, suppression of heparanase activity using an antisense approach inhibits tumor metastasis *in vivo* (Uno, *et al.*, 2001). Loss of HSGAGs in the subendothelial basement membrane of the blood vessels also enhances the ability of blood-borne tumor cells to leave the vasculature and to invade distant sites for

colonization. Because HSGAGs are capable of interacting with and activating numerous growth factors, the release of HSGAG fragments into the tumor's microenvironment is expected to exacerbate cell proliferation and migration. Therefore, the integrity of HSGAGs may be a key determinant in controlling the phenotype of cells.

In addition to gross structural changes, fine changes in HSGAG structures may provide another means to regulating biological functions during metastatic transformation. Several biochemical studies have identified specific structural changes in the disaccharide repeat units of HSGAGs by comparing tumor cells with their non-transformed counterparts. Elevated levels of 6-O-sulfation, and reduced levels of 2-O- and N-sulfation were found during the progression of human colon adenoma to carcinoma *in vitro* (Jayson, *et al.*, 1998). Up-regulation of 6-O sulfation was found in Lewis lung carcinoma cells with a higher metastatic potential (Nakanishi, *et al.*, 1992). In contrast, a marked decrease in 6-O-sulfation was observed during malignant transformation of mouse mammary epithelial cells (Safaiyan, *et al.*, 1998). Although significant structural alterations in HSGAG sequences were identified, it is still unclear whether such changes in HSGAG sequences have any biological significance in mediating malignant transformation.

Our laboratory has recently completed a mouse tumor transplantation study which demonstrates a divergent effect of heparinases in regulating tumor growth and metastasis (Liu, *et al.*, 2002b). HepIII treatment was shown to inhibit tumor growth and suppress the development of lung metastasis. In contrast, hepI treatment promoted tumor growth and was ineffective in suppressing metastasis. The growth inhibitory effect by hepIII was dose-dependent and was mediated by specific HSGAG fragments, which was shown to replicate the observed phenotype. In addition, heparinase was shown to regulate FGF2 signaling *in vivo*. Treating tumors with hepIII fragments inhibited the phosphorylation of FGFR1, Erk-1,2 and focal adhesion kinase, suggesting that the hepIII-generated HSGAG fragments targeted the cell proliferation and cell adhesion pathways. Importantly, a significant increase in apoptosis was observed in the tumor treated with the hepIII-generated fragments compared to the hepI fragments or negative control. The molecular mechanism by which hepIII treatment suppresses cell proliferation is explored in Chapter 6.

Endothelial cell proliferation in vitro *and* in vivo

It was shown in a chorioallantoic membrane assay that hepI and III were capable of inhibiting *in vivo* angiogenesis (Sasisekharan, *et al.*, 1994). The effect appears to be specific to endothelial cells but not smooth muscle cells or 3T3 fibroblasts. Moreover, *in vitro* proliferation assays revealed that both hepI and III suppressed FGF-mediated endothelial cell growth, with IC_{50} of 6 and 21 nM, respectively. Of note is the biphasic pattern of hepIII in that, at a lower concentration, the enzyme promotes proliferation while the enzyme suppresses proliferation in a dose-dependent manner at a higher concentration. It is not clear whether the growth inhibitory effect was due primarily to the HSGAG fragments released from the endothelial cells.

1.5 The HSGAG-FGF interactions

HSGAG-binding growth factors represent a unique class of signaling molecules in which the mitogenic potential can be modulated by distinct HSGAG sequences. As a result, variation in HSGAG sequences could impinge on various physiological and pathological processes such as neural development (Brickman, *et al.*, 1998; Nurcombe, *et al.*, 1993), carcinogenesis (Delehedde, *et al.*, 1996; Jayson, *et al.*, 1998) and aging (Feyzi, *et al.*, 1998). Given the structural heterogeneity of HSGAGs, it is possible that HSGAG expression may be specific to the microenvironment where the HSGAG-binding growth factors function. Consistent with this proposal, it was found that heparan sulfate extracted from different tissues displays distinct levels of N- and O-sulfation (Toida, *et al.*, 1997) and such variation may contribute to regulating biological functions such as FGF-induced cell proliferation. A detailed structural characterization on FGF2-binding HSGAG sequences has been performed by a number of research groups. HSGAG sequence of seven disaccharides with a 2-O sulfated iduronic acid and a N-sulfated glucosamine was indicated to be important in eliciting FGF activity (Habuchi, *et al.*, 1992; Turnbull, *et al.*, 1992; Walker, *et al.*, 1994). The minimal FGF2-binding sequence is believed to be a tetra- to hexasaccharide containing a N-sulfated glucosamine and a 2-

O sulfated iduronic acid (Habuchi, *et al.*, 1992; Maccarana, *et al.*, 1993) while the presence of a 6-O sulfate group and longer saccharide structures (deca- to dodecasaccharide) are needed for eliciting biological activity (Guimond, *et al.*, 1993; Lundin, *et al.*, 2000; Pye, *et al.*, 1998). Longer oligosaccharides tend to bind FGF2 at a higher affinity. A HSGAG fragment composed of 14 oligosaccharide units was shown to bind FGF2 with an affinity similar to heparin (Turnbull, *et al.*, 1992). However, hexasaccharides and disaccharides are also reported to exhibit biological activity in a few studies (Ornitz, *et al.*, 1995; Zhang, *et al.*, 1991). Therefore, it may be the case that the length of a saccharide *per se* is not the absolute requirement for eliciting a biological activity but whether the saccharide can induce an active FGF signaling complex. One possible mechanism leading towards the formation of an active signaling complex is by HSGAG-induced ligand dimerization. The molecular basis of HSGAG-induced FGF2 dimerization is explored in greater detail in Chapter 2.

The structural characteristics of HSGAG-binding proteins have been explored by several approaches. Electrostatic forces are believed to play an important role in the HSGAG-protein interactions since most, if not all, HSGAG-binding proteins display a high positive charge density at the binding sites for counteracting the high negative charges on HSGAGs. Upon examination of four different HSGAG-binding proteins, Cardin and Weintraub proposed that the primary sequences of XBBXBX and XBBBXXBX were important in HSGAG binding, where B and X represent basic and non-basic residues, respectively (Cardin and Weintraub, 1989). Basic residues tend to align on the same face of a α-helix or β-strand. Margalit *et al* observed a conserved distance of about 20 Å between two basic residues on a number of known heparin-binding peptides or proteins (Margalit, *et al.*, 1993), suggesting that a common structural motif for HSGAG binding may exist. Using synthetic peptides, Fromm *et al* reported that basic residues, such as arginine and lysine, bound HSGAGs with the highest affinity and that the spacing between those basic residues was important (Fromm, *et al.*, 1997). Comprehensive reviews on various topics of the HSGAG-FGF interactions have been published (Hileman, *et al.*, 1998; Jackson, *et al.*, 1991).

1.6 Crystal structures of FGF complexes

During the course of this thesis work, several high-resolution structures of FGF complexes have become available through the Protein Data Bank (PDB) (**Table 1.4**). In this section, selected crystal structures are discussed in the context of HSGAG-FGF, FGF-FGFR, and FGF-HSGAG-FGFR interactions. These crystal structures, prepared under different crystallographic conditions, reveal strikingly divergent molecular assemblages and, in some cases, stoichiometries. Detailed analysis of these structures not only provides important insights into the molecular interactions between the individual FGF signaling components, but also suggests the possible mechanisms for HSGAG-dependent FGF signaling.

PDB	FGF	FGFR	HSGAG	Assemblage*	Reference
1BFC	FGF2	---	hexa	---	(Faham, *et al.*, 1996)
1AXM	FGF1	---	penta (deca)	---	(DiGabriele, *et al.*, 1998)
1CVS	FGF2	FGFR1	---	2:2 symmetrical	(Plotnikov, *et al.*, 1999)
1DJS	FGF1	FGFR2	---	1:1	(Stauber, *et al.*, 2000)
1EV2	FGF2	FGFR2	---	2:2 symmetrical	(Plotnikov, *et al.*, 2000)
1EVT	FGF1	FGFR1	---	2:2 symmetrical	(Plotnikov, *et al.*, 2000)
1FQ9	FGF2	FGFR1	2 octa	2:2:2 symmetrical	(Schlessinger, *et al.*, 2000)
1E0O	FGF1	FGFR2	deca	2:2:1 asymmetrical	(Pellegrini, *et al.*, 2000)

Table 1.5: Recent crystal structures of FGF complexes. * Assemblage refers to the ligand:receptor or ligand:receptor:HSGAG ratio within a unit cell as well as the symmetry of the overall complex.

Faham *et al* provided the first molecular view of how a heparin fragment bound to the HSGAG-binding site on an FGF2 protein (Faham, *et al.*, 1996). In the crystal structure (**Figure 1.14**), the heparin chain adopted a helical conformation with a rotation of 174° per turn and an 8.6 Å translation per dissacharide. One of the two iduronic acids found in the FGF2-binding heparin chain adopted a twisted $^{2}S_{O}$ ring conformation, which is uncommon in unbound heparin. Such structural flexibility is likely to allow heparin to "fit" tightly to the HSGAG-binding site on FGF2 (Ernst, 1998). Two sets of HSGAG-

binding sites were identified from the crystal structure. The high-affinity site consists of residues that interact with the two pyranose rings near the non-reducing end of the HSGAG chain. Residues from the low-affinity site make contacts with the two terminal pyranose rings at the reducing end. In general, the HSGAG-binding residues identified from the crystal structure are in close agreement with those identified previously by site-directed mutagenesis.

Despite a wealth of biochemical evidence implicating FGF dimerization, earlier crystal structures only revealed a monomer of FGF in the asymmetric unit. From a structural point of view, it was unclear whether FGFs could self-associate to form stable complexes. The first crystal structure that revealed two FGFs in an asymmetric unit was provided by DiGabriele *et al* (DiGabriele, *et al.*, 1998). The structure was formed by FGF1 and a decasaccharide chain (of 10 monosaccharide units), in which only the five central pyranose rings were observed (**Figure 1.15**). Two sets of HSGAG-binding residues were identified, of which some residues were overlapped between the sets. The structure reveals a 2:1 FGF1:HSGAG complex and no FGF-FGF contact. The two FGF1 molecules are spatially related to each other in an approximate 2-fold symmetry (Waksman and Herr, 1998). Each of the FGF1 molecules can interact with the heparin chain oriented in both directions such that the primary HSGAG-binding site can interact with the pyranose rings at both the reducing and non-reducing ends.

The crystal structures of the FGF-FGFR assemblage were determined independently by Plotnikov *et al* (Plotnikov, *et al.*, 1999; Plotnikov, *et al.*, 2000) and Stauber *et al* (Stauber, *et al.*, 2000). These structures point to an overall symmetrical FGF-FGFR assemblage, with no FGF-FGF contact. More recently, another two crystal structures containing the FGF-FGFR-HSGAG complexes have been solved independently by two groups (Pellegrini, *et al.*, 2000; Schlessinger, *et al.*, 2000). Schlessinger *et al* reported the structure of an FGF2-FGFR1 crystal soaked with a decasaccharide. A number of intriguing features were observed from this complex. This ternary complex involves a dimeric assemblage of 2:2:2 FGF:FGFR:HSGAG. Shorter HSGAGs, such as hexa- and octasaccharide, were found by the authors to induce a similar stoichiometry. These observations are in sharp contrast with the notion of minimal HSGAG length requirement for FGF2 activity, in which octa- and

decasaccharides are proposed to be the shortest biologically active species that are long enough to bridge two FGF molecules for stabilization of the ternary complex (Guimond, *et al.*, 1993; Ornitz, *et al.*, 1992; Walker, *et al.*, 1994). The two decasaccharides are observed to bind with their non-reducing ends pointing in opposite directions to each other at the center of the HSGAG-binding groove, such that the symmetry of the complex was approximately 2-fold. Although the HSGAG-binding residues on FGF are the same as those identified previously from the FGF-hexasaccharide structure (Faham, *et al.*, 1996), the orientation of heparin binding on FGF is reversed. This observation raises the questions of whether the HSGAG-FGF interactions can occur in both orientations and if so, which one (or both) orientation is specific and biologically relevant. The "two-ends" configuration of HSGAGs as observed in the structure of Schlessinger *et al* would disallow a single HSGAG chain bridging the two FGF2 molecules because of both the symmetry and the HSGAG-FGF orientation constraints. In sharp contrast, Pellegrini *et al* reported a strikingly different co-crystal structure that revealed a 2:2:1 stoichiometry of FGF1:FGFR1:decasaccharide, in which a distorted decasaccharide chain made contacts with both FGF1 molecules but only with one FGFR (Pellegrini, *et al.*, 2000). Similar to a previous heparin-linked FGF1 dimer (DiGabriele, *et al.*, 1998), the two FGF1 molecules in the FGF1:FGFR1:decasaccharide crystal structure interacted with the decasaccharide without protein-protein contact. The decasaccharide was observed to interact with one of the two FGFRs with its non-reducing end.

The widely divergent assemblages observed from various crystal structures suggest that the molecular architecture of the ternary complex may be more diverse than previously expected (Jiang and Hunter, 1999). It is important to keep in mind that one structural architecture should not immediately exclude the others.

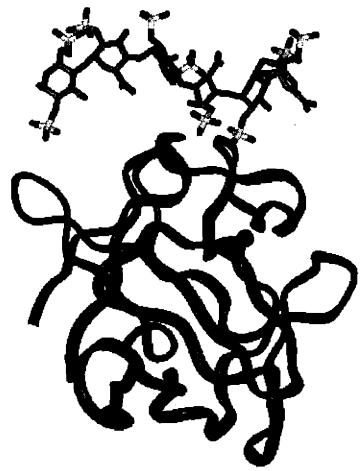

Figure 1.14: The FGF2-hexasaccharide co-crystal structure. The polypeptide chain of FGF2 is rendered as a blue ribbon. The hexasaccharide is colored by atom (green: carbon, blue: nitrogen, yellow: sulfate, red: oxygen). The structure is generated using the crystallographic coordinates of 1BFC (Faham, *et al.*, 1996).

Figure 1.15: The FGF1-pentasaccharide co-crystal structure. The polypeptide chains of FGF1 are colored as blue ribbons. Although a decasaccharide was used to form crystal with FGF1, only a pentasaccharide (colored by atom as above) is visible from the crystal structure. Note that the two FGF1 molecules do not make any direct protein contact. The structure is generated using the crystallographic coordinates of 1AXM (DiGabriele, *et al.*, 1998).

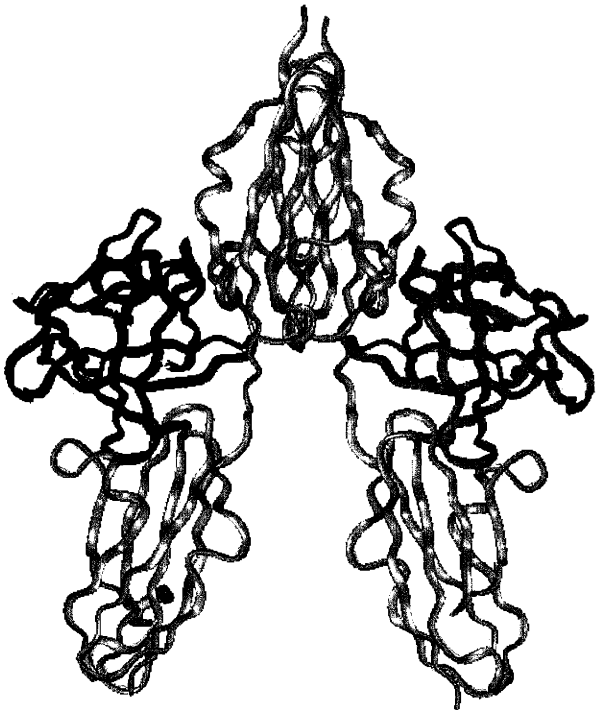

Figure 1.16: The FGF2-FGFR1 co-crystal structure. The polypeptide chains of the two FGF2 molecules are colored in either blue or green. The two FGFR1 ectodomains (each consisting of an upper IgII-like domain and a lower IgIII-like domain) are colored in gray. Note that there is no protein contact between the two FGF2 molecules and that there is substantial contact between the IgII-like domains of the two receptors. An overall 2:2 FGF:FGFR stoichiometry is observed from the assemblage. The structure is generated using the crystallographic coordinates of 1CVS (Plotnikov, *et al.*, 1999).

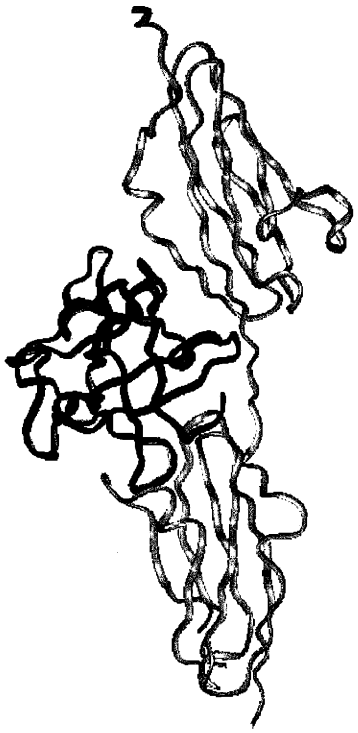

Figure 1.17: The FGF1-FGFR2 co-crystal structure. The polypeptide chain of FGF2 (colored as a blue ribbon) is complexed with the IgII-like and IgIII-like loops of FGFR2 in a 1:1 FGF:FGFR stoichiometry. The structure is generated using the crystallographic coordinates of 1DJS (Stauber, *et al.*, 2000).

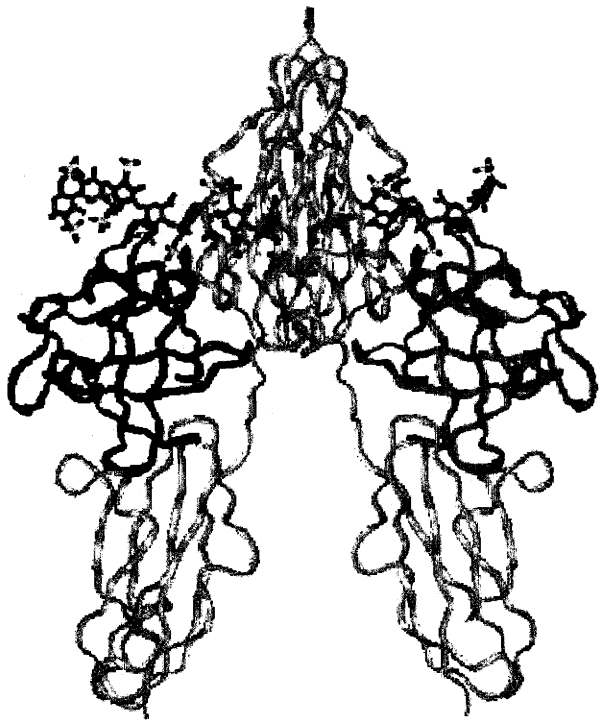

Figure 1.18: The dimeric 2:2:2 FGF:HSGAG:FGFR crystal structure. The polypeptide chains of the two FGF2 molecules are colored in blue and green. The receptors are colored in gray. The hexasaccharide is colored by atom as specified in the legend to Figure 1.14. The overall architecture is the same as the 1CVS structure as shown in Figure 1.16, except for the presence of two heparin fragments. The structure is generated using the crystallographic coordinates of 1DJS (Schlessinger, *et al.*, 2000).

Figure 1.19: The FGF2-hexasaccharide crystal structure. The polypeptide chains of FGF2 are colored as blue and green ribbons. The hexasaccharide is colored by atom as above. Note that the kicked HSGAG chain makes contact with one of the two IgII-like domains of FGFR. The structure is generated using the crystallographic coordinates of 1E0O (Pellegrini, *et al.*, 2000).

1.7 Specific objectives

As stated in Section 1.1, the overall objective of this thesis research is to develop a molecular understanding of the roles played by HSGAGs in cell signaling through FGF-dependent and FGF-independent mechanisms.

The specific research objectives are broadly grouped into two parts. Part I addresses the molecular aspects of HSGAG-induced FGF2 dimerization and its significance in biological systems. Part II relates to the functional roles of cell surface HSGAGs in modulating FGF-mediated cell proliferation and in regulating apoptotic cell phenotype. A general discussion on apoptosis and its potential role in tumor biology is provided in Chapter 6.

Accordingly, the specific objectives of this thesis work are summarized below:

1.	**Interactions of FGF2 with HSGAGs**
1a.	Rational design of mutant proteins for probing FGF-FGF interaction
1b.	Protein engineering and molecular characterization of a novel dimeric FGF2 fusion protein
1c.	*in vitro* and *in vivo* characterization of the dimeric FGF2 fusion protein
2.	**Cell Surface HSGAGs**
2a.	Investigation of the effect of heparinase-generated fragments on modulating FGF-mediated cell proliferation through different receptor isoforms
2b.	*in vitro* characterization and gene array analysis of the effect of heparinase III treatment on the induction of apoptosis in melanoma cells

Chapter 2:

Probing Protein-Protein Interaction in FGF2 Dimerization

Summary

Ligand dimerization is believed to be central in the formation of an active signaling complex for a number of growth factors and cytokines. In the case of fibroblast growth factor-2 (FGF2) signaling, heparan sulfate glycosaminoglycan (HSGAG) is involved through the interaction with both FGF2 and its receptors (FGFR) in assembling a tertiary complex and modulating FGF2 activity. Biochemical data have suggested different modes of HSGAG-induced FGF2 dimerization involving specific protein-protein contacts. In addition, several recent X-ray crystallography studies of FGF-FGFR and FGF-FGFR-HSGAG complexes have revealed other modes of molecular assemblage, with no FGF-FGF contacts. All these different biochemical and structural findings have clarified less and in fact raised more questions as to which mode of FGF2 dimerization, if any, is essential for cell signaling. The experimental studies described in this Chapter address the issue of FGF2 dimerization in signaling using a combination of biochemical, biophysical and site-directed mutagenesis approaches. The results provide direct evidence of FGF2 dimerization as a possible mechanism of growth factor activation.

2.1 Introduction

The FGF family of HSGAG-binding growth factors, consisting of at least 23 members, has been extensively studied for the past two decades. These growth factors are all monomeric proteins with molecular mass of ~15-45 kDa. One of the prototypic members of the FGF family, basic FGF or FGF2, has been demonstrated to play multiple fundamental roles in normal development (e.g. morphogenesis) as well as in disease states (e.g. tumor growth and metastasis). FGF signal is transduced primarily through high-affinity interaction with cell surface FGFRs, transmembrane polypeptides composed of immunoglobulin-like and tyrosine kinase domains (Jaye, *et al.*, 1992; Wilkie, *et al.*, 1995). FGF binding to different isoforms of FGFR is believed to trigger receptor dimerization followed by transphosphorylation of specific tyrosine residues (Schlessinger, *et al.*, 1995). Phosphorylated tyrosine residues in turn activate other signaling proteins such as mitogenic activating protein kinase and phosphoinositol-3 kinase, and subsequently lead to cell proliferation, migration and survival. One intriguing characteristic of FGF signaling is the involvement of HSGAGs as either positive or negative regulators of cell signaling (Guimond, *et al.*, 1993; Guimond and Turnbull, 1999; Liu, *et al.*, 2002b; Rapraeger, 1995). Many FGF family members exhibit an unusually high affinity towards heparin, which typically requires very high salt concentration for dissociating the protein from binding to a heparin column.

The molecular nature of FGF2 activation is controversial. A number of models have been proposed to explain how FGF2 activates FGFR for signaling and the role of HSGAGs, if any, in the FGF-FGFR interaction. Two of the widely debated models are described here. Using thermal titration calorimetry and ultracentrifugation, Pantoliano *et al* reported a 1:2 ratio of growth factor to receptor in the presence of HSGAGs and proposed a model of FGF2 activation (Pantoliano, *et al.*, 1994) similar to the activation mechanism of human growth hormone and erythropoietin (de Vos, *et al.*, 1992; Watowich, *et al.*, 1994). In this monomeric ligand model, a monomeric molecule of FGF2 is thought to facilitate FGFR dimerization through two distinct receptor-binding surfaces on FGF2. Pye *et al* reported that a monomeric FGF2 chemically crosslinked with an oligosaccharide was active in promoting cell growth in cultured cells (Pye and

Gallagher, 1999), suggesting that FGF2 might transduce signals through an overall 1:2 stoichiometry of ligand to receptors.

An alternative model of FGF activation is the dimer presentation model, which involves an overall 2:2 stoichiometry of growth factors to receptors in assembling the signaling complex. This model was proposed based on the early observations of heparin-induced FGF2 dimerization and oligomerization in chemical crosslinking experiments (Ornitz, *et al.*, 1992). Venkataraman *et al* reported that FGF2 molecules preferentially oligomerized by protein-protein interaction and that HSGAGs could serve to stabilize such interaction (Venkataraman, *et al.*, 1996). Other studies, such as chemical crosslinking (Davis, *et al.*, 1999), ultracentrifugation (Herr, *et al.*, 1997) and mass spectrometry (Venkataraman, *et al.*, 1999b), also suggested that HSGAGs induced FGF2 oligomerization. Perhaps the strongest evidence in supporting the dimer presentation model is the recent reports on the FGF-FGFR crystal structures, in which a 2:2 stoichiometry was clearly demonstrated (Plotnikov, *et al.*, 1999; Plotnikov, *et al.*, 2000). Another recent crystal structure of FGF1-FGFR2 complex also revealed a similar structural arrangement (Stauber, *et al.*, 2000), suggesting that the dimeric mode of FGF-FGFR interaction may apply to other members of the FGF family. However, like most other crystallographic analyses, exceedingly high protein and HSGAG concentrations were required in crystal packing. Therefore, questions remain with regards to the physiological relevance of the dimer presentation model and whether the observed crystal structure represents the biologically active form of the signaling complex *in vivo*. In addition, earlier crystal structures demonstrated that FGF2 molecule only crystallized as a monomer within an asymmetric unit (Eriksson, *et al.*, 1993; Faham, *et al.*, 1996; Zhang, *et al.*, 1991; Zhu, *et al.*, 1991), despite the biochemical evidence favoring FGF2 dimerization / oligomerization in the presence of HSGAGs. Furthermore, different modes of FGF-FGF interactions have been observed in various studies, drawing into question what modes of FGF oligomerization, if any, are biologically relevant.

In this Chapter, a combination of molecular modeling, protein engineering and biochemical analysis was used to distinguish various modes of FGF-FGF interactions in solution. A schematic illustration of the methodology is depicted in **Figure 2.1**. To test the dimer presentation hypothesis, a FGF2 mutant protein was designed based on the

computational modeling of a "side-by-side" FGF2 dimer (Venkataraman, *et al.*, 1996). Specific cysteine residues were incorporated into the protein by site-directed mutagenesis. The FGF2 mutant protein was expressed, purified and subject to the oxidative crosslinking analysis.

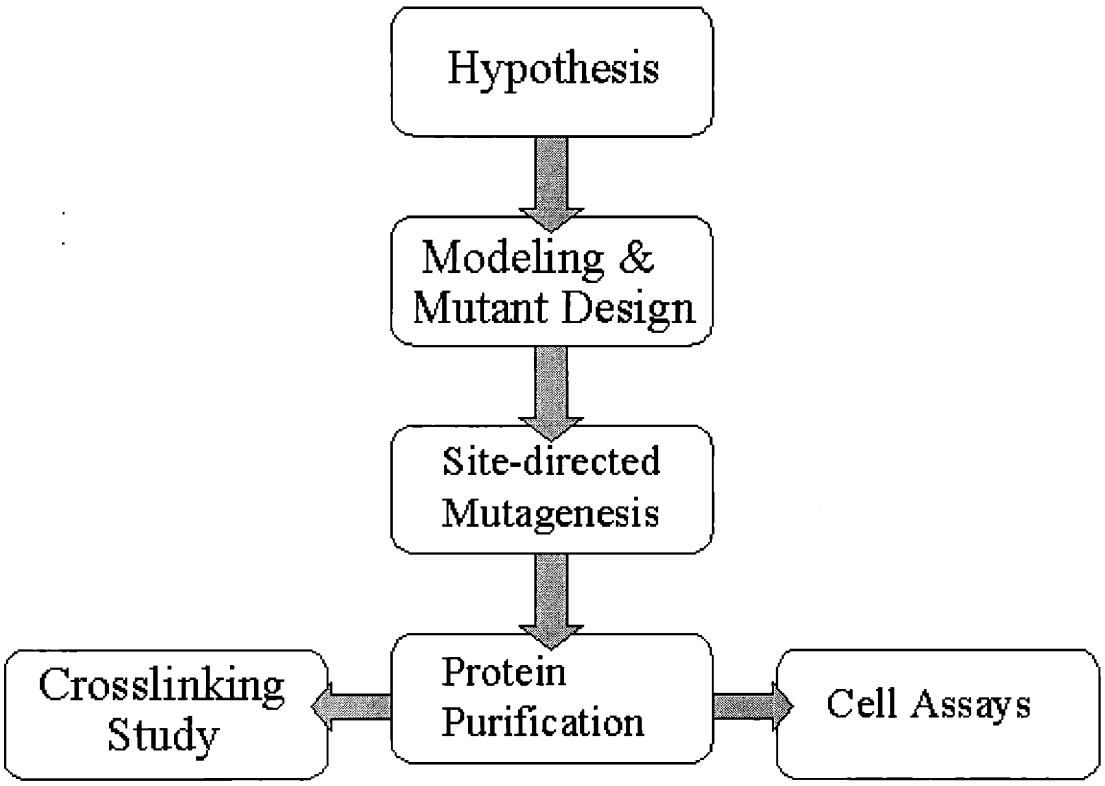

Figure 2.1: A flowchart of the overall experimental approach. A working hypothesis (specific FGF-FGF interaction in a "side-by-side" fashion is important in FGF dimerization / oligomerization) was formulated based on the existing knowledge of FGF crystal structures and experimental data. Computational modeling was employed to aid the design of the mutant protein based on the working hypothesis. A step-wise, PCR-based site-directed mutagenesis technique (see A1.2.3 in the Appendix) was used to introduce specific mutations into the cDNA construct of the protein. The mutant protein was recombinantly expressed in an expression system such as BL21 *E. coli*. The recombinant protein was extracted from the cell lysate and purified by a chromatographic method. The protein was subject to biochemical analysis using an oxidative crosslinking reagent and to cell proliferation assay for testing biological activity. Based on the results

of both the crosslinking study and cell assay, the working hypothesis was either accepted or rejected.

2.2 Framework for understanding FGF2 oligomerization

Our laboratory and others have attempted to address the issues of the role of HSGAGs in FGF2 activation by inspecting several independent apo-FGF and FGF-HSGAG crystal structures (Venkataraman, *et al.*, 1996). Through exhaustively examining the unit cells of FGF2 crystals, Venkataraman *et al* made the key observation that two of the three unit cell axes and an included angle were conserved in all the crystal structures examined. Translation of 31Å and 33Å along these two conserved axes led to two possible dimers for FGF2, namely dimer 31 and dimer 33, respectively (**Figure 2.2**).

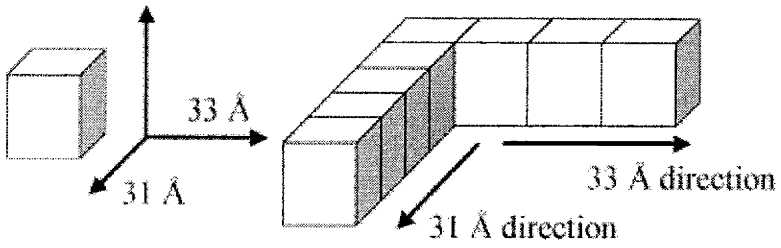

Figure 2.2: Schematic of FGF2 crystal packing. Left: a unit cell of FGF2 molecule is represented by a cube. Two of the three axes (indicated by their translational distance, 31Å and 33Å, respectively) are conserved in terms of the translational distance and the orientation (Venkataraman, *et al.*, 1996). Right: translation of the unit cell along the 31Å and 33Å directions results in two possible dimer forms, namely dimer 31 and dimer 33, respectively. Note that the two dimers involve distinct interfaces of the unit cell.

At the interfaces of dimers 31 and 33, a pair of protein-protein interaction sites (referred to as site p and p' for dimer 31, and site q and q' for dimer 33, respectively) can be identified. Based on the calculation of the van der Waals contact surface area and heparin modeling for the two possible dimers, dimer 31 was proposed to be the preferred

form of dimer in FGF2 dimerization (Venkataraman, *et al.*, 1996). As described in detail below, FGF2 dimerization / oligomerization is believed to be mediated through specific protein interaction between sites p and p' on the FGF2 molecules.

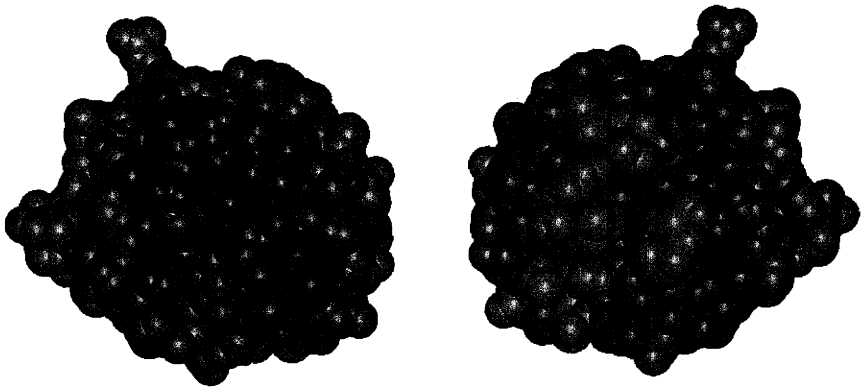

Figure 2.3: The protein-protein interaction sites on dimer 31. Space-filled models of FGF2 molecules (Faham, *et al.*, 1996) are shown. Left: residues within the protein-protein interaction site p are colored in purple. Right: the same molecule as in the left but rotated 180° along the y-axis. Residues within the protein-protein interaction site p' are highlighted in green. Note that the two sites are on the opposite surfaces of the molecule.

The model of FGF-FGF interactions proposed by Venkataraman *et al* (**Figure 2.2**) suggests that FGF2 molecules have an inherent tendency to oligomerize along the 31Å direction with or without binding to HSGAGs. Importantly, further stabilization of the dimeric state of FGF2 molecules can be achieved by binding to a HSGAG chain of at least 8 to 10 monosaccharide units. It is generally observed that an octa- to decasaccharide is the shortest oligosaccharide required for the activation of FGF2 signaling (Guimond, *et al.*, 1993; Ornitz, *et al.*, 1992). Hence, it is conceivable that HSGAGs may serve to stabilize the self-associated FGF2 molecules for proper presentation to the receptor at cell surface. This model predicts that:

(1) FGF2 molecules oligomerize asymmetrically in a "side-by-side" fashion involving two distinct interfaces with substantial protein-protein contacts;
(2) HSGAG is not absolutely required for FGF2 signaling but would enhance stability of the complex;
(3) the minimal functional unit of FGF2 signaling is a dimer.

2.3 Examining different proposed modes of FGF dimerization

Biochemical studies that are consistent with the "side-by-side" mode of FGF-FGF interactions include chemical crosslinking, analytical ultracentrifugation and mass spectrometry (Davis, *et al.*, 1999; Herr, *et al.*, 1997; Venkataraman, *et al.*, 1999b). However, NMR studies predict a different mode of FGF oligomerization, *viz.*, a symmetrical FGF2 dimer with possible disulfide bond formation between the two surface cysteines (Moy, *et al.*, 1997). Furthermore, the FGF1-decasaccharide co-crystal structure points to a FGF *trans* dimer involving no FGF-FGF contacts (DiGabriele, *et al.*, 1998), a mechanism for dimerization that may or may not extend to FGF2 and other members of the FGF family. More recently, several crystallographic studies of FGF-FGFR and FGF-FGFR-HSGAG complexes, including FGF2:FGFR1 (Plotnikov, *et al.*, 1999), FGF1:FGFR1 (Plotnikov, *et al.*, 2000), FGF2:FGFR2 (Plotnikov, *et al.*, 2000), FGF1:FGFR2 (Stauber, *et al.*, 2000), reveal an assemblage of two FGFs bound to two FGFRs with no FGF-FGF contacts in the complex. Thus, conflicting biochemical, biophysical and structural evidence makes it unclear whether FGF dimerization is important for cell signaling through FGFR and, if so, which dimerization mode of FGFs, involving either protein contact or no protein contact, mediates FGF signaling. This problem is compounded when one considers that the two recent crystal structures of the ternary complex involving FGF, FGFR, and HSGAGs (Pellegrini, *et al.*, 2000; Schlessinger, *et al.*, 2000) reveal different stoichiometries for the complex with markedly divergent geometries (Section 1.6). In this Chapter, conformational studies and molecular engineering techniques are applied to systematically explore various proposed modes of FGF2 dimerization.

2.4 Analysis on the FGF2 unit cell

The three dimensional structure of FGF2 has been thoroughly elucidated by a variety of biophysical techniques, including solution NMR and X-ray crystallography

(DiGabriele, *et al.*, 1998; Eriksson, *et al.*, 1993; Faham, *et al.*, 1996; Moy, *et al.*, 1996; Moy, *et al.*, 1997; Pellegrini, *et al.*, 2000; Plotnikov, *et al.*, 1999; Plotnikov, *et al.*, 2000; Schlessinger, *et al.*, 2000; Stauber, *et al.*, 2000; Zhang, *et al.*, 1991). All have pointed to roughly the same basic structure for FGF2, whether free, bound to its HSGAG ligand, or complexed with the receptor. An analysis of all of these structures suggests that three orthogonal surfaces exist on FGF2 (**Figure 2.4**).

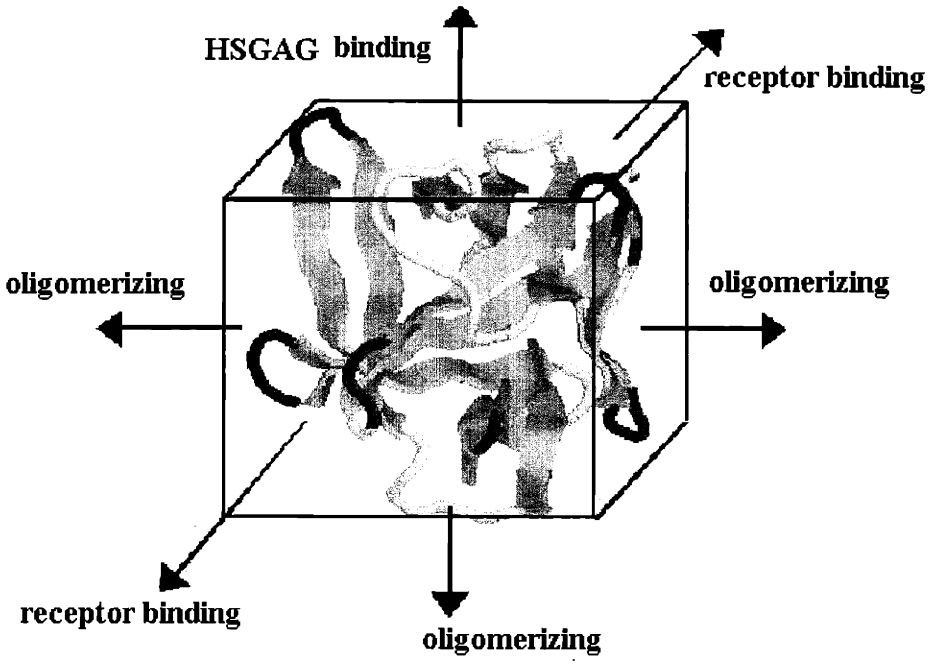

Figure 2.4: Analysis of various binding sites on FGF2. The surface of a FGF2 molecule (Faham, *et al.*, 1996) can be approximated as the faces of a parallelepiped. Of the six faces, two opposite faces represent the receptor binding sites (pointing into and out of the plane of the paper), while the other four (denoted as oligomerizing and HSGAG binding) represent directions about which FGF can associate. Note that two of the three oligomerizing directions are aligned along the same plane. Translation of the FGF2 molecules along these two directions forms the basis of FGF2 oligomerization.

As indicated in the figure, the first surface has been implicated in binding of FGF2 to its high affinity cell surface receptor. Through rigorous biochemical and site-directed mutagenesis studies, a second, orthogonal surface has been implicated in HSGAG binding (Eriksson, *et al.*, 1993). The third surface, orthogonal to both of the first two has been implicated in FGF2 dimerization / oligomerization. Within the third

surface, biochemical and structural studies have suggested different modes of FGF2 oligomerization both in the presence and absence of HSGAGs (DiGabriele, *et al.*, 1998; Moy, *et al.*, 1997; Venkataraman, *et al.*, 1996). As schematically represented in **Figure 2.5**, three modes of HSGAG-induced FGF2 dimerization have been proposed.

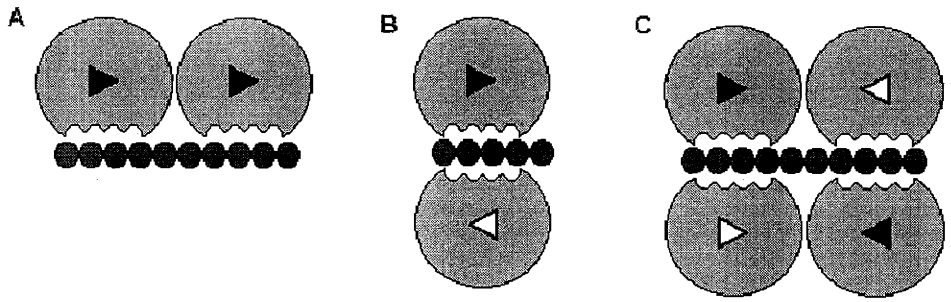

Figure 2.5: Proposed modes of FGF dimerization / oligomerization. Either a closed or an opened triangle is drawn inside each FGF molecule to distinguish different orientations. The round indentation within each FGF molecule represents the HSGAG-binding sites. A HSGAG molecule is depicted as a chain of beads. A, Two FGF molecules, oriented asymmetrically in *cis*, bind to the same side of the HSGAG chain in a "side-by-side" fashion (Herr, *et al.*, 1997; Venkataraman, *et al.*, 1999b; Venkataraman, *et al.*, 1996). B, Two FGF molecules are oriented by *trans* to the axis of the HSGAG chain in a "head-to-head" fashion (DiGabriele, *et al.*, 1998). C, A complex of four FGF molecules oriented both in *cis* and by *trans* with a chain of HSGAG are implicated in a NMR study (Moy, *et al.*, 1997). Note that, for the *trans* interaction, the two FGF molecules are symmetrically related as opposed to the *cis* dimer in A.

Specific protein-protein contacts are involved in both the sequential and symmetrical FGF2 dimers (**Figure 2.5A and C**, respectively) but not in the HSGAG-bridged or sandwich dimer (**Figure 2.5B**). Earlier it was demonstrated that FGF2 was capable of dimerization and oligomerization in the absence of heparin using an amine-specific chemical crosslinker with an 11 Å spacer (Davis, *et al.*, 1999). This observation is not consistent with the proposed HSGAG-bridged dimer in **Figure 2.5B** since, in this FGF sandwich model, there are no residues on neighboring FGF2 molecules proximate to one another and thus available for covalent crosslinking with an 11 Å spacer (additional experiments described below also are not consistent with this dimer mode). Therefore,

experiments were designed to determine whether either of the dimer models involving protein contacts (represented in **Figure 2.5, A** and **C**) are accurate representations of FGF2 dimerization mediated by HSGAGs.

2.5 Oxidative crosslinking of wildtype FGF2

To establish the presence of proximal contacts between FGF2 molecules and to distinguish between different modes of FGF2 dimerization, oxidative crosslinking experiments were performed to target specific cysteine residues using copper phenanthroline, or Cu^{2+}-$(phenanthroline)_2$. The oxidative property of copper phenanthroline was first described in the late 1960s (Kobashi, 1968) and it has been applied to study disulfide bridge formation in protein (Bisaccia, *et al.*, 1996; Costantini, *et al.*, 1998) and DNA (Veal, *et al.*, 1991). The redox reaction proceeds as below:

(1): 2 R-SH + 2 Cu^{2+}-$(phenanthroline)_2$ → R-S-S-R + 4 phenanthroline + 2 Cu^{+}+ 2 H^{+}

(2): 4 phenanthroline + 2 Cu^{+}+ ½ O_2 + 2 H^{+} → Cu^{2+}-$(phenanthroline)_2$ + H_2O

---

(1)+(2): 2 R-SH + ½ O_2 → R-S-S-R + H_2O

The reaction can be quenched with a metal chelating reagent such as EDTA. Disulfide bond formation can be reversed by incubating the crosslinked products with reducing agents such as dithiothreitol (DTT) or β-mercaptoethanol. Unreacted sulfhydryl groups can be blocked by alkylation using iodoacetic acid, a thiol modifying reagent. Blocking unreacted sulfhydryl groups after oxidative crosslinking reaction is necessary for SDS-PAGE analysis to avoid crosslinking between internal cysteines under denaturing conditions.

This oxidative crosslinking approach is anticipated to probe for atomic distance interactions between the FGF molecules through the introduction of a disulfide bond between two FGF2 molecules. As discussed below, by taking advantage of the surface exposed cysteine residues in FGF2 and through rationally engineering cysteine residues

on the surface of FGF2, we systematically explored all the possible modes of FGF2 dimerization.

There are four cysteines in FGF2, two of which are surface-exposed (C69 and C87), and two of which are buried in the protein core (C25 and C92). The surface positions of the two exposed cysteines (C69 and C87) in wildtype FGF2 are related to each other by 90°. Taking advantage of the surface-exposed cysteine residues in the wildtype structure of FGF2, we performed oxidative crosslinking studies to test the proposed symmetrical mode of FGF2 dimerization in **Figure 2.5C**, as this model predicted facile crosslinking between two FGF2 molecules (Moy, *et al.*, 1997). Under mild oxidative conditions, wildtype FGF2 showed very little oligomer formation in the presence and absence of heparin (**Figure 2.6**). Several control experiments were performed to ensure the authenticity of the data and are described below. The absence of significant dimers or oligomers suggested that either the FGF-FGF interface did not involve molecular contacts or that the contacts were such that the two surface exposed cysteines were not at the dimer interface. Our observation was not consistent with the proposed symmetrical mode of FGF2 dimerization wherein dimerization was mediated by disulfide bond formation between C69 of each monomer (Moy, *et al.*, 1997).

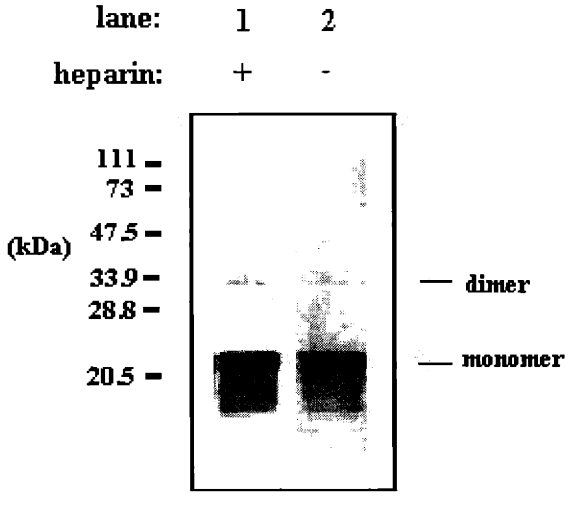

Figure 2.6: Oxidative crosslinking of wildtype FGF2. Wildtype FGF2 was oxidized with (lane 1) or without (lane 2) heparin as described in the Appendix (A1.2.5). A minor amount of dimer was detected, which was likely resulted from the crosslinking reaction between unfolded proteins. The approximate molecular weight in kDa is shown on the side. For heparin treatment, the wildtype protein was incubated with 3 μM heparin for 1 hour prior to crosslinking. The protein to heparin ratio was 10:1, which was previously shown to be optimal for FGF2 dimer formation (Davis, *et al.*, 1999).

2.6 Rational design of cysteine mutant

In a previous study, an extensive analysis was performed on all FGF2 crystal structures available at that time, and identified the protein-protein interfaces (p-p' and q-q') that were conserved along the two unit cell axes (Venkataraman, *et al.*, 1996). Based on exhaustive analysis on various FGF structures, a FGF2 dimerization model was proposed in which FGF2 molecules are preferentially self-associated in a sequential fashion and HSGAG binding stabilized FGF2 dimers and oligomers that were subsequently presented to FGFR for signaling. In this model, non-covalent FGF-FGF interactions translated along the oligomerization direction (**Figure 2.4**) are expected to lead to FGF2 oligomerization. If this model indeed describes a mode of FGF oligomerization, then substituting cysteine residues near the protein-protein interface between adjacent FGF2 molecules would lead to intermolecular disulfide bond formation under mild oxidative conditions. We reason that sequential dimer formed in this fashion is expected to be stabilized by significant protein-protein contacts.

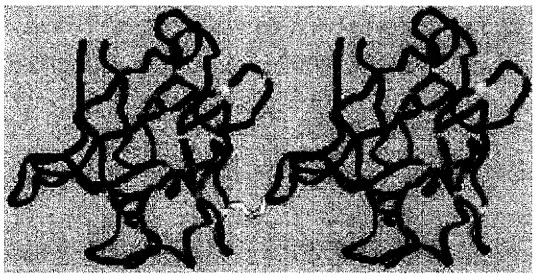

Figure 2.7: Molecular model of a "side-by-side" dimer of FGF2 cysteine mutant. Two FGF2 molecules (shown in red) are positioned in a "side-by-side" or *cis* fashion. The disulfide bridge formed between site p and p' of the two molecules is showed in yellow.

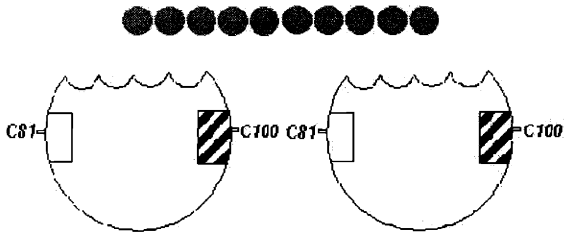

Figure 2.8: Schematic representation of the protein-protein and protein-HSGAG interactions in cysteine mutants. Two cysteine mutant molecules are shown, each with two dimer interfaces as represented by striped (site p) and open (site p') rectangles. Two solvent-exposed cysteines (C81 and C100 as shown at site p' and p, respectively) were engineered such that they would position in close proximity with each other at the interface. Modified from Herr *et al* (Herr, *et al.*, 1997).

As a first step towards testing this hypothesis, a search for candidate pairs of residues in the p-p' interface was conducted. When mutated to cysteine residues, these residues are expected to generate a disulfide linkage in a facile manner upon oxidative crosslinking. Through conformational studies, we found that optimal disulfide bond formation would be achieved when R81 and S100 were mutated into cysteines, as schematically represented in **Figure 2.8**. The two introduced cysteines are located on the opposite sides of FGF2 such that intramolecular disulfide bond formation would be disfavored. The two original cysteines, C69 and C87, were mutated to serines such that the total number of surface cysteines within the primary amino acid sequence of FGF2 remained the same. This protein, with four mutations (R81C/S100C/C69S/C87S), is hereafter referred to as the cysteine mutant. The cysteine mutant was constructed by a PCR-based site-directed mutagenesis method as described in the Appendix (A2.3). The protein retained biological activity to stimulate cell proliferation as compared to wildtype (data not shown), suggesting that the introduced mutations did not grossly alter protein folding.

2.7 Oxidative crosslinking of cysteine mutant

Under exactly the same oxidative conditions as applied to the wildtype protein, the cysteine mutant yielded a markedly higher amount of oligomers. Notably, the extent of oligomerization was markedly elevated by pre-incubating the protein with heparin (**Figure 2.9**). In addition, crosslinking of a mutant FGF that lacked one of these cysteines at the interface (*i.e.*, either the R81C or S100C mutation) resulted in significantly less oligomer formation, further suggesting that the covalent dimer was formed through disulfide bond formation between the designed C81 and C100. Together, these observations strongly support the sequential mode of FGF2 dimerization and also suggest that the extent and stability of FGF2 oligomers are increased by binding to HSGAGs such as heparin (Venkataraman, *et al.*, 1996).

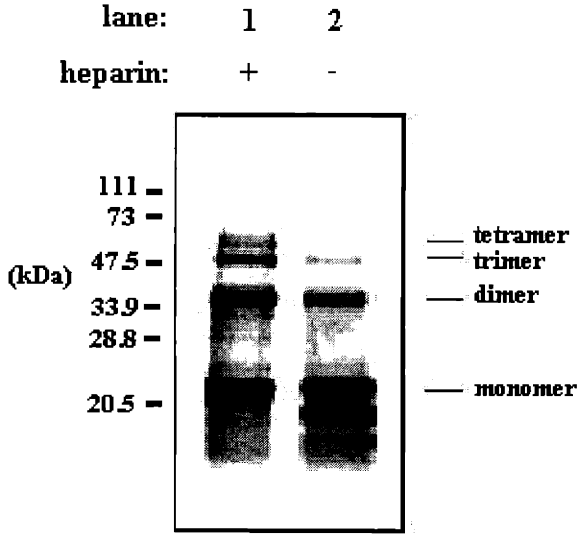

Figure 2.9: Oxidative crosslinking of cysteine mutant. Cysteine mutant (30 μM final), which was designed based on the model of FGF2 dimerization (Venkataraman, *et al.*, 1996), was oxidized with (lane 1) or without (lane 2) heparin under the same conditions as the wildtype protein in Figure 2.6. For heparin treatment, the mutant protein was incubated with 3 μM heparin for 1 hour prior to crosslinking. The protein to heparin ratio was 10:1, which was previously shown to be optimal for FGF2 dimer formation (Davis, *et al.*, 1999).

To ensure the authenticity of specific cysteine-mediated FGF2 oligomerization, several control experiments were performed. Addition of a reducing agent such as DTT converted the observed dimers and oligomers into monomers (**Figure 2.10**, lane 4), indicating the original crosslinking pattern was the result of disulfide-linked oligomers. Also, oligomerization was abolished when the cysteine mutant was denatured prior to crosslinking (**Figure 2.10**, lane 3), suggesting that oligomerization was mediated through

the native structure of protein and the observed oligomers were not formed due to non-specific protein aggregation. In addition, since two cysteines (C25 and C92) were buried in the protein core, they could potentially contribute to the observed oligomerization if the protein was unfolded during crosslinking. To exclude this possibility, the primary amino acid sequence of the cysteine mutant was further altered by substituting the two internal cysteines with serines (*i.e.*, additional C25S/C92S mutations were introduced). The introduction of these two additional mutations did not change the crosslinking pattern (data not shown), further indicating that only the surface exposed C81 and C100 contributed to disulfide-induced oligomerization.

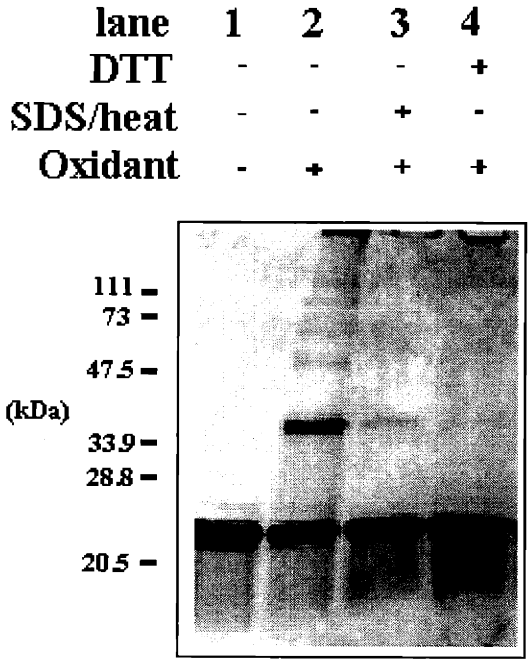

Figure 2.10: Dimerization and oligomerization of cysteine mutant were mediated by the native structure of the protein. Lane 1: cysteine mutant alone; lane 2: cysteine mutant oxidized without heparin; lane 3: same as lane 2 but protein was heat/SDS-denatured prior to oxidative crosslinking and lane 4: same as lane 2 but treated with 1 mM DTT. Note that oxidative crosslinking of cysteine mutant was abolished by either denaturing or reducing treatments.

To further explore the role of HSGAGs in FGF2 dimerization / oligomerization, cysteine mutant was oxidatively crosslinked in the presence of various concentrations of heparin. In a previous study from our laboratory, a 1:10 heparin to protein ratio was found to be optimal for inducing FGF2 dimerization and oligomerization (Davis, *et al.*, 1999). Consistent with this study, the extent of oligomerization was higher in the reaction that included the 1:10 heparin to protein ratio than the no heparin treatment (**Figure 2.11**). As the concentration of heparin increased (up to 10 fold in excess), the extent of oligomerization decreased. This observation can be explained if one considers heparin as a template for docking multiple FGF2 proteins. If the heparin to protein ratio is low, it is more likely for two or more FGF2 proteins to bind to a given chain of heparin for dimerization and oligomerization to occur. However, if an excess amount of heparin is present, it is more likely that the FGF2 proteins would bind to different heparin chains and therefore far fewer higher oligomers would be crosslinked. This finding lends further credence to the proposal that HSGAGs serve as a template for inducing FGF2 dimerization / oligomerization.

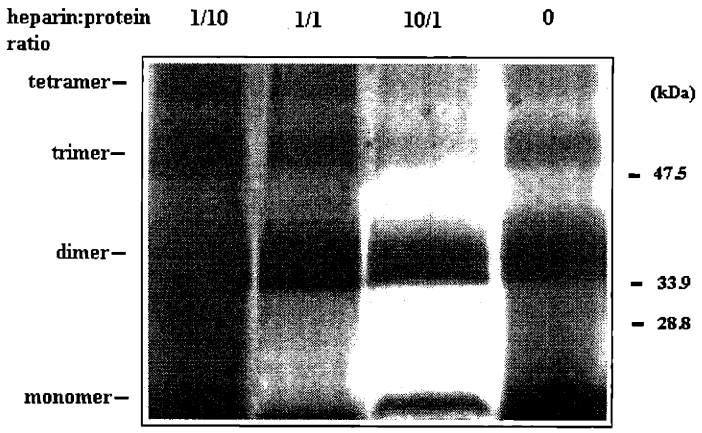

Figure 2.11: Oxidative crosslinking of cysteine mutant in different heparin:protein ratio. 30 μM cysteine mutant was oxidatively crosslinked in the presence of 3 μM (i.e., 1/10 ratio), 30 μM (1/1), 300 μM (10/1) heparin or in the absence of heparin. Note that the highest amount of oligomers was formed using the 1/10 ratio and that the amount of oligomerization (particularly for trimer and tetramer) decreases as the ratio increases. The SDS-PAGE gel was stained with silver stain reagent to show the amount of higher oligomers.

Taken all these results together, these oxidative crosslinking studies support a model wherein FGF2 monomers form sequential dimers via a substantial protein–protein interface and this interaction is further promoted by binding to HSGAGs. These results are consistent with other experimental studies including analytical ultracentrifugation of FGF2 with an octasaccharide, chemical crosslinking and mass spectrometry of FGF2 with or without the addition of exogenous HSGAGs (Davis, *et al.*, 1999; Herr, *et al.*, 1997; Ornitz, *et al.*, 1992; Venkataraman, *et al.*, 1999b).

Having demonstrated that cysteine mutant oligomerized through disulfide linkages under mild oxidative conditions, it was desired to isolate the dimerized protein from a pool of products for protein mapping study (to locate the peptides bridged by disulfide bonding) as well as for biological activity assay (to test whether a FGF dimer is more potent than a monomer). Attempts were made to isolate the dimerized FGF2 protein using size exclusion chromatography, reverse phrase-high pressure liquid chromatography and native polyacrylamide gel electrophoresis. Two major problems were encountered. First, the small size difference (~20 kDa) between monomer and oligomers made separation an extremely difficult task. In many instances, the fraction containing the majority of the dimerized protein was contaminated with a substantial amount of monomer and trimer. Second, because of the reversible nature of disulfide bond, it was speculated that a high proportion of the dimerized protein was converted back to monomer during the course of isolation. This may be caused by the very different buffer conditions used in the chromatographic procedures. Given the technical challenges in isolating disulfide-crosslinked FGF2 dimer, it was decided to take an alternative approach to engineer a fusion FGF2 dimeric protein for functional characterization (Chapters 3 and 4).

2.8 Conclusion

Several signaling pathways mediated by growth factors and cytokines involve binding of dimeric or oligomeric ligands to their cell surface receptors to facilitate receptor dimerization (Heldin, 1995), a key step leading towards activation of an

intracellular signaling cascade. For FGF family of growth factors, many biochemical studies have pointed to different modes of dimerization and oligomerization in the presence and absence of HSGAGs that is essential for signaling. In this study, three possible modes of HSGAG-mediated FGF2 association (**Figure 2.5, A-C**) was examined by evaluating earlier and current biochemical findings. The observation that FGF2 can oligomerize in the absence of HSGAGs (Davis, *et al.*, 1999) is inconsistent with the non-contacting, HSGAG-bridged dimerization mode (**Figure 2.5, B**). The results from the oxidative crosslinking studies of wildtype FGF2 do not support the proposed symmetric dimerization (**Figure 2.5, C**), which is potentially mediated by intermolecular disulfide bonds (Moy, *et al.*, 1997). Through rational design of a disulfide-mediated sequential dimer (the cysteine mutant) based on the earlier analysis of FGF2 crystal structures (Venkataraman, *et al.*, 1996), the results described in this Chapter demonstrated that:

(a) a marked increase in the amount of oligomers formed compared with wildtype FGF2, which has the same number of surface cysteines but at different positions,

(b) a higher extent of oligomerization by pre-incubating this cysteine mutant with heparin

(c) the observed oligomers involve specific protein contacts and are disulfide-mediated.

The above findings strongly support a model in which FGF2 molecules self-associate through specific FGF-FGF interactions in a sequential fashion (**Figure 2.5, A**) and that HSGAGs serve to provide a "platform" to stabilize the intermolecular interactions between FGF2 molecules, as previously proposed (Sasisekharan, *et al.*, 1997) (**Figure 2.12**).

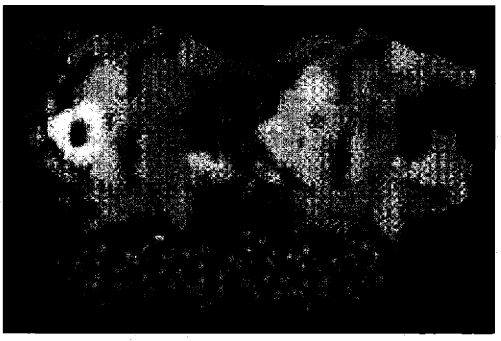

Figure 2.12: The "side-by-side" model of FGF2 dimerization. Two FGF2 molecules are positioned in a "side-by-side" or *cis* fashion along the 31Å axis with substantial protein contacts. An oligosaccharide chain (shown in green) binds to a different surface of the FGF2 dimer, providing further stabilization to the complex. Adapted from Sasisekharan *et al* (Sasisekharan, *et al.*, 1997).

Chapter 3:

Protein Engineering of Dimeric Fibroblast Growth Factor

Summary

Receptor dimerization at the cell surface is believed to be a key event that subsequently leads to cell signaling. In the case of FGF signaling, a number of structural studies have indicated a 2:2 FGF:FGFR assemblage, which might be biologically active in vivo. *It is hypothesized that ligand dimerization may facilitate receptor dimerization, which in turn may enhance biological activity. Conventional methods to force ligand dimerization (e.g. by chemical or oxidative crosslinking) often result in unwanted modification of the protein and generation of side products. These drawbacks not only complicate the interpretation of data, but also limit potential clinical applications. In this Chapter, a method is described to engineer a dimeric FGF2 (dFGF2) by fusing two FGF2 genes in tandem using conventional recombinant DNA technology. Conformational studies were completed to aid the design of linker for allowing optimal receptor dimerization. Molecular cloning strategies and biochemical characterization of the dimeric FGF2 protein are described.*

3.1. Introduction

FGF2 dimerization is believed to be an important prerequisite for triggering receptor dimerization on the cell surface, leading to the activation of a cascade of intracellular signaling events. Ligand dimerization is also implicated in other growth factors such as platelet-derived growth factor (Bishayee, *et al.*, 1989; Fretto, *et al.*, 1993; Heldin and Westermark, 1999; Heldin, *et al.*, 1989), transforming growth factor-β (Banner, *et al.*, 1993) and epidermal growth factor (Lemmon, *et al.*, 1997). Experimental data presented in Chapter 2 suggest that FGF2 exhibits an intrinsic self-association property in solution, reminiscent of their crystal packing patterns (Venkataraman, *et al.*, 1996). Moreover, it appears that HSGAGs serve to stabilize dimerization and oligomerization of FGF2 molecules by bridging two or more FGF2 molecules in a "side-by-side" or *cis* manner.

While the biochemical studies in Chapter 2 indicate that a *cis* FGF dimer does preferentially form in solution, it might only form under extreme conditions that are non-physiological (*i.e.*, high protein concentrations, heparin:protein ratios of 1:10, etc.). Through the construction of a defined FGF2 dimer (dFGF2) and testing its biological activity, the question of whether the oligomeric mode indicated by the biochemical studies, *viz.*, a *cis* dimer involving substantial protein contacts, is able to form an active signaling complex at the cell surface can be addressed directly (**Figure 3.1**).

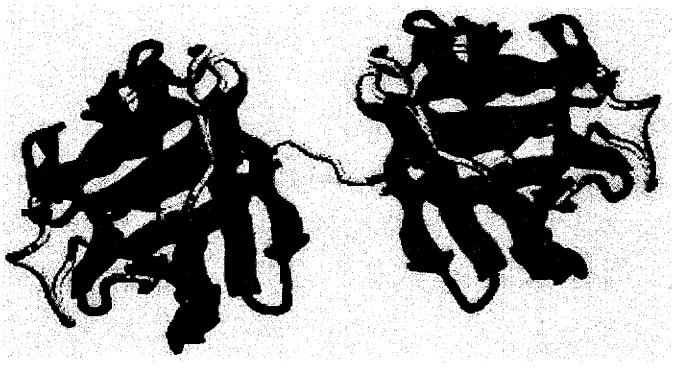

Figure 3.1: Model of dFGF2. A model of two FGF2 molecules linked in tandem is depicted here. Each FGF2 molecule consists of twelve β-sheets folded into a β-trefoil

structure. The linker between the two FGF2 molecules, shown as a structurally flexible loop, connects the C terminus of one FGF2 molecule to the N terminus of the other.

3.2 Method of approach:

The overall approach for constructing a dimeric FGF2 fusion protein is outlined in **Figure 3.2** and each individual module is described further in the subsequent sections. A molecular model of a "side-by-side" FGF2 dimer was constructed and the conformational characteristics of the introduced polypeptide linker were explored. A number of cloning strategies were proposed and attempted. PCR-based gene cloning techniques were employed to fuse the two FGF2 genes into a single construct for subcloning. After confirming the sequence and the directionality of the fused gene, the corresponding protein was expressed in *E. coli* and purified with an appropriate chromatographic method. After confirming the size of the fusion protein, a variety of assays were used to evaluate the biochemical, biophysical and biological properties of dFGF2.

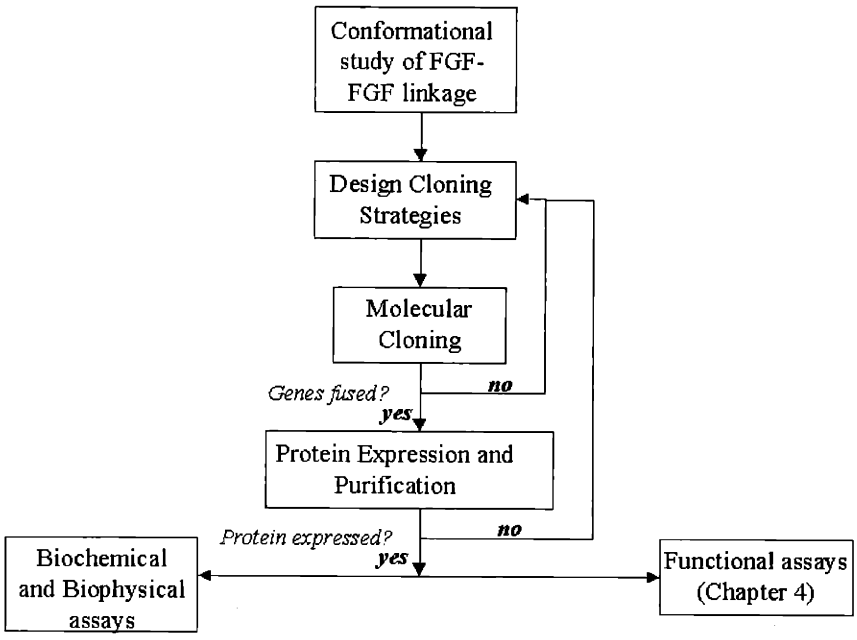

Figure 3.2: Flowchart illustrating the overall methodology of constructing dFGF2.

3.3 Conformational analysis

Conformational studies of FGF-FGFR interactions led to the proposal that receptor clustering is facilitated by receptor binding to a FGF2 dimer (Venkataraman, *et al.*, 1999a). However, as described in Section 1.6, the recently solved structures of 2:2 FGF-FGFR complexes, which are proposed to be the active FGF2 signaling complexes, revealed no contact between the two FGF molecules in the observed molecular assemblages (Pellegrini, *et al.*, 2000; Plotnikov, *et al.*, 1999; Plotnikov, *et al.*, 2000; Schlessinger, *et al.*, 2000; Stauber, *et al.*, 2000).

To determine whether FGF-FGF interaction is important for FGFR binding and concomitant signaling, it is desired to "force" FGF2 molecules into a *cis* dimerization mode by engineering a dimeric FGF2 protein containing a polypeptide linker. The size of the linker between the two FGF2 proteins could be controlled by deleting residues from the FGF2. Since there are at least 15 N terminal residues that are disordered in all the FGF2 crystal structures (including the proposed active FGF2-FGFR crystal structures), deletion of these residues is unlikely to significantly affect the folding of the protein. To find the optimal linker sequence length that would facilitate the distinction between the two modes of FGF-FGF interaction, the combinations of linker sequences with different lengths that could link the two FGF2 monomers in both the FGF-FGF interaction modes are explored as described in the Appendix (Section A1.3.2). Briefly, a linker was generated from the C-terminus of one of the FGF2 monomers to the N terminus of the other monomer in both the receptor-bound and the *cis* dimer by homology modeling. The modeled linker sequence in several randomly-generated structures was then subject to extensive energy minimization. Conformational studies showed that such a linker with 9 residues deleted from N terminus would optimally link two FGF2 molecules in the *cis* dimer (**Figure 3.3**, bottom), but would form a highly constrained structure when linking the two FGF2 molecules observed in the FGF2-FGFR1 crystal structure (**Figure 3.3**, top).

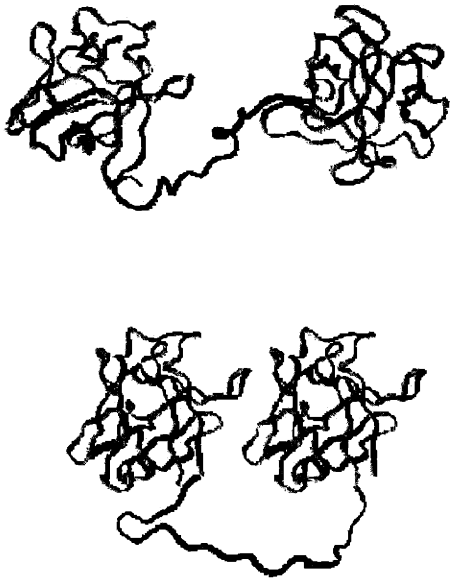

Figure 3.3. Comparison of the crosslinked *cis* dimer and the receptor-bound dimer of FGF2. Top: ribbon trace of FGF2 dimer bound to receptor (Plotnikov, *et al.*, 1999) (PDB code: 1CVS) colored in green. The disordered N and C termini and the modeled linker are shown as a ribbon trace colored in red. Bottom: the crosslinked *cis* dimer constructed from FGF2 crystal structure (Eriksson, *et al.*, 1993) (PDB: 4FGF). The ribbon trace of FGF2 dimer is colored in green and that of the linker is colored in red. Note that the linker is highly constrained in the FGF2 dimer bound to receptor and is much less constrained in the *cis* dimer.

3.4 Protein design

Based on the findings from the above conformational analysis, a fusion protein linking two FGF2 proteins was designed to investigate FGF2 dimerization and the role of HSGAGs in cell signaling. These two FGF2 proteins, both with their nine N-terminal residues deleted, was connected C to N through a tripeptide linker gly-ala-leu (**Figure 3.4**). To facilitate protein purification, a 13-residue 6x His tag and an 11-residue T7 tag were introduced to the N and C termini, respectively. Two 6-residue thrombin cleavage sites were located immediately adjacent to the tags such that the tags could be removed from the fusion protein if so desired. The distance between the two FGF2 proteins can be

controlled by adjusting the length of the linker or the N terminus of the second FGF2 protein. As described in the following sections, this engineered dFGF2 dimer is an ideal candidate to discriminate between a contacting FGF2 dimer and the non-contacting FGF2 dimer as observed in the FGF2-FGFR1 structure.

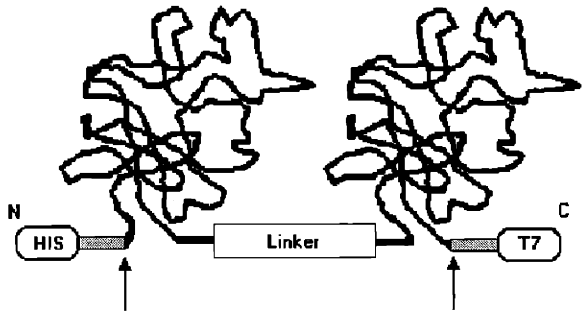

MGSSHHHHHHSSG*LVPRGS*HMPALPEDGGSGAFPPGHFKDPKRLYCKN
GGFFLRIHPDGRVDGVREKSDPHIKLQLQAEERGVVSIKGVCANRYLA
MKEDGRLLASKCVTDECFFFERLESNNYNTYRSRKYTSWYVALKRTGQ
YKLGSKTGPGQKAILFLPMSAKS**GAL**PALPEDGGSGAFPPGHFKDPKR
LYCKNGGFFLRIHPDGRVDGVREKSDPHIKLQLQAEERGVVSIKGVCA
NRYLAMKEDGRLLASKCVTDECFFFERLESNNYNTYRSRKYTSWYVAL
KRTGQYKLGSKTNPGQKAILFLPMSAK*SLVPRGS*MASMTGGQQMG

Figure 3.4: Protein design of dFGF2. Top: schematic representation of dFGF2. The two FGF2 proteins are connected in tandem by a tripeptide linker. Two tags (6x His and T7) are fused to the N and C termini, respectively. Thrombin cleavage sites (indicated by arrows) are adjacent to the tags to facilitate their removal by thrombin treatment. Bottom: protein primary sequence of dFGF2. Residues corresponding to 6x His tag are underlined with solid line. The tripeptide linker GAL is bolded. Residues corresponding to T7 tag are underlined with dashed line. Thrombin cleavage sites, which are located adjacent to the two tags, are italicized.

3.5 Molecular cloning strategies

Three different cloning strategies for generating dFGF2 were proposed, attempted and evaluated experimentally until the desired construct was obtained. Although only the last strategy was successful in generating the right construct for subsequent studies, it is

intended to document all three strategies here so as to provide a complete account of the cloning effort. To generate a DNA construct involving two FGF2 genes linked in tandem, it is required to duplicate the entire DNA sequence of FGF2 and to introduce a linker sequence for connecting the two FGF2 genes. For proper protein translation, it is also important to ensure that all the cloned sequences are in the correct reading frame. Based on prior experience in expressing FGF2, three different stop codes (TAG, TAA and TGA) were introduced at the 3' end of the construct to avoid translation "overrun."

I. Primer extension

In this approach, multiple rounds of PCR were performed to amplify and extend the gene sequence by about 50 base pairs per round of PCR (**Figure 3.5**). Amplified PCR products were analyzed by DNA gel electrophoresis and the DNA band was gel-purified to serve as template for subsequent rounds of PCR. Primers for annealing to the 3' end of the template were designed such that the primer sequence would flank a portion (~10 base pairs) of the template. After analyzing the PCR products from the first few rounds of PCR, it was realized that the 3' primers failed to anneal to the 3' end of the extended template due to low overlap in DNA sequences. This primer extension strategy, however, would have worked if the DNA sequences of the two genes were different.

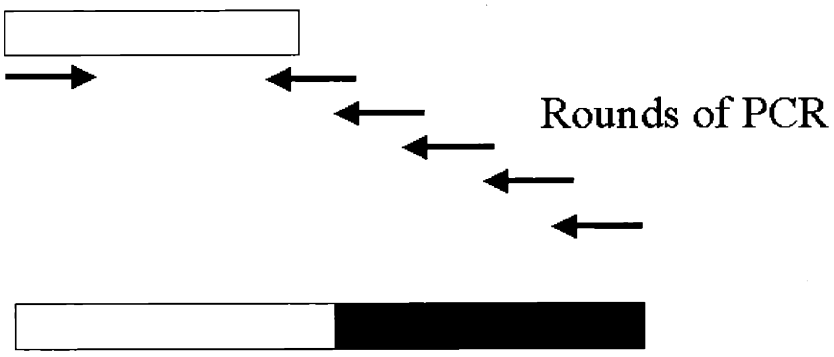

Figure 3.5: Schematic of the primer extension approach for fusing two genes into a single construct. The open rectangle represents the first gene while the closed rectangle represents the second gene. The primers are depicted as arrows. The proposed strategy involves performing multiple rounds of PCR using the first gene as a template. The

reverse primers are designed to anneal to the end of the cDNA such that the length of the PCR product is extended. The primer sequence is supposed to be same as the corresponding strand of the second gene, which in this case is the same as the first one.

II. The "cut-and-paste" strategy

A second approach to generate a fused FGF2 construct involved PCR-based cloning, restriction enzyme digestion and ligation (**Figure 3.6**). Restriction sites were introduced to the termini of the gene by PCR. PCR products were subcloned into a cloning vector (such as pCR2.1-TOPO of Invitrogen) and the DNA fragments were excised by digesting with the appropriate restriction enzymes. Another vector (such as pET15a of Novagen) was digested accordingly. Ligation of the DNA fragments and the linearized vector was expected to yield a fused FGF2 construct. The ligation mixture was then used to transform competent cells and colonies were screened by PCR or restriction digest. Unfortunately, it was found that most of the colonies only contained one copy of the FGF2 gene.

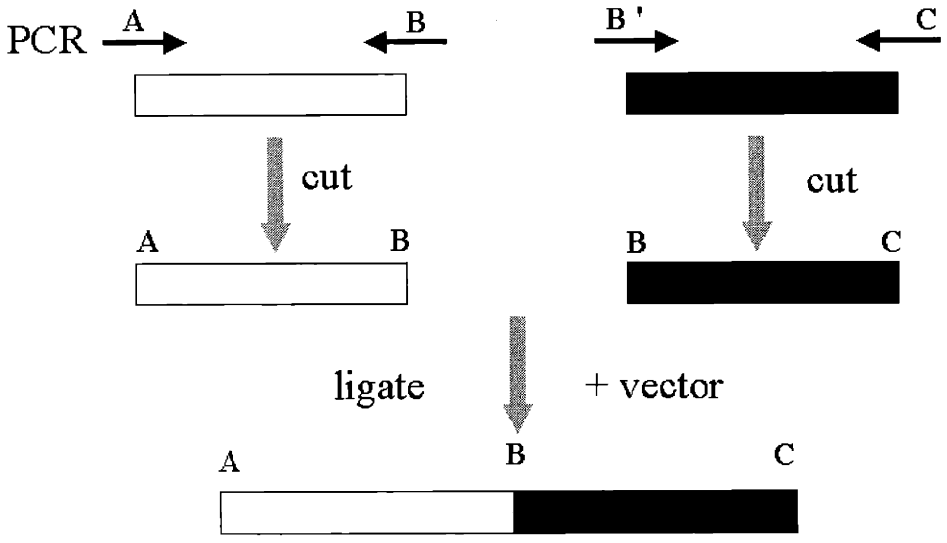

Figure 3.6: Schematic of the "cut-and-paste" strategy. Restriction sites (A, B and C) are introduced to the 5' and 3' ends of each gene by PCR. The PCR products are subcloned separately into cloning vectors such as pCR2.1-TOPO. Appropriate pairs of restriction enzymes are used to excise the gene (e.g. restriction enzymes A and B are used to digest the open-rectangle gene). After digestion, both genes contain restriction site B.

To subclone the two genes into a single construct, a three-way ligation is performed. The vector should have been cut with restriction enzymes A and C prior to ligation.

III. The sequential "cut-and-paste" strategy

In this approach, the two FGF2 genes were cloned one after another into a vector. DNA sequence containing the restriction site *SacI* was chosen to be the linker site connecting the two FGF2 genes (see A1.3.3 in the Appendix for other potential linker sites). As outlined in **Figure 3.7**, the first FGF2 gene containing the *NdeI*, *SacI* and *SpeI* restriction sites was subcloned into a vector. Subsequently, the second FGF2 gene was inserted behind the 3' end of the first FGF2 gene through the *SacI*/*SpeI* sites.

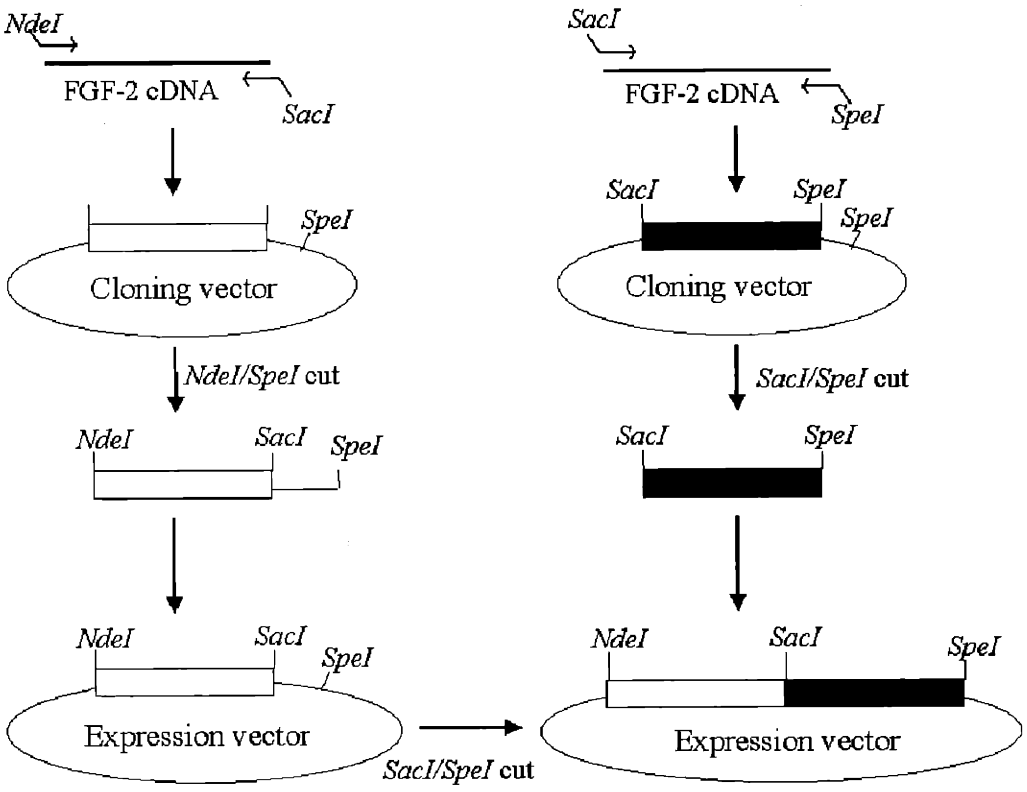

Figure 3.7: Schematic representation of the sequential "cut-and-paste" strategy. PCR was employed to introduce restriction sites (*NdeI, SacI* and *SpeI*) to the appropriate termini of the FGF2 gene. The PCR products were subcloned into a cloning vector that contained a *SpeI* site within the multiple cloning site. The first FGF2 gene (represented by the open rectangle) was excised with a double digest of *NdeI*/*SpeI* and the gene

fragment containing the *SacI* site was subcloned into an expression vector. The expression vector containing the first FGF2 gene was linearized by digesting with *SacI/SpeI*. Finally, the second FGF2 gene (represented by the filled rectangle) was subcloned to the vector through *SacI/SpeI* restriction sites.

The expression vector that was supposed to contain both FGF2 genes linked in tandem was subject to restriction digest analysis. As shown in **Figure 3.8**, a *NdeI/SpeI* digest yielded a ~1 kb product whereas both *NdeI/SacI* and *SacI/SpeI* digests yielded products of ~500 bp, suggesting that the two FGF2 constructs were positioned as anticipated. DNA sequencing with primers specific to the 5' end and the middle of the expression vector confirmed the identity of the final construct.

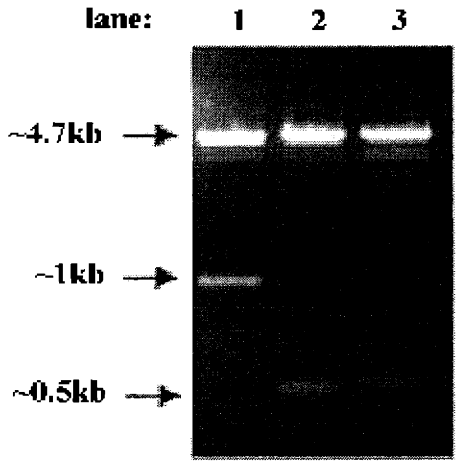

Figure 3.8: Restriction digest of the vector containing the dFGF2 construct. Lane 1, *NdeI/SpeI* digest of the expression vector; lane 2, *NdeI/SacI* digest and lane 3, *SacI/SpeI* digest. The approximate sizes of the bands were indicated on the left. DNA sequencing with primers specific to the 5' end and the middle of the expression vector further confirmed the identity of the final construct.

3.6 Protein purification

The dFGF2 fusion protein was recombinantly expressed in *E. coli* following the same procedures used for expressing cysteine mutant. To purify dFGF2, a combination of nickel-chelate and T7-affinity chromatographies was applied. Two species of M_r ~ 20kDa and ~40kDa were observed on SDS-PAGE after nickel-chelate chromatography (**Figure 3.9**). The protein was subject to further purification with an antibody-based T7 column (Novagen) for selecting the T7 epitope tagged at the C terminus of the protein. Flow-through and four fractions of eluted protein were collected for analysis on non-reducing SDS-PAGE. Fraction 2 was found to contain most of the ~40kDa species. Since the purification scheme selected for species that carried both the 6x His and T7 tags at the opposite termini, the ~40kDa species in fraction 2 was most likely the full-length dFGF2 fusion protein. Treating the ~40kDa species with a reducing agent (DTT) did not reduce the size, indicating that the dimer was not a product of disulfide crosslinking. The purified protein was stored in 100 µl aliquots in the presence of 1 mM DTT at –80°C.

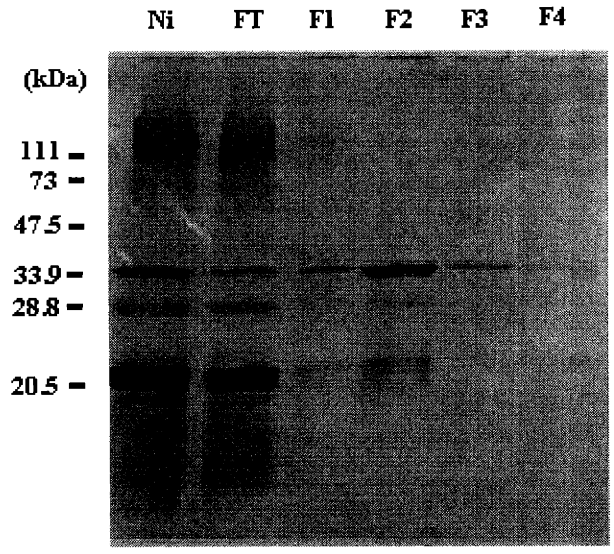

Figure 3.9: Purification of dFGF2 using Ni- and T7-chromatographies. SDS-PAGE analysis of different protein fractions collected from the Ni- and T7- columns. Molecular marker in kDa is shown on the side. Ni: purified after Ni-chromatography; FT: flow-through (FT) from the T7-column; F1 to F4: fractions eluted from the T7-column.

Heparin affinity chromatography was employed for protein purification purpose as well as for analytical purpose. Wildtype FGF2 protein binds heparin at a high affinity, requiring 1.2 M NaCl for eluting the protein from heparin column. Because each dFGF2 contains two FGF2 proteins, it was predicted that dFGF2 would exhibit an increased affinity towards heparin compared with its monomeric counterpart. To test the hypothesis, cell lysate was loaded to a heparin column and washed with a gradient of salt. It was found that the monomeric protein was eluted at ~1.2 M NaCl while the dimeric protein was eluted at ~1.8 M NaCl. These species were collected and desalted extensively for SDS-PAGE analysis (**Figure 3.10**). Not only did the heparin affinity chromatography data suggested that dFGF2 was properly folded, it also indicated that dFGF2 had a higher affinity for HSGAGs than did FGF2, perhaps through a cooperative binding interaction between the two linked FGF units and the heparin column (Section 3.8). If this is the case, then dFGF2 might have a reduced dependence on exogenous HSGAGs for activity.

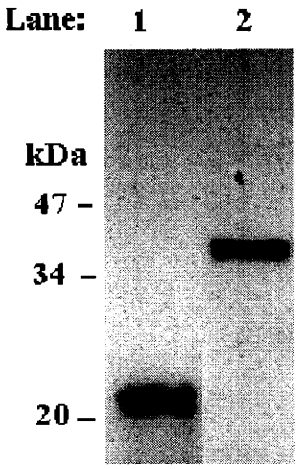

Figure 3.10: Heparin affinity chromatography. Two fractions collected from the heparin column were analyzed by SDS-PAGE. A monomeric species (lane 1) eluted with ~ 1.2 M NaCl and a dimeric species (lane 2) eluted with ~ 1.8 M NaCl were shown.

3.7 Biochemical properties

Immuno-blot study

Biochemical studies were performed to ensure that dFGF2 was properly folded prior to functional assays. The biological functions of FGF2 were mediated by proper folding of the structure into 12 anti-parallel β-strands (Murzin, *et al.*, 1992; Zhang, *et al.*, 1991; Zhu, *et al.*, 1991). To determine the folding status of the dimeric FGF2, an immuno-blot analysis employing monoclonal antibody that specifically recognized the properly folded form of wildtype FGF2 was performed. Protein samples collected from the nickel and T7 columns as well as wildtype FGF2 were applied onto a nitrocellulose membrane. As shown in **Figure 3.11**, all the samples were recognized by the antibody, with the highest intensity observed in the fraction 2. When the same amount of fraction 2 was heat-denatured in the presence of 1% SDS, the intensity was drastically reduced to background level. Therefore, the dFGF2 fusion protein was properly folded with respects to the epitope that was recognized by the monoclonal antibody.

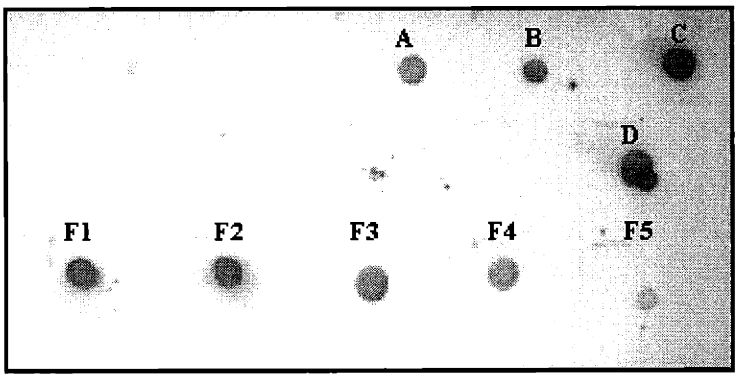

Figure 3.11: Folding properties of the dFGF2. Immuno-blot assay on the fractions collected from the T7-column by monoclonal antibody that recognized the properly-folded structure of FGF2. Three different amounts of wildtype FGF2 was spotted on the membrane: (A) 0.1μg, (B) 0.5 μg and (C) 1.0 μg. 3 μl of flow-through from T-7 column was spotted (D). 3 μl each of fraction 1 to 5 from T7-column was spotted (F1 to F5).

Circular dichroic study

To assess the overall secondary structure, the banding positions of near UV circular dichroic (CD) spectroscopy of dFGF2 was analyzed. The CD spectrum showed a negative minima near 210 nm (**Figure 3.12**), which is characteristic of the native FGF2 (Arakawa, *et al.*, 1989; Davis, *et al.*, 1999; Fox, *et al.*, 1988).

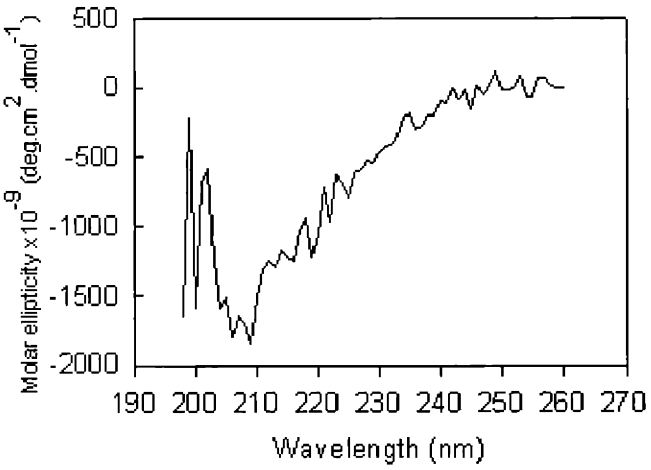

Figure 3.12: Structural properties of dFGF2. The near UV CD spectrum of dFGF2 is shown. dFGF2 was concentrated to 1 μM and buffer-exchanged into 10 mM sodium phosphate, pH 7.2. Data were recorded in an average of 20 scans between 195 nm and 260 nm. Of note is the characteristic intense negative CD signals observed near 210 nm that is indicative of properly folded FGF2.

Mass spectrometry study

Mass spectrometry was used to determine whether dFGF2 could compete with wildtype FGF2 for binding to FGFR2. Matrix assisted laser desorption ionization-mass spectrometry (MALDI-MS) analysis of dFGF2 yielded a species consistent with the expected mass for dFGF2 of 37,066 Da. As a next step, the nature of wildtype FGF2-FGFR interactions both in the presence as well as in the absence of HSGAGs was investigated. These studies indicated that, in the absence of HSGAGs, wildtype FGF2 bound FGFR with a stoichiometry of 1:1 (**Figure 3.13, A**), consistent with FGF-FGFR crystal structures (Plotnikov, *et al.*, 1999; Plotnikov, *et al.*, 2000). However, addition of a

HSGAG decasaccharide (consisting of a trisulfated disaccharide repeat unit which is known to bind with high affinity to FGF2 and support FGF2-mediated signaling), resulted in the formation of a detectable 2:2:1 FGF:FGFR:HSGAG complex (**Figure 3.13, B**). Addition of dFGF2 to this complex resulted in the formation of a new 1:2 complex of dFGF2:FGFR (inset in **Figure 3.13, B**). Notably, no dFGF2:FGFR species with decasaccharide bound was detected. The absence of this species could be either because the complex does not form in solution or that it is not ionized and detected under the conditions of this experiment. In addition, since the ionization efficacies of the various species undoubtedly differ from one another, with the larger species (especially those containing the decasaccharide) being less amenable to ionization than the smaller species, quantitative estimates of the amount of complex formed in this case is not warranted. However, detection of a 1:2 dFGF2:FGFR complex indicated that this species did form at protein levels that approximate those present at the cell surface.

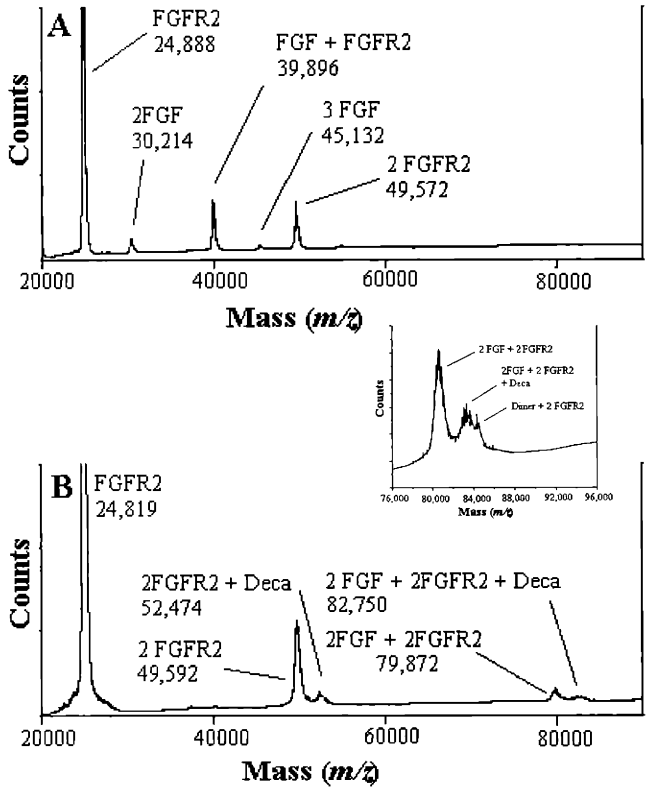

Figure 3.13: Competitive binding of dFGF2 for FGFR2. A: MALDI-MS profile of a mixture of wildtype FGF2 and the ectodomain of FGFR2. Observed in the mass spectrum are $(M+H)^+$ ion for an FGF2 dimer (*m/z* 30,214) and trimer (*m/z* 45,132),

FGFR2 monomer (*m/z* 24,888) and dimer (*m/z* 49,572), and an a 1:1 FGF2-FGFR2 complex (*m/z* 39,896). The theoretical molecular masses for FGF2 and FGFR2 are 15,114 and 24,864, respectively. B: Mass spectrum of the FGF2/FGFR2 mixture in the presence of a homogenous HSGAG decasaccharide. Addition of a decasaccharide (Deca) to FGF2/FGFR2 promotes the formation of a 2:2 FGF2:FGFR2 complex with an observed $(M+H)^+$ ion at *m/z* 82,750 (with Deca) or *m/z* 79,872 (without Deca). The $(M+H)^+$ ion for two dimeric FGFR2 species are also observed, the first at *m/z* 49,592 represents the apo complex and the second, at *m/z* 52,474 is a 2:1 FGFR2:Deca complex. *Inset*: mass spectrum of dFGF2 added to the mixture of Deca/FGF2/FGFR2 shown above. Three high molecular weight complexes are observed: 2:2 FGF2:FGFR2 complexes with or without Deca and a 1:2 dFGF2:FGFR2 complex without Deca.

3.8 Conclusion

Ligand dimerization is believed to be important in activating receptor dimerization, which in turn triggers a cascade of intracellular signaling events. Although previous biochemical evidence demonstrated that FGF2 dimerized in solution, it was unclear whether ligand dimerization is a physiologically relevant phenomenon. To address the question of whether ligand dimerization is important in cell signaling, it is desired to isolate a pure FGF2 dimer for assaying its biochemical, biophysical and biological properties. As detailed in Chapter 2, FGF2 proteins were found to interact with one another through specific interfaces on the protein surface and HSGAG binding is believed to stabilize such protein-protein interaction. Initially, it was attempted to isolate oxidatively crosslinked FGF2 dimer. Because of the inherent limitation in protein separation techniques, it was decided to construct a genetically defined fusion protein of FGF2 dimer. This novel FGF2 dimer was subject to a series of biochemical and biophysical assays for assessing its properties. Together with the results from Chapter 2, it is concluded that:

(1) one molecule of dFGF2 having protein contacts is able to support receptor dimerization;

(2) one of the roles of HSGAGs in FGF binding to FGFR is to support FGF and/or FGFR oligomerization; and

(3) biochemically one mode of FGF oligomerization and receptor binding involves a dimer with substantial protein-protein contact.

It is important to note that a much higher ionic strength is needed to dissociate dFGF2 from binding to heparin (1.8 M NaCl for dFGF2 as opposed to 1.2 M NaCl for wildtype FGF2), as demonstrated by heparin affinity chromatography in section 3.6. This increased heparin affinity can be rationalized using a cooperative binding model as schematically illustrated in **Figure 3.14**. In this model, binding of any one of the two FGF2 proteins to a HSGAG chain would help bring the other unbound FGF2 protein closer to an adjacent site on the HSGAG chain. In another word, it is more favorable for two FGF proteins to bind to an adjacent site on a HSGAG chain. As a result of this "forced" configuration of ligand, it is speculated that receptor dimerization would take place more readily and at a lower ligand concentration compared with the monomeric ligand. Hence, dFGF2 is expected to activate FGF2 signaling more efficiently than the monomeric wildtype. To test the hypothesis of elevated dFGF2 potency, *in vitro* and *in vivo* functional assays are employed as detailed in Chapter 4.

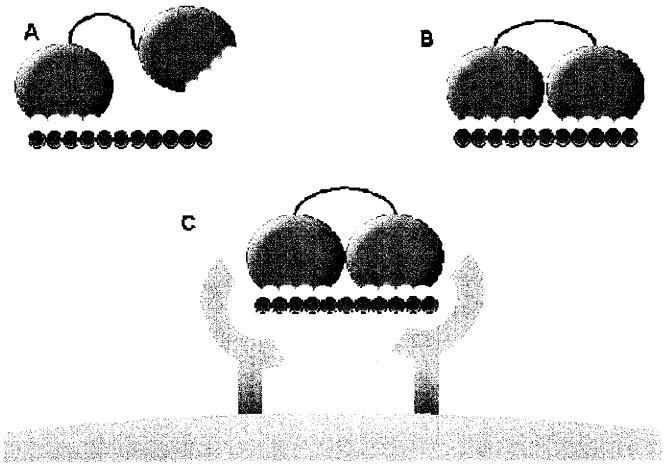

Figure 3.14: Proposed cooperative binding model of HSGAG-mediated dFGF2 signaling. Two FGF2 molecules are fused together by a tripeptide linker. HSGAG is represented by a string of beads. Binding of the first FGF2 molecule to a site on HSGAG

(A) helps bring the second molecule into close proximity to an adjacent site (B), leading to dimerization of FGF2 molecules. The dFGF2-HSGAG complex then diffuse to the cell surface where receptor binding occurs followed by the formation of a 2:2:1 FGF-FGFR-HSGAG ternary complex (C). The presence of the linker "forces" the two FGF2 molecules to interact with each other more readily and facilitates ligand dimerization as well as receptor dimerization.

A number of macromolecules, including HSGAG fragments and protein, have been shown to regulate FGF2 binding and/or activity. It is logical to assert that macromolecules that either promote or inhibit dimerization would be of biological significance. For naturally found HSGAG fragments, the minimal length required to promote FGF2 activity is found to be 8 monosaccharide units, which is about the translational distance between two *cis*-oriented FGF2 molecules (Venkataraman, *et al.*, 1996). Shorter fragments are able to bind FGF2 but fail to induce mitogenic activity (Faham, *et al.*, 1996), suggesting that a minimum of two FGF2 molecules is needed for activity. Sucrose octasulfate, a disaccharide drug used in ulcer treatment, also binds FGF1 and FGF2 without promoting biological activity (Zhu, *et al.*, 1993). It is of interest to note that shorter synthetic HSGAG fragments also promoted FGF2 activity (Ornitz, *et al.*, 1995), presumably by intercalating between two FGF2 molecules at the interface (Sasisekharan, *et al.*, 1997). Beside glycosaminoglycans, platelet factor 4, an anti-angiogenic protein used clinically in treating cancer, was found to inhibit FGF2 activity by complexing with the growth factor and presumably blocking ligand dimerization (Perollet, *et al.*, 1998). Given the potent angiogenic activity of FGF2, further understanding on how such macromolecules promote or inhibit dimerization may lead to the development of therapeutics for controlling vasculature growth.

Chapter 4:

Functional Characterization of Dimeric Fibroblast Growth Factor

Summary

The FGF dimerization model predicts that a dimer of FGF2 proteins with substantial protein interaction is the minimal functional unit to induce receptor dimerization. Although HSGAG-induced FGF2 dimerization has been observed in solution through biochemical and biophysical means, it was unclear whether the process has any biological significance in living systems. To test the hypothesis of FGF dimerization, a dimeric fusion growth factor dFGF2, which was designed to contain two wildtype FGF2 proteins linked in tandem, was constructed by molecular cloning as described in Chapter 3. This recombinant protein was an ideal candidate to investigate the biological significance of FGF2 dimerization in vitro *as well as* in vivo. *Using a combination of cell proliferation assay, survival assay and angiogenesis animal model, we performed side-by-side comparisons of the biological activities exhibited by wildtype FGF2 and dFGF2. The results not only indicated that dFGF2 was more active than wildtype FGF2, but also demonstrated that dFGF2 was less dependent on HSGAGs for signaling. Therefore, the results are consistent with the FGF2 dimerization hypothesis. The current study also suggests that genetically dimerized growth factors may be useful for clinical applications.*

4.1 Introduction

FGF2 is currently in clinical trials for its therapeutic effects in treating ischemic vascular diseases and healing wounds (Ferrara and Alitalo, 1999; Freedman and Isner, 2001; Mazue, *et al.*, 1991). The potent biological activity of FGF2 is mediated by cell surface HSGAGs on recipient cells, which serve as a low affinity receptor, modulating binding of the growth factor to its high affinity receptor on the cell surface. As discussed in Chapter 2, one of the functions of HSGAGs is proposed to serve as a template for orientating two FGF2 proteins in a "side-by-side" fashion for presentation to cell surface receptors, facilitating receptor clustering and dimerization. Numerous studies provided structural, biochemical and biophysical evidence that heparin induced FGF2 dimerization and oligomerization in solution under non-physiological conditions. However, critics argued that FGF2 dimerization, which was observed under extreme conditions, may have little or no biological significance in living systems under physiological conditions (Pye and Gallagher, 1999).

To directly test the biological significance of FGF2 dimerization in living systems, we developed a molecular cloning scheme for engineering a novel dimeric FGF2 fusion protein to be used *in vitro* and *in vivo* studies. As described in Chapter 3, this dimeric fusion protein dFGF2 contained two FGF2 proteins linked C to N by a tripeptide. Biochemical studies confirmed that dFGF2 exhibited proper protein folding and elevated heparin affinity. Mass spectrometry study also indicated that the dimeric fusion protein interacted with FGFR in a 1:2 stoichiometry. With these experimental findings, we continued to explore the functional attributes of FGF2 dimerization. Using *in vivo* and *in vitro* assays, we compared biological activities exhibited by the monomeric wildtype FGF2 and the dimeric dFGF2. The two growth factors were subject to a series of functional characterizations including smooth muscle cell (SMC) proliferation assay (Section 4.2), human umbilical vein endothelial cell (HUVEC) survival assay (Section 4.3) and rat corneal pocket assay (Section 4.4). These assays allow quantitative comparison between the two growth factors, and therefore provide important insights into the molecular mechanism of FGF2 signaling. Implication and significance of the results from these studies are provided in Section 4.6.

By rationally designing FGF2 dimer, we demonstrated the feasibility in engineering growth factors with desired characteristics (such as elevated potency and lowered heparin dependency) for therapeutic protein applications (McCafferty and Glover, 2000). Our approach provides a framework towards engineering dimerized growth factors at the genetic level.

4.2 Cell proliferation assay

FGF2 is a potent mitogenic and survival factor on many cell types including fibroblasts, smooth muscle cells and endothelial cells. To study the effects of HSGAG-dependent FGF2 signaling, bovine aortic smooth muscle cells, pretreated with or without chlorate, were incubated with various concentrations of the growth factors. Chlorate, which competitively inhibits the formation of a cofactor required in sulfation, disrupts the biosynthesis of cell surface HSGAGs by drastically lowering its O-sulfation level (Safaiyan, *et al.*, 1999).

In untreated cells (with intact cell surface HSGAGs), both wildtype FGF2 and dFGF2 were capable of stimulating cell proliferation (**Figure 4.1, A**). Importantly, the molar concentrations required to achieve half maximal proliferation by wildtype FGF2 and dFGF2 were found to be 270 pM and 60 pM, respectively. Hence, dFGF2 exhibited 4.5 fold more activity as compared to wildtype in promoting cell proliferation under these *in vitro* conditions. Hence, the data suggested that dFGF2 was more potent then wildtype monomeric FGF2 in stimulating SMC proliferation in the presence of intact cell surface HSGAGs. Alternatively, the elevated potency exhibited by dFGF2 may be explained by a high stability or a lower turnover rate of the protein.

In chlorate-treated cells (with diminished cell surface HSGAGs), wildtype FGF2 protein only elicited a moderate response in cell proliferation (**Figure 4.1, B**), consistent with previous finding that chlorate exposure was associated with low or lack of mitogenic activity (Rapraeger, *et al.*, 1991). On the other hand, dFGF2 was able to achieve about 80% full proliferation even though the cells were depleted in cell surface HSGAGs. This result suggested that dFGF2 was less dependent on HSGAGs for biological activity

compared with wildtype FGF2. The apparent diminished HSGAG dependency exhibited by dFGF2 can be rationalized if one considers that HSGAGs serve to stabilize the dimeric state of FGF2 for receptor dimerization. Since dFGF2 was already in a dimeric state, it would be less dependent on the level of HSGAGs expressed on the cell surface for signaling.

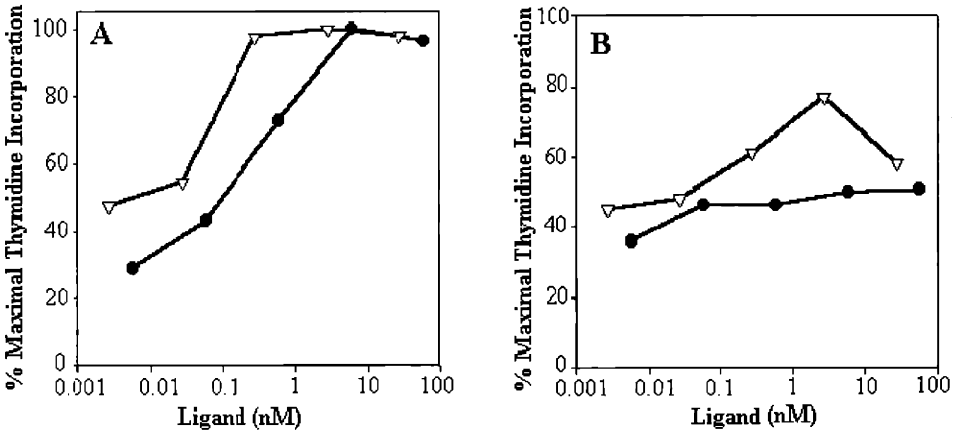

Figure 4.1: Smooth muscle cell proliferation assay. Serum-starved SMCs were stimulated with the indicated molar concentrations of wildtype FGF2 (●) and dFGF2 (▽). SMCs were grown (A) in the absence of chlorate or (B) upon addition of 75 mM chlorate. After 21 hours at 37°C, [^{3}H] thymidine was added for an additional 3 hours. Cells were harvested, washed and [^{3}H] thymidine incorporation was counted. Maximal count/minute for wildtype FGF2 and dFGF2 were about the same. Unprocessed data for this set of experiments are provided in Appendix 3. Note that the proliferation curve of dFGF2 is shifted towards the left of wildtype FGF2. Molar concentrations of growth factors were calculated based on the theoretical molecular weights of the wild-type FGF2 (18702) and dimeric FGF2 (37066). The molar concentrations for half-maximal proliferation by wildtype FGF2 and dFGF2 are 270 pM and 60 pM, respectively.

4.3 Cell survival assay

To confirm the *in vitro* biological activities of dFGF2, we performed cell survival assays using early passage HUVEC isolated from human umbilical cords. Using the colorimetric MTS dye that reflects the mitochondrial integrity of viable cells (Tepper, *et*

al., 1995), the HUVEC survival assay provides a sensitive way to measure endothelial cell viability mediated by the growth factors added exogenously. FGF2 is known to act as a survival factor by suppressing apoptosis triggered by growth factor deprivation (Araki, *et al.*, 1990; Karsan, *et al.*, 1997) and radiation (Haimovitz-Friedman, *et al.*, 1994). In serum-deprived HUVEC, cell viability was about 50% of that grown in 10% serum (**Figure 4.2**). Addition of various concentrations of wildtype FGF2 and dFGF2 partially recovered cell viability in a dose-dependent manner. Consistent with the results from the SMC proliferation assay, dFGF2 was more active than wildtype FGF2 in stimulating survival in HUVEC on a molar basis, with maximal activity achieved at 5.2 nM for wildtype FGF2 and 2.7 nM for dFGF2. It must be emphasized that the molar concentration of FGF2 binding sites in dFGF2 and that in the monomeric form are roughly equivalent such that the biological activity per binding site can be interpreted as similar in this assay. Together, the biological activity of dFGF2 from the two independent cell types demonstrated that dFGF2 was biologically active under physiological conditions in cell culture.

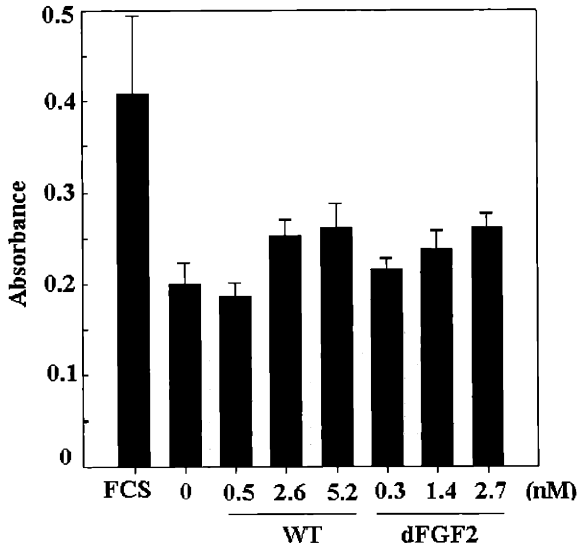

Figure 4.2: HUVEC survival assay. HUVECs were serum-starved overnight and were stimulated with the indicated concentrations of wildtype FGF2 and dFGF2, or without any growth factor. Cells supplemented with 10% FCS served as a positive control. After 18 hours, cell viability was determined colorimetrically using the MTS reagent. Note that both wildtype FGF2 and dFGF2 restored HUVEC viability following serum starvation and that dFGF2 achieved the same levels of cell viability at a lower molar concentration than wildtype FGF2. Unprocessed data for this experiment are provided in Appendix 3. Error bars indicate the standard deviation of a single experiment. Representative data from 3 independent experiments are shown here.

4.4 *in vivo* angiogensis assay

The ability of dFGF2 to induce new blood vessel formation was investigated using a rat corneal angiogenesis model. The concept and biological significance of angiogenesis are briefly summarized below. Further information on different topics of angiogenesis can be found in other reviews (Campochiaro, 2000; Carmeliet, 2000; Carmeliet and Jain, 2000; Ferrara and Alitalo, 1999; Folkman, 2001; Hanahan and Folkman, 1996).

The pathophysiological significance of angiogenesis

Angiogenesis is an important biological process in which new blood vessel is formed from the existing vasculature (**Figure 4.3**). One of the most potent pro-angiogenic factors is FGF2, which is well known for its ability to stimulate endothelial cell proliferation and migration, capillary tube formation, and endothelial cell invasion into the ECM (Desai and Libutti, 1999). In addition to cancer, uncontrolled angiogenesis also contributes to the pathogenesis of a number of hypoxia-driven diseases such as diabetic retinopathy as well as inflammation-induced diseases such as gastric ulcer (Carmeliet and Jain, 2000). Normal physiological processes such as mammary gland development, wound healing and embryogenesis also depend on angiogenesis.

Under most circumstances, angiogenesis in adult tissues is tightly regulated and the turnover rate of endothelial cells, the key constituent of a blood vessel, is exceedingly low (Folkman, 1995b). However, under certain physiological as well as pathological conditions, angiogenesis is activated as a result of excessive endothelial cell proliferation and migration. In the case of solid tumor development, it was first hypothesized by Folkman in 1971 that establishing new capillary sprouts from the pre-existing vasculature was critical for the survival and proliferation of a tumor mass (Folkman, 1971). Tumor angiogenesis involves a series of distinct subcellular events including hyperpermeability of the basement membrane, extravasation of plasma proteins, endothelial cell proliferation and migration. In the absence of angiogenesis, solid tumors would not be supplied with oxygen and nutrients from the blood vessels, and subsequently the tumor

mass would hardly exceed 2-3 mm in size (Folkman, 1995b). A considerable amount of excitement has been generated from the studies that demonstrated the possibility of blocking tumor growth by administrating angiogenesis inhibitors (Bergers, *et al.*, 1999; Boehm, *et al.*, 1997; Cao, *et al.*, 1998; O'Reilly, *et al.*, 1995; O'Reilly, *et al.*, 1996; O'Reilly, *et al.*, 1997). The molecular mechanism by which angiogenesis is regulated is under intense investigation.

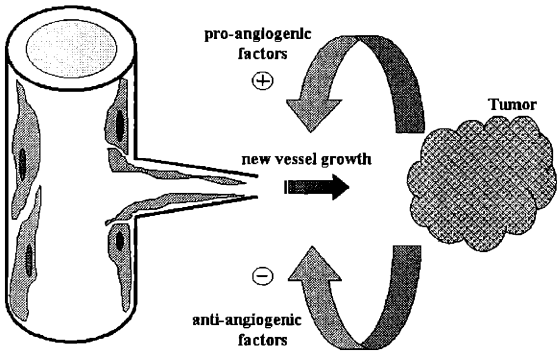

Figure 4.3: Schematic drawing of tumor angiogenesis. Sprouting of new blood vessel from the existing vasculature proximal to a tumor mass is depicted. Soluble pro-angiogenic (+) and anti-angiogenic (-) factors are secreted from the tumor to regulate endothelial cell proliferation and migration. Oxygen and nutrients carried in blood vessels are fed to the tumor through the newly established vascular network.

Assays for angiogenesis

Interests in identifying pro-angiogenic and anti-angiogenic factors have propelled the development of more sensitive and reliable angiogenesis assays for screening purpose (Auerbach, *et al.*, 1991). Among the most common models are chick chorioallantoic membrane (CAM) assay and intrastromal cornea pocket assay. The CAM assay involves grafting an angiogenic factor onto the chorioallantoic membrane of a chick embryo and monitoring vascularization with the aid of a dissecting microscope. The drawbacks of this assay are associated with the quantification method (subjective scoring of the extent of neovascularization on a graded scale) and the false positives (the irritation and wound induced by the procedure itself). The intrastromal cornea pocket model is by far the most

reliable angiogenesis assay. Unlike the CAM where existing blood vessels are actively growing, the cornea is essentially an avascular environment under normal conditions. In addition, the transparent nature of cornea makes monitoring of vessel growth a lot easier than the CAM assay. Therefore, the cornea model represents a non-traumatic method of assaying *in vivo* angiogenesis with minimal tissue damage. More importantly, it allows the monitoring of vessel growth over an extended period of time. The assay involves implanting an angiogenic stimulus in a pellet form to a micro pocket created surgically about 2 mm away from the limbal vascular network of the cornea (see A1.4.3 in the Appendix). Vascular sprouting can be detected from 36 hours to 1 week after the implantation. The extent of angiogenesis is measured in terms of the maximal vessel length (the linear distance of the sprouting vessels measured from the limbal vascular plexus) and the circumferential neovascularization (the degree of the circumference covered by the newly-formed vessels). The assay has been established in several animal species including rabbit, mouse, rat and guinea pig.

in vivo *angiogenic activity by wildtype FGF2 and dFGF2*

To extend the *in vitro* observation, the *in vivo* angiogenic activity of wildtype FGF2 and dFGF2 were compared, side-by-side, using the rat corneal pocket assay (**Figure 4.4**). In the absence of the hydrolysis inhibitor sucralfate, FGF2 is released rapidly from the pellet whereas sucralfate incorporation allows sustained release over a 6-day period (Kenyon, *et al.*, 1996). Control pellets containing no FGF2 (*i.e.* no angiogenic stimulus) failed to induce appreciable angiogenesis, suggesting that the pellet itself and the implantation procedure *per se* did not induce new blood vessel growth (**Figure 4.4, A**). Wildtype FGF2 induced an angiogenic response in a dose-dependent manner with little angiogensis induced at a protein level of 1.5 pmole (**Figure 4.4, B**) and more extensive angiogenesis induced at 6 pmole (**Figure 4.4, C**). The extent of angiogenesis induced by wildtype FGF2 was accurately reflected both by the length of the induced vessels as well as the circumference of those vessels (**Table 4.1**). Compared to wildtype FGF2, dFGF2 induced more extensive angiogenesis in the corneas of rats at a lower concentration of 0.7 pmole (**Figure 4.4, D**). With dFGF2, induced blood vessels were

longer, of larger circumference, and more plentiful, as measured by the "clock hours" or the extent of angiogenesis around the limbus. In fact, 0.7 pmole of dFGF2 was a better angiogenic stimulus than was FGF2 at an 8-fold higher level, *viz.*, 6 pmole. Thus, the biological potency of dFGF2, as measured in *in vitro* cell culture experiments (Section 4.2 and 4.3), was retained in an *in vivo* animal model, suggesting that the dFGF2 construct was a potent biological mediator.

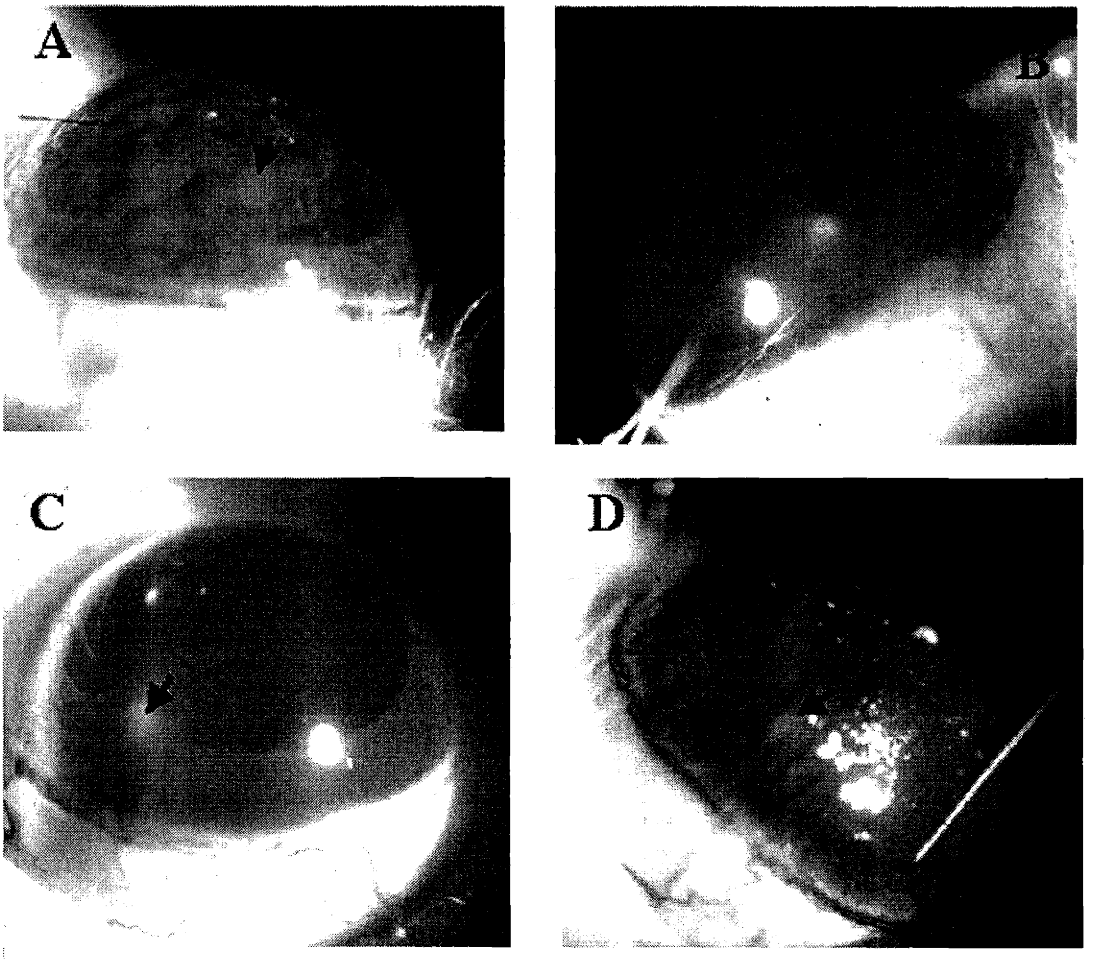

Figure 4.4: ***In vivo*** **potency of dFGF2.** Slit lamp photographs of rat corneas on day 6 after implantation with Hydron pellets containing (A) no FGF2 as control, (B) 1.5 pmole FGF2, (C) 6.0 pmole FGF2, or (D) 0.7 pmole dFGF2. The area of pellet implantation is designated with an arrow. The control pellet did not induce a significant angiogenic response, while pellets containing dFGF2 induced an intense neovascular response

originating from the limbal vessels and reaching the pellet on day 6 after the implantation. Pellets containing FGF2 (B, C) induced a less vigorous, but still detectable, angiogenic response on day 6 after implantation (see Table 4.1 below).

Treatment	FGF2 1.5 pmole	FGF2 6.0 pmole	dFGF2 0.7 pmole
Linear length (mm)	0.24 ± 0.05*	1.56 ± 0.04	1.84 ± 0.05
Clock hours	0.38 ± 0.07	1.50 ± 0.07	2.06 ± 0.16

Table 4.1: Comparison between wildtype FGF2 and dFGF2 in promoting angiogenesis in rat cornea. The extent of corneal angiogenic response was expressed as linear length, which is the linear distance of the sprouting vessels measured from the limbal vascular plexus, and circumferential clock hours, which is the degree of the circumference covered by the newly-formed vessels. * indicates Standard Error.

4.6 Conclusion

To test our hypothesis of an active FGF2 dimer involving protein-protein contact and to distinguish it from the FGF2 dimer observed in the FGF-FGFR co-crystal structures that lack protein-protein contact, we constructed a tandemly-linked dFGF2 molecule using conformational studies and genetic engineering tools. The dimeric fusion protein dFGF2 was designed such that the short distance between the two FGF2 molecules within the dimeric protein would allow for substantial FGF-FGF interactions while making non-contacting dimer mode less favorable and therefore enable us to dissect whether a contacting FGF2 dimer can elicit biological activity. We show through mass spectrometry that dFGF2 interacts with FGFR in a ratio of 1:2, suggesting that dFGF2 is capable of binding to a dimer of FGFR. Furthermore, these results indicate that one mode, involving substantial protein contact, by which FGF2 and its receptor can interact is through the binding of FGFR to a FGF2 dimer. These biochemical findings are further supported by the biological activity of the dFGF2 molecule.

To test whether a contacting FGF2 dimer can elicit biological activity, dFGF2 was subject to two independent *in vitro* assays. From both the SMC proliferation and HUVEC survival assays, dFGF2 exhibited elevated biological activities compared with

wildtype FGF2. This effect is especially pronounced in the SMC proliferation assay where dFGF2 is several fold more active than wildtype and only 20% less active in the absence of HSGAGs as in their presence (as opposed to wildtype FGF2 wherein activity is markedly reduced in the absence of cell surface HSGAGs). These findings suggest that dFGF2, in which FGF-FGF interactions are predicted to be substantial, forms an active signaling complex with the receptor. In addition, proliferation of chlorate-treated SMCs demonstrated that dFGF2 was less HSGAG-dependent for signaling. This observation can be rationalized if one considers that one primary mechanism by which HSGAGs modulate FGF2 activity is by stabilizing two FGF2 molecules in a dimeric mode to facilitate receptor dimerization. Because dFGF2 is already dimeric, its dependency on HSGAGs for proper presentation to the receptor is lower compared to wildtype FGF2 (**Figure 4.5**). An alternative explanation to the elevated potency exhibited by dFGF2 is that the turnover rate of dFGF2 may be lower than that of wildtype FGF2. We have also extended these studies to show that the dFGF2 construct is a potent pro-angiogenic agent *in vivo*, much more so than is wildtype FGF2, thus providing compelling evidence that the dFGF2 construct, involving substantial protein-protein contact, forms an active signaling complex at the cell surface. It appears that dFGF2 exhibits a much higher activity in the *in vivo* cornea pocket model than in other *in vitro* assays compared to wildtype FGF2. This may be explained by the lack of HSGAGs in cornea. Because dFGF2 has a lower dependence on HSGAGs for activity than wildtype FGF2, it may exhibit a higher activity in a HSGAG-free environment.

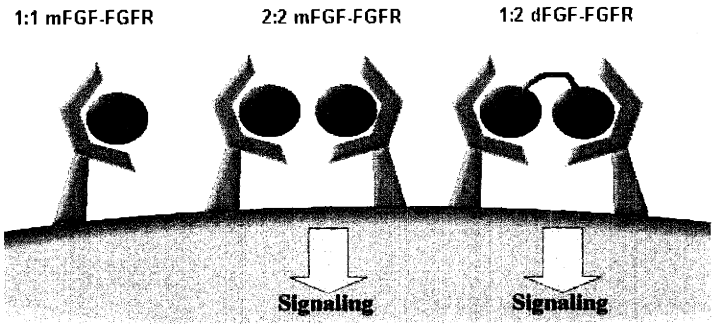

Figure 4.5: Schematic representation of FGF2 signaling mediated by wildtype FGF2 and dFGF2. (from left to right) A wildtype FGF2 binds to FGFR to form a 1:1 complex.

Clustering of two 1:1 FGF-FGFR complex leads to the formation of a 2:2 FGF-FGFR complex and receptor dimerization. As a result, an intracellular signaling cascade is activated. dFGF2, which is made up of two monomeric FGF2s fused by a linker, binds to two FGFRs and initiate receptor dimerization followed by intracellular signaling.

Thus the biochemical, cell culture, and *in vivo* assays are consistent with the proposal that a contacting FGF2 dimer is involved in the active signaling complex. These findings appear to be inconsistent with the different FGF2-FGFR crystal structures, which show no FGF-FGF interactions. Such an inconsistency may reflect the inherent complexity and the multifaceted nature of the FGF system. One possible explanation is that the different structural configurations of FGF-FGFR may reflect the different states, *viz.*, "on" or "off" states, of the signaling complex. A similar observation has been made in other systems (Ballinger and Wells, 1998; Jiang and Hunter, 1999). For instance, in the case of erythropoietin, it has been noted that certain mimetic peptides can dimerize the receptor but fail to induce signaling (Livnah, *et al.*, 1998) due to the formation of an inactive complex at the cell surface. Furthermore, the ultimate biological endpoint of erythropoietin signaling, *i.e.*, whether erythropoietin signaling results in proliferation or differentiation, is sensitive to how the receptors are brought together (Ballinger and Wells, 1998). Another system where the mode of dimerization plays a critical role in determining the biological activity is the tumor necrosis factor (TNF) binding to TNF receptor-1. Unliganded TNF receptor-1 exists as an inactive dimer with its catalytic domains over 100 Å apart (Naismith, *et al.*, 1995). Binding of TNF to its receptor brings the catalytic domains of the receptors proximate to one another, initiating intracellular signaling cascades (Naismith, *et al.*, 1996). Thus, similar to these cases, it is conceivable that a mode of FGF2 dimerization involving protein-protein interactions could lead to a cooperative FGF2-FGFR interaction by promoting subsequent receptor dimerization and signaling whereas the non-contacting FGF2 dimerization may lead to an inactive complex.

In addition, it must be noted that other studies have suggested that the monomeric forms of FGF2 may form an active signaling complexe (Pantoliano, *et al.*, 1994; Pye and Gallagher, 1999). For instance in a recent study, it was found that a covalently linked complexe of monomer FGF with a pool of heparin dodecasaccharides was able to

promote cell proliferation *in vitro* (Pye and Gallagher, 1999). However, as observed in that study, the covalent FGF-HSGAG complex was less active than uncomplexed FGF in promoting [^{3}H] thymidine incorporation. In contrast, the dFGF2 construct presented in this study is several times *more* potent in biological assays than is wildtype FGF, with reduced dependence on exogenous HSGAGs for activity. Nevertheless, it is possible that monomer complexes of FGF do signal, albeit with less apparent activity than do oligomeric forms of FGF2.

In summary, it is concluded that FGF2 does have a preference to oligomerize, and the studies contained herein point to the fact that this oligomerization interface involves protein-protein contact. In addition, a dFGF2 construct based on these biochemical findings has potent biological activity, consistent with the hypothesis that FGF dimers are potent mediators of FGFR dimerization and concomitant signaling.

PART III: CELL SURFACE HEPARAN SULFATE GLYCOSAMINOGLYCANS

Chapter 5:

Modulation of FGF activity by cell surface heparan sulfate glycosaminoglycans

Summary

Cell surface heparan sulfate glycosaminoglycans (HSGAGs) are believed to play an important role in regulating a variety of biological functions through interactions with specific mediators. In this Chapter, the effect of cell surface HSGAGs derived from smooth muscle cells (SMCs) on FGF signaling was investigated. HSGAGs interact specifically with both FGF and FGFR, forming a multimeric signaling complex at the cell surface. To characterize how SMC-derived HSGAGs affect FGF signaling, a panel of heparinases was employed as a tool to depolymerize HSGAGs and their abilities to modulate FGF activity on engineered cell lines expressing defined FGFR isoforms were assayed. The results indicated that FGF2-mediated proliferation was dependent on the composition of the SMC-derived HSGAG fragments as well as the type of FGFR isoforms expressed. The data presented here support the hypothesis that the chemical sequence of HSGAGs dictates the specificity of interactions between FGF2 and a given FGFR. By altering the HSGAG sequences expressed on the cell surface, cells may be able to fine-tune their responses to growth factors released from the extracellular matrix (ECM) upon vascular damage. This study may add to our knowledge of developing carbohydrate-based drug in treating vascular diseases such as atherosclerosis.

5.1. Introduction

Cell surface HSGAGs have long been considered an inert scaffold of little biological significance. With the advent of new tools to study HSGAGs in the past decade, the functional significance of HSGAGs in regulating cell behavior has received broader attention. Landmark studies in the early 1990s indicated that depletion of HSGAGs by chlorate or heparinase treatments abrogates cell's responsiveness to growth factors like FGFs. Moreover, several recent studies lend credence to the idea that specific HSGAG sequences expressed on the cell surface may function either as a promoter or an inhibitor of a given biological response (Guimond and Turnbull, 1999; Liu, *et al.*, 2002b). The ability of HSGAGs to regulate a plethora of biological functions stems from the polymers' structural heterogeneity. Various structural modifications create unique sequences within the HSGAG chain; diversity among sequences allows HSGAGs to interact with a number of growth factors, cytokines, and morphogens (Perrimon and Bernfield, 2000; Tumova, *et al.*, 2000). As such, specific HSGAG structures have been implicated as important modulators in a number of biological processes, including anticoagulation, angiogenesis, embryonic development, and tumor growth (Hahnenberger, *et al.*, 1993; Jin, *et al.*, 1997; Lin, *et al.*, 1999).

Smooth muscle cell (SMC) proliferation plays an important role in the pathophysiology of many disease conditions such as atherosclerosis and restenosis. Among the stimulatory molecules that act on SMCs is FGF2, a potent mitogen that is normally stored extracellularly and is released to the endothelium upon injury (Klagsbrun and Edelman, 1989; Ross, 1993). HSGAGs, found ubiquitously on the cell surface and in the ECM, are believed to inhibit the migration and proliferation of SMCs (Castellot, *et al.*, 1985; Fritze, *et al.*, 1985). As discussed in Chapter 1, HSGAGs are known to interact with both FGF (Faham, *et al.*, 1996; Ornitz, *et al.*, 1995) and FGFR (Kan, *et al.*, 1993). Such specific interaction is important in eliciting a diverse array of biological functions. In addition to the inherent selectivity of each member of the FGFR family for various FGFs (Ornitz, *et al.*, 1996), it appears that receptor specificity is also dictated by the sequence of HSGAGs present at the cell surface. Several recent crystal structures of FGF-FGFR complexes have indicated a 2:2 assemblage of ligand to receptor (Plotnikov,

et al., 1999; Plotnikov, *et al.*, 2000; Stauber, *et al.*, 2000). It is hypothesized that FGF activity is dependent on specific HSGAG sequences that regulate FGF-FGFR interactions, through dimerization or oligomerization of FGF (Sasisekharan, *et al.*, 1997).

Our laboratory and others have examined the role of HSGAGs in modulating FGF2 activity in SMC proliferation. Porcine mucosal heparin, a highly sulfated form of HSGAGs, was found to inhibit SMC proliferation (Guyton, *et al.*, 1980; Majack and Clowes, 1984). Similarly, the HSGAG component of conditioned medium from aortic endothelial cells was found to inhibit FGF2-mediated SMC proliferation (Forsten, *et al.*, 1997; Han, *et al.*, 1997). This inhibitory effect can be abrogated by treating the conditioned medium with hepI and/or III (Han, *et al.*, 1997; Nugent, *et al.*, 1993). Earlier our laboratory generated SMC-derived HSGAG fragments enzymatically and examined their effects on FGF2-mediated SMC proliferation (Natke, *et al.*, 2000). The heparinases are a series of bacterial enzymes that depolymerize HSGAGs with defined substrate specificities (Section 1.4.5). Whereas hepI cleaves the highly sulfated domains (or heparin-like regions) of HSGAGs leaving intact undersulfated regions, hepIII digests the undersulfated domains, (or heparan sulfate-like regions), instead leaving intact the highly sulfated regions. HepII, with the broadest substrate specificity of the enzymes, cleaves both highly sulfated and undersulfated regions of HSGAGs. Although it is suggested that FGF2-HSGAG interactions, at the cell surface, are important for SMC proliferation, whether HSGAGs elicited the modulatory effect through specific FGFR isoforms remains unclear. To dissect the effect of distinct HSGAG fragments on FGF's ability to signal through different FGFR isoforms, a panel of BaF3 cell lines transfected with FGFR1c, FGFR2b, FGFR2c or FGFR3c was employed. BaF3 cells have been extensively used in the past to investigate such interactions (Ornitz, *et al.*, 1992; Ornitz, *et al.*, 1995; Ornitz, *et al.*, 1996). Because BaF3 cells do not express any endogenous FGFR and generally lack cell surface HSGAGs, proliferation is dependent on the transfected FGFR isoform expressed at the cell surface, the exogenously added FGF2, and the HSGAG fragments added to the cell culture medium (Ornitz, *et al.*, 1992; Wang, *et al.*, 1994). As such, the system is unfettered from complications associated with other cell types, allowing us to dissect individual interactions important for FGF-mediated signaling that involves the formation of a ternary FGF-FGFR-HSGAG complex at the cell surface.

In this Chapter, the key observation that FGF2-mediated cell proliferation is differentially modulated by distinct SMC-derived HSGAG fragments depending on the expression of FGFR isoform is presented. A model of FGF-HSGAG-FGFR interaction proposed here provides a framework for understanding the structure-function relationship of HSGAG sequences in modulating biological functions mediated by HSGAG-binding growth factors.

5.2 Method of approach

The methodology employed in this Chapter is schematically represented in **Figure 5.1**. To investigate the effect of cell surface HSGAGs on modulating FGF-mediated cell proliferation, HSGAGs were isolated from the donor cells (SMCs) and then applied to the recipient cells (BaF3) that lack endogenous HSGAG expression. HepI, II and III were used to release HSGAGs from the cell surface of SMCs. Conditioned medium from hep-treated SMCs was subject to compositional analysis and activity assays. The recipient cells were transfected with distinct FGFR isoforms and their FGFR expression profile was studied. The approach used in this study would enable us to systematically evaluate the modulatory effect mediated by different HSGAG fragments on cell proliferation in different FGFR backgrounds.

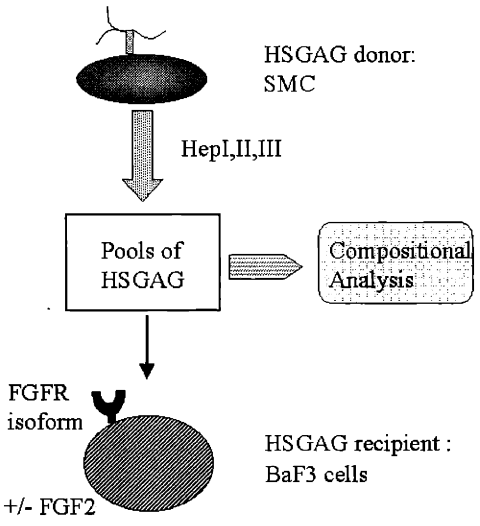

Figure 5.1: Schematic representation of methodology. Cell surface HSGAGs were released from the donor cells (SMCs) using heparinase treatment. The pools of HSGAG fragments, generated from the digestion with hepI, II and III, were subject to compositional analysis for comparing their structural differences. In addition, the pools of HSGAG fragments were added to individual recipient cells (BaF3 cells) that were transfected with distinct FGFRs. The effect of various HSGAG fragments on modulating FGF-dependent and FGF-independent proliferation was examined.

5.3 Expression profile of FGF receptor isoforms

Proliferation assays were performed using four separate BaF3 cell lines, each expressing a distinct FGFR isoform (Ornitz, *et al.*, 1996). To determine the types of FGFR isoforms expressed, BaF3 cells transfected with FGFR1c, FGFR2b, FGFR2c, and FGFR3c were assayed by RT-PCR to determine their FGFR "profile." FGF2 signaling is mediated through various isoforms of FGFR, whose expression and distribution are developmentally regulated (Givol and Yayon, 1992). Hence, the BaF3 cell lines provide a unique opportunity to dissect FGF2 signaling through distinct FGFR isoforms. As a first step in this investigation, we confirmed that the four cell lines used in this study expressed defined FGFR isoforms. Since the protein expression level of these receptors has previously been shown to be comparable (Ornitz, *et al.*, 1996), differences in proliferative response can be attributed to the type of FGFR expressed and not the expression level. In SMCs and ECs, FGFR1c was determined to be the predominant form of FGFR (**Figure 5.2**).

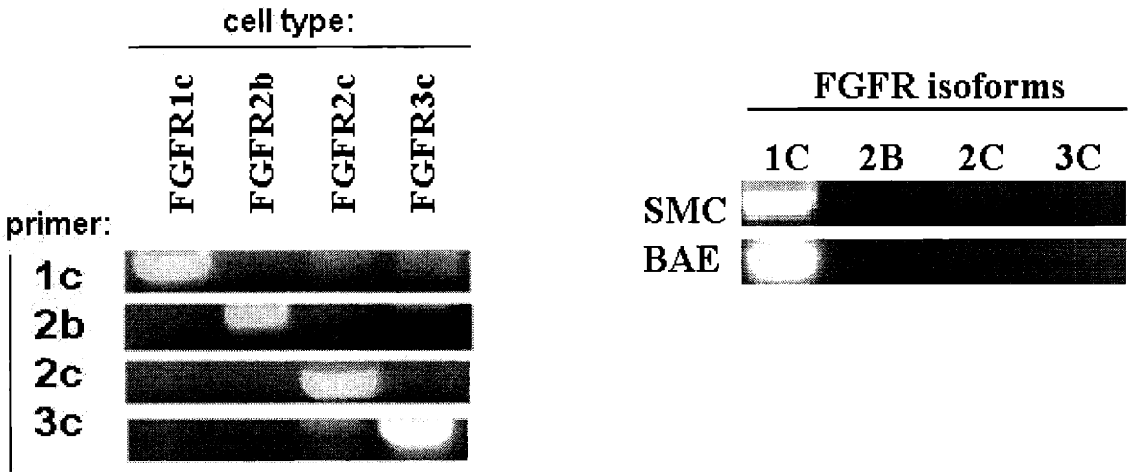

Figure 5.2: Expression profiles of FGFR in smooth muscle cells, endothelial cells and the BaF3 cell lines. RT-PCR was performed using primers specific to various FGFR isoforms to confirm the expression pattern of receptors from the BaF3 cell lines, SMCs and bovine aortic endothelial cells (BAE).

5.4 Modulation of FGF activity by heparin

To characterize functionally these four cells lines, each was cultured in the presence or absence of FGF2 with heparin. It is well known that heparin binds with high affinity to FGF2 and is able to potentiate FGF2-mediated signaling with certain FGFR isoforms. As shown in **Figure 5.3**, FGF2 with heparin elicited a significant proliferative response in cells expressing FGFR1c, FGFR2c and FGFR3c, but not FGFR2b, consistent with previous findings (Ornitz, *et al.*, 1996).

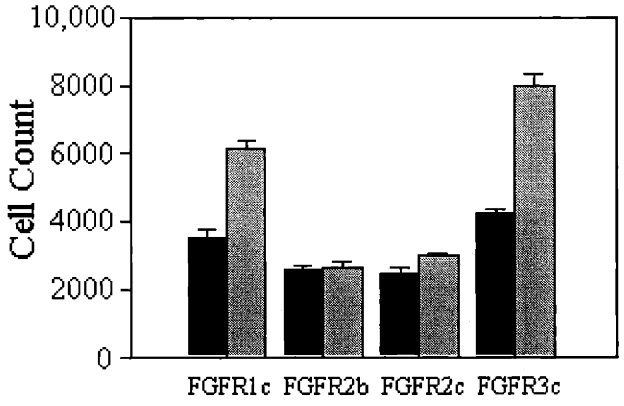

Figure 5.3: Functional characterization of the BaF3 cell lines used in this study. Cell lines were incubated for 72 hours in DMEM media in the presence of 500 ng/ml heparin either without (dark) or with (gray) 50 ng/mL FGF2. Whole cell count is used as a measure of proliferation. Error bars indicate standard deviation of this set of experiments.

5.5 Chemical properties of cell surface HSGAGs

Approximately 100 ng of cell surface HSGAGs were isolated from SMCs by incubating the cells with either hepI, II or III. As a negative control, the cells were also incubated in PBS without any enzyme. The isolated fragments were subject to compositional analysis (Duteil, *et al.*, 1999; Park, *et al.*, 1999; Rhomberg, *et al.*, 1998; Venkataraman, *et al.*, 1999c) and cell proliferation assays (Section 4.5).

Disaccharide	PEN*	m/z	hepI	hepII	hepIII
ΔU_{2S}-$H_{NS,6S}$	D	577.5	5	4	16
ΔU_{2S}-H_{NS}	9	497.4	22	24	30
ΔU-$H_{NS,6S}$	5	497.4	6	8	8
ΔU_{2S}-$H_{NAc,6S}$	C	539.5	0	0	0
ΔU-H_{NS}	1	417.4	31	18	20
ΔU_{2S}-H_{NAc}	8	459.4	0	0	0
ΔU-$H_{NAc,6S}$	4	459.4	8	12	7
ΔU-H_{NAc}	0	379.4	28	24	19

Table 5.1: Compositional analysis of HSGAGs derived from SMCs. All numbers are reported as a percentage of total disaccharide. Each disaccharide consists of an unsaturated uronic acid (ΔU) with or without 2-O sulfation (2S), and a glucosamine (H) with or without N-sulfation (NS), N-acetylation (NAc) or 6-O sulfation (6S). * stands for property encoded nomenclature (Venkataraman, *et al.*, 1999c).

As expected from the known substrate specificities of the heparinases (Ernst, *et al.*, 1995; Godavarti and Sasisekharan, 1996), the HSGAG fragments derived from hepI digestion were less highly sulfated than those fragments resulting from hepII or III treatment (**Table 5.1**). The hepIII fragments were the most highly sulfated, and accordingly, the content of 6-O sulfated disaccharide units was found to be highest in the hepIII-treated HSGAG fragments, particularly with regard to ΔU_{2S}-$H_{NS,6S}$. Conversely, the hepI fragments were relatively deficient in 6-O sulfation and 2-O sulfation. Notably, all three heparinase treated samples generated approximately the same amount of HSGAG fragments, *viz.*, ~50 ng/ml. These same fragments, isolated from the SMC cell surface, were used in the proliferation assays to determine their ability to promote or inhibit FGF2 binding to the four FGFR isoforms used in this study. Importantly, very little HSGAG fragments could be isolated from the PBS-treated cells, demonstrating that it is a good negative control for this set of experiments. In every case, the response of the engineered BaF3 cell lines was the same whether the supernatant from the PBS-treated cells was used or whether the BaF3 cells were treated with DMEM medium, free of exogenous HSGAGs.

5.6 FGF activity modulated by cell surface HSGAGs

Heparinase generated HSGAG fragments are biologically active

The proliferative response of the cell surface HSGAG fragments prepared by different heparinase treatment was tested by culturing transfected BaF3 cells with or without FGF2. For the ease of comparison, all values are expressed as a fraction of the PI where a PI of 1 indicates maximal response and a PI of 0 indicates negligible response, using a formula derived in a previous paper (Padera, *et al.*, 1999). The reference point (PI=1) for this set of experiments was BaF3 cells stimulated with 50 ng/ml FGF2 and 500 ng/ml heparin. This point was chosen based on our previous study and is based on a rigorous determination of the dose-response relationship for FGF2/heparin on BaF3 cells expressing each FGFR isoform. Importantly, establishing this reference point provides a mechanism by which the cell data can be standardized such that comparisons between HSGAG preparations and across receptor isoforms can be accomplished.

Upon addition of FGF2, and either heparin or the SMC-derived HSGAG fragments, a pronounced increase in the PI was observed in all cells except FGFR2b expressing cells, consistent with literature reports and the results outlined in **Figure 5.3.**

HepIII generated HSGAG fragments effectively promote FGF2 signaling through FGFR1c

In the absence of FGF2, none of the added heparinase-treated HSGAG fragments significantly altered cell proliferation of the BaF3 cells transfected with FGFR1c (**Figure 5.4, A,** dark bars). In the presence of FGF2, the HSGAG fragments derived from either hepIII or hepII treatment elicited a significantly higher PI than the PBS control. The potency of these fragments rivaled that of heparin itself. Conversely, the hepI fragments were unable to significantly promote FGF2 activity in FGFR1c-expressing BaF3 cells beyond the response obtained by PBS alone, where significant stimulation was observed upon addition of FGF2.

In FGFR1c-transfected cells, the observation that hepIII treatment produces the highest PI and the finding that the hepIII-treated HSGAG fragments contain the most 6-O sulfated disaccharide units (particularly ΔU_{2S}-$H_{NS,6S}$ or D) are in agreement with the suggestion of Pye *et al* that 6-O sulfated oligosaccharides generated by heparinase treatment promote FGF2 activity (Pye, *et al.*, 1998). In contrast, the hepI fragments, which are relatively deficient in 6-O sulfation, produce the lowest PI. Several studies have indicated that 6-O desulfated oligosaccharides reduce the mitogenic activity mediated by FGF2 (Guimond, *et al.*, 1993; Ishihara, *et al.*, 1995; Krufka, *et al.*, 1996; Lundin, *et al.*, 2000).

SMC-derived HSGAG fragments are inefficient for FGF2 signaling through FGFR2c

BaF3 cells expressing FGFR2c gave a significant response to FGF2 stimulation, regardless of whether exogenous HSGAG fragments were present (**Figure 5.4, B**). The PI of PBS treated cells was not significantly different from those of cells treated with SMC fragments derived from either hepII or III treatment. Thus, in this case, it appears that the HSGAG fragments from SMCs do not potentiate FGF2 signaling through FGFR2c, and by comparison with the heparin results in **Figure 5.3**, exogenous HSGAGs at best only slightly promote FGF2 signaling through FGFR2c. In the presence of hepI-treated HSGAG fragments, FGF2-mediated proliferation is decreased, such that there is no significant difference in the PI for FGFR2c–transfected cells in the presence and the absence of FGF2. In FGFR2c-transfected cells, the effect of hepII and III in modulating FGF2 activity is insignificant when compared with the PBS control. It is possible that SMCs may not express the "correct" HSGAG sequences for facilitating FGF2 signaling through FGFR2c. Interestingly, in the presence of hepI-derived HSGAG fragments, FGF2 signaling is slightly suppressed, such that there is no significant difference in the PI for FGFR2c-transfected cells in the presence and the absence of FGF2. Thus, it may be the case that the hepI-derived fragments actually inhibit FGF2 binding to its receptor.

HepI generated HSGAG fragments effectively mediate FGF2 signaling through FGFR3C

With BaF3 cells expressing FGFR3c, it appears that HSGAG fragments are required for significant FGF2 signaling (**Figure 5.4, C**) as was observed in the FGFR1c-expressing cell line (**Figure 5.4, A**). In direct contrast to FGFR1c-transfected cells, however, the hepI or II-treated HSGAG fragments elicited a significantly higher PI than the PBS control in the FGFR3c engineered cell line while the hepIII-derived fragments failed to elicit a significant response in this cell line. Also in contrast to FGFR1c and FGFR2c transfected cells, no significant response is seen in FGFR3c cells upon the addition of FGF2 unless exogenous HSGAGs are present, that is the PI for the PBS-treated sample in this case is 0.02 ± 0.17 as compared to the PIs' of 0.78 ± 0.12 and 0.67 ± 0.20 for FGFR1c and FGFR2c transfected cells, respectively (**Figure 5.4, D**).

Importantly, as a control for the above studies and to investigate whether our results are extendable to other members of the FGF family, we completed experiments with the BaF3 cell lines, but used FGF1 as the ligand instead of FGF2. Previously it has been shown that FGF1 signals equally through each FGFR isoform used in this study (Ornitz, *et al.*, 1996), including FGFR2b (to which FGF2 does not appreciably bind). Notably, with FGFR1c, 2c, and 3c the results obtained with FGF1 are consistent with the observed effect of the SMC fragments on FGF2-mediated proliferation (data not shown). This is even true when one considers the effect of fragments on FGF-mediated signaling through FGFR2c, where FGF1 is a better ligand than FGF2. Thus, in each case, the effect of the SMC-derived HSGAG fragments on FGF1-mediated signaling paralleled its effect on FGF2-mediated signaling. The one notable exception to this observation was with FGFR2b. Unlike FGF2, FGF1 induced significant proliferation of BaF3 cells expressing the FGFR2b isoform in the presence of either heparin or the hepIII-generated SMC fragments, consistent with its known receptor specificity (Ornitz, *et al.*, 1996) and ensuring the authenticity of our findings.

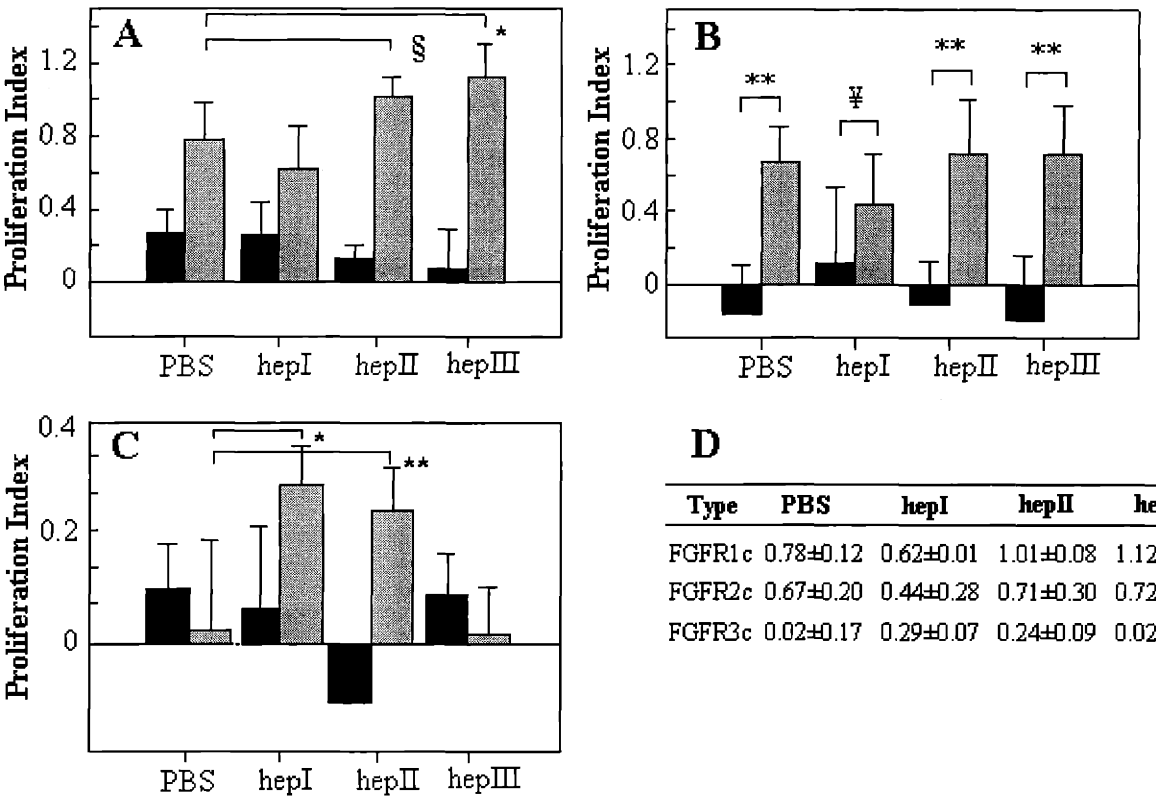

D

Type	PBS	hepI	hepII	hepIII
FGFR1c	0.78±0.12	0.62±0.01	1.01±0.08	1.12±0.21
FGFR2c	0.67±0.20	0.44±0.28	0.71±0.30	0.72±0.26
FGFR3c	0.02±0.17	0.29±0.07	0.24±0.09	0.02±0.08

Figure 5.4: FGF-mediated proliferation of BaF3 cells encoding various FGFR isoforms in the presence of SMC HSGAGs treated with either hepI, II or III. BaF3 cells expressing (A) FGFR1c, (B) FGFR2c, or (C) FGFR3c were grown with 50 ng/ml FGF2 (gray) or without (dark). The PI is calculated as described in the Appendix (section A1.5.8). The significance of the results are also presented; $p<0.01$ (*), $p<0.02$ (**), $p<0.05$ (§), $p>0.3$ (¥). (D) Summary of the PIs resulting from treatment of each cell type with FGF2 and the corresponding SMC HSGAG oligosaccharide preparation. Error bars indicate standard deviation of this set of experiments. Unprocessed data for these three sets of experiments are provided in Appendix 3.

5.7 Conclusion

Cell surface HSGAGs are believed to be important in modulating proliferation of a wide variety of cell types including SMCs. It is believed that SMC proliferation is maintained by a fine balance between growth stimulatory factors such as FGF2 and growth inhibitory factors such as HSGAGs (Ross, 1993). In the case of endothelial injury, FGF2 and other signaling molecules are released from the ECM, the basement membrane or intact cells, which subsequently lead to SMC proliferation and migration. Under quiescent conditions, SMC proliferation is tightly controlled in part by limiting the exposure of SMCs to FGF2. Binding of FGF2 to HSGAGs protects the growth factor from proteolytic degradation (Sommer and Rifkin, 1989). In addition, HSGAGs are involved in facilitating FGF2 binding and activation (Rapraeger, *et al.*, 1991; Yayon, *et al.*, 1991). Our laboratory and others have previously demonstrated that HSGAGs serve to induce dimerization and oligomerization of FGF2 (Davis, *et al.*, 1999; Ornitz, *et al.*, 1992; Spivak-Kroizman, *et al.*, 1994; Venkataraman, *et al.*, 1999b), presumably to facilitate receptor dimerization. In addition, HSGAGs are involved in the internalization of FGF2 for intracellular processing (Roghani and Moscatelli, 1992; Sperinde and Nugent, 1998) and in the control of FGF2 transport within the ECM (Dowd, *et al.*, 1999). Although FGF2-mediated SMC proliferation is well studied, the physiological role of SMC-derived HSGAGs on modulating signaling is unclear.

The current study extends the earlier work from our laboratory on SMC-derived HSGAGs by utilizing two well-established systems: the BaF3 cell lines which express distinct FGFR isoforms and the heparinases which cleave HSGAGs with known substrate specificity. The data presented here show that FGF2 signaling is differentially modulated by HSGAG fragments of distinct structural characteristics through different FGFR isoforms. In contrast to the results obtained with FGFR2c, it appears that with certain receptor isoforms, *viz.* FGFR1c and FGFR3c, that HSGAG fragments of proper length and sulfation pattern are important for signaling to occur. This conclusion is reinforced by the fact that hepI or II-treated HSGAG fragments significantly increase FGF2 signaling whereas hepIII abrogates it, indicating that sulfation number and position is of utmost importance. These results are in stark contrast to the response of BaF3 cells

expressing FGFR1c to FGF2, where hepIII treatment results in the production of SMC-derived HSGAG fragments that strongly potentiate FGF2 activity while the hepI-derived SMC fragments do not support proliferation. Notably, the hepII-treated HSGAG fragments supported a significant FGF2 response in both FGFR1c and FGFR3c expressing cells as compared to the PBS control as would be expected from its broad substrate specificity. Hence, a structure-function relationship between the different SMC-derived HSGAG fragments and FGF2-mediated proliferation through various FGFR isoforms is established in this study. The exact chemical sequences of the HSGAG fragments responsible for modulating FGF2 activity are being characterized by others in the laboratory.

Consistent with a previous study that employed porcine mucosal HSGAGs (Guimond and Turnbull, 1999), our results indicate that FGF2 signaling through a given FGFR is differentially modulated by chemically distinct HSGAG fragments. We extend this prevailing notion to SMC-derived HSGAGs, which is the physiologically relevant form found in most cell types. We find that its ability to modulate FGF2 signaling is highly dependent on the composition and length of the fragments as well as the FGFR isoform expressed by the recipient cells. The modulatory effect of the HSGAG fragments is not restricted only to FGF2 but is also true for FGF1 based on the following observations.

(1) HSGAG fragments that activate FGF2 also activate FGF1 signaling for all receptor isoforms;
(2) in BaF3 cells expressing FGFR2b, the hepIII fragments are more active than the hepI and II fragments in FGF1-stimulated proliferation and
(3) in FGFR2c-expressing cells, FGF1 is an more effective ligand in stimulating cell proliferation than FGF2.

Taken together, the differences in chemical contents of HSGAGs from the cell surface can lead to a potential mechanism for the fine control of FGF2-mediated biological processes. For instance, FGFR1 is predominantly expressed in proliferating adult rat SMCs whereas FGFR3 is the preferred type in newborn rat SMCs (van Neck, *et*

al., 1995). Thus, cells could take advantage of the inherent structural diversity of HSGAGs to regulate FGF signaling through a receptor or set of receptors by dynamically altering the HSGAG sequences on the cell surface (Brickman, *et al.*, 1998; Guimond and Turnbull, 1999). **Figure 5.5** shows a schematic representation to account for the differential effects on FGF2 signaling mediated by the HSGAG fragments generated by hepI and hepIII, respectively. In this model, a proper spatial display of 2 O-, 6 O- and N-sulfated groups on HSGAGs (as is the case in the "hepIII-HSGAG") would allow optimal interaction with both FGF2 and FGFR isoforms. On the other hand, the hepI-HSGAG fragment fails to interact with high affinity through the display of its sulfate groups, resulting in less efficient signal transduction. Further characterization of the "active" HSGAG fragments that provide the required specificity for FGF2 activity would not only enable important insight into identifying the structural requirement of the ternary complex, but also aid the development of therapeutics for targeting proliferative vascular disorders.

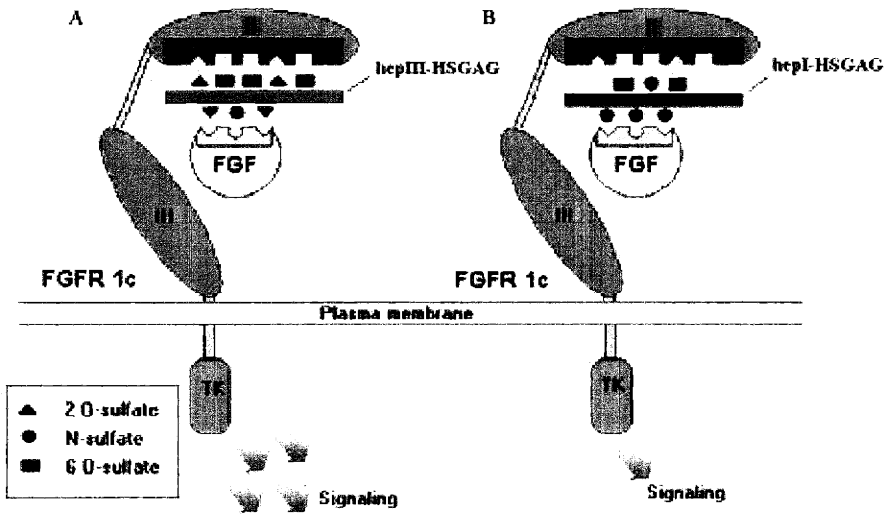

Figure 5.5: Model of differential modulating effects mediated by HSGAGs on FGF2 signaling. Interaction of HSGAGs with the HSGAG-binding domains of FGF (colored yellow) and FGFR (red) forms the basis of FGF2 signaling. Domains of the immunoglobulin-like loop II, III and tyrosine kinase (TK) of FGFR1c are shown. For simplicity, only one FGF and FGFR are shown although several recent crystal structures indicated that FGF-FGFR forms a 2:2 complex. The spatial display of 2 O-, 6 O- and N-

sulfated groups in the hepIII-generated HSGAG fragment (green) would allow an optimal "fit" to both FGF2 and FGFR1c, leading to signaling through tyrosine kinase (A). On the other hand, the hepI-generated HSGAG fragment (blue) displays another pattern of sulfated groups that interact less efficiently with FGF2 and FGFR1c for transmitting signals (B).

Chapter 6:

Heparinase III-induced apoptosis in melanoma cells

Summary

Cell surface HSGAGs are involved in regulating a wide variety of cellular processes including cell proliferation, survival and migration. Using heparinases as tools to release HSGAG fragments from the cell surface, our laboratory has presented in vivo *evidence that HSGAGs can serve as cryptic promoters as well as inhibitors of tumor growth and metastasis. In this Chapter, the effect of tumor cell-derived HSGAGs on modulating cell proliferation in the absence of exogenously-added growth factor is explored. Consistent with the previous studies from our laboratory, heparinase III (hepIII) was found to suppress cell proliferation in two different tumor cell lines. In addition, conditioned medium from hepIII-treated cells was capable of suppressing cell proliferation. A combination of biochemical and activity assays was performed to confirm the involvement of apoptosis in the observed growth suppression. Gene array experiments coupled with caspase activity assays indicated that hepIII treatment induced apoptosis through a caspase 8-dependent pathway. The findings presented here provide a framework towards dissecting the molecular mechanism of HSGAG-mediated cell signaling.*

6.1 Introduction

In recent years, dramatic progress has been made in demonstrating the critical roles of HSGAGs in orchestrating various facets of tumor progression and metastasis (Blackhall, *et al.*, 2001; Liu, *et al.*, 2002a; Sanderson, 2001). One of the earlier indications that HSGAGs may serve as an important regulator in tumorigenesis comes from the observation that modifications in HSGAG structures correlate with malignant transformation. Specific structural changes were observed in the HSGAGs extracted from tumor cells but not from their normal counterparts. For example, it was reported that cancerous liver tissues yielded lower amounts of sulfate and uronic acid than normal tissues (Nakamura and Kojima, 1981). Down-regulation of 6-O sulfation was associated with malignant transformation in a mouse mammary carcinoma cell line (Safaiyan, *et al.*, 1998). On the other hand, a higher content of 6-O-sulfation was observed in the HSGAGs extracted from the highly metastatic Lewis lung carcinoma (LLC) cells (Nakanishi, *et al.*, 1992). 6-O-sulfation was also found to be elevated in colon carcinoma cells as compared to adenoma cells (Jayson, *et al.*, 1998). In addition to the observed structural changes in HSGAGs, over-expression of the mammalian HSGAG-degrading enzyme, or heparanase, has been shown to correlate with the extent of malignant transformation (Hulett, *et al.*, 1999; Vlodavsky, *et al.*, 1999). Consistent with this proposal, antisense expression of the full-length heparanase gene suppressed tumor metastasis *in vivo* (Uno, *et al.*, 2001). More recently, our laboratory has demonstrated that tumor cell-derived HSGAGs could serve either as a promoter or an inhibitor of tumor progression and metastasis in a tumor transplantation model (Liu, *et al.*, 2002b). Together, these studies suggest that cell surface HSGAGs are capable of regulating various aspects of tumor biology. These findings also raise the intriguing question of how HSGAGs mediate critical changes in cell behavior. Liu *et al* demonstrated that one of the mechanisms by which cell surface HSGAGs modulate cell proliferation is by regulating FGF-mediated phosphorylation of protein tyrosine kinases such as FGFR1, Erk and focal adhesion kinase (Liu, *et al.*, 2002b). In addition, increased apoptosis was also evident from the tumors treated with specific HSGAG fragments. However, little is known about the effect of HSGAGs in the absence of exogenous growth factors.

The broader objective of this study is to develop an understanding of the structure-function relationship of a variety of HSGAG-mediated biological functions. To this end, we investigated the anti-proliferative effect of heparinase III (hepIII) treatment on cell proliferation with two primary goals: first, to optimize the experimental conditions used in the *in vitro* assays for investigating the effect of hepIII treatment on cell proliferation; second, to develop a pilot gene array study to identify candidate genes involved in hepIII-mediated growth suppression. The use of gene array for systematic profiling of transcriptional changes would expedite the identification of cell signaling pathways affected by the HSGAG fragments. The study described in this Chapter serves to provide a framework towards understanding the molecular mechanism of HSGAG-mediated cell signaling.

6.2 Apoptosis: an overview

An overview of several key concepts in apoptosis is presented here. General reviews on different aspects of the topic have been published (Evan and Vousden, 2001; Green and Reed, 1998; Hengartner, 2000; Smyth, *et al.*, 2002; Thornberry and Lazebnik, 1998; Yuan, 1997). Also known as programmed cell death, apoptosis is a tightly regulated, genetically controlled process by which cells are genetically programmed to die in response to environmental stress or developmental signals. Apoptosis is widely conserved in phylogeny, from nematode to human. Extensive genetic and biochemical studies performed in the past two decades have uncovered a repertoire of critical apoptotic components, including transcription factors, cell surface receptors, proteases and protease inhibitors. Concerted action of these components allows a multi-cellular organism to get rid of excessive or damaged cells during normal development and tissue homeostasis. On the other hand, aberrant action in any of the components of the apoptotic machinery often compromises the organism's ability to survive. Noticeably, abnormal apoptosis is associated with a number of pathological conditions in humans, including cancers, autoimmune diseases, viral infections and neurodegenerative disorders.

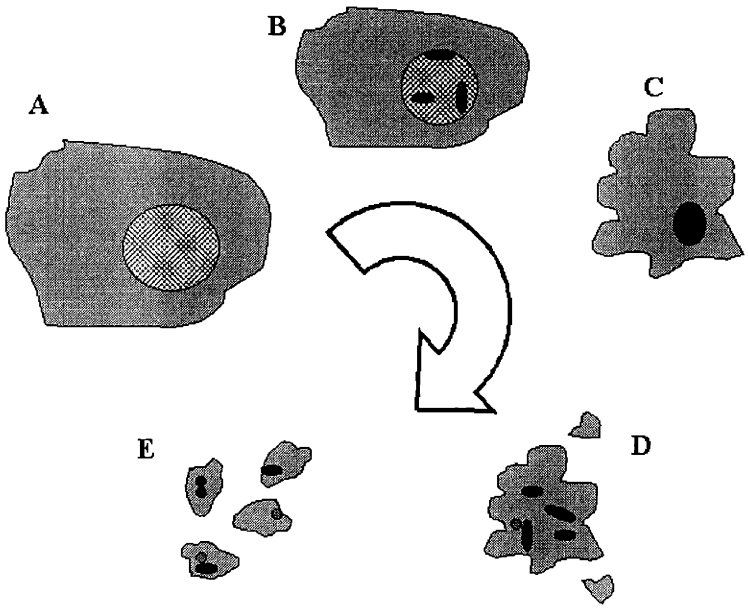

Figure 6.1: Morphological changes of a cell undergoing apoptosis. As a normal cell becomes committed to apoptosis (A), a sequence of ultrastructural morphological changes takes place. Early signs of apoptosis are characterized by chromatin segregation (B), chromatin condensation, membrane blebbing and cell shrinkage (C). Late phase of apoptosis is characterized by fragmentation of the nucleus and the cytoplasm (D). Finally, the cell is fragmented into several membrane-bound apoptotic bodies (E) that can be phagocytosed by nearby cells or immune cells.

Cells undergoing apoptosis exhibit a number of distinctive morphological features, including cell shrinkage, membrane blebbing and chromatin condensation, that are readily recognizable under a high-power light microscope (**Figure 6.1**). In addition to morphological markers, a variety of biochemical markers specific to defined stages of apoptosis have been identified. These include externalization of phosphatidylserine on the plasma membrane (Martin, *et al.*, 1995), fragmentation of nucleosomal DNA (Wyllie, *et al.*, 1984) and elevated mitochondrial permeability (Green and Reed, 1998). Most, if not all, of these morphological and biochemical changes are catalysized by a class of proteolytic enzyme known as **c**ysteine-directed **a**spartate **prot**e**ase**, or caspase (Thornberry and Lazebnik, 1998). This class of proteases is unique in its substrate

specificity wherein protein targets are cleaved exclusively after the aspartate residues. There are at least 12 human caspases described in the literature to date, with about 100 substrates identified (Earnshaw, *et al.*, 1999). These caspases act on specific cellular targets to elicit various apoptotic phenotypes. In the cells that are committed to apoptosis, cell shrinkage occurs in part due to the collapse of cytoskeleton network resulting from caspase-mediated cleavage of gelsolin (Kothakota, *et al.*, 1997). Activation of caspase leads to the cleavage of DNA fragmentation factor DFF (Liu, *et al.*, 1997) and nuclear inhibitor ICAD (Enari, *et al.*, 1998), which in turn trigger DNA fragmentation. Cleavage of the nuclear envelope protein lamin by caspase leads to chromatin condensation (Buendia, *et al.*, 1999). To assert the presence of apoptosis in cells, generally accepted criteria include the identification of a morphological change and the detection of at least one other biochemical marker (Smyth, *et al.*, 2002).

General mechanisms of apoptosis

There are two general mechanisms by which cells undergo apoptosis, namely mitochondria-mediated and death receptor-mediated mechanisms (**Figure 6.2**). In a normal cell, the anti-apoptotic protein Bcl-2 is localized on the outer membrane of the mitochondria and is bound to its adaptor protein Apaf-1. Once apoptosis is induced, the electron carrier cytochrome c exits the outer mitochondrial membrane to the cytoplasm and causes Apaf-1 to dissociate from Bcl-2. Free cytochrome c and Apaf-1 aggregate with caspase 9, forming a complex called apoptosome. Activated caspase 9 in turn initiates the cleavage of other downstream substrates, including the "executioner" caspase, or caspase 3. A second mechanism of apoptosis involves the death receptors, which include the tumor necrosis factor (TNF) family of cell surface receptors. In many immune-response cells, apoptosis is induced by the activation of death receptors through binding with ligands displayed on the cell surface of other cells (such as cytotoxic T cells). Death signal is transduced to the cytoplasm as a result of receptor clustering, followed by the formation of an intracellular complex involving adaptor proteins such as TNF-associated protein (TRAF). Activation of the adaptor proteins in turn induces

caspase 8 activity, which subsequently triggers caspase 3 activity for executing various apoptotic phenotypes.

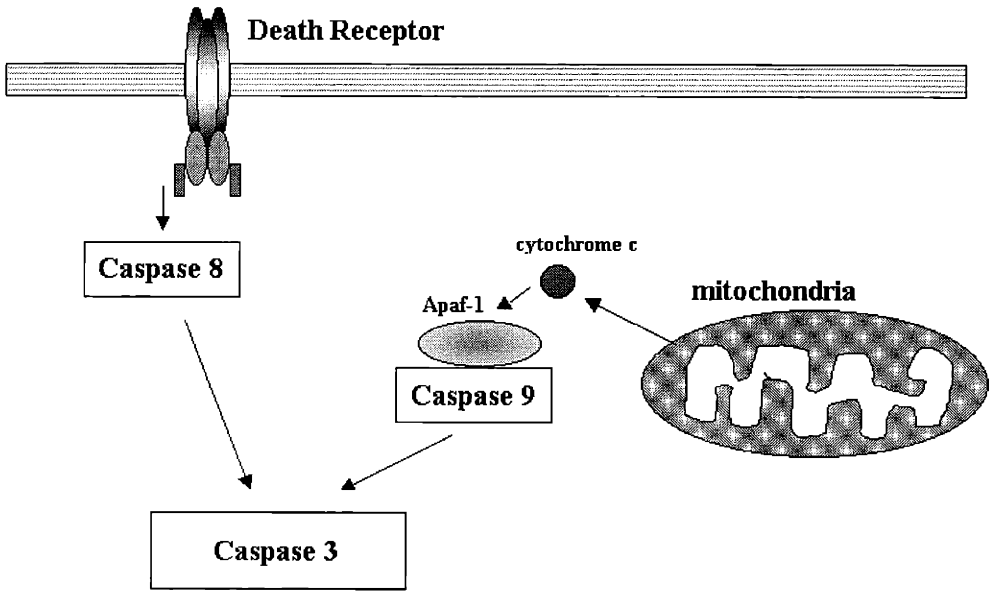

Figure 6.2: Two distinct mechanisms of apoptosis. Right: mitochondria-initiated pathway involving cytochrome c, Apaf-1 and caspase 9. Left: death receptor pathway involving caspase 8. Both caspase 8 and 9 are capable of activating caspase 3. Modified from Smyth *et al* (Smyth, *et al.*, 2002).

6.3 Method of approach

An overview of the methodology employed in this Chapter is outlined in **Figure 6.3**. HepIII was added to the medium of melanoma cells for a defined period of time. Cell proliferation was determined by whole cell counting and was expressed as a percentage of the maximal cell count achieved in a set of experiment. DNA extracted from hepIII-treated and control cells was used for detecting DNA fragmentation. To identify differentially expressed genes, RNA was isolated from the cells for cDNA microarray analysis. Enzymatic activity of caspase 3, 8 and 9 was detected from the whole cell lysate of the hepIII-treated and control cells. Details of the methodology are provided in the Appendix (A1.6).

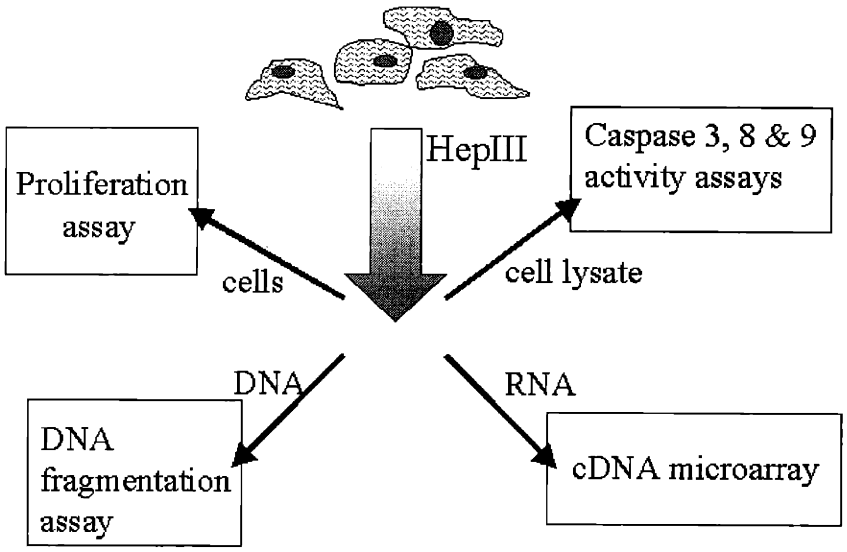

Figure 6.3: Schematic representation of methods used in the study. A combination of cell biology, molecular biology and biochemical assays was used in this study to investigate the effect of hepIII treatment on cell proliferation. The effect of hepIII treatment on cell proliferation was examined by whole cell counting. The effect of the conditioned medium derived from hepIII-treated cells was also studied. Cell lysate isolated from the treated and untreated cells was subject to caspase activity assays. The integrity of nucleic acid was determined by DNA fragmentation assay. The transcriptional profile of the treated and untreated cells was compared by analyzing their gene expressions using cDNA microarray.

6.4 The anti-proliferative effect of hepIII treatment on B16 melanoma cells

Three HSGAG-degrading lyases, hepI-III, have been cloned from the genome of *Flavobacterium heparinum* (Godavarti and Sasisekharan, 1996; Sasisekharan, *et al.*, 1993; Su, *et al.*, 1996). Their distinct substrate specificities (see section 1.3 in Chapter 1) make these enzymes important tools for investigating the biological functions of cell surface HSGAGs (Liu, *et al.*, 2002b; Natke, *et al.*, 1999; Sasisekharan, *et al.*, 1994). HepIII, which digests undersulfated domains of HSGAGs and releases highly sulfated fragments from the cell surface, was shown to inhibit endothelial cell proliferation *in vitro* and *in vivo* (Sasisekharan, *et al.*, 1994). Recently, hepIII treatment as well as hepIII-generated fragments were demonstrated to suppress tumor progression and

metastasis in a tumor transplantation model (Liu, *et al.*, 2002b). Unlike hepIII, hepI, which cleaves highly sulfated domains of HSGAGs and releases undersulfated fragments, was shown to either promote or exhibit no effect on cell proliferation. Hence, the two heparinases appear to have a divergent effect on cell proliferation, which may result from the distinct substrate specificities of the enzymes. In this section, the *in vitro* characteristics of hepIII treatment on melanoma cells are investigated through a series of cell culture experiments.

Time course study

To extend the previous studies on hepIII-mediated growth suppression (Liu, *et al.*, 2002b; Sasisekharan, *et al.*, 1994), we treated melanoma cells daily with the enzyme for 5 consecutive days by adding the enzyme to the culture medium (without changing the medium unless specified otherwise). HepIII was expressed as a 6xHis-tagged recombinant protein in *E. Coli* and the enzymatic activity was determined as described previously (Godavarti, *et al.*, 1996). The enzyme was extensively buffer-exchanged into PBS to remove any traces of chemicals used in the protein purification procedure. As a first step in this experiment, a much higher concentration of hepIII was used to the medium for determining if a growth inhibitory effect could be observed. Subsequently, the concentration tested was narrowed to a lower range. The determination of the optimal concentration used in this experiment is discussed in the next session. As shown in **Figure 6.4**, proliferation of the hepIII-treated cells increased markedly and peaked at day 3. After day 3, cell number decreased drastically and, on day 5, cell number dropped markedly to ~10% of the maximal cell count. As a control, untreated cells were grown over the same period of time in parallel and the cell count was found to be ~90% of the maximal cell count on day 5. Based on this experiment, it was determined that 3 daily doses of hepIII would minimally impact cell proliferation while longer treatment would result in excessive growth suppression.

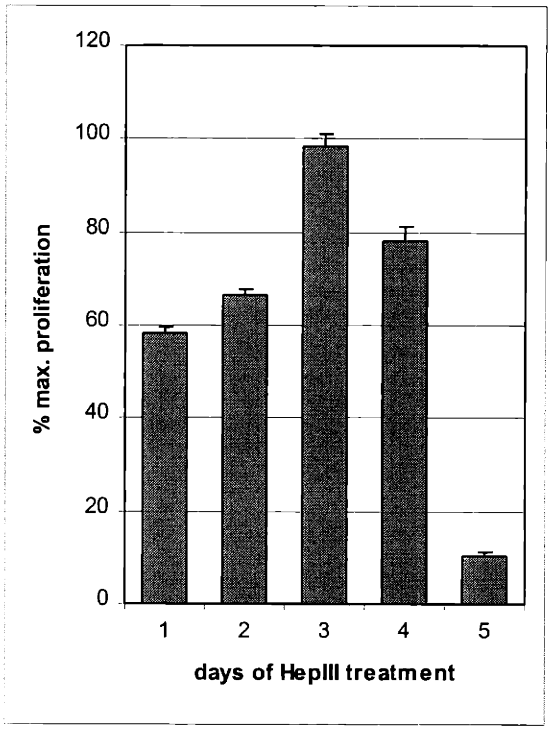

Figure 6.4: Time course study of hepIII treatment on melanoma cells. Melanoma cells were seeded at ~10^4 cells/ml in 24-well format and were allowed to grow overnight to reach ~70% confluence. 50 nM HepIII was added to the medium for 5 consecutive days (see the next section for determination of the optimal concentration). At the end of each day, cells were washed, trypsinized and counted by whole cell counting. Control experiment was set up with no hepIII treatment and the cell count on day 5 was about 90% of maximal proliferation. Appendix 3 provides the unprocessed data of this figure. Each experimental condition was carried out in four wells. The error bars indicate standard deviation of the data set.

Dose-response relationship

To determine the dose-response relationship, we examined the anti-proliferative effect of hepIII over a range of enzyme concentrations over 3 days (**Figure 6.5**). At higher concentration ranges (1-100 nM), a dose-dependent inhibition on cell proliferation was observed with an IC_{50} value of 54 nM. At very low concentration ranges (0.1-1 nM), the inhibitory effect of hepIII appears to be more efficient. The dose-response curve of

hepIII-treated melanoma cells exhibits a biphasic response pattern, which is reminiscent of the curve of the hepIII-treated bovine capillary endothelial cells (Sasisekharan, *et al.*, 1994). This biphasic response pattern has been reported in other studies (Iozzo and San Antonio, 2001; Krufka, *et al.*, 1996; Landau, *et al.*, 2001), in which a lower concentration of HSGAGs appears to promote a biological activity while a higher concentration inhibits. The result presented here suggests that the growth inhibitory effect is correlated to hepIII treatment in a concentration-dependent manner over a higher concentration range. Based on this result, 50 nM hepIII was determined to be the optimal concentration as it was within the linear portion of the dose-response curve.

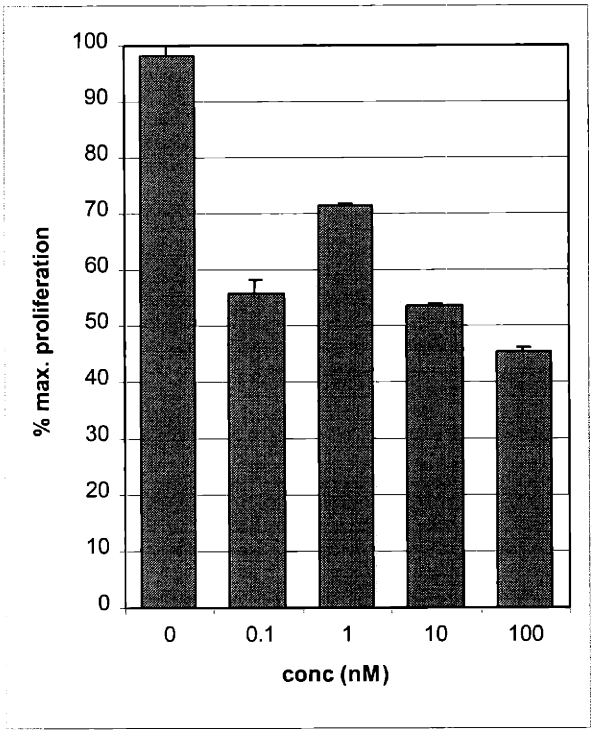

Figure 6.5: Dose-response relationship of hepIII treatment. Melanoma cells were treated daily with the indicated concentrations of hepIII for three consecutive days. The enzyme was added to the culture medium on each day for 3 days. At the end of day 3, cells were trypsinized and counted. The unprocessed data of this experiment are provided in Appendix 3. Note that a dose-dependent decrease in cell proliferation was observed over the higher concentration range. The profile of the dose-response curve exhibits a biphasic pattern. Its significance is discussed in Section 1.4 under "Endothelial

cell proliferation *in vitro* and *in vivo*." Each experimental condition was carried out in four wells. The error bars indicate standard deviation of the data set.

Effect of enzyme folding

To test if the inhibitory effect was specific to the native state of the enzyme, denatured hepIII was used to treat melanoma cells in the proliferation assay. Initially, it was intended to completely denature the enzyme by heating at a high temperature such as 60°C. However, severe precipitation of the enzyme preparation resulted. Subsequently, the enzyme was partially denatured by warming at 42°C with a mild detergent. Cells were treated daily with either PBS, heat-denatured hepIII or native hepIII for 5 days to allow extensive cell death to occur. As shown in **Figure 6.6**, the PBS control had no inhibitory effect on cell proliferation after 5 days of treatment. The heat-denatured hepIII exhibited only 30% growth inhibitory effect compared to the PBS control. As expected, the native enzyme produced about 100% growth inhibitory effect. The result indicated that the heat-denatured enzyme was much less effective than the native one in inhibiting cell proliferation. This finding was consistent with the assertion that the enzymatic activity (i.e. cleavage of cell surface HSGAGs) accounted for the observed growth inhibitory effect in melanoma cells. The result also argued against the possibility that growth inhibition was largely due to cytotoxic impurity that might be present in the enzyme preparation.

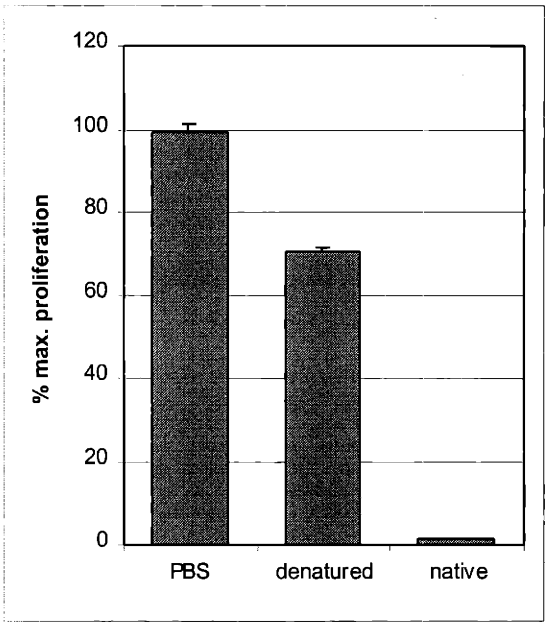

Figure 6.6: The anti-proliferative effect of hepIII is dependent on the native state of the enzyme. Melanoma cells were treated with either PBS (negative control), hepIII denatured at 42°C, or the native hepIII (positive control). After 5 days of treatment, cell proliferation was determined. Unprocessed data of this experiment are provided in Appendix 3. Each experimental condition was carried out in four wells. The error bars indicate standard deviation of the data set.

Conditioned medium of hepIII suppressed cell proliferation

The observed anti-proliferative effect of hepIII treatment can be explained by two possible mechanisms. Enzymatic cleavage of cell surface HSGAGs would lead to the release of specific fragments into the conditioned medium, some of which may in turn signal cells to alter their growth pattern. Alternatively, hepIII treatment can chemically modify cell surface HSGAGs in such a way that the HSGAGs remaining on the cell surface can serve as a signal to regulate cell proliferation. The first proposal predicts that the conditioned medium derived from the hepIII-treated cells would retain the anti-proliferative effect while the second proposal predicts the opposite. To distinguish these two possibilities, experiments were designed in which the conditioned medium from the

hepIII-treated cells was applied to the untreated cells. Two experiments with different culture conditions were performed as described below.

In the first experiment, melanoma cells were treated with hepIII for two days while the untreated cells were cultured in parallel. On the third day, the conditioned medium from the hepIII-treated cells was transferred to the wells of the untreated cells for one day of incubation (**Figure 6.7,** top). A positive control was set up in which the cells were treated with hepIII for two days and left untreated on the third day. The untreated cells served as a negative control and were expected to display maximal proliferation after 3 days. All cells were counted on day 3. As expected, the 2-day hepIII treatment (positive control) significantly inhibited melanoma growth compared with the negative control (**Figure 6.7,** bottom). Importantly, the hepIII conditioned medium was as effective as the positive control in suppressing cell proliferation. Consistent with the first proposed mechanism, the result here indicated that the observed anti-proliferative effect was mediated by the conditioned medium derived from the hepIII-treated cells.

In the second experiment, conditioned medium collected from both hepIII-treated and untreated cells were tested. To remove any residual enzymatic activity, the conditioned medium was heated at 50°C for 10 minutes and centrifuged briefly to remove cell debris. Three sets of melanoma cells were set up for a three-day assay: the first two sets were cultured in the conditioned medium derived from the hepIII-treated and untreated cells, respectively, and the last set was cultured in fresh medium (positive control). As shown in **Figure 6.8**, the hepIII conditioned medium displayed a significant anti-proliferative effect ($p<0.05$) compared with the untreated conditioned medium. Hence, the findings from these two experiments are consistent with the hypothesis that HSGAG fragments released to the conditioned medium by hepIII treatment mediate the observed growth suppression in melanoma cells.

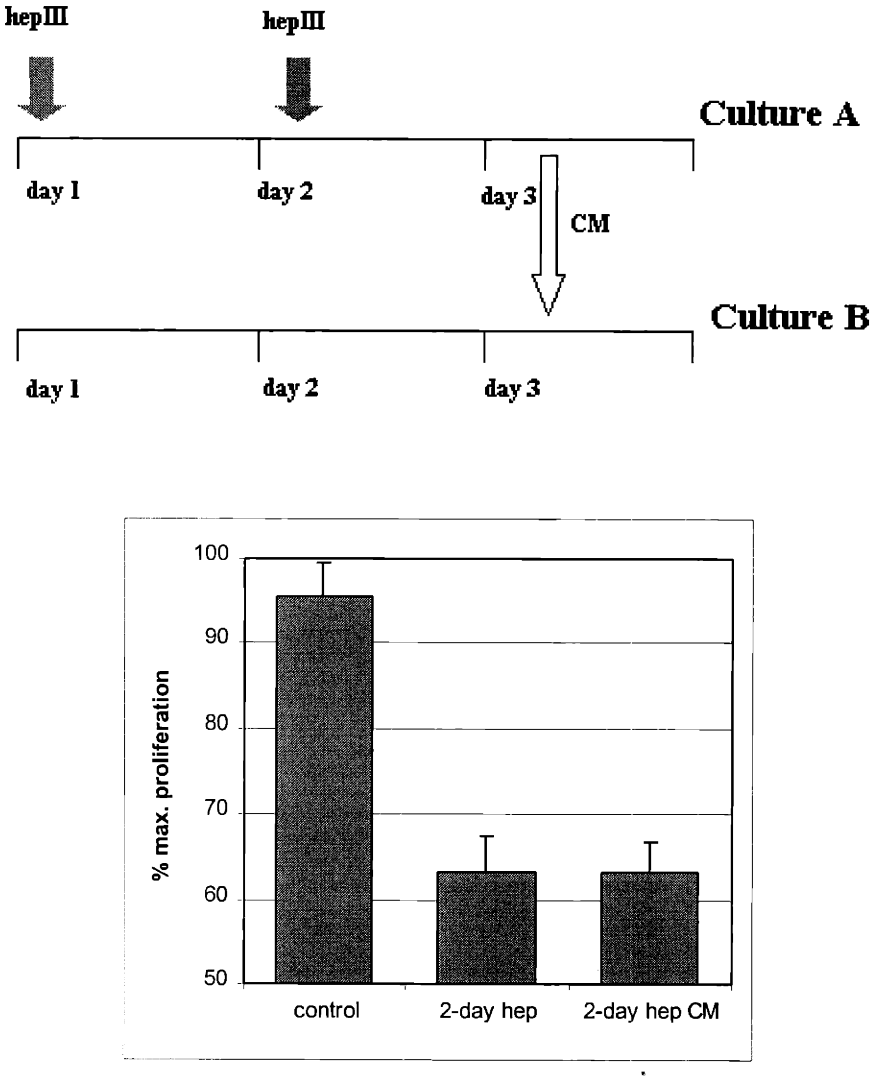

Figure 6.7: Effect of 2-day hepIII treatment and conditioned medium from the hepIII-treated cells. Top: experimental design. HepIII was added to the cells of culture A on days 1 and 2. On the third day, the conditioned medium from culture A was transferred to the cells in culture B for a day. Bottom: proliferation of the untreated cells (positive control), the cells treated with hepIII for 2 days (2-day hep), and the cells treated with hepIII conditioned medium for 2 days (2-day hep CM). Each experimental condition was carried out in four wells. The error bars indicate standard deviation of the data set.

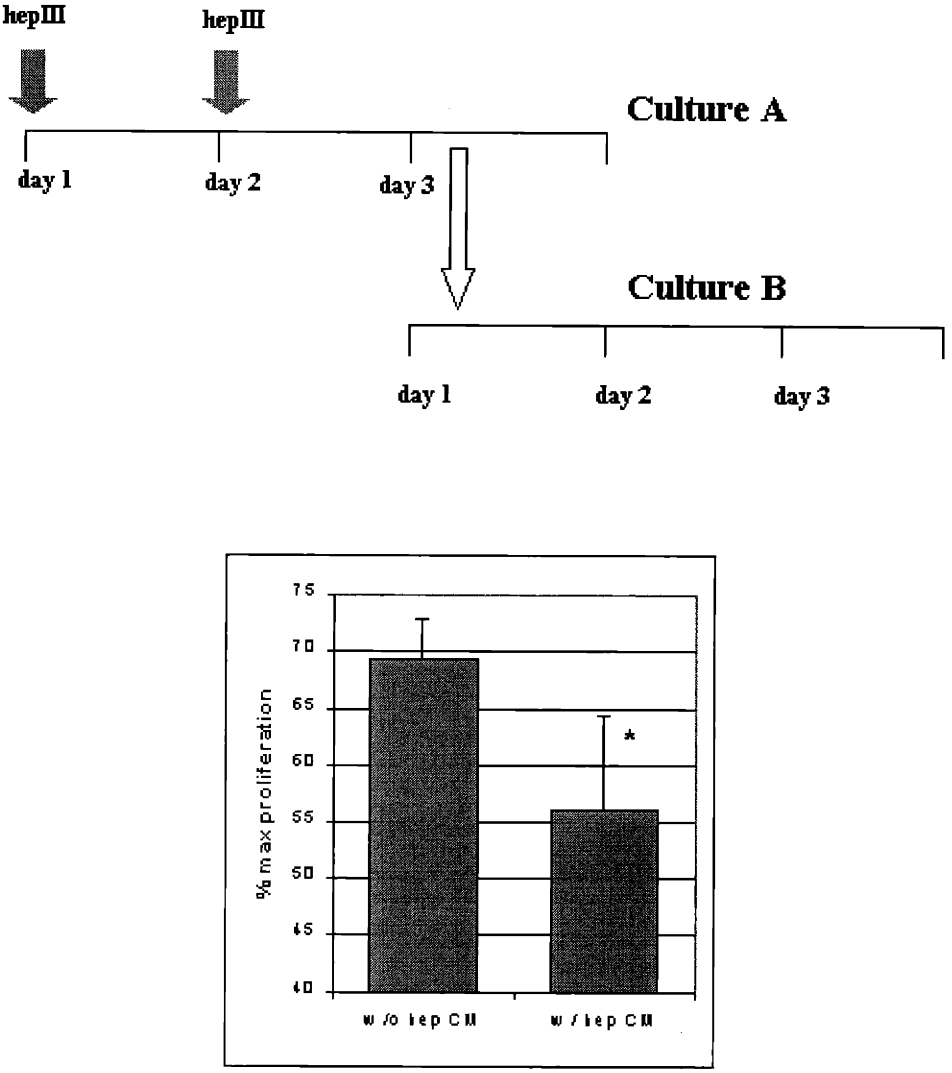

Figure 6.8: Conditioned medium from the hepIII-treated and untreated cells. Top: experimental design. HepIII was added to the cells of culture A on days 1 and 2 (top timeline). On the third day, the conditioned medium from culture A was transferred to a set of freshly seeded cells (culture B) for three days. Bottom: cell proliferation in the conditioned medium derived from the untreated cells (w/o hep CM) and treated cells (w/ hep CM). Proliferation of cells cultured in fresh medium (positive control) was about 100%. Each experimental condition was carried out in four wells. The error bars indicate standard deviation of the data set. *, $p < 0.05$ (student's t-test).

Effect of heparin

Because hepIII is known to release highly sulfated fragments (Ernst, *et al.*, 1995), the observed growth inhibitory effect may be due to the high sulfation level found in the hepIII-generated HSGAGs rather than the HSGAG sequences specific to melanoma cells *per se*. To test if the high level of sulfation was sufficient to elicit the observed growth inhibition, we treated cells with up to 1 mg/ml heparin over 5 days. Heparin, an intracellular form of HSGAGs extracted from mast cells, is unique in its unusually high sulfation level compare to cell surface HSGAGs. A high dose of heparin was only found to modestly suppress cell proliferation (~15%) over a 5-day period (**Figure 6.9**), in contrast to more than 50% suppression exhibited by hepIII treatment. It was concluded that high sulfation alone is not sufficient to account for the observed growth inhibition of hepIII treatment.

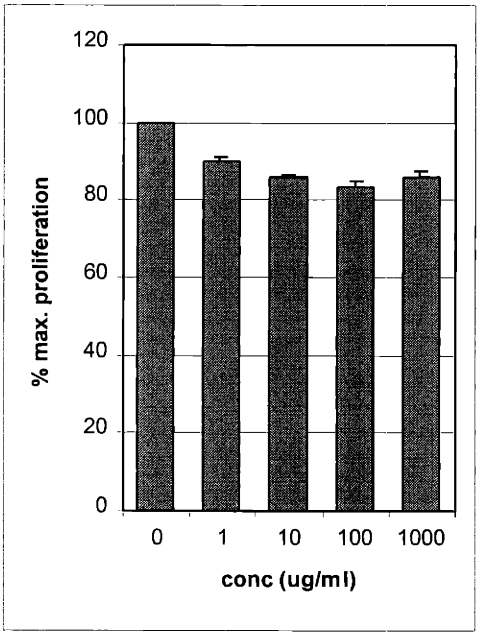

Figure 6.9: The effect of heparin on melanoma cell proliferation. Melanoma cells were treated daily with heparin at the designated concentrations for 5 days. At the end of day 5, cell count was measured by whole cell counting. Each experimental condition was carried out in four wells. The error bars indicate standard deviation of the data set.

Is hepIII-mediated growth suppression restricted to melanoma cells?

To address the question of cell type specificity, we tested the effect of hepIII treatment on the proliferation of Lewis lung carcinoma (LLC) cells. It was observed that untreated LLC organized into an extended web-like morphology. Upon treating the cells with hepIII for 3 days, it was found that most cells lost their morphological features. Proliferation assays showed that hepIII treatment significantly suppressed LLC growth compared with the untreated control (**Figure 6.10**). Therefore, the anti-proliferative effect mediated by hepIII is not restricted to melanoma cells.

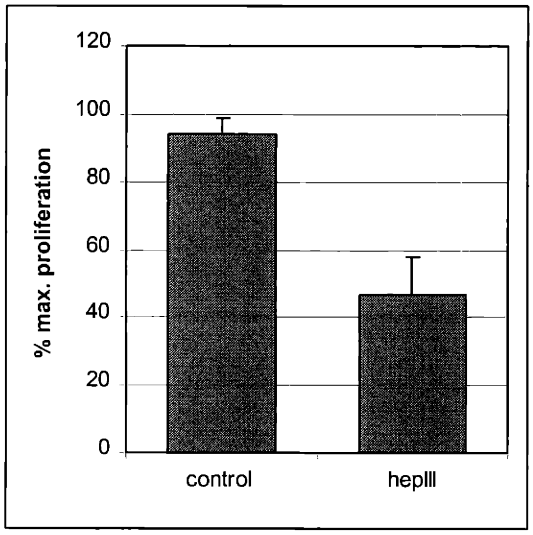

Figure 6.10: The anti-proliferative effect of hepIII on Lewis lung carcinoma cell proliferation. HepIII (50 nM) was added to LLC for 3 days. Proliferation was determined by whole cell counting at the end of day 3. Each experimental condition was carried out in four wells. The error bars indicate standard deviation of the data set.

6.5 HepIII treatment induced apoptosis in melanoma cells

It was recognized that melanoma cells treated with hepIII exhibited a number of prominent morphological features such as cell shrinkage, condensation and fragmentation

of nuclei, and loss of cell adhesion. Together with the report by Liu *et al* that increased apoptosis was detected from hepIII-treated tumor (Liu, *et al.*, 2002b), it was hypothesized that apoptosis was involved in the antiproliferative effect mediated by hepIII treatment. To test this hypothesis, a series of assays were performed to determine the nature of the effect as described below.

HepIII treatment induced DNA fragmentation

DNA fragmentation is considered a hallmark of apoptosis (Wyllie, *et al.*, 1984). Activation of DNA nucleases triggers double-stranded breaks of DNA between evenly spaced nucleosomal regions of about 180 base pairs. To determine if apoptosis contributed to the observed growth suppression, we analyzed the integrity of nucleosomal DNA in the hepIII-treated and control cells using a ligation-mediated PCR method as described in section A1.6.2. As shown in **Figure 6.11**, genomic DNA isolated from the hepIII-treated cells displayed a prominent pattern of nucleosomal DNA laddering compared with the untreated cells, suggesting that apoptosis might play a role in the growth suppression.

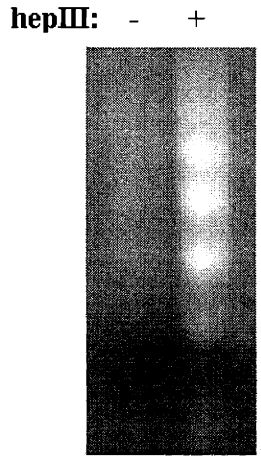

Figure 6.11: Ligation-mediated PCR assay for detecting DNA fragmentation. Genomic DNA extracted from the hepIII-treated cells and control cells was subject to

ligation-mediated PCR assay. Note the prominent DNA laddering pattern from the hepIII-treated cells.

HepIII treatment increased caspase 3 activity

As discussed in section 6.2, activation of caspases is a pivotal biochemical event during apoptosis. Caspase 3 is regarded as the downstream "effector" that, upon activation, is involved in the execution phase of apoptosis (Bratton and Cohen, 2001; Thornberry and Lazebnik, 1998). The activity of caspase 3 in cell lysate can be determined by a simple colorimetric method developed by Gurtu *et al* (Gurtu, *et al.*, 1997). In this assay, a synthetic tetrapeptide (Asp-Glu-Val-Asp or DEVD) was labeled with a chromophore p-nitroanilide. The protease activity of caspase 3, which cleaves the tetrapeptide to release the chromophore, is proportional to the amount of free chromophore detected. To detect caspase 3 activity, cell lysate was harvested from melanoma cells that had been treated with hepIII for one and five days. As a control, cell lysate was extracted from the untreated cells during the same time period. A three-fold increase in caspase 3 activity was observed from the cells treated with hepIII for 1 day (**Table 6.1**). The activity decreased to about 2 fold after 5 days of treatment. This result confirmed the above findings that apoptosis was involved in the observed growth suppression. In order to gain further insights into the molecular nature of hepIII-mediated apoptosis, we employed a cDNA microarray analysis to identify differentially regulated genes as described in the following sections.

days of HepIII treatment	fold induction
1 day	2.8
5 days	1.9

Table 6.1: Caspase 3 activity in the whole cell lysate of hepIII-treated cells. The "fold induction" of caspase 3 activity refers to the ratio of the background-adjusted average absorbance from the hepIII-treated sample to that from the untreated control sample. Unprocessed data of this experiment are provided in Appendix 3. The results shown here are representative of two experiments.

6.6 cDNA microarray analysis

An important step towards understanding the role of HSGAGs in tumor progression and metastasis is the identification of key genetic markers, whose expression are differentially regulated upon heparinase treatment. Because many facets of cell signaling are regulated at the transcription level, a gene expression profiling approach represents a promising way for identifying differentially regulated genes. Traditional methods for profiling gene expression (such as RT-PCR and Northern hybridization) have the inherent limitation that only a handful of genes can be analyzed at a time. The cDNA microarray or gene array approach has become an increasingly powerful tool for profiling gene expression (Khan, *et al.*, 1999). It has the advantage of scalability—allowing simultaneous analysis of a large number of genes in a high-throughput fashion.

Principle

In a way, cDNA microarray is similar to Northern hybridization but is performed in a reverse fashion. In Northern hybridization, the RNA immobilized on a membrane is hybridized with a labeled gene tag. The cDNA microarray involves immobilization of a large collection of gene tags on a support (such as nylon membrane, plastic or glass) and hybridization with the labeled cDNA reverse-transcribed from the RNA of interest. The cDNA probes are either labeled with radioisotope such as α-^{32}P or with fluorescent dyes such as Cy3 or Cy5. The methodology is schematically represented in **Figure 6.12**. The cDNA microarray approach has been successfully applied to investigate many biological and disease processes (Martin, *et al.*, 2000; Perou, *et al.*, 2000; Ross, *et al.*, 2000; Sorlie, *et al.*, 2001). In most of these applications, comparison in gene expression levels was made in two or more samples, or in a time series. The complexity of data would increase massively as the number of comparisons as well as the number of gene tags increase. An emerging area of genomic research is to develop computer algorithms to simplify the identification of clusters of genes that are similarly expressed under a given condition (Eisen, *et al.*, 1998).

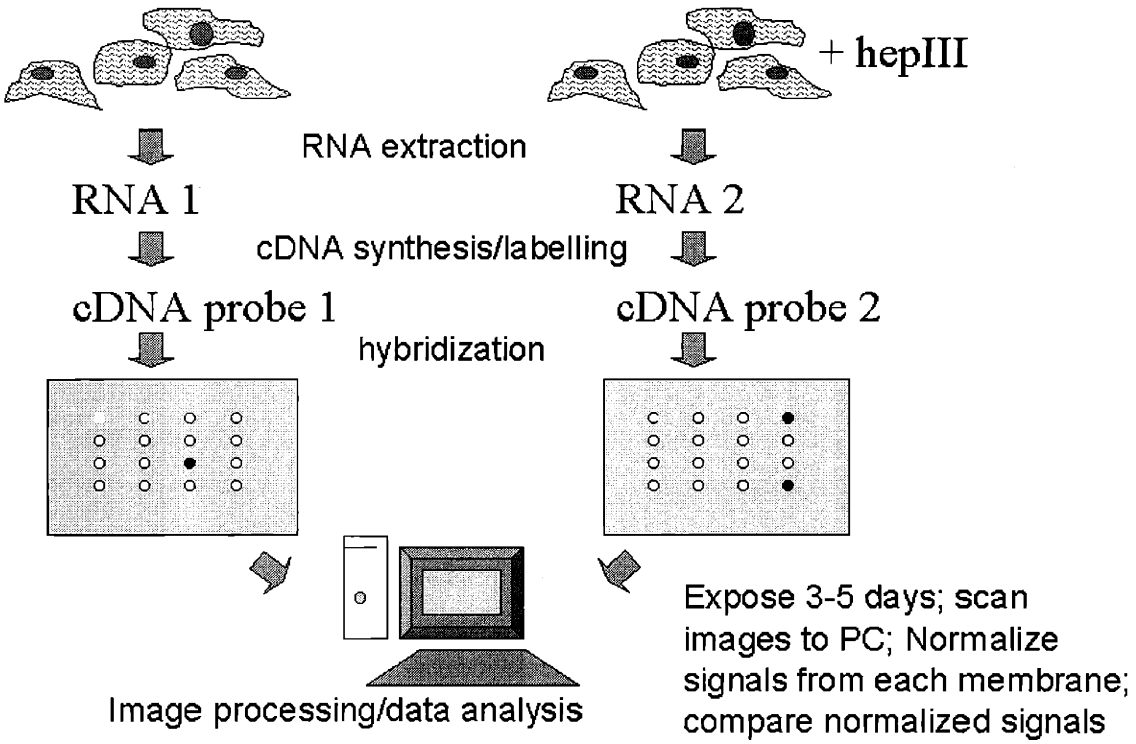

Figure 6.12: Schematic representation of the cDNA microarray methodology. RNA is extracted from the control (left) and hepIII-treated cells (right). Labeled cDNA probes are synthesized by reverse transcription in the presence of radioactive or fluorescent nucleotides. Side-by-side hybridizations of the cDNA probes with the gene arrays (nylon membranes in this case) allow simultaneous comparison of expression profiles of the two samples. The membranes are washed using high stringency conditions and are exposed to a phosphorimaging screen for 3-5 days. Hybridization signals are acquired by scanning the phosphorimager screen and the images are analyzed by the ImageQuant software on a PC workstation.

The Clontech Atlas Mouse Cancer 1.2 Array

A large number of cDNA microarray products are available from several vendors for a variety of applications (e.g. cell cycle, cancer and toxicology) and systems (e.g. membrane, plastic and glass). We surveyed four different membrane-based products and subsequently chose the Atlas Mouse Cancer 1.2 cDNA microarray system from Clontech. This relatively low-cost system is compatible with the conventional hybridization and phosphorimaging equipment. The array contains 1176 unique genes and 12 control genes

for normalization purpose. The 1176 genes are grouped into six categories: (1) apoptosis, oncogenes and tumor suppressor genes, (2) growth factors and cytokines, (3) DNA damage response, repair and recombination, cell fate and developmental receptor, (4) angiogenesis, cell adhesion and motility, (5) invasion regulators and cell-cell interactions, and (6) cell-cycle regulators, growth regulators and intermediate filament markers. According to the manufacturer, these gene tags are considered unique as they are derived from regions that are free of repetitive, poly-A or high homology sequences. The size of these genes ranges from 200 to 600 base pairs. A complete list of all the genes included on the cDNA microarray can be downloaded from the manufacturer's website (http://www.clontech.com/atlas/genelists/index.shtml).

Summary of experiments

One of the single most important factors in determining the quality of hybridization signals is the integrity of RNA used for probe synthesis. All the glassware and plasticware used in the experiment were autoclaved and were used exclusively for RNA work. All buffers were made with DEPC-treated water. Prior to probe synthesis, RNA samples were treated with RNase-free DNase I to remove traces of contaminating genome DNA. Initially, RNA was extracted from the cells treated with hepIII for 5 days. However, it was noticed that both the yield and quality of RNA was poor. As a result, RNA was harvested after 3 days of hepIII treatment, a time when minimal cell death was observed. 5 μg of RNA was reverse-transcribed into cDNA in the presence of α-^{32}P dATP. Control reaction with RNA supplied by the manufacturer was set up in parallel for assessing the labeling efficiency. The labeled cDNA was purified using a G50 sepharose column to remove any unincorporated isotope. The cDNA probes of approximately equal radioactive activity were added to the array membrane for an overnight hybridization. The membranes were then washed several times using high stringency conditions to remove any non-specific binders. For signal detection and analysis, the membranes were exposed to a phosphorimaging screen for 3 to 5 days and the images were acquired by a PC workstation for data analysis.

Hybridization signals were normalized based on the averaged signals from four of the housekeeping genes provided on each membrane. The expression of housekeeping

genes remains relatively constant under most physiological and pathological conditions (Adams, *et al.*, 1995). Hence, hybridization signals from housekeeping genes provide an estimate of the relative abundance of the two cDNA probes being tested.

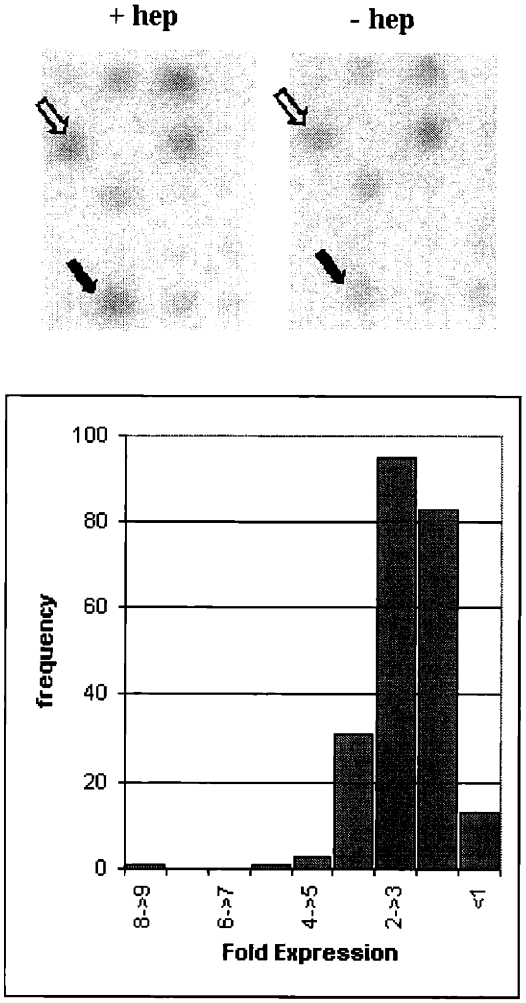

Figure 6.13: The cDNA microarray analysis. Top: magnified images of the representative hybridization signals (indicated by the arrow pairs) from the hepIII-treated and untreated cells. The open and filled arrows point to two different gene tags on each of the two membranes. Note that the spots on the left panel (+ hep) yield a stronger hybridization signal than those on the right (- hep). These signals were acquired by scanning the phosphorimaging screen that had been exposed to the cDNA microarray membranes for 3 days. Bottom: distribution of the fold expression upon hepIII treatment of the 245 selected candidate genes. The fold expression of each individual gene is

calculated by normalizing the hybridization signals of the housekeeping genes provided on each membrane.

Selected candidate genes up-regulated by hepIII treatment

Among the 1176 genes included in the microarray, 245 produced high enough signals (above the background hybridization signal) for detection and were selected for further analysis. Representative spots with markedly different signal intensity were shown in **Figure 6.13**, top. Most of these selected genes are up-regulated upon hepIII treatment, with the highest frequency in the 2- to 3-fold increase group (**Figure 6.13,** bottom). Genes with an expression level above 3-fold were considered further. Most of these genes fall into one of the following categories: cell-cell or cell-matrix adhesion, cytokine ligands or receptors, and intracellular signal transduction. We narrowed our search to those genes that were related to apoptosis and cell cycle control. It was found that the following genes were up-regulated upon hepIII treatment for 3 days: CD40 ligand or tumor necrosis factor superfamily 5 (5.5 fold), tumor necrosis factor-related association factor 6 (TRAF6) (4.0 fold), p27 (3.4 fold) and TWEAK or tumor necrosis factor superfamily 12 (2.4 fold). In another microarray experiment, expression of caspase 8 as well as several tumor necrosis factor ligands was found to be up-regulated as well. As discussed below, the expression pattern of these genes appeared to be closely related to the apoptotic phenotype observed in the hepIII-treated melanoma cells.

CD40 ligand, a member of the tumor necrosis factor superfamily, is an integral membrane protein expressed on antigen-presenting cells, endothelial cells, activated mast cells and basophiles (Henn, *et al.*, 1998). Binding of CD40 ligand to its cognate receptor, CD40, triggers the induction of apoptosis in a wide variety of cell types, including ovarian carcinoma cells (Eliopoulos, *et al.*, 2000), malignant melanoma cells (von Leoprechting, *et al.*, 1999), myeloma cells (Bergamo, *et al.*, 1997), biliary epithelial cells (Afford, *et al.*, 2001), hepatocytes (Afford, *et al.*, 1999), transformed mesenchymal, and epithelial cells (Hess and Engelmann, 1996). The mechanism by which CD40 activation induces apoptosis is shown to be caspase 8- and 3-dependent (Eliopoulos, *et al.*, 2000), which is similar to the mechanism of TNF-induced apoptosis (Miura, *et al.*, 1995). TRAF6 is a cytoplasmic protein that associates with the cytoplasmic tail of CD40 upon

activation (Inoue, *et al.*, 2000). TWEAK, a newly-discovered member of the TNF superfamily, has been shown to induce mild apoptosis in adenocarcinoma cells (Chicheportiche, *et al.*, 1997). p27 is a cyclin-dependent kinase inhibitor whose function is to inhibit cell cycle progression by initiating G_1 growth arrest. Over-expression of p27 has been shown to induce apoptosis in a number of cell types including mammary, colon, lung, cervical carcinoma and melanoma (D'Agnano, *et al.*, 2001; Katayose, *et al.*, 1997; Wang, *et al.*, 1997). One mechanism by which beta-lapachone, an anti-neoplastic drug, induces apoptosis in cancer cells is by up-regulating p27 expression (Don, *et al.*, 2001). The known biological functions of these candidate genes prompted us to speculate that the caspase-8 dependent death receptor pathway was activated upon hepIII treatment.

6.7 Caspase 8 activity but not 9 was up-regulated by hepIII treatment

As described in section 6.2, apoptotic cell death is mediated by two general mechanisms—one initiated from within the mitochondria and the other initiated by death receptor activation. Distinct upstream initiator caspases are activated in the two mechanisms. While the death receptor pathway promotes apoptosis through caspase 8, the mitochondria-initiated pathway transduces apoptotic signal through caspase 9. To distinguish between these two pathways, we assayed the activities of caspase 8 and 9 in the cell extracts. Cells were either treated with hepIII or untreated for one and five days. Caspase activities were determined using specific substrates linked with either a chromophore or a fluorophore. As shown in **Figure 6.14**, while caspase 9 activity remained unchanged on days 1 and 5, a marked increase in caspase 8 activity was observed on day 5. This finding, together with the results from the microarray analysis, strongly suggested that hepIII treatment induced apoptotic cell death through the caspase-8 dependent death receptor pathway.

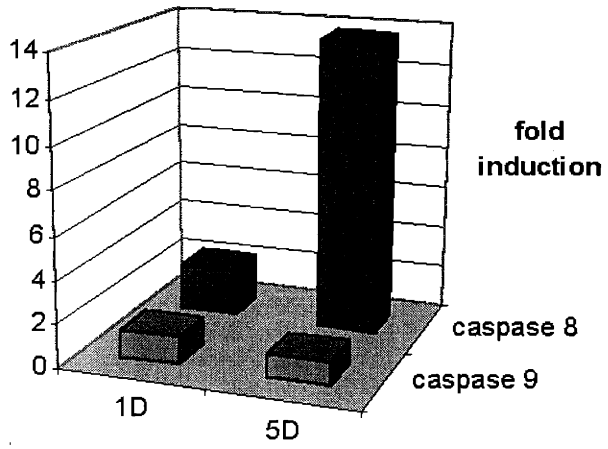

Figure 6.14: Caspase 8 and 9 activities in the whole cell lysate of the hepIII-treated cells. Caspase activity assays were performed as described in the Appendix (A1.6). The "fold induction" of caspase activity refers to the ratio of the background-adjusted average of the absorbance from the hepIII-treated sample to that from the untreated control sample. The number of "fold induction" for caspase 9 activity on days 1 and 5 is 1.3 and 1.1, respectively. That for caspase 8 activity on days 1 and 5 is 2.2 and 13.7, respectively. Unprocessed data of these experiments are provided in Appendix 3. The results shown here are representative of two experiments.

6.8 Conclusion

Cell surface HSGAGs modulate a broad spectrum of biological functions through interacting with specific cellular mediators. HSGAG fragments derived from tumor cells have been demonstrated to either promote or inhibit tumor progression and metastasis *in vitro* and *in vivo* (Liu, *et al.*, 2002b). In the current Chapter, *in vitro* cell culture assays were developed to investigate the effect of heparinase III treatment on cell proliferation. HepIII was found to suppress cell proliferation in a dose-dependent manner with an IC_{50} value of 54 nM, which was very close to a previously determined value (21 nM) in a separate study (Sasisekharan, *et al.*, 1994). The anti-proliferative effect was largely mediated by the enzymatic activity of hepIII, which cleaves under-sulfated HSGAG domains and leaves behind highly-sulfated fragments. Conditioned medium derived

from the hepIII-treated cells were shown to elicit a similar anti-proliferative effect on melanoma cells. LLC was also found to be susceptible to hepIII treatment, suggesting that the observed anti-proliferative effect was not restricted to melanoma cells alone.

The role of apoptosis in the hepIII-mediated growth suppression was assessed using standard morphological examination criteria, DNA fragmentation assay and caspase 3 activity assay. In agreement with a previous study (Liu, *et al.*, 2002b), the current results suggested that apoptosis was induced as a result of hepIII treatment. To gain further insights into the mechanism of apoptotic cell death, a cDNA microarray approach was employed to profile transcriptional changes in melanoma cells following hepIII treatment. Based on the gene expression pattern, it was speculated that a death receptor-mediated, caspase 8-dependent apoptotic pathway was activated by hepIII treatment. As mentioned in section 6.2, apoptosis is initiated through two distinct mechanisms; one involves cell surface death receptor and caspase 8 activity while the other involves the mitochondria and caspase 9 activity. Activation of either caspase 8 or 9 would subsequently lead to the induction of caspase 3. To distinguish the two possible apoptotic mechanisms, cell lysate from the treated and control cells was subject to caspase 8 and 9 activity assays. Consistent with the microarray data, caspase 8 activity was significantly higher than caspase 9 activity. Therefore, the data from cDNA microarray analysis and caspase activity assays strongly suggested that hepIII induced caspase-8 dependent apoptotic cell death in melanoma cells. The present study provides the foundation for further investigation into the molecular mechanisms by which cell surface HSGAGs modulate cell growth and death.

PART IV: IMPLICATION

Chapter 7:

Conclusions and Significance

7.1 Conclusions of Thesis Research

Heparan sulfate glycosaminoglycans are ubiquitous biopolymers expressed by most, if not all, multi-cellular organisms. A broad spectrum of physiological processes, such as anti-coagulation and angiogenesis, are regulated by HSGAGs through specific interactions with various biological mediators. In this thesis research, the FGF family of growth factors is chosen as the model system for investigating the functional role of HSGAGs in modulating cell signaling. FGF2 is not only an important mitogenic factor under normal and pathological circumstances, but also a prime therapeutic candidate for treating vascular diseases and healing wounds. By dissecting the molecular mechanism of HSGAG-FGF interactions, it is expected to expand our knowledge of HSGAG-dependent growth factor signaling and to facilitate engineering of therapeutic growth factors with higher activity and stability.

- Based on exhaustive modeling studies of FGF2 crystal structures, a FGF2 mutant protein was rationally designed for testing various possible modes of ligand dimerization. Cysteine residues were engineered at the specific protein interfaces such that the mutant protein was amenable to oxidative crosslinking. While wildtype FGF2 failed to dimerize significantly under oxidative conditions, the mutant protein exhibited extensive dimerization and oligomerization, particularly in the

presence of heparin. Control experiments verified that the observed dimers and oligomers were disulfide-mediated and that denatured protein failed to dimerize. These findings strongly suggest that one role of HSGAGs in FGF2 signaling is to facilitate ligand dimerization.

- A novel dimeric FGF2 fusion protein was engineered to investigate the biochemical as well as the functional aspects of FGF2 dimerization. The fusion protein contains two FGF2 proteins linked in tandem with a tripeptide linker. The genetic construct was cloned by a combination of PCR, restriction enzyme digestion and ligation. The fusion protein was expressed in bacteria and purified with two chromatographic steps. Biochemical assays indicated that the fusion protein was grossly folded properly and that the protein interacted with heparin at a much higher affinity. The dimeric protein also appears to interact with FGFR in a 1:2 stoichiometry, suggesting that the protein was capable of inducing receptor dimerization.

- Three independent biological assays were employed to study the functions of the dimeric FGF2 protein under conditions close to physiological states. Two *in vitro* assays confirmed that dFGF2 was several folds more potent than the monomeric FGF2 on a molar basis. In addition, dFGF2 exhibited less dependency on heparin for activity. An *in vivo* angiogenesis assay further corroborated the *in vitro* results.

The roles of cell surface HSGAGs in modulating cell signaling through FGF-dependent and FGF-independent mechanisms were examined in this thesis research. With the aid of a panel of heparinases and the knowledge of their substrate specificities, we were able to investigate the effect of distinct HSGAG sequences on modulating cell growth and death. Hence, the studies described in Chapters 5 and 6 provide a framework for studying the diverse effects of cell surface HSGAGs on modulating cell signaling.

- It was found that FGF2 signaling was differentially modulated by both the composition of the SMC-derived HSGAGs and the type of FGFR isoforms expressed on the cell surface. Cell proliferation assays indicated that the hepIII-generated fragments were most effective in promoting FGF2 signaling through FGFR1C whereas the hepI fragments acted most effectively through FGFR3C. The hepIII fragments were found to be the most highly sulfated, with the highest content in ΔU_{2S}-$H_{NS,6S}$. Conversely, the hepI fragments were relatively undersulfated. These findings promoted us to propose a model in which a dynamic alternation of HSGAG sequences expressed on the cell surface enabled cells to fine-tune their responsiveness to growth factors through a receptor or set of receptors.

- The effect of hepIII treatment on cell proliferation was investigated using a series of *in vitro* cell culture studies. Melanoma cell proliferation was found to be suppressed by both the enzymatic treatment as well as the conditioned medium derived from the treated cells. The anti-proliferative effect was mediated by apoptosis. Gene expression profiling by cDNA microarray analysis and caspase activity assays suggested that a death receptor-dependent, caspase 8-mediated apoptotic pathway was involved.

7.2 Significance:

HSGAGs have emerged as one of the most intensely studied macromolecules for their importance in a myriad of biological systems. With the advent of several key enzymatic and analytical tools, we are beginning to address the pivotal question of how HSGAGs modulate biological functions at both the molecular and the functional levels. In this thesis research, FGF2 was chosen as the model system for investigating the molecular mechanism by which HSGAGs facilitate the assemblage of an active signaling

complex. Based on exhaustive structural analysis on FGF2, a rational design approach was employed to engineer a FGF2 mutant that would form disulfide bridged dimers and oligomers. Oxidative crosslinking of this mutant and wildtype FGF2 allowed us to probe FGF-FGF interaction and thereby enabled us to dissect various modes of HSGAG-induced dimerization. A novel dimeric FGF2 fusion protein was constructed, which enabled us to directly test the biological significance of FGF2 dimerization *in vitro* as well as *in vivo*. Our findings not only provided further support to the dimer presentation model, but also provided a framework for engineering dimerized growth factors for therapeutic purposes.

At the functional levels, we demonstrated how specific HSGAG fragments and/or heparinase treatment could be used to regulate cellular processes in an FGF-dependent and FGF-independent manner. Developing a better understanding on the structure-function relationship of HSGAG fragments is fundamental to achieving the long term goal of identifying or synthesizing specific HSGAG sequences (or their derivatives) for therapeutic applications. For example, a HSGAG fragment of defined sequences may serve as a growth inhibitor that triggers certain apoptotic pathway while a similar fragment with slightly different sequence may serve as a growth promoter. By analyzing the functional effect of distinct HSGAG fragments in a systematic fashion, it is anticipated to uncover even more biologically important HSGAG sequences that may have various applications.

7.3 Recommendations for Future Research

Based on the findings obtained from this thesis research, two areas are recommended for consideration of future investigation. The first is in the area of protein engineering of dimeric growth factor, and the second area relates to the chemical and functional characterization of cell surface HSGAGs.

1) The present work has provided the groundwork for 're-engineering' the dimeric growth factors. For example, different dimeric FGF2 fusion

proteins can be designed based on the different co-crystal structures in order to test for various structural requirements of ligand dimerization. In addition, other linker sequences can be designed for different purposes. For example, a protease- or pH-sensitive linker sequence could be engineered into the dimeric protein such that one could turn a high activity dimer back to a low activity monomer. Because of the angiogenic potential of FGF2 in treating ischemia and healing wounds, dimeric FGF2 with higher potency and lower heparin dependency may be an ideal therapeutic protein for clinical applications. Pathological animal models can be used to evaluate the efficacy of such a dimer.

2) In the second area, this work lays the foundation for characterizing the functions of cell surface HSGAGs. Two approaches can be considered for future work. First, improved preparative methods for isolating specific HSGAG fragments from cultured cells and tissues are needed. It is desired to isolate a library of HSGAG fragments in large quantities from cells or tissues under defined pathophysiological conditions. Second, the microarray study can be expanded to profile gene expression changes in cells treated with different HSGAG fragments. It is conceivable that certain HSGAG fragments may induce one gene expression profile (such as pro-apoptosis) while others may induce another (such as anti-apoptosis).

Appendix 1. Materials and Methods

A1.1 General

Equipments

A thermal cycler (Perkin Elmer Cetus, Norwalk, Connecticut) was used for PCR applications. A bench-top Eppendorf centrifuge (Model 5417, Westbury, New York) was used to centrifuge 1.5 ml or 0.5 ml microcentrifuge tubes at room temperature. Centrifugation of samples in larger volume (15 ml and 50 ml) was carried out in refrigerated centrifuge (Model IEC Centra-7R, International Equipment Company, Needham Heights, Massachusetts). Pelleting of bacterial cells (up to 1 L) was carried out in a refrigerated centrifuge (Sorvall RC3B Plus, Sorvall Products, L.P., Newton, Connecticut). An UV/VIS spectrophotometer (Model 8452A, Hewlett Packard Diode Array Spectrophotometer, Avondale, Pennsylvania) was used to measure optical density (OD). Gel electrophoresis was carried out using a computer controlled electrophoresis power supply (Model 3000Xi, Bio-red, Hercules, California). A digital imaging system (FotoDyne, Inc, Hartland, Wisconsin) was used to record images of DNA and protein gels. An Accumet® model 15 pH meter (Fisher Scientific, Pittsburgh, Pennsylvania) was used to adjust pH of all buffers. Equipments for tissue culture include incubators (Forma Scientific, Norwood, Massachusetts), tissue culture hoods (SterilGard Hood, BakerCom, Inc, Sanford, Maine) and an electronic cell counter (Coulter, Inc., Hialeah, Florida). An Olympus CK40 microscope (Optical Analysis Corporation, Nashua, New Hampshire) was used to observe cell morphology.

Glassware and plasticware

All glassware used was either from Pyrex or Kimax. Glassware for RNA work was autoclaved to inhibit RNase activity. Polypropylene centrifuge tubes of 1.5 ml, 15 ml and 50 ml sizes were either from Corning (Corning, New York) or Falcon (Franklin Lakes, New Jersey). T75 tissue culture flasks and 100 mm dishes were from Corning Inc

(Corning, New York). Individually packaged serological pipets were from Falcon (Becton Dickinson, Franklin Lakes, New Jersey).

Miscellaneous

All solutions were made with double distilled water (Reagent Grade Water System, Photronix, Medway, Massachusetts). Buffers for protein purification were further sterilized by filtering through 0.2 μm filter paper (Versapor®-200, Gelman Laboratory, Ann Arbor, Michigan). Water for RNA work was treated with 0.1% diethyl pyrocarbonate (DEPC). Acetonitrile (HPLD grade) was from J.T. Baker (Phillipsbury, New Jersey). Difco Luria-Bertani (LB) medium (Beckon Dickinson, Sparks, Maryland) was used for making LB broth and plates. Oligonucleotide primers were synthesized by GibcoBRL (Rockville, Maryland).

A1.2 Probing Protein-Protein Interaction in FGF2 Dimerization

(Materials and methods related to Chapter 2)

A1.2.1 Materials

Ampicillin, isopropyl ß-D-thiogalactopyranoside (IPTG), iodoacetic acid, 1,10-phenthroline, and dithiothreitol (DTT) were purchased from Sigma (St. Louis, Missouri). Ultra-pure 2-mercaptoethanol was from American Bioanalytical (Natick, Massachusetts). Recombinant human wildtype FGF2 was a gift from Scios Nova (Mountain View, California). The expression vector pET14b variant (which has an introduced *SpeI* site) was a generous gift from Professor David M. Ornitz (Department of Molecular Biology and Pharmacology, Washington University, St. Louis, Missouri). The *Escherichia coli* strain BL21 (bacterial phage resistant) was obtained from Professor Lawrence Stern (Department of Chemistry, MIT). Heparin sodium USP porcine intestinal mucosa was purchased from Kabi Pharmacia (Franklin, Ohio). Ready-Gel (15% polyacrylamide gel), Bradford assay and silver staining kits were from Bio-rad (Hercules, California).

A1.2.2 Buffers

Buffers for protein purification were used within two weeks after preparation. The buffers used were as follows: binding buffer (5 mM imidazole, 20 mM Tris and 500 mM NaCl, pH 7.9), elution buffer (500 mM imidazole, 20 mM Tris and 500 mM NaCl, pH 7.9), solubilization buffer (4M guanidine HCl and 0.5% 2-mercaptoethanol in binding buffer), nickel buffer (200 mM $NiSO_4$), strip buffer (100 mM EDTA, 20 mM Tris and 500 mM NaCl, pH 7.2). All buffers were filtered to remove particulates. Precaution was taken to ensure that the buffer was free of precipitation.

A1.2.3 Site-directed Mutagenesis

Specific point mutations were introduced by the PCR-based site-directed mutagenesis method as described previously (Higuchi, 1990). A plasmid containing the tetra-mutant of FGF2 (R81C/S100C/C69S/C87S) was obtained from Dr. Ranga Godavarti (Health Science and Technology, MIT) and was used as a template for further site-directed mutagenesis. Additional primers were designed to replace the two internal cysteines with serines (**Table A1.2.1**).

Primers	Sequences (5' → 3')
C25S 5'	CGGCTGTACTCCAAGAACGGG
C25S 3'	CCC GTT CTT GGA GTA CAG CCG
C92S 5'	ACA GAC GAG TCT TTC TTT
C92S 3'	AAA GAA AGA CTC GTC TGT

Table A1.2.1: Primer sequences for replacing internal cysteines with serines

PCR products were gel-purified with the Quantum Prep® spin columns (Bio-rad, Hercules, California) and subcloned into the pCR2.1-TOPO vector (Invitrogen, Carlsbad, California). Positive clones were selected by blue/white screens and plasmid DNA was isolated. Inserts were excised with the appropriate restriction enzymes and were subcloned into a variant of pET14b expression vector through the *NdeI/SpeI* sites. DNA

sequencing was performed by the Nucleic Acid and Protein core facility at the Children Hospital of Philadelphia, Pennsylvania.

A1.2.4 Protein Expression and Purification of Cysteine Mutant

BL21 cell was used as a host for protein expression. Bacterial cultures were carried out aerobically at 37°C in LB medium supplemented with ampicillin. Approximately 1 ng of the expression plasmid was used to transform a vial of frozen BL21 cells following standard bacterial transformation procedure. Transformed cells were plated on LB agar plate supplemented with 100 μg/ml ampicillin. A single colony was picked and grown in 50-100 ml LB supplemented with ampicillin at room temperature overnight with shaking. About 10 ml of the overnight culture was transferred to two shake flasks (2 L Erlenmeyer flasks), each containing 500 ml LB medium supplemented with ampicillin (400 mg/L). The shake flasks were secured on an orbital shaker (Model G10 Gyrotory® shaker, New Brunswick, Edison, New Jersey) and shaked at 200 rotations per minute. Bacterial cell growth was measured by cell density. Measuring optical density at 600 nm (OD_{600}) provides a convenient and real-time estimate of cell density. All measurements were blanked against plain LB medium. The cultures were allowed to grow at 37°C until cell density reached OD_{600} of ~0.8 and induced with 1 mM IPTG for 2 hours. Cells were resuspended in chilled binding buffer for sonication (Ultrasonic processor XL, Misonix Inc, Farmingdale, New York). Protein purification by Ni-chromatography was performed as previously described (Ernst, *et al.*, 1996; Padera, *et al.*, 1999). Purity of the protein was assessed by SDS-PAGE under non-reducing conditions and concentration was determined by Bradford assay using recombinant wildtype FGF2 as control.

A1.2.5 Oxidative Crosslinking

Purified protein was buffer-exchanged into HEPES buffer with 10kDa molecular mass cut-off membranes (Millipore, Beverly, MA). Oxidative crosslinking was performed by incubating 50 μg protein (30 μM final) with 750 μM Cu^{2+}-phenanthroline (made from a 1:1 mixture of 25 mM $CuSO_4$ and 130 mM phenanthroline) in a 100 μl reaction volume

at room temperature for 10 minutes. Longer incubation times (up to 2 hours) did not significantly increase the amount of oligomer formed. For heparin treatment, the protein was incubated with 3 μM heparin for 1 hour prior to crosslinking. The protein to heparin ratio was 10:1, which was previously shown to be optimal for FGF2 dimer formation (Davis, *et al.*, 1999). Other reaction conditions are indicated in the legend to the figures. The reaction was terminated with 0.1 M EDTA and 10 mM iodoacetic acid. Crosslinked products were analyzed by electrophoresis in 15% non-reducing SDS-PAGE gels followed by silver staining.

A1.3 Protein engineering of dimeric fibroblast growth factor

(Materials and methods related to Chapter 3)

A1.3.1 Materials

Restriction enzymes were either from New England Biolab (Beverly, Massachusetts) or GibcoBRL (Rockville, Maryland). Antibody against native FGF2 was a gift from Scios Nova (Mountain View, California). Dulbecco's Modified Eagle's Medium (DMEM), RPMI-164 and M199 media were from BioWhittaker (Walkerville, Maryland). Fetal bovine serum (FBS) and bovine calf serum (BCS) were from HyClone Inc (Logan, Utah). Bovine brain extract was from Clonetics Corp (San Diego, California). Trypsin-EDTA and phosphate buffered saline (PBS) were from GibcoBRL (Rockville, Maryland). Sodium chlorate and alcian blue were from Sigma (St. Louis, Missouri). Immun-blot® assay kit was purchased from Bio-rad (Hercules, California). HUVEC were supplied by the laboratory of Dr. Jeffrey Isner in the department of cardiovascular research, St. Elizabeth Medical Center, Boston, Massachusetts.

A1.3.2 Conformational Studies

Conformational studies were performed with the Insight II package (Molecular Simulations, Burlington, Massachusetts) on a Silicon Graphics workstation (Mountain

View, California). The coordinates of FGF2 dimer in the FGF2-FGFR1 crystal structure (PDB entry: 1CVS) and that of free FGF2 (PDB entry: 4FGF) were obtained from the Protein Data Bank. The sequential "side-by-side" dimer was constructed from 4FGF by translating the coordinates along the 31Å axis.

The linker used in the experiment contained a tripeptide with the sequence of gly-ala-leu, or GAL. However, since the N and C termini of FGF2 in most of the crystal structures are disordered, the modeled linker included the tripeptide sequence and the disordered residues of FGF2. The sequence of the linker was of the form C_{term}-GAL-N_{term}, where C_{term} and N_{term} are the disordered C and N termini of FGF2, respectively. By deleting residues from the disordered N terminus, linkers of different lengths could be obtained. The most optimal structure for each of the linkers was obtained as follows. Combinations of structures for the linker were generated from the C-terminus of one of the FGF2 monomers to the N terminus of the other monomer in both the receptor-bound and sequential dimer using the homology modeling module of Insight II. A good starting structure from the randomly generated linker structures in each FGF2 dimer was subject to energy minimization with the Newton-Raphson method until convergence. Potentials were assigned using the Consistent Valence forcefield, or cvff. Interchanging the N and C termini among monomers did not lead to significant changes in the model of the crosslinked dimer, and therefore it did not affect the interpretation of the results.

A1.3.3 Construction of dimeric FGF2

Based on the results from the conformational studies, the two DNA sequences of FGF2 were ligated and subcloned into an expression vector as outlined in **Figure 3.7**. Selection of *SacI* as part of the linker sequence is based on a detailed analysis on all possible restriction sites in FGF2 and in the expression vector (**Table A1.3**). The *NdeI/SacI* sites were introduced by PCR to the 5' and 3' of the first sequence while *SacI/SpeI* sites were introduced to the second. Both the first and the second sequences encode for the FGF2 with the first 9 N-terminal residues removed.

Aat II	BspH I	**Hpa I**	**Sac I**
Acc I	BspM I	**Kpn I**	**Sac II**
Afl III	BssH II	Mae II	Sal I
AlwN I	BstB I	Mlu I	Sca I
Apa I	**BstE II**	Mme I	Sfe I
ApaL I	**BstX I**	Msc I	**Sfi I**
Ase I	**Bsu36 I**	Nae I	SgrA I
Asp718	Dra I	Nco I	**Sma I**
Avr II	**Dra III**	Nhe I	Sna I
Ban II	Drd I	Nla III	**SnaB I**
Bbs I	Dsa I	**Not I**	Spe I
Bcl I	Ec1136 I	Nru I	Sph I
Bgl I	Eco47 III	**Nsi I**	Spl I
Bgl II	Eco57 I	Nsp I	**Sse8337 I**
Bsa I	EcoR I	Nsp7524 I	Ssp I
BsaA I	EcoR V	NspC I	**Stu I**
BsaB I	Esp I	**Pac I**	Sty I
Bsg I	**Fse I**	PflM I	**Swa I**
Bsm I	Gsu I	**Pml I**	Tfi I
BsmA I	Hae I	Pst I	Xba I
Bsp120 I	Hga I	Pvu I	Xca I
Bsp1286 I	Hinc II	Pvu II	Xma I
BspE I	Hind III	**Rsr II**	Xmn I

Table A1.3.1: The complete list of restriction sites that are absent in wildtype FGF2. Enzymes that are also absent in the pET-14b vector are highlighted in bond. These sites are considered to be used as linker sequence.

To facilitate purification of dFGF2, a 6x His tag and a thrombin cleavage site were introduced by PCR to the 5' of the first sequence, and a T7 tag and another thrombin cleavage site were introduced similarly to the 3' of the second sequence. Upon subcloning of the PCR product of the first sequence into pCR2.1-TOPO (which carries an internal *SpeI* site), a *SacI/SpeI* double digest was performed to linearize the vector. The PCR product from the second sequence was subcloned similarly and the insert was excised by a *SacI/SpeI* double digest. Ligation between the linearized vector and the insert from second sequence resulted in a fused DNA of two tandemly-linked FGF2 DNA sequences. DNA sequencing was performed to confirm the identities of the fused DNA sequences. Protein expression and purification were performed as above except that a T7-affinity column was used as described below (Novagen, Madison, Wisconsin) after Ni-chromatography.

Primer names	Primer sequence (5'→ 3')
BFGF-5'	CAT CAT CAC AGC AGC GGC CTG
Sac-5'	GAG CTC GAC CAG CCC TGC CGG AG
Sac-3'	TCG AGC TCC GCT CTT AGC AGA CAT
THR2	CAT GCT AGC CAT GCT GCC GCG CGG
THR1	GCC GCG CGG CAC CAG GCT CTT AGC
T7TAG2	CAT TTG CTG TCC ACC AGT CAT GCT AGC
T7TAG3	TAC TAG TCA CTA TTA ACC CAT TTG CTG

Table A1.3.2: Primer sequences used for constructing dFGF2.

T7 affinity purification

T7 affinity chromatography was performed essentially as described by the manufacturer (Novagen, Madison, Wisconsin). Briefly, sepharose conjugated with T7 antibodies was loaded to a plastic column (Bio-rad) and the charged column was washed extensively with 10 ml of buffer. Partially purified protein from Ni-chelate chromatography was loaded to the column, washed with 10 ml of buffer and eluted with a low-pH elution buffer. 1-ml fractions were collected for SDS-PAGE analysis.

Immunoblot assay

Immunoblot assays were performed with the 48.1 antibody that specifically recognized the properly-folded form of FGF2. Nitrocellulose membrane (Protran-BA85, Schleicher & Schuell, Keene, New Hampshire) was soaked briefly in Tris-buffered saline or TBS (20 mM Tris, 500mM NaCl, pH 7.5) and was allowed to air-dry. Wildtype FGF2 and sample protein from various elution fractions were applied to the membrane by spotting with a P10 pipette. The membrane was then blocked with 3% gelatin in TBS. After washing in Tween-20/TBS (20 mM Tris, 500mM NaCl, 0.05% Tween-20, pH 7.5), the membrane was incubated overnight with the primary antibody solution (1:1000 dilution of primary antibody in 1% gelatin in TBS). Chemilluscience detection of signals was performed according to manufacturer's instruction (Bio-rad, Hercules, California).

CD spectroscopy

dFGF2 was concentrated to 1 μM and buffer-exchanged into 10 mM sodium phosphate pH 7.2. CD spectroscopy of dFGF2 was performed in a quartz cell with a 1 mm pathlength (Starnz, Atascadero, California) at room temperature. Data were recorded in an average of 20 scans between 195 nm and 260 nm on an Aviv 62SD spectropolarimeter located in the Peter Kim laboratory at the Whitehead Institute.

Protein Mass Spectrometry

MALDI-MS was completed by diluting a solution of FGF2, FGFR1, and a heparinase-derived HSGAG decasaccharide (consisting of a disaccharide repeat unit of [$I_{2S}H_{NS,6S}$]) to 20 μM in 10 mM sodium phosphate pH 7.0. To 1μL of this sample was added an equimolar amount of the purified dFGF2 construct. The sample was allowed to come to equilibrium for 30 minutes at 4°C. 1 μL of the sample was then immediately spotted on the MALDI target with 1μL of a saturated sinapinic acid solution in 50% acetonitrile. After drying, the sample was washed with water, dried under a stream of nitrogen, and subjected to mass spectral analysis. MALDI-MS spectra were acquired in the linear mode using a Voyager Elite reflectron time-of-flight instrument (PerSeptive Biosystems, Framingham, MA) fitted with a 337-nm nitrogen laser. Delayed extraction was used to increase resolution (25 kV, grid at 91%, guide wire at 0.25%, pulse delay 350ns, low mass gate at 2000).

A1.4. Functional Characterization of Dimeric Fibroblast Growth Factor

(Materials and methods related to Chapter 4)

A1.4.1 SMC Proliferation Assay

Smooth muscle cells (SMC) isolated from bovine aorta were maintained in propagation medium supplemented with 10% BCS, 2 mM L-glutamine and antibiotics. The proliferation assay of SMC, as measured by tritium incorporation, was performed as follows. Cells were passaged at 95% confluence and seeded onto 24 well plates at 1 ml per well. After 24 hours, cells were serum-starved in medium supplemented with 0.1% BCS for another 24 hours. An appropriate amount of growth factor was added to 8 wells for each protein concentration tested. 75 mM sodium chlorate was added to half of the wells for each condition. After 21 hours, [^{3}H] thymidine (1μCi/ml) was applied to each well and incubated for 3 hours. Cells were washed with PBS and 0.5 ml 1M NaOH was subsequently added. The contents of each well were transferred to scintillation vials filled with 5 ml ScintiSafe Plus scintillation fluid (Fisher Scientific, Pittsburgh, Pennsylvania). Total [^{3}H] thymidine incorporation was measured by liquid scintillation counting.

A1.4.2 HUVEC Survival Assay

Human umbilical vein endothelial cells (HUVEC) were isolated from human umbilical cords after labor as previously described (Jaffe, *et al.*, 1973) and were cultured on 1% gelatin-coated tissue culture plates in M199 medium supplemented with 20% FBS and bovine brain extract as previously described (Namiki, *et al.*, 1995). Cells in passage three or four were used for the assay. After 24 hours, HUVEC were trypsinized briefly by rinsing with 1 ml trypsin-EDTA and incubating at 37°C for 1 minute. The cells were then rinsed with M199 medium, spun down, washed twice with PBS and resuspended in M199 medium containing 0.5% FBS and 1% BSA. The cells were seeded at a density of approximately 1-2 x 10^4 per well onto 96-well plates coated with fibronectin-like polymer (Sigma, St Louis, Missouri). Appropriate amounts of growth factor were added

to the wells using a multi-channel pipette. Each experimental condition was tested in six different wells. Cell viability was accessed after 18 hours using a colorimetric CellTiter 96 AQ assay (Promega, Madison, Wisconsin). MTS dye containing a tetrazolium salt was added to the cells for 4 hours at 37°C before measuring OD_{490}.

A1.4.3 Angiogenic Assay in the Rat Cornea

Pellets containing sucralfate (a peptic hydrolysis inhibitor) with FGF2 or sucralfate alone were prepared as described by Kenyon *et al* (Kenyon, *et al.*, 1996). Briefly, suspensions of sterile FGF2 solution containing the appropriate amount of wildtype FGF2 (5 μg and 20 μg) and dFGF2 (5 μg) were prepared and speed vacuumed for 5 minutes. 10 μl of 12% Hydron, a non-imflammatory slow release polymer (Langer and Folkman, 1976) in ethanol, was added and the suspension was deposited onto an autoclave-sterilized nylon mesh (pore size 0.4 x 0.4 mm). The mesh was stacked between two layers of fiber covered with a thin film of Hydron. After drying on a sterile petri dish for 30 minutes, the fibers of the mesh were pulled apart. With the aid of a dissecting microscope, uniformly sized pellets were selected from approximately 200 pellets produced. Each pellet contained approximately 1.5 pmole and 6 pmole wildtype FGF2 or 0.7 pmole dFGF2. Control pellets containing no FGF2 were also prepared.

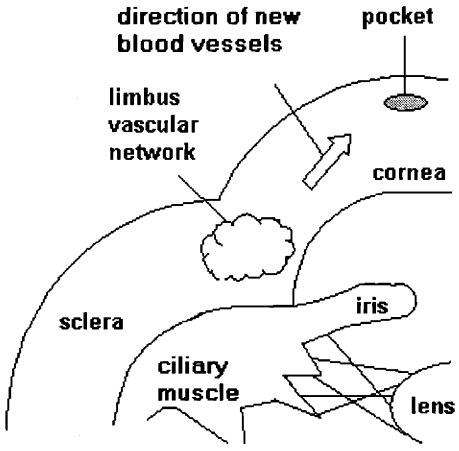

Figure A1.4.1: Schematic representation of implanting of an angiogenic pellet to the cornea.

For pellet implantation, Sprague Dawley rats (male, 400-450 g, n= 5) were anesthetized with Ketamine (80 mg/kg) or Xylazine (10 mg/kg). Using an operating microscope, an intrastromal linear keratomy was performed with a surgical blade (Bard-Parker no. 15; Becton Dickenson, Franklin Lakes, New York) parallel to and 2 mm away from the limbus. A lamellar micropocket was dissected toward the limbus. A single pellet was placed to the base of the pocket with jeweler's forceps. On day 6 after the implantation, the corneal angiogenesis was photographed with a slit lamp. The extent of angiogenesis was quantified in terms of maximum vessel length (VL), which is the linear distance of the sprouting vessels measured from the limbal vascular plexus, and circumferential neovascularization (CN), which is the degree of the circumference covered by the newly-formed vessels.

A1.5 Cell surface HSGAGs

(Materials and methods related to Chapter 5)

A1.5.1 Materials

Recombinant heparinases were expressed as described (Ernst, *et al.*, 1996; Natke, *et al.*, 2000). Heparin was purchased from Celsus Laboratories (Columbus, Ohio). Isopropyl alcohol of spectrophotometric grade was from Mallinckrodt Chemicals (Paris, Kentucky). The BaF3 cell lines transfected with FGFR1c, FGFR2b, FGFR2c and FGFR3c were generously provided by Professor David M. Ornitz (Washington University, St. Louis, Misssouri). DMEM and RPMI-1640 media were from BioWhittaker (Walkerville, Maryland).

A1.5.2 RNA extraction from cultured cells

Total RNA was extracted using the Trizol® reagent (GibcoRBL, Rockville, Maryland). Cells grown at approximately 80-90% confluence were used. For non-adherent cells such as BaF3, ~10^5-10^6 cells were pelleted by centrifugation and washed once with PBS.

1 ml Trizol was added to the cells. For adherent cells such as SMC and EC, cells were rinsed once with PBS followed by addition of 1 ml Trizol. After mixing vigorously for several times, a slurry of granular debris could be observed. The slurry was transferred to a 1.5 ml microcentrifuge tube. 200 μl chloroform was added to the tube followed by vigorous vortexing at room temperature. The tube was centrifuged at 12,000 rpm for 15 minutes at 4°C. The upper aqueous phase was transferred to a new microcentrifuge tube followed by adding 500 μl isoproyl alcohol. The tube was thoroughly vortexed and was placed at room temperature for 10 minutes. After centrifugation at 12,000 rpm for 15 minutes at 4°C, the supernatant was carefully removed without disturbing the pellet at the bottom of the tube. The pellet was washed once with 1 ml 75% chilled DEPC-treated ethanol and was subjected to another centrifugation at 7,500 rpm for 5 minutes at 4°C. The supernatant was carefully removed by aspiration and the pellet was air-dried at room temperature. Once the pellet was fairly dry, 50 μl DEPC-treated water was added for resuspension. The concentration and the quality of the total RNA were determined by measuring OD_{260} and OD_{280}.

A1.5.3 RT-PCR

Complementary DNA (cDNA) was generated by reverse transcription using the SuperScript™ first-strand synthesis system (GibcoRBL, Rockville, Maryland). To detect the expression of different FGFR isoforms, specific oligomers were designed based on the published cDNA sequences of FGFR1c (accession number: X51803), FGFR2b (M97193), FGFR2c (X52832) and FGFR3c (M61881). Sequences of primer pairs specific to different FGFR isoforms were shown in **Table A1.5**.

FGFR1c	Forward	5′-TGG AGC TGG AAG TGC CTC CTC-3′
	Reverse	5′-GTG ATG GGA GAG TCC GAT AGA-3′
FGFR2b	Forward	5′-GTC AGC TGG GGT CGT TTC ATC-3′
	Reverse	5′-CTG GTT GGC CTG CCC TAT ATA-3′
FGFR2c	Forward	5′-GTC AGC TGG GGT CGT TTC ATC-3′
	Reverse	5′-GTG AAA GGA TAT CCC AAT AGA-3′
FGFR3c	Forward	5′-GTA GTC CCG GCC TGC GTG CTA-3′
	Reverse	5′-TCC TTG CAC AAT GTC ACC TTT-3′

Table A1.5: Primer sequences for detecting different isoforms of FGFR.

PCR was performed using the Advantage®-GC cDNA PCR kit (Clontech, Palo Alto, California) following manufacturer's instructions. Each reaction contained 0.5 M GC melt, 10 μM primer, 1 mM dNTP and Advantage-GC cDNA polymerase mix. GC cDNA PCR reaction buffer contains 40 mM tricine-KOH (pH 9.2), 15 mM KOAc, 3.5 mM $Mg(OAc)_2$, 5% dimethyl sulfoxide (DMSO) and 3.75 μg/ml BSA.

A1.5.4 Cell Culture

Bovine SMCs were isolated from fresh calf aortas as described (Nugent, *et al.*, 1993) and maintained in DMEM medium supplemented with 10% calf serum, 100 μg/ml penicillin, 100 U/ml streptomycin and 500 μg/ml L-glutamine. Cells between passage 2 to 8 were used. SMCs were grown in 75 cm^2 flasks at 37°C in a 5% CO_2 humidified incubator and were passaged 1:10 every three days. Cultures were discarded after passage eight. BaF3 cells transfected with various FGFR isoforms were maintained as suspension culture in propagation medium consisting of RPMI-1640 (BioWhittaker) supplemented with 10% calf serum, 2 mM L-glutamine, 100 U/ml penicillin and 100 μg/ml streptomycin and 500 ng/ml mouse recombinant IL-3. Cultures were grown in 75 cm^2 flasks at 37°C/5% CO_2 and were passaged 1:10 by dilution two to three times each week.

A1.5.5 Isolation of HSGAGs from SMCs

Cell surface HSGAG fragments were collected from SMCs as follows. Fully confluent SMCs were trypsinized and diluted 1:10 with the supplemented DMEM medium. 20 ml of suspension culture was added to each of the 12 75 cm^2 tissue culture flasks and the flasks were incubated for 72 hours at 37°C. The flasks were washed once with 20 ml Dulbecco's Modified PBS, and the medium was replaced with 2 ml PBS. HepI, II and III were added to three flasks each to produce concentrations of 200 nM. An equivalent volume of PBS was added to the remaining three flasks. The cells were subsequently incubated for 30 minutes at 37°C. Each of the heparinase- or PBS-treated preparations was collected and centrifuged 10 minutes at 4°C at 4500 x g. The pellet was discarded, and the samples were heated to 50°C for 10 minutes to eliminate residual enzymatic activity. Samples were stored at 4°C until use.

A1.5.6 Compositional analysis

SMC-derived HSGAGs were purified and exchanged into water by centrifugation using a 3,000 MWCO membrane (Millipore Corporation, Bedford, MA). After lyophilization, saccharide amounts were assessed using Alcian Blue with slight modifications from a previous published method (Bjornsson, 1998). For compositional analysis, the sample was treated with 200 nM of hepI, II and III in 25 mM sodium acetate, 100 mM NaCl, 5mM calcium acetate buffer, pH 7.0 (Duteil, *et al.*, 1999; Park, *et al.*, 1999; Rhomberg, *et al.*, 1998; Venkataraman, *et al.*, 1999c). The reaction was allowed to proceed at 30°C overnight to ensure that all HSGAGs were fully digested and then analyzed by capillary electrophoresis in reverse polarity with a running buffer of 50 mM tris/phosphate, 10 μM dextran sulfate pH 2.5. The identity of each disaccharide is shown based on comigration with a known standard.

A1.5.7 Proliferation assay with heparin

BaF3 cells expressing FGFR1c, FGFR2b, FGFR2c or FGFR3c were independently collected by washing three times with propagation medium lacking IL-3. Cells were counted and resuspended to a density of 1 x 10^5 cells/ml in the IL-3 deficient medium. Each of the four resulting cell suspensions was added to a 24-well tissue culture plate at 1 ml/well. Heparin was added to each well to produce a concentration of 500 ng/ml. FGF2 was added to half the wells within each cell type to yield a final concentration of 50 ng/ml. The concentrations of heparin and FGF2 were the equivalent as that shown to elicit the maximal FGF2 mediated cellular response via FGFR1 (Padera, *et al.*, 1999). The cells were incubated for 72 hours at 37°C/5% CO_2. Whole cell number was counted at the experimental endpoint by a Coulter counter. This procedure was repeated three times with each of the cell lines.

A1.5.8 Proliferation assay with SMC-derived HSGAGs

Similar to the proliferation assay with heparin, BaF3 cells expressing various FGFR isoforms were washed and resuspended to a density of 1 x 10^5 cells/ml in IL-3 deficient propagation medium. The cell suspension was divided into 12 samples, 6 ml each. Each sample of cells was centrifuged 3 minutes at room temperature at 1085 x g, and resuspended in 3 ml of the SMC-derived HSGAG preparations in PBS, producing two sets of cells in the same medium. One of each set was supplemented with 50 ng/ml FGF2 while the other was unsupplemented. 1 ml from each set was added to each of the 3 wells on a 24-well tissue culture plate. After 72 hours, whole cell number was counted at the experimental endpoint by the Coulter counter. This procedure was repeated three times. Collected data were normalized using a proliferative index (PI), as previously described (Padera, *et al.*, 1999). The index is defined as the increase in cell number for the experimental case divided by the increase in cell number for the positive control. The positive control was cells in DMEM with 50 ng/ml FGF2, 500 ng/ml heparin, 10% BCS, 2 mM L-glutamine, 100 U/ml penicillin and 100 μg/ml streptomycin. The negative control was same as the positive control except lacking FGF2. The PI was calculated independently for each cell type and each experiment.

A1.6 Apoptosis induced by hepIII-treatment of melanoma cells

(Materials and methods related to Chapter 6)

A1.6.1 Cell proliferation assays

Melanoma cells (B16BL6) and LLC were cultured in DMEM medium supplemented with 10% calf serum, 100 μg/ml penicillin, 100 U/ml streptomycin and 500 μg/ml L-glutamine. For cell proliferation assay, approximately 10^4 cells/ml were seeded in 24-well plates and were allowed to glow to ~70% confluence. HepIII, which had been extensively desalted and buffer-exchanged into PBS, was added to the medium at the designated concentrations. Each experimental condition was tested in four wells. Other conditions were specified in the legends to the figures. Cell proliferation was measured by whole cell counting using Coulter counter and was expressed as a percentage of the averaged maximal cell counts achieved in an experiment.

A1.6.2 Ligation-mediated PCR assay for detection of DNA fragmentation

Detection of DNA laddering pattern was performed using the ApoAlert ligation-mediated PCR (LM-PCR) assay kit from Clontech (Palo Alto, California). Unlike conventional gel electrophoresis method, LM-PCR method provides a semi-quantitative and sensitive means to compare the extent of DNA fragmentation in different samples. Because of the amplification nature of PCR, the LM-PCR method is capable of detecting DNA fragmentation from even a small portion of apoptotic cells. The principle of the assay is schematically illustrated in **Figure A1.6**.

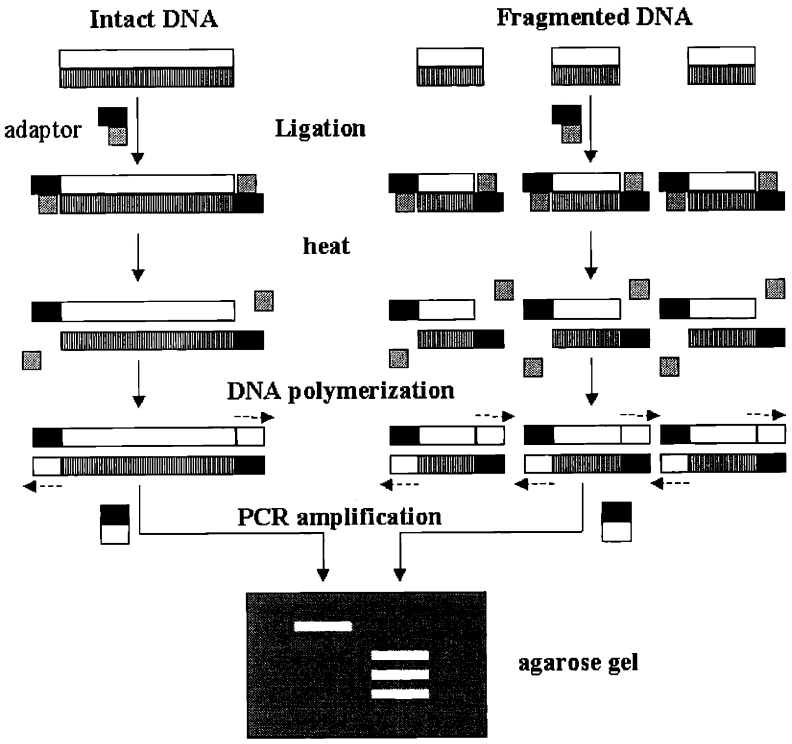

Figure A1.6: Schematic representation illustrating the principle of ligation-mediated PCR assay. Equal amount of genomic DNA is ligated with the ligation adaptors (one strand with 24 nucleotides while the other with 12). After overnight ligation, the DNA's ends are ligated with the adaptors. Note that only the 24-mer is ligated to the DNA fragments due to the presence of 5' phosphorylated blunt ends. The mixture is heated to release the 12-nucleotide strand. The ends of the genomic DNA are then filled up with nucleotides by DNA polymerization. The genomic DNA ligated with specific sequences at both ends, are then ready for PCR. The expected pattern of gel electrophoresis of the PCR products is shown.

LM-PCR was performed following the manufacturer's instruction. Briefly, genomic DNA was isolated from cells treated with 50 nM hepIII for three days as well as untreated cells following standard protocol (Ausubel, *et al.*, 1994). Ligation was carried out overnight with 0.5 μg genomic DNA, the adaptor primer and T4 DNA ligase. Approximately 150 ng of the adaptor-ligated DNA mixture was used as a template in the PCR (94°C, 1 minute and 72°C, 3 minutes for 30 cycles). The PCR products were analyzed by DNA gel electrophoresis.

A1.6.3 Caspase activity assays

The activity of caspase 3, 8 and 9 was determined using the appropriate ApoAlert Caspase kits from Clontech (Palo Alto, California). Apoptosis was induced in melanoma cells by treating with hepIII for 1 or 5 days. Untreated cells served as control. 5 x 10^6 cells were harvested, resuspended in chilled lysis buffer and centrifuged at 4°C. The appropriate reaction mixture and substrates were applied to the cell lysate as described in the manufacturer's instruction. The reaction mixtures were incubated at 37 °C for 2 hours in the dark. A microplate reader was used to measure the emission from the reaction mixtures. Background readings were subtracted from the sample readings. The fold-increase in caspase activity is determined by comparing the reading of the samples with that of the uninduced control.

A1.6.4 cDNA microarray

The cDNA microarray membranes (Atlas Mouse Cancer 1.2 Array) and reagents for labeling cDNA probes were purchased from Clontech (Palo Alto, California). Total RNA was isolated from hepIII-treated and control cells on day 3 using the protocol described in **A1.5.2**. Procedures for RT and hybridization were performed as recommended by the manufacturer (Clontech) with slight modifications. Briefly, 5 μg total RNA was first DNase-treated with DNaseOUT (GibcoBRL, Rockville, Maryland) prior to reverse-transcription. The DNase treatment ensured the removal of contaminating genomic DNA in the RNA sample. The cDNA was labeled by

incorporating [α-^{32}P] dATP during first strand synthesis. Control poly A+ RNA was used as control to assess the labeling efficiency. The labeled cDNA probes were purified using Sephadex G-50 Quick Spin columns (Roche, Indianapolis, Indiana). The two cDNA probes of approximately equal radioactivity were added to the respective microarray membranes and hybridization was performed in a hybridization oven (Bellco, Vineland, New Jersey) at 68°C overnight. The membranes were washed three times with 2X SSC, 1%SDS for 30 minutes each at 68°C with continuous agitation, followed by another 30-minute wash with 0.1X SSC, 0.5%SDS for 30 minutes at 68°C. The membranes, wrapped in plastic wrap, were exposed to a phosphorimaging screen in an exposure cassette (Molecular Dynamic, Sunnyvale, California) for 3 to 5 days. The hybridization images were acquired with a Storm 840 optical scanner (Molecular Dynamic, Sunnyvale, California) interfaced with a PC workstation. Image analysis was carried out with the ImageQuant software (version 5).

Appendix 2. HSGAG-binding sites in FGF1, 2 and KGF

Summary:

The mechanism of signal transduction by the fibroblast growth factors involves binding to their transmembrane tyrosine kinase receptors (FGFRs) and heparan sulfate glycosaminoglycans (HSGAGs) that are present ubiquitously on the cell surface and in the extracellular space. HSGAGs have been implicated to play a role in modulating the FGF-FGFR interaction, which induces receptor dimerization that subsequently triggers a cascade of intracellular signaling events. Although there is abundant biochemical and structural information on the FGF-HSGAG interactions particularly in the case of FGF1 and FGF2, there is little knowledge on the structural determinants of specificity in these interactions. In this study through homology modeling we have investigated the structure of keratinocyte growth factor (KGF), characterized the molecular features of the HSGAG binding site on KGF and compared these features with those on FGF1 and FGF2. Our study indicates that there are distinct differences in the molecular features of the HSGAG binding domains in these proteins, and these are manifested by the differences in the number and spatial distribution of basic residues (lysines and arginines), thereby imposing different structural requirements on the HSGAG chain for optimal interaction.

A2.1 Introduction

Glycosaminoglycan-protein interaction is important in dictating a broad spectrum of biological functions including anticoagulation, morphogenesis and viral infection (see section 1.4.6 in Chapter 1). There is abundant structural and biochemical information on the interaction of HSGAG with FGF1 and FGF2. Site-directed mutagenesis studies (Wong and Burgess, 1998), co-crystal structures (DiGabriele, *et al.*, 1998; Faham, *et al.*, 1996; Pellegrini, *et al.*, 2000; Schlessinger, *et al.*, 2000) and NMR structures (Moy, *et al.*, 1997) all point to a specific interaction between a unique HSGAG sequence and the basic HSGAG binding pocket in FGF1 and FGF2. It is probable that distinct structural determinants on FGFs confer specificity towards binding with distinct sequences on HSGAGs (Guimond, *et al.*, 1993; Ishihara, *et al.*, 1995; Rahmoune, *et al.*, 1998). Heparin, which is commonly used in experiments as a substitute for heparan sulfate, was well known for its ability to enhance FGF1 and FGF2 activities but inhibit KGF (FGF7) mitogenic signaling (LaRochelle, *et al.*, 1999). HSGAGs have been reported to cause differential effects in the binding of FGF1 and KGF to KGFR (Reich-Slotky, *et al.*, 1994). The specificity of interaction between different HSGAGs with FGF2 and KGF has also been demonstrated *in vivo* where these proteins were shown to interact with distinct HSGAGs in different extracellular compartments of tissues (Friedl, *et al.*, 1997). However, the sequence and structural basis of such differences in interaction between HSGAGs and KGF as compared to FGF1 or FGF2 is poorly understood.

In this study, we examined the structural features of KGF in comparison to FGF1 and FGF2 so as to elucidate the molecular basis for structural specificity for HSGAG binding to these proteins. We found that in addition to the differences in the number of basic residues in the HSGAG binding pocket, there were significant differences in the distribution of these basic residues. The spacing and the topology of the basic residues not only provided differential features to the HSGAG binding pocket in the protein, but also provided the specificity associated with HSGAG binding.

A2.2 Homology modeling of KGF

The crystal structure of a biologically active KGF, in which the first 23 residues were deleted and a R144Q mutation was introduced, has been described (Osslund, *et al.*, 1998) although the coordinates are not available for public access. The structure revealed striking similarity in C_α trace to FGF1 and FGF2 (except in a loop region that was believed to be the receptor-binding site) (Osslund, *et al.*, 1998), suggesting that all members in the FGF family may share a common structural foil (Eriksson, *et al.*, 1993; Zhang, *et al.*, 1991; Zhu, *et al.*, 1991). Based on the sequence alignment of KGF and FGF2 (Osslund, *et al.*, 1998), we modeled KGF structure by using the homology module of INSIGHT II (Molecular Simulations, Burlington, Massachusetts). This KGF structure was subject to energy minimization (potentials assigned using CVFF force field) first without charges then with charges using steepest descent method, until convergence. Superposition of this structure to the FGF2-hexasaccharide co-crystal structure (rms deviation = 0.82) fixed the spatial orientation of the HSGAG hexasaccharide (H1) with respect to KGF. It is important to note that our KGF (human) structure is in good agreement with the recently solved rat KGF structure (PDB code: 1QQL) (Ye, *et al.*, 2001). KGF adopted a β-trefoil core comprising of three 4-stranded β-sheets related by an approximate three-fold symmetry. The C_α trace of FGF2 and KGF coincided in most regions except for a loop region between β9 and β10 on KGF that has been implicated to play a role in conferring specificity to KGF-KGFR interactions (Osslund, *et al.*, 1998; Sher, *et al.*, 1999). By superimposing the modeled KGF structure over the FGF2-hexasaccharide structure and by removing FGF2 but not the hexasaccharide, a modeled structure of KGF complexed with a HSGAG chain was generated (**Figure A2.1-3**).

Inspection on the modeled KGF-hexasaccharide structure (**Figure A2.4**) revealed nine residues that made contact with various groups on H1 (**Table A2.1**). Three of those residues (K147, N137 and K139) have not been identified previously from the structural alignment of HSGAG-binding residues based on the FGF2-hexasaccharide co-crystal (Faham, *et al.*, 1998; Faham, *et al.*, 1996).

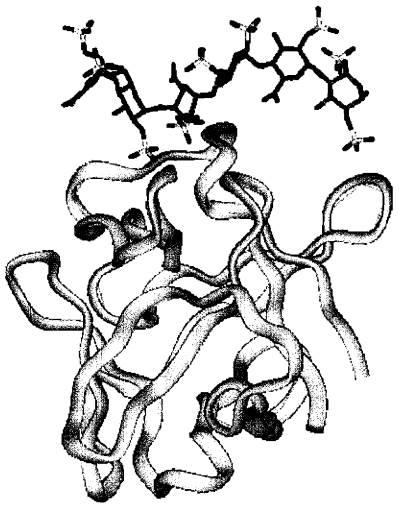

Figure A2.1: FGF2-hexasaccharide co-crystal structure. FGF2 is rendered in gray while the hexasaccharide HSGAG chain is colored by atom (green for carbon, red for oxygen, blue for nitrogen and yellow for sulfur). The structure (PDB code: 1BFC) was solved by Faham *et al.*

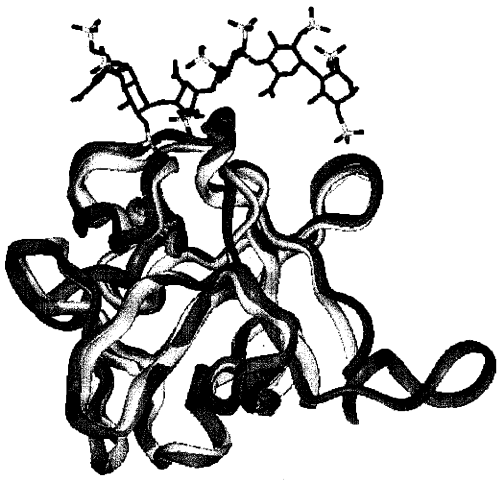

Figure A2.2: Superposition of KGF onto the FGF2-hexasaccharide co-crystal structure. The KGF structure (colored in cyan) was modeled by homology modeling and was superimposed onto the FGF2-hexasaccharide structure for visualization.

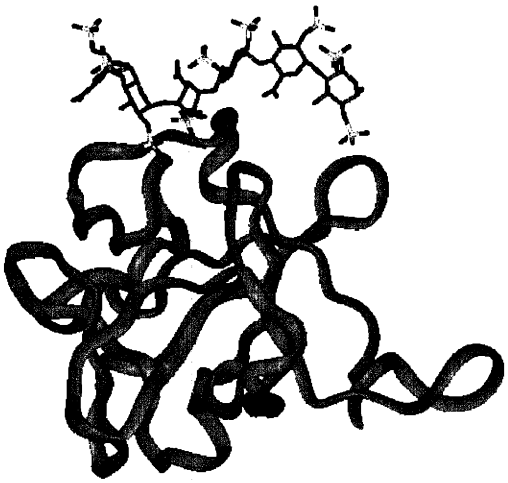

Figure A2.3: The modeled KGF-hexasaccharide structure. A KGF-hexasaccharide structure was generated by removing the FGF2 structure.

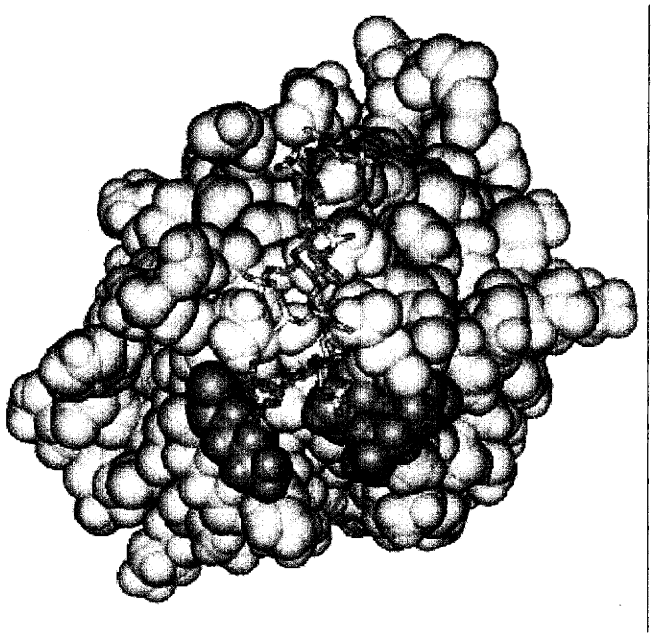

Figure A2.4: KGF-hexasaccharide structure. The CPK rendered structure of the KGF obtained from homology modeling is shown in gray with the docked structure of H1 (rendered as stick representation) colored by atom. The putative HSGAG-binding residues inferred from sequence homology with FGF2 are colored yellow. Three additional HSGAG-binding residues inferred from the KGF structure are shown in red.

HSGAG residue	Group	KGF residue	Group
I-1	COO-	**Lys 147**	NZ
H-2	NS	**Asn 137**	ND2
H-2	NS	Gln 138	NH
H-2	NS	Gln 152	NE22
H-2	NS	Thr 154	NH
H-2	NS	**Lys 139**	NH
I-3	OH (C3)	Thr 42	OG1
I-3	COO-	Gln 138	NE2
I-3	2S	Thr 154	NH
I-3	OH (C3)	Lys 153	NZ
I-3	2S	Gln 152	NE2
I-3	2S	Lys 153	NZ
I-5	COO-	Lys 153	NZ
H-6	NS	Arg 41	NH1
H-6	OH (C3)	Arg 41	NH2

Table A2.1: Putative residues in the HSGAG binding site of KGF. Column 1 shows the monosaccharide and its sequence number (numbering starting at 1 from non-reducing

end). Column 2 shows the groups on the monosaccharide (for the hydroxyls, the atom to which it is attached is indicated in parenthesis) that make ionic contacts with the corresponding groups (shown in column 4) on the residues of KGF shown in column 3. The three residues other than those which have homology with the residues described in the HSGAG binding site on FGF2 (Faham, *et al.*, 1998) are bolded.

The sequence comparison of the eight HSGAG-binding residues identified previously (Faham, *et al.*, 1998; Faham, *et al.*, 1996) and the three residues identified in this study is tabulated in **Table A2.2**. The eight residues are all located in the loop regions between adjacent β-sheets: R41 and T42 between β1 and β2, N115, Q138, V143, Q152, K153 and T154 between β9 and β10. These residues were clustered on one side of the molecule to form a region resembling a triangle (colored yellow in **Figure A2.4**). For the other three residues identified from the KGF-hexasaccharide structure (N137, K139, K147; colored red), they were located between β9 and β10. Topologically, these residues were positioned outside the base of the HSGAG-binding domain (colored red in **Figure A2.4**) and the side chains were in close proximity to the non-reducing end of the HSGAG chain. In the FGF1 crystal structure (DiGabriele, *et al.*, 1998), two molecules of FGF1 were shown to bind to the opposite sides of a decasaccharide through two sets of overlapping heparin-binding residues (Faham, *et al.*, 1998). Interestingly, the corresponding residues of the three additional heparin-binding residues of KGF identified here were also represented in the FGF1 dimeric structure: R122 (K147 in KGF) in one FGF1 molecule, and K112, N114 and R122 (N137, K139 and K147 in KGF) in the other FGF1 molecule. Across the HSGAG-binding domain of KGF, N115 and N137 were positioned near the distal ends of the hexasaccharide covering a distance of 20.96 Å between of the two residues.

	KGF	FGF2	FGF1	affinity
	R (41)	**K (27)**	S (17)	low
	T (42)	N (28)	N (18)	high
	N (115)	N (102)	N (92)	low
	Q (138)	**R (121)**	**K (113)**	high
	V (143)	**K (126)**	**K (118)**	high
	Q (152)	Q (135)	Q (127)	high
	K (153)	**K (136)**	**K (128)**	low
	T (154)	A (137)	A (129)	low
Number of basic residues:	2	4	3	

	KGF	FGF2	FGF1
	N (137)	**K (120)**	**K (112)**
	K (139)	T (122)	N (114)
	K (147)	**K (130)**	**R (122)**
Number of basic residues:	2	2	2
Total number of basic residues:	4	6	5

Table A2.2: Sequence comparison of the HSGAG binding site in KGF with FGF1 and FGF2. Comparison of the structurally homologous residues in the HSGAG binding site of KGF, FGF2 and FGF1 is shown. The top panel shows the sequence comparison of HSGAG-binding residues identified from the FGF2-hexasaccharide co-crystal. The lower panel shows the three additional residues implicated for HSGAG binding. The basic residues R and K are bolded and the total number of basic residues in the HSGAG binding site in each protein is shown in the last row. Note that there is very little sequence homology between the residues in the HSGAG binding site of these three proteins.

A2.3 Sequence comparison of the HSGAG-binding domains in FGF1, FGF2 and KGF

Members of the FGF family were believed to bind HSGAG with different affinities. Wong *et al* demonstrated that FGF2 bound heparin with the highest affinity (1.2M NaCl for elution), compared to FGF1 (0.9M-1.1M) and KGF (0.6M-0.8M) (Wong and Burgess, 1998). Differential heparin affinity might be attributed to sequence

variation within the HSGAG-binding domain since sequence alignment of HSGAG-binding residues in the FGF family showed that none of those residues was absolutely conserved (Faham, *et al.*, 1998). To make general observations on the patterns of HSGAG-binding residues, we aligned the 11 residues identified from the KGF-hexasaccharide structure and compared sequence variation in FGF1, FGF2 and KGF. The FGF2-hexasaccharide co-crystal structure (Faham, *et al.*, 1996) revealed eight residues that made either high or low affinity contacts with the heparin chain (**Table A2.2**). All except one residue (A137) interacted with heparin by side chain interaction. Four out of eight residues in FGF2 were basic (one arginine and three lysines) and two of them occupied high affinity sites. Sequence alignment of those eight residues showed that three were basic in FGF1 (all lysines and two in high affinity site) and two in KGF (one arginine, one lysine and both in low affinity site). Basic residues had been shown to play an important role in HSGAG binding, with higher affinity contributed by arginine than lysine (Fromm, *et al.*, 1995). As a result, the frequency of basic residues and their occupancy in high affinity sites may correlate with the observed highest heparin affinity in FGF2. Likewise, the lack of basic residue in the high affinity site of KGF may correlate with the lowest heparin affinity. In addition, the presence of threonine and valine in the high affinity site of KGF might lower the affinity of KGF towards heparin (Faham, *et al.*, 1996). Sequence alignment of the other three residues located outside the HSGAG-binding domain showed that two of the three residues were basic in each of the growth factors (**Table 2A.2**). Taking all 11 residues into consideration, FGF2 had the most (six) HSGAG-binding basic residues followed by FGF1 (five) and KGF (four). Therefore, the number of HSGAG-binding basic residues may correlate with the affinities exhibited by different FGF proteins.

A2.4 Topological mapping of basic residues on FGF1, FGF2 and KGF

It was long observed that the HSGAG-binding domain in FGF2 carried an unusually high positive electrostatic potential contributed by a cluster of basic residues. Lysine and arginine were frequently represented in heparin-binding peptides (Fromm, *et*

al., 1995) and they were able to make efficient ionic interactions with the sulfate or carboxylate groups on heparin. To extend the observations based on sequence alignment, we mapped the basic and non-basic residues onto the corresponding structures for visualization (**Figure A2.5**). All the structures were positioned the same way such that the hexasaccharide chain would align vertically in the center of each structure for comparison purpose. As expected, the 11 residues in each of the three structures were mapped closely to one another on the same side of the proteins although their primary sequences were located on two separate loops. Of particular interest were the different patterns observed among the three structures due to uneven distribution of the basic residues As shown in **Figure A2.5**, the basic residues in FGF2 and FGF1 implicated in HSGAG binding are more localized than that of KGF. In KGF, the HSGAG binding residues are distributed in the periphery, leaving a pocket of non-basic residues in the center. The spacing between the clusters of basic residues at the periphery of the HSGAG binding pocket of FGF1 and FGF2 is about 17 Å and that in KGF is about 19 Å. As discussed below, this wider spatial distribution of the basic residues in KGF as compared to FGF1 and FGF2 may reflect the differential HSGAG affinities exhibited by different FGF members.

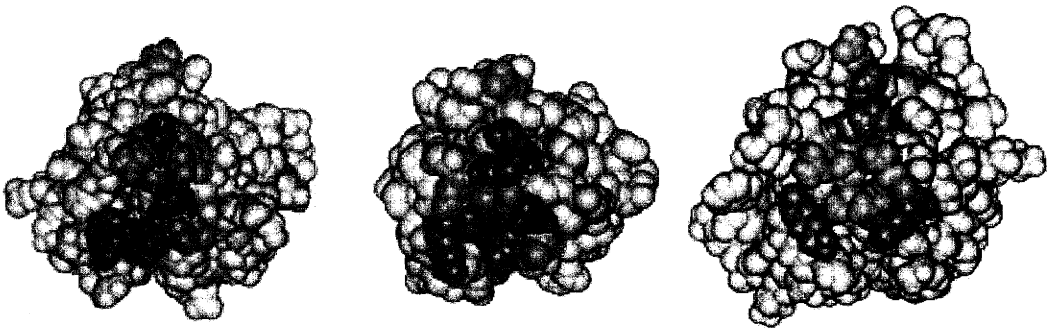

Figure A2.5: Topological mapping of HSGAG-binding residues in FGF1, FGF2 & KGF. All three growth factors are aligned the same way such that the hexasaccharide chain would be vertically positioned across the protein as in **Figure A2.4**. Basic residues (lysine and arginine) are colored purple and non-basic residues are colored green. Note

that there are two clusters of basic residues in the periphery of the binding site separated by non-basic (mostly hydrophilic) residues forming a pocket in all the three proteins. The spacing between the cluster of basic residues in FGF1 and FGF2 are very similar and is significantly less than that in KGF.

A2.5 Discussion

To explore the molecular interaction between FGFs and HSGAGs, we examined the HSGAG-binding domains of FGF1, FGF2 and KGF by comparing their sequence alignments and three-dimensional structures. Three aspects make these growth factors ideal for comparison. First, crystal structures of the growth factors are available for detailed structural analysis. In particular, the FGF2-hexasaccharide co-crystal structure enabled us to examine the interactions between various groups on the protein and on the HSGAG chain. Second, the affinities toward heparin differ significantly among these FGF proteins, with the highest affinity exhibited by FGF2 and lowest by KGF. Third, the biological properties of these growth factors are distinct. For instance, FGF1 and FGF2 are potent mitogens on cell types derived from mesoderm and neuroectoderm whereas KGF acts exclusively on epithelial cells in a paracrine fashion (Gospodarowicz, *et al.*, 1987). The modulating effect by heparin may also be specific to the type of growth factors. It is well known that heparin was able to enhance proliferation in cells treated with FGF1 but the opposite pattern was observed in KGF-stimulated cells (LaRochelle, *et al.*, 1999; Ron, *et al.*, 1993). Our observations on sequence alignment and topological mapping of HSGAG-binding basic residues pointed to a possible mechanism by which favorable interaction between FGFs and HSGAGs of different sulfation levels could be achieved. In this model, the spatial arrangement of basic residues in the HSGAG-binding domain on FGF would determine the affinity towards a particular HSGAG sequence. FGF2, with more basic residues centrally clustered in the HSGAG-binding domain, would interact more favorably with a highly sulfated HSGAG such as heparin. KGF, with fewer basic residues dispersed in the periphery of the HSGAG-binding domain, would favor interaction with a less sulfated HSGAG such as heparan sulfate. This model extends a previous proposal by Fromm *et al* in which the linear spacing between basic

residues on a protein conferred the specificities of heparin-binding versus heparan sulfate-binding (Fromm, *et al.*, 1997). Consistent with the present model, Reich-Slotky *et al* reported that the level of sulfation in HSGAGs correlated with KGF binding to its receptor and that KGF binding was about three-fold higher with heparan sulfate than heparin (Reich-Slotky, *et al.*, 1994). Despite the low heparin affinity exhibited by KGF, its disperse arrangement of HSGAG-binding basic residues could favor interaction with less-sulfated HSGAG such as heparan sulfate. In tissue staining of renal carcinoma, KGF binding to heparan sulfate on basement membrane was stronger than FGF2 although FGF2 staining was generally higher in most other tissues examined (Friedl, *et al.*, 1997), suggesting that KGF-heparan sulfate interaction may be highly specific to the subcellular location and the pathological stage. Further, an optimal KGF-heparan sulfate interaction may modulate the activity induced by KGF. Bonneh-Barkay *et al* reported that heparan sulfate isolated from glypican was more potent in inhibiting KGF-stimulated cell proliferation than heparin (Bonneh-Barkay, *et al.*, 1997). Together, these reports pointed to the biological significance of differential HSGAG affinities exhibited by different FGF proteins in modulating the activity of growth factors.

Appendix 3. Experimental data

A3.1 Data for the SMC proliferation study

(Chapter 4)

Experimental protocol for the SMC proliferation assay is provided in Section A1.4.1. Molar concentrations of growth factors were calculated based on the theoretical molecular weights of the wildtype (18702) and dimeric FGF2 (37066). Each experimental condition was duplicated in two wells. Scintination counts of the two samples are shown in the following table. The average and standard deviation of the two samples in a single experiment are provided.

WT (without chlorate)

Conc (pM)	Scintination count of Sample 1 (cpm)	Scintination count of Sample 2 (cpm)	Average (cpm)	Standard deviation
0	1272	1509.6	1390.8	168.0086
5.8	1297.2	1484.2	1390.7	132.229
58	2037.4	1481	1759.2	393.4342
580	2304.6	2736.4	2520.5	305.3287
5800	3740	2576.8	3158.4	822.5066
58000	2838.4	2732.8	2785.6	74.67048

dFGF2 (without chlorate)

Conc (pM)	Scintination count of Sample 1 (cpm)	Scintination count of Sample 2 (cpm)	Average (cpm)	Standard deviation
0	1416.6	1509.2	1462.9	65.47809
2.7	1600.4	1359.8	1480.1	170.1299
27	1743.8	1663.4	1703.6	56.85139
270	3111.4	2993.8	3052.6	83.15576
2700	2865.2	3383.4	3124.3	366.4227
27000	3458.4	2661	3059.7	563.8469

WT (with chlorate)

Conc (pM)	Scintination count of Sample 1 (cpm)	Scintination count of Sample 2 (cpm)	Average (cpm)	Standard deviation
0	1394.8	1414.2	1404.5	13.71787
5.8	1685.2	1564.6	1624.9	85.27708
58	2320.6	2069	2194.8	177.9081
580	3299.3	3630.7	3465	234.3352
5800	2978.1	3068.9	3023.5	64.2053
58000	1958	1851.8	1904.9	75.09474

dFGF2 (with chlorate)				
Conc (pM)	Scintination count of Sample 1 (cpm)	Scintination count of Sample 2 (cpm)	Average (cpm)	Standard deviation
0	1285.4	1594.8	1440.1	218.7788
2.7	1527.2	1296.6	1411.9	163.0588
27	1413.2	1603.8	1508.5	134.7746
270	2117.2	1700.4	1908.8	294.7221
2700	2417.4	2404.6	2411	9.050967
27000	1897	1740.4	1818.7	110.7329

Table A3.1: Unprocessed data of the SMC proliferation assay. Column one: molar concentration of the protein tested; column two: scintination count of sample 1; column three: scintination count of sample 2; column four: the average of columns two and three; column five: the standard deviation of columns two and three. This set of data is obtained from a single experiment.

A3.2 Data for the HUVEC survival study

(Chapter 4)

Experimental protocol for the HUVEC survival assay is provided in Section A1.4.2. The OD_{490} readings of the positive control (10% FCS), negative control (0), and various growth factor concentrations are shown below. The average and standard deviation (S.D.) are provided.

	10% FCS	0	WT 515 pM	WT 2.575 nM	WT 5.150 nM	dFGF2 270 pM	dFGF2 1.350 nM	dFGF2 2.7 nM
	0.39	0.187	0.189	0.219	0.246	0.216	0.27	0.276
	0.305	0.215	0.195	0.246	0.254	0.193	0.242	0.272
	0.526	0.24	0.187	0.254	0.299	0.221	0.231	0.271
	0.503	0.186	0.162	0.264	0.285	0.211	0.216	0.239
	0.355	0.178	0.186	0.275	0.255	0.216	0.246	0.257
	0.372	0.197	0.203	0.248	0.228	0.232	0.223	0.256
Average:	0.4085	0.2005	0.187	0.251	0.2612	0.215	0.238	0.262
S.D.:	0.087	0.023	0.014	0.019	0.026	0.013	0.019	0.014

Table A3.2: Unprocessed data of the HUVEC survival assay. The results are representative of three sets of experiments. Each experimental condition was repeated in six wells.

A3.3 Data for the HSGAG-mediated FGF activity study

(Chapter 5)

Experimental protocol for the BaF3 cell proliferation assay is provided in Section A1.5.8. Six sets of unprocessed data from three different receptor isoforms, with and without FGF2 treatment, are presented in the following tables. Cell counts from different

experimental conditions are reported below. The average and standard deviation (S.D.) are provided.

FGFR1C/+FGF

	PBS	+ heparin	HepI	HepII	HepIII
	4958	6028	5302	6139	5876
	5996	6160	5689	5889	6734
	5729	6249	4510	6480	6732
Average:	5561	6145.5	5166.8	6169.2	6447.2
S.D.:	539.1	111	600.9	296.7	495.1

FGFR1C/-FGF

	PBS	+ heparin	HepI	HepII	HepIII
	4518	3599	4515	3898	3522
	4304	3753	3652	3630	4349
	3906	3264	4424	4056	3338
Average:	4242.5	3538.3	4196.7	3861.2	3736.2
S.D.:	310.5	250.1	474.3	215.6	538.6

FGFR2C/+FGF

	PBS	+ heparin	HepI	HepII	HepIII
	2714	2874	2819	2978	2814
	2820	3032	2550	2840	2722
	2907	3026	2731	2684	2976
Average:	2813.7	2976.8	2700	2834	2837.3
S.D.:	96.7	89.5	137.2	147.1	128.6

FGFR2C/-FGF

	PBS	+ heparin	HepI	HepII	HepIII
	2304	2482	2309	2459	2271
	2551	2649.5	2625	2308	2307
	2358	2320.5	2694	2528	2587
Average:	2404.3	2484	2542.7	2431.7	2388.3
S.D.:	129.9	164.5	205.3	112.5	173

FGFR3C/+FGF

	PBS	+ heparin	HepI	HepII	HepIII
	4940	7736.5	5104.5	5430	3993
	4268	8208	5486	5103	4203
	3699	7972	5295	4828	4632
Average:	4302.3	7972.3	5295	5120.2	4275.7
S.D.:	621.2	333.4	269.4	301.4	326

	FGFR3C/-FGF				
	PBS	+ heparin	HepI	HepII	HepIII
	4267	4060	3917	4164	4230
	4865	4356	4405	3487	4602
	4633	4238	5034	3776	4799
Average:	4587.8	4218	4451.8	3809	4543.3
S.D.:	301.5	149	559.7	339.7	289

Table A3.3: Unprocessed data of the HSGAG-mediated FGF2 activity assay. BaF3 cells transfected with three different FGFR isoforms (FGFR1C, FGFR2C and FGFR3C) were stimulated in the presence and absence of FGF2. Proliferation was measured by whole cell counting.

A3.4 Data for the hepIII-mediated growth suppression study
(Chapter 6)

Experimental protocol for the following assays is provided in Section A1.6.1. Cell counts from different experimental conditions were reported below. The average and standard deviation (S.D.) are provided.

	Day 1	Day 2	Day 3	Day 4	Day 5
	2760	3100	4545	3564	471
	2655	3025	4669	3789	513
	2794	3124	4729	3509	514
	2697	3178	4451	3726	459
Average:	2726.5	3106.8	4598.5	3647	489.3
S.D.:	62.35	63.52	124.66	132.1	28.4

Table A3.4: Unprocessed data of the time-course study of hepIII treatment. HepIII was added each day for up to 5 days to culture medium where B16 melanoma cells grew. Proliferation was measured by whole cell counting.

	0 nM	0.1 nM	1 nM	10 nM	100 nM
	3262	1887	2412	1797	1550
	3339	1950	2410	1807	1499
	3246	1910	2414	1775	1527
	3368	1778	2382	1824	1538
Average:	3303.8	1881.3	2404.5	1800.8	1528.5
S.D.:	59	73.6	15.1	20.5	21.8

Table A3.5: Unprocessed data of the dose-response study of hepIII treatment. B16 melanoma cells were treated with different concentrations of hepIII for 3 days. Proliferation was measured by whole cell counting.

	PBS	Denatured hepIII	Native hepIII
	3270	2359	57
	3304	2366	48
	3417	2333	48
	3366	2414	34
Average:	3339.3	2368	46.8
S.D.:	65.3	33.8	9.5

Table A3.6: Unprocessed data of the denaturation study. PBS serves as a negative control. HepIII was partially heat-denatured (Denatured hepIII) and was added to the culture medium. Native hepIII serves as a positive control.

	Control	2 day hep	2 day hep CM
	3223	2113	1927
	3305	2260	2198
	3080	1933	2134
	3026	2064	2089
Average:	3158	2092.4	2086.9
S.D.:	128.5	135	115.7

Table A3.7: Unprocessed data of the 2-day hepIII conditioned medium study. As described in the figure legend to Figure 6.7, B16 melanoma cells were treated with hepIII for 2 days (2 day hep) or were cultured in the conditioned medium derived from the conditioned medium derived from hep-treated cells (2 day hep CM).

	Control	w/o hep CM	w/ hep CM
	2351	1586	1151
	2369	1650	1540
	2290	1755	1459
	2338	1576	1167
Average:	2336.6	1641.5	1329
S.D.:	33.9	82.2	199.2

Table A3.8: Unprocessed data of the conditioned medium study. As described in the figure legend to Figure 6.8, conditioned media derived from untreated cells (w/o hep CM) and hepIII-treated cells (w/ hep CM) were assayed for their ability to inhibit cell proliferation.

	Control	Hep III
	3918	1564
	3928	2050
	4185	1824
	4346	2684
Average:	4094.1	2030.3
S.D.:	208.2	478.6

Table A3.9: Unprocessed data of the Lewis lung carcinoma cell proliferation study. Lewis lung carcinoma cells were treated with 50 nM hepIII for three days. Cell proliferation was measured by whole cell counting.

Caspase 3 activity assay

OD 405
Negative control (medium only): 0.040

	Untreated control	HepIII-treated	Untreated control minus background	HepIII-treated minus background	Induction
1 Day	0.069	0.120	0.029	0.08	2.8
5 Day	0.087	0.128	0.047	0.088	1.9

Caspase 8 activity assay

OD 405
Negative control (medium only): 0.047

	Untreated control	HepIII-treated	Untreated control minus background	HepIII-treated minus background	Induction
1 Day	0.162	0.302	0.115	0.255	2.2
5 Day	0.065	0.294	0.018	0.247	13.7

Caspase 9 activity assay

OD 405 (Fluorescence)
Negative control (medium only): 27.045

	Untreated control	HepIII-treated	Untreated control minus background	HepIII-treated minus background	Induction
1 Day	41.3	45.9	14.3	18.8	1.3
5 Day	57.0	59.7	30.0	32.6	1.1

Table A3.10: Unprocessed data of the caspase activity assays. Readings of the negative control (medium only, with substrate but no cells), untreated cells and hepIII-treated cells are presented above. The background-adjusted readings for the untreated controls and treated samples are shown. Induction of caspase activity is calculated as the ratio of the background-adjusted hepIII-treated reading to the untreated reading. Representative results are presented here.

Effect of HSGAG fragments isolated from the cell surface

	Control (without fragment)				
	Day 1	Day 2	Day 3	Day 4	Day 5
	486	962	1079	1083	968
	456	912	1021	1020	864
	460	944	1075	1078	885
	419	956	1005	1028	861
Average:	455.3	943.5	1045	1052.3	894.5
S.D.:	27.6	22.3	37.6	32.8	50.1

	HSGAG fragment				
	Day 1	Day 2	Day 3	Day 4	Day 5
	479	919	995	1088	1120
	392	860	965	1063	1031
	396	866	964	985	1041
	395	842	934	1016	1035
Average:	415.5	871.8	964.5	1038	1056.8
S.D.:	42.4	33.1	24.9	46.3	42.4

Table A3.11: Unprocessed data of the HSGAG fragment study. Unpublished data from the time-course proliferation study using HSGAG fragments isolated from B16 cells by Nishla Keiser.

Abbreviation

2S	2-O sulfation
6S	6-O sulfation
ATIII	Antithrombin III
BCS	bovine calf serum
CAM	Chorioallantoic membrane
CD	Circular dichroic
CVFF	Consistent Valence forcefield
dFGF2	Dimeric FGF2
Dpp	Decapentaplegic
EC	Endothelial cell
ECM	Extracellular matrix
FBS	Fetal bovine serum
FCS	Fetal calf serum
FGF	Fibroblast growth factor
FGFR	Fibroblast growth factor receptor
GPI	Glycosylphosphatidylinositol
H	Hexosamine
Hep	Heparinase
Hh	Hedgehog
HSGAG	Heparan sulfate glycosaminoglycan
HUVEC	Human umbilical vein endothelial cell
IAA	Iodoacetic acid
Ig	Immunoglobulin
IL	Interleukin
LLC	Lewis lung carcinoma
MALDI-MS	Matrix assisted laser desorption ionization-mass spectrometry
NGF	Nerve growth factor
NAc	N-acetylation
NS	N-sulfation
OD	Optical density
PAPS	3'-phosphoadenosine-5'-phosphosulfate
PCR	Polymerase chain reaction
PDB	Protein Data Bank
PDGF	Platelet derived growth factor
PEN	Property encoded nomenclature
PI	Proliferation index
RT	Reverse transcription
SH	Src-homology
SMC	Smooth muscle cell
TGF	Transforming growth factor
TOPO	Topoisomerase
U	Uronic acid
UV	Ultraviolet
Wg	Wingless

Bibliography

Adachi, T., Fukushima, T., Usami, Y., and Hirano, K. (1993) Binding of human xanthine oxidase to sulphated glycosaminoglycans on the endothelial-cell surface. *Biochem J* **289**(Pt 2):523-527.

Adams, M. D., Kerlavage, A. R., Fleischmann, R. D., Fuldner, R. A., Bult, C. J., Lee, N. H., Kirkness, E. F., Weinstock, K. G., Gocayne, J. D., White, O., and et al. (1995) Initial assessment of human gene diversity and expression patterns based upon 83 million nucleotides of cDNA sequence. *Nature* **377**(6547 Suppl):3-174.

Afford, S. C., Randhawa, S., Eliopoulos, A. G., Hubscher, S. G., Young, L. S., and Adams, D. H. (1999) CD40 activation induces apoptosis in cultured human hepatocytes via induction of cell surface fas ligand expression and amplifies fas-mediated hepatocyte death during allograft rejection. *J Exp Med* **189**(2):441-446.

Afford, S. C., Ahmed-Choudhury, J., Randhawa, S., Russell, C., Youster, J., Crosby, H. A., Eliopoulos, A., Hubscher, S. G., Young, L. S., and Adams, D. H. (2001) CD40 activation-induced, Fas-dependent apoptosis and NF-kappaB/AP-1 signaling in human intrahepatic biliary epithelial cells. *Faseb J* **15**(13):2345-2354.

Ameer, G. A., Harmon, W., Sasisekharan, R., and Langer, R. (1999a) Investigation of a whole blood fluidized bed Taylor-Couette flow device for enzymatic heparin neutralization. *Biotechnol Bioeng* **62**(5):602-608.

Ameer, G. A., Raghavan, S., Sasisekharan, R., Harmon, W., Cooney, C. L., and Langer, R. (1999b) Regional heparinization via simultaneous separation and reaction in a novel Taylor-Couette flow device. *Biotechnol Bioeng* **63**(5):618-624.

Ameer, G. A., Barabino, G., Sasisekharan, R., Harmon, W., Cooney, C. L., and Langer, R. (1999c) Ex vivo evaluation of a Taylor-Couette flow, immobilized heparinase I device for clinical application. *Proc Natl Acad Sci U S A* **96**(5):2350-2355.

Anderson, K. J., Dam, D., Lee, S., and Cotman, C. W. (1988) Basic fibroblast growth factor prevents death of lesioned cholinergic neurons in vivo. *Nature* **332**(6162):360-361.

Arakawa, T., Hsu, Y. R., Schiffer, S. G., Tsai, L. B., Curless, C., and Fox, G. M. (1989) Characterization of a cysteine-free analog of recombinant human basic fibroblast growth factor. *Biochem Biophys Res Commun* **161**(1):335-341.

Araki, S., Simada, Y., Kaji, K., and Hayashi, H. (1990) Role of protein kinase C in the inhibition by fibroblast growth factor of apoptosis in serum-depleted endothelial cells. *Biochem Biophys Res Commun* **172**(3):1081-1085.

Armelin, H. A. (1973) Pituitary extracts and steriod hormones in the control of 3T3 cell growth. *Proc Natl Acad Sci U S A* **70**:2702-2706.

Ascencio, F., Fransson, L. A., and Wadstrom, T. (1993) Affinity of the gastric pathogen Helicobacter pylori for the N- sulphated glycosaminoglycan heparan sulphate. *J Med Microbiol* **38**(4):240-244.

Atkins, E. D. T., and Nieduszynski, I. A. (1976) *Heparin - Chemistry and clinical usage.* Academic Press, London.

Auerbach, R., Auerbach, W., and Polakowski, I. (1991) Assays for angiogenesis: a review. *Pharmacol Ther* **51**(1):1-11.

Ausubel, F. M., Brent, R., Kingston, R. E., Moore, D. D., Sidman, J. G., Smith, J. A., and Struhl, K. (1994) *Current Protocols in Molecular Biology*. Greene Publishing Associates and John Wiley & Sons, Inc, New York.

Ay, H., Ay, I., Koroshetz, W. J., and Finklestein, S. P. (1999) Potential usefulness of basic fibroblast growth factor as a treatment for stroke. *Cerebrovasc Dis* **9**(3):131-135.

Bae, Y. H., Huh, K. M., Kim, Y., and Park, K. (2000) Biodegradable amphiphilic multiblock copolymers and their implications for biomedical applications. *J Control Release* **64**(1-3):3-13.

Baeg, G. H., Lin, X., Khare, N., Baumgartner, S., and Perrimon, N. (2001) Heparan sulfate proteoglycans are critical for the organization of the extracellular distribution of Wingless. *Development* **128**(1):87-94.

Baird, A., Schubert, D., Ling, N., and Guillemin, R. (1988) Receptor- and heparin-binding domains of basic fibroblast growth factor. *Proc Natl Acad Sci U S A* **85**(7):2324-2328.

Ballinger, M. D., and Wells, J. A. (1998) Will any dimer do? *Nat Struct Biol* **5**(11):938-940.

Banner, D. W., D'Arcy, A., Janes, W., Gentz, R., Schoenfeld, H. J., Broger, C., Loetscher, H., and Lesslauer, W. (1993) Crystal structure of the soluble human 55 kd TNF receptor-human TNF beta complex: implications for TNF receptor activation. *Cell* **73**(3):431-445.

Beck, K., Hunter, I., and Engel, J. (1990) Structure and function of laminin: anatomy of a multidomain glycoprotein. *Faseb J* **4**(2):148-160.

Bellaiche, Y., The, I., and Perrimon, N. (1998) Tout-velu is a Drosophila homologue of the putative tumour suppressor EXT-1 and is needed for Hh diffusion. *Nature* **394**(6688):85-88.

Bergamo, A., Bataille, R., and Pellat-Deceunynck, C. (1997) CD40 and CD95 induce programmed cell death in the human myeloma cell line XG2. *Br J Haematol* **97**(3):652-655.

Berger, W., Setinek, U., Mohr, T., Kindas-Mugge, I., Vetterlein, M., Dekan, G., Eckersberger, F., Caldas, C., and Micksche, M. (1999) Evidence for a role of FGF-2 and FGF receptors in the proliferation of non-small cell lung cancer cells. *Int J Cancer* **83**(3):415-423.

Bergers, G., Javaherian, K., Lo, K. M., Folkman, J., and Hanahan, D. (1999) Effects of angiogenesis inhibitors on multistage carcinogenesis in mice. *Science* **284**(5415):808-812.

Bikfalvi, A., Klein, S., Pintucci, G., and Rifkin, D. B. (1997) Biological roles of fibroblast growth factor-2. *Endocr Rev* **18**(1):26-45.

Binari, R. C., Staveley, B. E., Johnson, W. A., Godavarti, R., Sasisekharan, R., and Manoukian, A. S. (1997) Genetic evidence that heparin-like glycosaminoglycans are involved in wingless signaling. *Development* **124**(13):2623-2632.

Bisaccia, F., Zara, V., Capobianco, L., Iacobazzi, V., Mazzeo, M., and Palmieri, F. (1996) The formation of a disulfide cross-link between the two subunits demonstrates the dimeric structure of the mitochondrial oxoglutarate carrier. *Biochim Biophys Acta* **1292**(2):281-288.

Bishayee, S., Majumdar, S., Khire, J., and Das, M. (1989) Ligand-induced dimerization of the platelet-derived growth factor receptor. Monomer-dimer interconversion occurs independent of receptor phosphorylation. *J Biol Chem* **264**(20):11699-11705.

Bjornsson, S. (1998) Quantitation of proteoglycans as glycosaminoglycans in biological fluids using an alcian blue dot blot analysis. *Anal Biochem* **256**(2):229-237.

Blackhall, F. H., Merry, C. L., Davies, E. J., and Jayson, G. C. (2001) Heparan sulfate proteoglycans and cancer. *Br J Cancer* **85**(8):1094-1098.

Boehm, T., Folkman, J., Browder, T., and O'Reilly, M. S. (1997) Antiangiogenic therapy of experimental cancer does not induce acquired drug resistance. *Nature* **390**(6658):404-407.

Bonneh-Barkay, D., Shlissel, M., Berman, B., Shaoul, E., Admon, A., Vlodavsky, I., Carey, D. J., Asundi, V. K., Reich-Slotky, R., and Ron, D. (1997) Identification of glypican as a dual modulator of the biological activity of fibroblast growth factors. *J Biol Chem* **272**(19):12415-12421.

Bos, G. W., Scharenborg, N. M., Poot, A. A., Engbers, G. H., Beugeling, T., van Aken, W. G., and Feijen, J. (1999) Proliferation of endothelial cells on surface-immobilized albumin- heparin conjugate loaded with basic fibroblast growth factor. *J Biomed Mater Res* **44**(3):330-340.

Bowman, K. G., and Bertozzi, C. R. (1999) Carbohydrate sulfotransferase: mediators of extracellular communication. *Curr Biol* **6**:R9-R22.

Bratton, S. B., and Cohen, G. M. (2001) Apoptotic death sensor: an organelle's alter ego? *Trends Pharmacol Sci* **22**(6):306-315.

Brickman, Y. G., Ford, M. D., Gallagher, J. T., Nurcombe, V., Bartlett, P. F., and Turnbull, J. E. (1998) Structural modification of fibroblast growth factor-binding heparan sulfate at a determinative stage of neural development. *J Biol Chem* **273**(8):4350-4359.

Brogi, E., Winkles, J. A., Underwood, R., Clinton, S. K., Alberts, G. F., and Libby, P. (1993) Distinct patterns of expression of fibroblast growth factors and their receptors in human atheroma and nonatherosclerotic arteries. Association of acidic FGF with plaque microvessels and macrophages. *J Clin Invest* **92**(5):2408-2418.

Browning, P. J., Roberts, D. D., Zabrenetzky, V., Bryant, J., Kaplan, M., Washington, R. H., Panet, A., Gallo, R. C., and Vogel, T. (1994) Apolipoprotein E (ApoE), a novel heparin-binding protein inhibits the development of Kaposi's sarcoma-like lesions in BALB/c nu/nu mice. *J Exp Med* **180**(5):1949-1954.

Buendia, B., Santa-Maria, A., and Courvalin, J. C. (1999) Caspase-dependent proteolysis of integral and peripheral proteins of nuclear membranes and nuclear pore complex proteins during apoptosis. *J Cell Sci* **112 (Pt 11)**:1743-1753.

Calabro, A., Plaas, A., Midura, R. J., Goodstone, N. J., Roden, L., and Hascall, V. (2000) Structure and biosynthesis of chondroitin sulfate and hyaluronan, in *Proteoglycans: structure, biology, and molecular interactions* (Iozzo, R. V., ed.). Marcel Dekker, Inc, New York, 5-26.

Campochiaro, P. A. (2000) Retinal and choroidal neovascularization. *J Cell Physiol* **184**:301-310.

Cao, Y., O'Reilly, M. S., Marshall, B., Flynn, E., Ji, R. W., and Folkman, J. (1998) Expression of angiostatin cDNA in a murine fibrosarcoma suppresses primary tumor growth and produces long-term dormancy of metastases. *J Clin Invest* **101**(5):1055-1063.

Cardin, A. D., and Weintraub, H. J. (1989) Molecular modeling of protein-glycosaminoglycan interactions. *Arteriosclerosis* **9**(1):21-32.

Carmeliet, P. (2000) Mechanisms of angiogenesis and arteriogenesis. *Nat Med* **6**(4):389-395.

Carmeliet, P., and Jain, R. K. (2000) Angiogenesis in cancer and other diseases. *Nature* **407**(6801):249-257.

Carreira, C. M., LaVallee, T. M., Tarantini, F., Jackson, A., Lathrop, J. T., Hampton, B., Burgess, W. H., and Maciag, T. (1998) S100A13 is involved in the regulation of fibroblast growth factor-1 and p40 synaptotagmin-1 release in vitro. *J Biol Chem* **273**(35):22224-22231.

Castellot, J. J., Jr., Cochran, D. L., and Karnovsky, M. J. (1985) Effect of heparin on vascular smooth muscle cells. I. Cell metabolism. *J Cell Physiol* **124**(1):21-28.

Chellaiah, A. T., McEwen, D. G., Werner, S., Xu, J., and Ornitz, D. M. (1994) Fibroblast growth factor receptor (FGFR) 3. Alternative splicing in immunoglobulin-like domain III creates a receptor highly specific for acidic FGF/FGF-1. *J Biol Chem* **269**(15):11620-11627.

Chen, Y., Li, X., Eswarakumar, P., Seger, R., and Lonai, P. (2000) Fibroblast growth factor (FGF) signaling through PI 3-kinase and Akt/PKB is required for embryoid body differentiation. *Oncogene* **19**:3750-3756.

Cheng, H., Cao, Y., and Olson, L. (1996) Spinal cord repair in adult paraplegic rats: partial restoration of hind limb function. *Science* **273**(5274):510-513.

Chicheportiche, Y., Bourdon, P. R., Xu, H., Hsu, Y. M., Scott, H., Hession, C., Garcia, I., and Browning, J. L. (1997) TWEAK, a new secreted ligand in the tumor necrosis factor family that weakly induces apoptosis. *J Biol Chem* **272**(51):32401-32410.

Conrad, H. E. (1998) *Heparin-Binding Proteins*. Academic Press, San Diego.

Costantini, P., Colonna, R., and Bernardi, P. (1998) Induction of the mitochondrial permeability transition by N-ethylmaleimide depends on secondary oxidation of critical thiol groups. Potentiation by copper-ortho-phenanthroline without dimerization of the adenine nucleotide translocase. *Biochim Biophys Acta* **1365**(3):385-392.

Cumberledge, S., and Reichsman, F. (1997) Glycosaminoglycans and WNTs: just a spoonful of sugar helps the signal go down. *Trends Genet* **13**(11):421-423.

D'Agnano, I., Valentini, A., Fornari, C., Bucci, B., Starace, G., Felsani, A., and Citro, G. (2001) Myc down-regulation induces apoptosis in M14 melanoma cells by increasing p27(kip1) levels. *Oncogene* **20**(22):2814-2825.

Davis, J. C., Venkataraman, G., Shriver, Z., Raj, P. A., and Sasisekharan, R. (1999) Oligomeric self-association of basic fibroblast growth factor in the absence of heparin-like glycosaminoglycans. *Biochem J* **341**(Pt 3):613-620.

De Cat, B., and David, G. (2001) Developmental roles of the glypicans. *Semin Cell Dev Biol* **12**(2):117-125.

de Vos, A. M., Ultsch, M., and Kossiakoff, A. A. (1992) Human growth hormone and extracellular domain of its receptor: crystal structure of the complex. *Science* **255**(5042):306-312.

Delehedde, M., Deudon, E., Boilly, B., and Hondermarck, H. (1996) Heparan sulfate proteoglycans play a dual role in regulating fibroblast growth factor-2 mitogenic activity in human breast cancer cells. *Exp Cell Res* **229**(2):398-406.

Dell, K. R., and Williams, L. T. (1992) A novel form of fibroblast growth factor receptor 2. Alternative splicing of the third immunoglobulin-like domain confers ligand binding specificity. *J Biol Chem* **267**(29):21225-21229.

Dellacono, F. R., Spiro, J., Eisma, R., and Kreutzer, D. (1997) Expression of basic fibroblast growth factor and its receptors by head and neck squamous carcinoma tumor and vascular endothelial cells. *Am J Surg* **174**(5):540-544.

Desai, S. B., and Libutti, S. K. (1999) Tumor angiogenesis and endothelial cell modulatory factors. *J Immunother* **22**(3):186-211.

DiGabriele, A. D., Lax, I., Chen, D. I., Svahn, C. M., Jaye, M., Schlessinger, J., and Hendrickson, W. A. (1998) Structure of a heparin-linked biologically active dimer of fibroblast growth factor. *Nature* **393**(6687):812-817.

Don, M. J., Chang, Y. H., Chen, K. K., Ho, L. K., and Chau, Y. P. (2001) Induction of CDK inhibitors (p21(WAF1) and p27(Kip1)) and Bak in the beta-lapachone-induced apoptosis of human prostate cancer cells. *Mol Pharmacol* **59**(4):784-794.

Dowd, C. J., Cooney, C. L., and Nugent, M. A. (1999) Heparan sulfate mediates bFGF transport through basement membrane by diffusion with rapid reversible binding. *J Biol Chem* **274**(8):5236-5244.

Dudas, J., Ramadori, G., Knittel, T., Neubauer, K., Raddatz, D., Egedy, K., and Kovalszky, I. (2000) Effect of heparin and liver heparan sulphate on interaction of HepG2- derived transcription factors and their cis-acting elements: altered potential of hepatocellular carcinoma heparan sulphate. *Biochem J* **350 Pt 1**:245-251.

Duncan, G., McCormick, C., and Tufaro, F. (2001) The link between heparan sulfate and hereditary bone disease: finding a function for the EXT family of putative tumor suppressor proteins. *J Clin Invest* **108**(4):511-516.

Duteil, S., Gareil, P., Girault, S., Mallet, A., Feve, C., and Siret, L. (1999) Identification of heparin oligosaccharides by direct coupling of capillary electrophoresis/ionspray-mass spectrometry. *Rapid Commun Mass Spectrom* **13**(19):1889-1898.

Earnshaw, W. C., Martins, L. M., and Kaufmann, S. H. (1999) Mammalian caspases: structure, activation, substrates, and functions during apoptosis. *Annu Rev Biochem* **68**:383-424.

Edelman, E. R., Mathiowitz, E., Langer, R., and Klagsbrun, M. (1991) Controlled and modulated release of basic fibroblast growth factor. *Biomaterials* **12**(7):619-626.

Ehrlich, H. J., Keijer, J., Preissner, K. T., Gebbink, R. K., and Pannekoek, H. (1991) Functional interaction of plasminogen activator inhibitor type 1 (PAI-1) and heparin. *Biochemistry* **30**(4):1021-1028.

Eisen, M. B., Spellman, P. T., Brown, P. O., and Botstein, D. (1998) Cluster analysis and display of genome-wide expression patterns. *Proc Natl Acad Sci U S A* **95**(25):14863-14868.

Elenius, K., Vainio, S., Laato, M., Salmivirta, M., Thesleff, I., and Jalkanen, M. (1991) Induced expression of syndecan in healing wounds. *J Cell Biol* **114**(3):585-595.

Eliopoulos, A. G., Davies, C., Knox, P. G., Gallagher, N. J., Afford, S. C., Adams, D. H., and Young, L. S. (2000) CD40 induces apoptosis in carcinoma cells through activation of cytotoxic ligands of the tumor necrosis factor superfamily. *Mol Cell Biol* **20**(15):5503-5515.

Enari, M., Sakahira, H., Yokoyama, H., Okawa, K., Iwamatsu, A., and Nagata, S. (1998) A caspase-activated DNase that degrades DNA during apoptosis, and its inhibitor ICAD. *Nature* **391**(6662):43-50.

Eriksson, A. E., Cousens, L. S., and Matthews, B. W. (1993) Refinement of the structure of human basic fibroblast growth factor at 1.6 A resolution and analysis of presumed heparin binding sites by selenate substitution. *Protein Sci* **2**(8):1274-1284.

Ernst, S. (1998) Molecular characterization of the glycosaminoglycan interactions with fibroblast growth factor and heparinase I, in *Ph.D thesis in Chemical Engineering.* Massachusetts Institute of Technology, Cambridge

Ernst, S., Langer, R., Cooney, C. L., and Sasisekharan, R. (1995) Enzymatic degradation of glycosaminoglycans. *Crit Rev Biochem Mol Biol* **30**(5):387-444.

Ernst, S., Venkataraman, G., Winkler, S., Godavarti, R., Langer, R., Cooney, C. L., and Sasisekharan, R. (1996) Expression in Escherichia coli, purification and characterization of heparinase I from Flavobacterium heparinum. *Biochem J* **315**(Pt 2):589-597.

Evan, G. I., and Vousden, K. H. (2001) Proliferation, cell cycle and apoptosis in cancer. *Nature* **411**(6835):342-348.

Evans, D. L., Marshall, C. J., Christey, P. B., and Carrell, R. W. (1992) Heparin binding site, conformational change, and activation of antithrombin. *Biochemistry* **31**(50):12629-12642.

Faham, S., Linhardt, R. J., and Rees, D. C. (1998) Diversity does make a difference: fibroblast growth factor-heparin interactions. *Curr Opin Struct Biol* **8**(5):578-586.

Faham, S., Hileman, R. E., Fromm, J. R., Linhardt, R. J., and Rees, D. C. (1996) Heparin structure and interactions with basic fibroblast growth factor. *Science* **271**(5252):1116-1120.

Ferrara, N., and Alitalo, K. (1999) Clinical applications of angiogenic growth factors and their inhibitors. *Nat Med* **5**(12):1359-1364.

Feyzi, E., Trybala, E., Bergstrom, T., Lindahl, U., and Spillmann, D. (1997) Structural requirement of heparan sulfate for interaction with herpes simplex virus type 1 virions and isolated glycoprotein C. *J Biol Chem* **272**(40):24850-24857.

Feyzi, E., Saldeen, T., Larsson, E., Lindahl, U., and Salmivirta, M. (1998) Age-dependent modulation of heparan sulfate structure and function. *J Biol Chem* **273**:13395-13398.

Flaumenhaft, R., Moscatelli, D., and Rifkin, D. B. (1990) Heparin and heparan sulfate increase the radius of diffusion and action of basic fibroblast growth factor. *J Cell Biol* **111**(4):1651-1659.

Folkman, J. (1971) Tumor angiogenesis: therapeutic implications. *N Engl J Med* **285**:1182-1186.

Folkman, J. (1995a) Angiogenesis in cancer, vascular, rheumatoid and other disease. *Nat Med* **1**(1):27-31.

Folkman, J. (1995b) Clinical applications of research on angiogenesis. *N Engl J Med* **333**:1757-1763.

Folkman, J. (2001) Angiogenesis-dependent diseases. *Semin Oncol* **28**(6):536-542.

Forsten, K. E., Courant, N. A., and Nugent, M. A. (1997) Endothelial proteoglycans inhibit bFGF binding and mitogenesis. *J Cell Physiol* **172**(2):209-220.

Fox, G. M., Schiffer, S. G., Rohde, M. F., Tsai, L. B., Banks, A. R., and Arakawa, T. (1988) Production, biological activity, and structure of recombinant basic fibroblast growth factor and an analog with cysteine replaced by serine. *J Biol Chem* **263**(34):18452-18458.

Freedman, S., and Isner, J. M. (2001) Therapeutic angiogenesis for ischemic cardiovascular disease. *J Mol Cell Cardiol* **33**(3):379-393.

Fretto, L. J., Snape, A. J., Tomlinson, J. E., Seroogy, J. J., Wolf, D. L., LaRochelle, W. J., and Giese, N. A. (1993) Mechanism of platelet-derived growth factor (PDGF) AA, AB, and BB binding to alpha and beta PDGF receptor. *J Biol Chem* **268**(5):3625-3631.

Friedl, A., Chang, Z., Tierney, A., and Rapraeger, A. C. (1997) Differential binding of fibroblast growth factor-2 and -7 to basement membrane heparan sulfate: comparison of normal and abnormal human tissues. *Am J Pathol* **150**(4):1443-1455.

Friesel, R. E., and Maciag, T. (1995) Molecular mechanisms of angiogenesis: fibroblast growth factor signal transduction. *Faseb J* **9**(10):919-925.

Fritze, L. M., Reilly, C. F., and Rosenberg, R. D. (1985) An antiproliferative heparan sulfate species produced by postconfluent smooth muscle cells. *J Cell Biol* **100**(4):1041-1049.

Fromm, J. R., Hileman, R. E., Caldwell, E. E., Weiler, J. M., and Linhardt, R. J. (1995) Differences in the interaction of heparin with arginine and lysine and the importance of these basic amino acids in the binding of heparin to acidic fibroblast growth factor. *Arch Biochem Biophys* **323**(2):279-287.

Fromm, J. R., Hileman, R. E., Caldwell, E. E., Weiler, J. M., and Linhardt, R. J. (1997) Pattern and spacing of basic amino acids in heparin binding sites. *Arch Biochem Biophys* **343**(1):92-100.

Frommherz, K. J., Faller, B., and Bieth, J. G. (1991) Heparin strongly decreases the rate of inhibition of neutrophil elastase by alpha 1-proteinase inhibitor. *J Biol Chem* **266**(23):15356-15362.

Fuks, Z., Persaud, R. S., Alfieri, A., McLoughlin, M., Ehleiter, D., Schwartz, J. L., Seddon, A. P., Cordon-Cardo, C., and Haimovitz-Friedman, A. (1994) Basic fibroblast growth factor protects endothelial cells against radiation-induced programmed cell death in vitro and in vivo. *Cancer Res* **54**(10):2582-2590.

Gabizon, R., Meiner, Z., Halimi, M., and Ben-Sasson, S. A. (1993) Heparin-like molecules bind differentially to prion-proteins and change their intracellular metabolic fate. *J Cell Physiol* **157**(2):319-325.

Gallagher, J. T. (1997) Structure-activity relationship of heparan sulphate. *Biochem Soc Trans* **25**(4):1206-1209.

Gallo, R., Kim, C., Kokenyesi, R., Adzick, N. S., and Bernfield, M. (1996) Syndecans-1 and -4 are induced during wound repair of neonatal but not fetal skin. *J Invest Dermatol* **107**(5):676-683.

Giroglou, T., Florin, L., Schafer, F., Streeck, R. E., and Sapp, M. (2001) Human papillomavirus infection requires cell surface heparan sulfate. *J Virol* **75**(3):1565-1570.

Giuffre, L., Cordey, A. S., Monai, N., Tardy, Y., Schapira, M., and Spertini, O. (1997) Monocyte adhesion to activated aortic endothelium: role of L-selectin and heparan sulfate proteoglycans. *J Cell Biol* **136**(4):945-956.

Givol, D., and Yayon, A. (1992) Complexity of FGF receptors: genetic basis for structural diversity and functional specificity. *Faseb J* **6**(15):3362-3369.

Godavarti, R., and Sasisekharan, R. (1996) A comparative analysis of the primary sequences and characteristics of heparinases I, II, and III from Flavobacterium heparinum. *Biochem Biophys Res Commun* **229**(3):770-777.

Godavarti, R., Davis, M., Venkataraman, G., Cooney, C., Langer, R., and Sasisekharan, R. (1996) Heparinase III from Flavobacterium heparinum: cloning and recombinant expression in Escherichia coli. *Biochem Biophys Res Commun* **225**(3):751-758.

Goncalves, L. M. (1998) Fibroblast growth factor-mediated angiogenesis for the treatment of ischemia. Lessons learned from experimental models and early human experience. *Rev Port Cardiol* **17 Suppl 2**:II11-20.

Goretzki, L., Burg, M. A., Grako, K. A., and Stallcup, W. B. (1999) High-affinity binding of basic fibroblast growth factor and platelet-derived growth factor-AA to the core protein of the NG2 proteoglycan. *J Biol Chem* **274**(24):16831-16837.

Gospodarowicz, D. (1974) Localisation of a fibroblast growth factor and its effect alone and with hydrocortisone on 3T3 cell growth. *Nature* **249**(453):123-127.

Gospodarowicz, D., and Cheng, J. (1986) Heparin protects basic and acidic FGF from inactivation. *J Cell Physiol* **128**(3):475-484.

Gospodarowicz, D., Weseman, J., and Moran, J. (1975) Presence in brain of a mitogenic agent promoting proliferation of myoblasts in low density culture. *Nature* **256**(5514):216-219.

Gospodarowicz, D., Bialecki, H., and Thakral, T. K. (1979) The angiogenic activity of the fibroblast and epidermal growth factor. *Exp Eye Res* **28**(5):501-514.

Gospodarowicz, D., Neufeld, G., and Schweigerer, L. (1986) Fibroblast growth factor. *Mol Cell Endocrinol* **46**(3):187-204.

Gospodarowicz, D., Moran, J., Braun, D., and Birdwell, C. (1976) Clonal growth of bovine vascular endothelial cells: fibroblast growth factor as a survival agent. *Proc Natl Acad Sci U S A* **73**(11):4120-4124.

Gospodarowicz, D., Brown, K. D., Birdwell, C. R., and Zetter, B. R. (1978) Control of proliferation of human vascular endothelial cells. Characterization of the response of human umbilical vein endothelial cells to fibroblast growth factor, epidermal growth factor, and thrombin. *J Cell Biol* **77**(3):774-788.

Gospodarowicz, D., Ferrara, N., Schweigerer, L., and Neufeld, G. (1987) Structural characterization and biological functions of fibroblast growth factor. *Endocr Rev* **8**(2):95-114.

Gospodarowicz, D., Cheng, J., Lui, G. M., Baird, A., and Bohlent, P. (1984) Isolation of brain fibroblast growth factor by heparin-Sepharose affinity chromatography: identity with pituitary fibroblast growth factor. *Proc Natl Acad Sci U S A* **81**(22):6963-6967.

Green, D. R., and Reed, J. C. (1998) Mitochondria and apoptosis. *Science* **281**(5381):1309-1312.

Guimond, S., Maccarana, M., Olwin, B. B., Lindahl, U., and Rapraeger, A. C. (1993) Activating and inhibitory heparin sequences for FGF-2 (basic FGF). Distinct requirements for FGF-1, FGF-2, and FGF-4. *J Biol Chem* **268**(32):23906-23914.

Guimond, S. E., and Turnbull, J. E. (1999) Fibroblast growth factor receptor signalling is dictated by specific heparan sulphate saccharides. *Curr Biol* **9**(22):1343-1346.

Gurtu, V., Kain, S. R., and Zhang, G. (1997) Fluorometric and colorimetric detection of caspase activity associated with apoptosis. *Anal Biochem* **251**(1):98-102.

Guyton, J. R., Rosenberg, R. D., Clowes, A. W., and Karnovsky, M. J. (1980) Inhibition of rat arterial smooth muscle cell proliferation by heparin. In vivo studies with anticoagulant and nonanticoagulant heparin. *Circ Res* **46**(5):625-634.

Habuchi, H., Suzuki, S., Saito, T., Tamura, T., Harada, T., Yoshida, K., and Kimata, K. (1992) Structure of a heparan sulphate oligosaccharide that binds to basic fibroblast growth factor. *Biochem J* **285**(Pt 3):805-813.

Hacker, U., Lin, X., and Perrimon, N. (1997) The Drosophila sugarless gene modulates Wingless signaling and encodes an enzyme involved in polysaccharide biosynthesis. *Development* **124**(18):3565-3573.

Haerry, T. E., Heslip, T. R., Marsh, J. L., and O'Connor, M. B. (1997) Defects in glucuronate biosynthesis disrupt Wingless signaling in Drosophila. *Development* **124**(16):3055-3064.

Hahnenberger, R., Jakobson, A. M., Ansari, A., Wehler, T., Svahn, C. M., and Lindahl, U. (1993) Low-sulphated oligosaccharides derived from heparan sulphate inhibit normal angiogenesis. *Glycobiology* **3**(6):567-573.

Haimovitz-Friedman, A., Balaban, N., McLoughlin, M., Ehleiter, D., Michaeli, J., Vlodavsky, I., and Fuks, Z. (1994) Protein kinase C mediates basic fibroblast growth factor protection of endothelial cells against radiation-induced apoptosis. *Cancer Res* **54**(10):2591-2597.

Hallgren, J., Karlson, U., Poorafshar, M., Hellman, L., and Pejler, G. (2000) Mechanism for activation of mouse mast cell tryptase: dependence on heparin and acidic pH for formation of active tetramers of mouse mast cell protease 6. *Biochemistry* **39**(42):13068-13077.

Han, R. O., Ettenson, D. S., Koo, E. W., and Edelman, E. R. (1997) Heparin/heparan sulfate chelation inhibits control of vascular repair by tissue-engineered endothelial cells. *Am J Physiol* **273**(6 Pt 2):H2586-2595.

Hanahan, D., and Folkman, J. (1996) Patterns and emerging mechanisms of the angiogenic switch during tumorigenesis. *Cell* **86**(3):353-364.

Hart, A. W., Baeza, N., Apelqvist, A., and Edlund, H. (2000) Attenuation of FGF signalling in mouse beta-cells leads to diabetes. *Nature* **408**(6814):864-868.

Hedner, U. (2000) Development of tinzaparin: a heparinase-digested low-molecular-weight heparin. *Semin Thromb Hemost* **26**(1):23-29.

Heldin, C. H. (1995) Dimerization of cell surface receptors in signal transduction. *Cell* **80**(2):213-223.

Heldin, C. H., and Westermark, B. (1999) Mechanism of action and in vivo role of platelet-derived growth factor. *Physiol Rev* **79**(4):1283-1316.

Heldin, C. H., Ernlund, A., Rorsman, C., and Ronnstrand, L. (1989) Dimerization of B-type platelet-derived growth factor receptors occurs after ligand binding and is closely associated with receptor kinase activation. *J Biol Chem* **264**(15):8905-8912.

Hengartner, M. O. (2000) The biochemistry of apoptosis. *Nature* **407**(6805):770-776.

Henn, V., Slupsky, J. R., Grafe, M., Anagnostopoulos, I., Forster, R., Muller-Berghaus, G., and Kroczek, R. A. (1998) CD40 ligand on activated platelets triggers an inflammatory reaction of endothelial cells. *Nature* **391**(6667):591-594.

Herr, A. B., Ornitz, D. M., Sasisekharan, R., Venkataraman, G., and Waksman, G. (1997) Heparin-induced self-association of fibroblast growth factor-2. Evidence for two oligomerization processes. *J Biol Chem* **272**(26):16382-16389.

Hess, S., and Engelmann, H. (1996) A novel function of CD40: induction of cell death in transformed cells. *J Exp Med* **183**(1):159-167.

Higuchi, R. (1990) *PCR Protocols: A guide to Methods and Applications*. Academic Press, San Diego.

Hileman, R. E., Fromm, J. R., M., W. J., and Linhardt, R. J. (1998) Glycosaminoglycan-protein interactions: definition of consensus sites in glycosaminoglycan binding proteins. *Bioessays* **20**(156-167)

Houchen, C. W., George, R. J., Sturmoski, M. A., and Cohn, S. M. (1999) FGF-2 enhances intestinal stem cell survival and its expression is induced after radiation injury. *Am J Physiol* **276**(1 Pt 1):G249-258.

Hulett, M. D., Freeman, C., Hamdorf, B. J., Baker, R. T., Harris, M. J., and Parish, C. R. (1999) Cloning of mammalian heparanase, an important enzyme in tumor invasion and metastasis. *Nat Med* **5**(7):803-809.

Huntington, J. A., and Gettins, P. G. (1998) Conformational conversion of antithrombin to a fully activated substrate of factor Xa without need for heparin. *Biochemistry* **37**(10):3272-3277.

Inoue, J., Ishida, T., Tsukamoto, N., Kobayashi, N., Naito, A., Azuma, S., and Yamamoto, T. (2000) Tumor necrosis factor receptor-associated factor (TRAF) family: adapter proteins that mediate cytokine signaling. *Exp Cell Res* **254**(1):14-24.

Iozzo, R. V., and San Antonio, J. D. (2001) Heparan sulfate proteoglycans: heavy hitters in the angiogenesis arena. *J Clin Invest* **108**(3):349-355.

Ishihara, M., Takano, R., Kanda, T., Hayashi, K., Hara, S., Kikuchi, H., and Yoshida, K. (1995) Importance of 6-O-sulfate groups of glucosamine residues in heparin for activation of FGF-1 and FGF-2. *J Biochem (Tokyo)* **118**(6):1255-1260.

Jackson, R. L., J., B. S., and D., C. A. (1991) Glycosaminoglycans: molecular properties, protein interactions, and role in physiological processes. *Physiol Reviews* **71**:481-522.

Jaffe, E. A., Nachman, R. L., Becker, C. G., and Minick, C. R. (1973) Culture of human endothelial cells derived from umbilical veins. Identification by morphologic and immunologic criteria. *J Clin Invest* **52**(11):2745-2756.

Jaye, M., Schlessinger, J., and Dionne, C. A. (1992) Fibroblast growth factor receptor tyrosine kinases: molecular analysis and signal transduction. *Biochim Biophys Acta* **1135**(2):185-199.

Jayson, G. C., Lyon, M., Paraskeva, C., Turnbull, J. E., Deakin, J. A., and Gallagher, J. T. (1998) Heparan sulfate undergoes specific structural changes during the progression from human colon adenoma to carcinoma in vitro. *J Biol Chem* **273**(1):51-57.

Jayson, G. C., Vives, C., Paraskeva, C., Schofield, K., Coutts, J., Fleetwood, A., and Gallagher, J. T. (1999) Coordinated modulation of the fibroblast growth factor dual receptor mechanism during transformation from human colon adenoma to carcinoma. *Int J Cancer* **82**(2):298-304.

Jiang, G., and Hunter, T. (1999) Receptor signaling: when dimerization is not enough. *Curr Biol* **9**(15):R568-571.

Jin, L., Abrahams, J. P., Skinner, R., Petitou, M., Pike, R. N., and Carrell, R. W. (1997) The anticoagulant activation of antithrombin by heparin. *Proc Natl Acad Sci U S A* **94**(26):14683-14688.

Johnson, D. E., Lee, P. L., Lu, J., and Williams, L. T. (1990) Diverse forms of a receptor for acidic and basic fibroblast growth factors. *Mol Cell Biol* **10**(9):4728-4736.

Jones, C. P., and Sawyer, R. T. (1989) Heparin inhibits mammalian, but not leech, hyaluronidase. *Thromb Res* **55**(6):791-796.

Junqueira, L. C., Carneiro, J., and Kelley, R. O. (1992) *Basic histology*. Appleton & Lange, Norwalk.

Kan, M., Wu, X., Wang, F., and McKeehan, W. L. (1999) Specificity for fibroblast growth factors determined by heparan sulfate in a binary complex with the receptor kinase. *J Biol Chem* **274**(22):15947-15952.

Kan, M., Wang, F., Xu, J., Crabb, J. W., Hou, J., and McKeehan, W. L. (1993) An essential heparin-binding domain in the fibroblast growth factor receptor kinase. *Science* **259**(5103):1918-1921.

Kannan, K., and Givol, D. (2000) FGF receptor mutations: dimerization syndromes, cell growth suppression, and animal models. *IUBMB Life* **49**(3):197-205.

Karsan, A., Yee, E., Poirier, G. G., Zhou, P., Craig, R., and Harlan, J. M. (1997) Fibroblast growth factor-2 inhibits endothelial cell apoptosis by Bcl-2- dependent and independent mechanisms. *Am J Pathol* **151**(6):1775-1784.

Karumanchi, S. A., Jha, V., Ramchandran, R., Karihaloo, A., Tsiokas, L., Chan, B., Dhanabal, M., Hanai, J. I., Venkataraman, G., Shriver, Z., Keiser, N., Kalluri, R., Zeng, H., Mukhopadhyay, D., Chen, R. L., Lander, A. D., Hagihara, K., Yamaguchi, Y., Sasisekharan, R., Cantley, L., and Sukhatme, V. P. (2001) Cell surface glypicans are low-affinity endostatin receptors. *Mol Cell* **7**(4):811-822.

Katayose, Y., Kim, M., Rakkar, A. N., Li, Z., Cowan, K. H., and Seth, P. (1997) Promoting apoptosis: a novel activity associated with the cyclin-dependent kinase inhibitor p27. *Cancer Res* **57**(24):5441-5445.

Kawamata, T., Dietrich, W. D., Schallert, T., Gotts, J. E., Cocke, R. R., Benowitz, L. I., and Finklestein, S. P. (1997) Intracisternal basic fibroblast growth factor enhances functional recovery and up-regulates the expression of a molecular marker of neuronal sprouting following focal cerebral infarction. *Proc Natl Acad Sci U S A* **94**(15):8179-8184.

Kenyon, B. M., Voest, E. E., Chen, C. C., Flynn, E., Folkman, J., and D'Amato, R. J. (1996) A model of angiogenesis in the mouse cornea. *Invest Ophthalmol Vis Sci* **37**(8):1625-1632.

Khan, J., Bittner, M. L., Chen, Y., Meltzer, P. S., and Trent, J. M. (1999) DNA microarray technology: the anticipated impact on the study of human disease. *Biochimica et Biophysica Acta* **1423**:M17-M28.

Kim, I., Moon, S., Yu, K., Kim, U., and Koh, G. Y. (2001) A novel fibroblast growth factor receptor-5 preferentially expressed in the pancreas(1). *Biochim Biophys Acta* **1518**(1-2):152-156.

Kitagawa, H., Shimakawa, H., and Sugahara, K. (1999) The tumor suppressor EXT-like gene EXTL2 encodes an alpha1, 4-N-acetylhexosaminyltransferase that transfers N-acetylgalactosamine and N-acetylglucosamine to the common glycosaminoglycan-protein linkage region. The key enzyme for the chain initiation of heparan sulfate. *J Biol Chem* **274**(20):13933-13937.

Kitagawa, H., Tone, Y., Tamura, J., Neumann, K. W., Ogawa, T., Oka, S., Kawasaki, T., and Sugahara, K. (1998) Molecular cloning and expression of glucuronyltransferase I involved in the biosynthesis of the glycosaminoglycan-protein linkage region of proteoglycans. *J Biol Chem* **273**(12):6615-6618.

Klagsbrun, M., and Edelman, E. R. (1989) Biological and biochemical properties of fibroblast growth factors. Implications for the pathogenesis of atherosclerosis. *Arteriosclerosis* **9**(3):269-278.

Kobashi, K. (1968) Catalytic oxidation of sulfhydryl groups by o-phenanthroline copper complex. *Biochim Biophys Acta* **158**(2):239-245.

Kothakota, S., Azuma, T., Reinhard, C., Klippel, A., Tang, J., Chu, K., McGarry, T. J., Kirschner, M. W., Koths, K., Kwiatkowski, D. J., and Williams, L. T. (1997) Caspase-3-generated fragment of gelsolin: effector of morphological change in apoptosis. *Science* **278**(5336):294-298.

Krufka, A., Guimond, S., and Rapraeger, A. C. (1996) Two hierarchies of FGF-2 signaling in heparin: mitogenic stimulation and high-affinity binding/receptor transphosphorylation. *Biochemistry* **35**:11131-11141.

Kuzuya, M., Satake, S., Ramos, M. A., Kanda, S., Koike, T., Yoshino, K., Ikeda, S., and Iguchi, A. (1999) Induction of apoptosis cell death in vascular endothelial cells cultured in three-dimensional collagen lattice. *Exp Cell Research* **248**:498-508.

Kwan, C. P., Venkataraman, G., Shriver, Z., Raman, R., Liu, D., Qi, Y., Varticovski, L., and Sasisekharan, R. (2001) Probing fibroblast growth factor dimerization and role of heparin-like glycosaminoglycans in modulating dimerization and signaling. *J Biol Chem* **276**(26):23421-23429.

Laham, R. J., Sellke, F. W., Edelman, E. R., Pearlman, J. D., Ware, J. A., Brown, D. L., Gold, J. P., and Simons, M. (1999) Local perivascular delivery of basic fibroblast growth factor in patients undergoing coronary bypass surgery: results of a phase I randomized, double-blind, placebo-controlled trial. *Circulation* **100**(18):1865-1871.

Laham, R. J., Rezaee, M., Post, M., Novicki, D., Sellke, F. W., Pearlman, J. D., Simons, M., and Hung, D. (2000) Intrapericardial delivery of fibroblast growth factor-2 induces neovascularization in a porcine model of chronic myocardial ischemia. *J Pharmacol Exp Ther* **292**(2):795-802.

Lam, L. H., Silbert, J. E., and Rosenberg, R. D. (1976) The separation of active and inactive forms of heparin. *Biochem Biophys Res Commun* **69**(2):570-577.

Landau, Z., David, M., Aviezer, D., and Yayon, A. (2001) Heparin-like inhibitory activity to fibroblast growth factor-2 in wound fluids of patients with chronic skin ulcers and its modulation during wound healing. *Wound Repair Regen* **9**(4):323-328.

Langer, R., and Folkman, J. (1976) Polymers for the sustained release of proteins and other macromolecules. *Nature* **263**(5580):797-800.

LaRochelle, W. J., Sakaguchi, K., Atabey, N., Cheon, H. G., Takagi, Y., Kinaia, T., Day, R. M., Miki, T., Burgess, W. H., and Bottaro, D. P. (1999) Heparan sulfate proteoglycan modulates keratinocyte growth factor signaling through interaction with both ligand and receptor. *Biochemistry* **38**(6):1765-1771.

LaVallee, T. M., Trantini, F., Gamble, S., Carreira, C. M., Jackson, A., and Maciag, T. (1998) Synaptotagmin-1 is required for fibroblast growth factor-1 release. *J Biol Chem* **273**:22217-22223.

Lemmon, M. A., Bu, Z., Ladbury, J. E., Zhou, M., Pinchasi, D., Lax, I., Engelman, D. M., and Schlessinger, J. (1997) Two EGF molecules contribute additively to stabilization of the EGFR dimer. *Embo J* **16**(2):281-294.

Lin, X., and Perrimon, N. (1999) Dally cooperates with Drosophila Frizzled 2 to transduce Wingless signalling. *Nature* **400**(6741):281-284.

Lin, X., Buff, E. M., Perrimon, N., and Michelson, A. M. (1999) Heparan sulfate proteoglycans are essential for FGF receptor signaling during Drosophila embryonic development. *Development* **126**(17):3715-3723.

Lindahl, B., Westling, C., Gimoez-Gallego, G., Lindahl, U., and Salmivirta, M. (1999) Common binding sites for beta-amyloid fibrils and fibroblast growth factor-2 in heparan sulfate from human cerebral cortex. *J Biol Chem* **274**:30631-30635.

Lindahl, U., Kusche-Gullberg, M., and Kjellen, L. (1998) Regulated diversity of heparan sulfate. *J Biol Chem* **273**(39):24979-24982.

Liu, D., Shriver, Z., Qi, Y., Venkataraman, G., and Sasisekharan, R. (2002a) Dynamic regulation of tumor growth and metastasis by heparan sulfate glycosaminoglycans. *Semin Thromb Hemost* **28**(1):67-78.

Liu, D., Shriver, Z., Venkataraman, G., El Shabrawi, Y., and Sasisekharan, R. (2002b) Tumor cell surface heparan sulfate as cryptic promoters or inhibitors of tumor growth and metastasis. *Proc Natl Acad Sci U S A* **99**(2):568-573.

Liu, X., Zou, H., Slaughter, C., and Wang, X. (1997) DFF, a heterodimeric protein that functions downstream of caspase-3 to trigger DNA fragmentation during apoptosis. *Cell* **89**(2):175-184.

Livnah, O., Johnson, D. L., Stura, E. A., Farrell, F. X., Barbone, F. P., You, Y., Liu, K. D., Goldsmith, M. A., He, W., Krause, C. D., Pestka, S., Jolliffe, L. K., and Wilson, I. A. (1998) An antagonist peptide-EPO receptor complex suggests that receptor dimerization is not sufficient for activation. *Nat Struct Biol* **5**(11):993-1004.

Lobb, R. R., and Fett, J. W. (1984) Purification of two distinct growth factors from bovine neural tissue by heparin affinity chromatography. *Biochemistry* **23**(26):6295-6299.

Lookene, A., Chevreuil, O., Ostergaard, P., and Olivecrona, G. (1996) Interaction of lipoprotein lipase with heparin fragments and with heparan sulfate: stoichiometry, stabilization, and kinetics. *Biochemistry* **35**(37):12155-12163.

Lopez, J. J., Edelman, E. R., Stamler, A., Hibberd, M. G., Prasad, P., Thomas, K. A., DiSalvo, J., Caputo, R. P., Carrozza, J. P., Douglas, P. S., Sellke, F. W., and Simons, M. (1998) Angiogenic potential of perivascularly delivered aFGF in a porcine model of chronic myocardial ischemia. *Am J Physiol* **274**(3 Pt 2):H930-936.

Lundin, L., Larsson, H., Kreuger, J., Kanda, S., Lindahl, U., Salmivirta, M., and Claesson-Welsh, L. (2000) Selectively desulfated heparin inhibits fibroblast growth factor- induced mitogenicity and angiogenesis. *J Biol Chem* **275**(32):24653-24660.

Lyon, M., Deakin, J. A., and Gallagher, J. T. (1994) Liver heparan sulfate structure. *J Biol Chem* **269**:11208-11215.

Maccarana, M., Casu, B., and Lindahl, U. (1993) Minimal sequence in heparin/heparan sulfate required for binding of basic fibroblast growth factor. *J Biol Chem* **268**(32):23898-23905.

Maciag, T. (1984) Angiogenesis. *Prog Hemost Thromb* **7**:167-182.

Majack, R. A., and Clowes, A. W. (1984) Inhibition of vascular smooth muscle cell migration by heparin-like glycosaminoglycans. *J Cell Physiol* **118**(3):253-256.

Mansukhani, A., Dell'Era, P., Moscatelli, D., Kornbluth, S., Hanafusa, H., and Basilico, C. (1992) Characterization of the murine BEK fibroblast growth factor (FGF) receptor: activation by three members of the FGF family and requirement for heparin. *Proc Natl Acad Sci U S A* **89**(8):3305-3309.

Marcum, J. A., and Rosenberg, R. D. (1984) Anticoagulantly active heparin-like molecules from vascular tissue. *Biochemistry* **23**(8):1730-1737.

Marcum, J. A., and Rosenberg, R. D. (1985) Heparinlike molecules with anticoagulant activity are synthesized by cultured endothelial cells. *Biochem Biophys Res Commun* **126**(1):365-372.

Marcum, J. A., McKenney, J. B., and Rosenberg, R. D. (1984) Acceleration of thrombin-antithrombin complex formation in rat hindquarters via heparinlike molecules bound to the endothelium. *J Clin Invest* **74**(2):341-350.

Margalit, H., Fischer, N., and Ben-Sasson, S. A. (1993) Comparative analysis of structurally defined heparin binding sequences reveals a distinct spatial distribution of basic residues. *J Biol Chem* **268**(26):19228-19231.

Marics, I., Adelaide, J., Raybaud, F., Mattei, M. G., Coulier, F., Planche, J., de Lapeyriere, O., and Birnbaum, D. (1989) Characterization of the HST-related FGF.6 gene, a new member of the fibroblast growth factor gene family. *Oncogene* **4**(3):335-340.

Martin, K. J., Kritzman, B. M., Price, L. M., Koh, B., Kwan, C. P., Zhang, X., Mackay, A., O'Hare, M. J., Kaelin, C. M., Mutter, G. L., Pardee, A. B., and Sager, R. (2000) Linking gene expression patterns to therapeutic groups in breast cancer. *Cancer Res* **60**(8):2232-2238.

Martin, S. J., Reutelingsperger, C. P., McGahon, A. J., Rader, J. A., van Schie, R. C., LaFace, D. M., and Green, D. R. (1995) Early redistribution of plasma membrane phosphatidylserine is a general feature of apoptosis regardless of the initiating

stimulus: inhibition by overexpression of Bcl-2 and Abl. *J Exp Med* **182**(5):1545-1556.

Mason, I. J. (1994) The ins and outs of fibroblast growth factors. *Cell* **78**:547-552.

Mazue, G., Bertolero, F., Jacob, C., Sarmientos, P., and Roncucci, R. (1991) Preclinical and clinical studies with recombinant human basic fibroblast growth factor. *Ann N Y Acad Sci* **638**:329-340.

McCafferty, J., and Glover, D. R. (2000) Engineering therapeutic proteins. *Curr Opin Struct Biol* **10**(4):417-420.

McCormick, C., Duncan, G., Goutsos, K. T., and Tufaro, F. (2000) The putative tumor suppressors EXT1 and EXT2 form a stable complex that accumulates in the Golgi apparatus and catalyzes the synthesis of heparan sulfate. *Proc Natl Acad Sci U S A* **97**(2):668-673.

Milev, P., Monnerie, H., Popp, S., Margolis, R. K., and Margolis, R. U. (1998) The core protein of the chondroitin sulfate proteoglycan phosphacan is a high-affinity ligand of fibroblast growth factor-2 and potentiates its mitogenic activity. *J Biol Chem* **273**(34):21439-21442.

Miura, M., Friedlander, R. M., and Yuan, J. (1995) Tumor necrosis factor-induced apoptosis is mediated by a CrmA-sensitive cell death pathway. *Proc Natl Acad Sci U S A* **92**(18):8318-8322.

Mohammadi, M., Honegger, A. M., Rotin, D., Fischer, R., Bellot, F., Li, W., Dionne, C. A., Jaye, M., Rubinstein, M., and Schlessinger, J. (1991) A tyrosine-phosphorylated carboxy-terminal peptide of the fibroblast growth factor receptor (Flg) is a binding site for the SH2 domain of phospholipase C-gamma 1. *Mol Cell Biol* **11**(10):5068-5078.

Mongiat, M., Taylor, K., Otto, J., Aho, S., Uitto, J., Whitelock, J. M., and Iozzo, R. V. (2000) The protein core of the proteoglycan perlecan binds specifically to fibroblast growth factor-7. *J Biol Chem* **275**(10):7095-7100.

Moore, R., Casey, G., Brookes, S., Dixon, M., Peters, G., and Dickson, C. (1986) Sequence, topography and protein coding potential of mouse int-2: a putative oncogene activated by mouse mammary tumour virus. *Embo J* **5**(5):919-924.

Mourey, L., Samama, J. P., Delarue, M., Choay, J., Lormeau, J. C., Petitou, M., and Moras, D. (1990) Antithrombin III: structural and functional aspects. *Biochimie* **72**(8):599-608.

Moy, F. J., Seddon, A. P., Bohlen, P., and Powers, R. (1996) High-resolution solution structure of basic fibroblast growth factor determined by multidimensional heteronuclear magnetic resonance spectroscopy. *Biochemistry* **35**(42):13552-13561.

Moy, F. J., Safran, M., Seddon, A. P., Kitchen, D., Bohlen, P., Aviezer, D., Yayon, A., and Powers, R. (1997) Properly oriented heparin-decasaccharide-induced dimers are the biologically active form of basic fibroblast growth factor [published erratum appears in Biochemistry 1997 Jun 24;36(25):7936]. *Biochemistry* **36**(16):4782-4791.

Mulloy, B., and Forster, M. (2000) Conformation and dynamics of heparin and heparan sulfate. *Glycobiology* **10**:1147-1156.

Murano, G., Williams, L., Miller-Andersson, M., Aronson, D. L., and King, C. (1980) Some properties of antithrombin-III and its concentration in human plasma. *Thromb Res* **18**(1-2):259-262.

Murzin, A. G., Lesk, A. M., and Chothia, C. (1992) beta-Trefoil fold. Patterns of structure and sequence in the Kunitz inhibitors interleukins-1 beta and 1 alpha and fibroblast growth factors. *J Mol Biol* **223**(2):531-543.

Nabel, E. G., Yang, Z. Y., Plautz, G., Forough, R., Zhan, X., Haudenschild, C. C., Maciag, T., and Nabel, G. J. (1993) Recombinant fibroblast growth factor-1 promotes intimal hyperplasia and angiogenesis in arteries in vivo. *Nature* **362**(6423):844-846.

Nagendra, H. G., Harrington, A. E., Harmer, N. J., Pellegrini, L., Blundell, T. L., and Burke, D. F. (2001) Sequence analyses and comparative modeling of fly and worm fibroblast growth factor receptors indicate that the determinants for FGF and heparin binding are retained in evolution. *FEBS Lett* **501**(1):51-58.

Naismith, J. H., Devine, T. Q., Brandhuber, B. J., and Sprang, S. R. (1995) Crystallographic evidence for dimerization of unliganded tumor necrosis factor receptor. *J Biol Chem* **270**(22):13303-13307.

Naismith, J. H., Devine, T. Q., Kohno, T., and Sprang, S. R. (1996) Structures of the extracellular domain of the type I tumor necrosis factor receptor. *Structure* **4**(11):1251-1262.

Nakajima, M., Irimura, T., Di Ferrante, D., Di Ferrante, N., and Nicolson, G. L. (1983) Heparan sulfate degradation: relation to tumor invasive and metastatic properties of mouse B16 melanoma sublines. *Science* **220**(4597):611-613.

Nakamura, N., and Kojima, J. (1981) Changes in charge density of heparan sulfate isolated from cancerous human liver tissue. *Cancer Res* **41**(1):278-283.

Nakanishi, H., Oguri, K., Yoshida, K., Itano, N., Takenaga, K., Kazama, T., Yoshida, A., and Okayama, M. (1992) Structural differences between heparan sulphates of proteoglycan involved in the formation of basement membranes in vivo by Lewis-lung-carcinoma-derived cloned cells with different metastatic potentials. *Biochem J* **288 (Pt 1)**:215-224.

Namiki, A., Brogi, E., Kearney, M., Kim, E. A., Wu, T., Couffinhal, T., Varticovski, L., and Isner, J. M. (1995) Hypoxia induces vascular endothelial growth factor in cultured human endothelial cells. *J Biol Chem* **270**(52):31189-31195.

Naski, M. C., and Ornitz, D. M. (1998) FGF signaling in skeletal development. *Front Biosci* **3**:D781-794.

Natke, B., Venkataraman, G., Nugent, M. A., and Sasisekharan, R. (1999) Heparinase treatment of bovine smooth muscle cells inhibits fibroblast growth factor-2 binding to fibroblast growth factor receptor but not FGF-2 mediated cellular proliferation. *Angiogenesis* **3**:249-257.

Natke, B., Venkataraman, G., Nugent, M. A., and Sasisekharan, R. (2000) Heparinase treatment of smooth muscle cells inhibits FGF-2 binding to FGFR1 but not FGF-2 mediated cellular proliferation. *Angiogenesis* **3**:249-257.

Nieduszynski, I. A. (1985) Connective tissue polysaccharides, in *Polysaccharides* (Atkins, E. D. T., ed.). VCH, Weinheim, 107-139.

Nugent, M. A., and Iozzo, R. V. (2000) Fibroblast growth factor-2. *Int J Biochem Cell Biol* **32**(2):115-120.

Nugent, M. A., Karnovsky, M. J., and Edelman, E. R. (1993) Vascular cell-derived heparan sulfate shows coupled inhibition of basic fibroblast growth factor binding and mitogenesis in vascular smooth muscle cells. *Circ Res* **73**(6):1051-1060.

Nurcombe, V., Ford, M. D., Wildschut, J. A., and Bartlett, P. F. (1993) Developmental regulation of neural response to FGF-1 and FGF-2 by heparan sulfate proteoglycan. *Science* **260**(5104):103-106.

Ong, S. H., Hadari, Y. R., Gotoh, N., Guy, G. R., Schlessinger, J., and Lax, I. (2001) Stimulation of phosphatidylinositol 3-kinase by fibroblast growth factor receptors is mediated by coordinated recruitment of multiple docking proteins. *Proc Natl Acad Sci U S A* **98**(11):6074-6079.

O'Reilly, M. S., Brem, H., and Folkman, J. (1995) Treatment of murine hemangioendotheliomas with the angiogenesis inhibitor AGM-1470. *J Pediatr Surg* **30**(2):325-329; discussion 329-330.

O'Reilly, M. S., Holmgren, L., Chen, C., and Folkman, J. (1996) Angiostatin induces and sustains dormancy of human primary tumors in mice. *Nat Med* **2**(6):689-692.

O'Reilly, M. S., Pirie-Shepherd, S., Lane, W. S., and Folkman, J. (1999) Antiangiogenic activity of the cleaved conformation of the serpin antithrombin. *Science* **285**(5435):1926-1928.

O'Reilly, M. S., Boehm, T., Shing, Y., Fukai, N., Vasios, G., Lane, W. S., Flynn, E., Birkhead, J. R., Olsen, B. R., and Folkman, J. (1997) Endostatin: an endogenous inhibitor of angiogenesis and tumor growth. *Cell* **88**(2):277-285.

Ornitz, D. M. (2000) FGFs, heparan sulfate and FGFRs: complex interactions essential for development. *Bioessays* **22**(2):108-112.

Ornitz, D. M., and Leder, P. (1992) Ligand specificity and heparin dependence of fibroblast growth factor receptors 1 and 3. *J Biol Chem* **267**(23):16305-16311.

Ornitz, D. M., Yayon, A., Flanagan, J. G., Svahn, C. M., Levi, E., and Leder, P. (1992) Heparin is required for cell-free binding of basic fibroblast growth factor to a soluble receptor and for mitogenesis in whole cells. *Mol Cell Biol* **12**(1):240-247.

Ornitz, D. M., Herr, A. B., Nilsson, M., Westman, J., Svahn, C. M., and Waksman, G. (1995) FGF binding and FGF receptor activation by synthetic heparan-derived di- and trisaccharides. *Science* **268**(5209):432-436.

Ornitz, D. M., Xu, J., Colvin, J. S., McEwen, D. G., MacArthur, C. A., Coulier, F., Gao, G., and Goldfarb, M. (1996) Receptor specificity of the fibroblast growth factor family. *J Biol Chem* **271**(25):15292-15297.

Osslund, T. D., Syed, R., Singer, E., Hsu, E. W., Nybo, R., Chen, B. L., Harvey, T., Arakawa, T., Narhi, L. O., Chirino, A., and Morris, C. F. (1998) Correlation between the 1.6 A crystal structure and mutational analysis of keratinocyte growth factor. *Protein Sci* **7**(8):1681-1690.

Padera, R., Venkataraman, G., Berry, D., Godavarti, R., and Sasisekharan, R. (1999) FGF-2/fibroblast growth factor receptor/heparin-like glycosaminoglycan interactions: a compensation model for FGF-2 signaling. *Faseb J* **13**(13):1677-1687.

Pantoliano, M. W., Horlick, R. A., Springer, B. A., Van Dyk, D. E., Tobery, T., Wetmore, D. R., Lear, J. D., Nahapetian, A. T., Bradley, J. D., and Sisk, W. P. (1994) Multivalent ligand-receptor binding interactions in the fibroblast growth

factor system produce a cooperative growth factor and heparin mechanism for receptor dimerization. *Biochemistry* **33**(34):10229-10248.

Papkoff, J., and Schryver, B. (1990) Secreted int-1 protein is associated with the cell surface. *Mol Cell Biol* **10**(6):2723-2730.

Park, Y., Yu, G., Gunay, N. S., and Linhardt, R. J. (1999) Purification and characterization of heparan sulphate proteoglycan from bovine brain. *Biochem J* **344 Pt 3**:723-730.

Pellegrini, L., Burke, D. F., von Delft, F., Mulloy, B., and Blundell, T. L. (2000) Crystal structure of fibroblast growth factor receptor ectodomain bound to ligand and heparin. *Nature* **407**(6807):1029-1034.

Perollet, C., Han, Z. C., Savona, C., Caen, J. P., and Bikfalvi, A. (1998) Platelet factor 4 modulates fibroblast growth factor 2 (FGF-2) activity and inhibits FGF-2 dimerization. *Blood* **91**:3289-3299.

Perou, C. M., Sorlie, T., Eisen, M. B., van de Rijn, M., Jeffrey, S. S., Rees, C. A., Pollack, J. R., Ross, D. T., Johnsen, H., Akslen, L. A., Fluge, O., Pergamenschikov, A., Williams, C., Zhu, S. X., Lonning, P. E., Borresen-Dale, A. L., Brown, P. O., and Botstein, D. (2000) Molecular portraits of human breast tumours. *Nature* **406**(6797):747-752.

Perrimon, N., and Bernfield, M. (2000) Specificities of heparan sulphate proteoglycans in developmental processes. *Nature* **404**(6779):725-728.

Plotnikov, A. N., Schlessinger, J., Hubbard, S. R., and Mohammadi, M. (1999) Structural basis for FGF receptor dimerization and activation. *Cell* **98**(5):641-650.

Plotnikov, A. N., Hubbard, S. R., Schlessinger, J., and Mohammadi, M. (2000) Crystal structures of two FGF-FGFR complexes reveal the determinants of ligand-receptor specificity. *Cell* **101**(4):413-424.

Powell, P. P., Wang, C.-C., Horinouchi, H., Shepherd, K., Jacobson, M., Lipson, M., and Jones, R. (1998) Differential expression of fibroblast growth factor receptors 1 to 4 and ligand genes in late fetal and early postnatal rat lung. *Am J Respir Cell Mol Biol* **19**:563-572.

Powers, C. J., McLeskey, S. W., and Wellstein, A. (2000) Fibroblast growth factors, their receptors and signaling. *Endocr Relat Cancer* **7**(3):165-197.

Pratt, C. W., and Church, F. C. (1991) Antithrombin: structure and function. *Semin Hematol* **28**(1):3-9.

Pye, D. A., and Gallagher, J. T. (1999) Monomer complexes of basic fibroblast growth factor and heparan sulfate oligosaccharides are the minimal functional unit for cell activation. *J Biol Chem* **274**(19):13456-13461.

Pye, D. A., Vives, R. R., Turnbull, J. E., Hyde, P., and Gallagher, J. T. (1998) Heparan sulfate oligosaccharides require 6-O-sulfation for promotion of basic fibroblast growth factor mitogenic activity. *J Biol Chem* **273**(36):22936-22942.

Raballo, R., Rhee, J., Lyn-Cook, R., Leckman, J. F., Schwartz, M. L., and Vaccarino, F. M. (2000) Basic fibroblast growth factor (Fgf2) is necessary for cell proliferation and neurogenesis in the developing cerebral cortex. *J Neurosci* **20**(13):5012-5023.

Radomsky, M. L., Aufdemorte, T. B., Swain, L. D., Fox, W. C., Spiro, R. C., and Poser, J. W. (1999) Novel formulation of fibroblast growth factor-2 in a hyaluronan gel accelerates fracture healing in nonhuman primates. *J Orthop Res* **17**(4):607-614.

Rahmoune, H., Chen, H.-L., Gallagher, J. T., Rudland, P. S., and Fernig, D. G. (1998) Interaction of heparan sulfate from mammary cells with acidic fibroblast growth factor (FGF) and basic FGF. *J Biol Chem* **273**:7303-7310.

Rapraeger, A. C. (1995) In the clutches of proteoglycans: how does heparan sulfate regulate FGF binding? *Chem Biol* **2**(10):645-649.

Rapraeger, A. C., Krufka, A., and Olwin, B. B. (1991) Requirement of heparan sulfate for bFGF-mediated fibroblast growth and myoblast differentiation. *Science* **252**(5013):1705-1708.

Reich-Slotky, R., Bonneh-Barkay, D., Shaoul, E., Bluma, B., Svahn, C. M., and Ron, D. (1994) Differential effect of cell-associated heparan sulfates on the binding of keratinocyte growth factor (KGF) and acidic fibroblast growth factor to the KGF receptor. *J Biol Chem* **269**(51):32279-32285.

Reichsman, F., Smith, L., and Cumberledge, S. (1996) Glycosaminoglycans can modulate extracellular localization of the wingless protein and promote signal transduction. *J Cell Biol* **135**(3):819-827.

Rhomberg, A. J., Ernst, S., Sasisekharan, R., and Biemann, K. (1998) Mass spectrometric and capillary electrophoretic investigation of the enzymatic degradation of heparin-like glycosaminoglycans. *Proc Natl Acad Sci U S A* **95**(8):4176-4181.

Robertson, S. C., Meyer, A. N., Hart, K. C., Galvin, B. D., Webster, M. K., and Donoghue, D. J. (1998) Activating mutations in the extracellular domain of the fibroblast growth factor receptor 2 function by disruption of the disulfide bond in the third immunoglobulin-like domain. *Proc Natl Acad Sci U S A* **95**(8):4567-4572.

Roden, L. (1989) Highlights in the history of heparin, in *Heparin: Chemical and Biological Properties, Clinical Applications* (Lanes, D. A., Lindhal, U, ed.). CRC Press, Inc, Boca Raton, 1-23.

Roghani, M., and Moscatelli, D. (1992) Basic fibroblast growth factor is internalized through both receptor-mediated and heparan sulfate-mediated mechanisms. *J Biol Chem* **267**(31):22156-22162.

Ron, D., Bottaro, D. P., Finch, P. W., Morris, D., Rubin, J. S., and Aaronson, S. A. (1993) Expression of biologically active recombinant keratinocyte growth factor. Structure/function analysis of amino-terminal truncation mutants. *J Biol Chem* **268**(4):2984-2988.

Rosenberg, R. D., Shworak, N. W., Liu, J., Schwartz, J. J., and Zhang, L. (1997) Heparan sulfate proteoglycans of the cardiovascular system. *J. Clin. Invest.* **99**(9):2062-2070.

Ross, D. T., Scherf, U., Eisen, M. B., Perou, C. M., Rees, C., Spellman, P., Iyer, V., Jeffrey, S. S., Van de Rijn, M., Waltham, M., Pergamenschikov, A., Lee, J. C., Lashkari, D., Shalon, D., Myers, T. G., Weinstein, J. N., Botstein, D., and Brown, P. O. (2000) Systematic variation in gene expression patterns in human cancer cell lines. *Nat Genet* **24**(3):227-235.

Ross, R. (1993) The pathogenesis of atherosclerosis: a perspective for the 1990s. *Nature* **362**(6423):801-809.

Rousseau, F., Bonaventure, J., Legeai-Mallet, L., Pelet, A., Rozet, J. M., Maroteaux, P., Le Merrer, M., and Munnich, A. (1994) Mutations in the gene encoding fibroblast growth factor receptor-3 in achondroplasia. *Nature* **371**(6494):252-254.

Rusnati, M., Tulipano, G., Spillmann, D., Tanghetti, E., Oreste, P., Zoppetti, G., Giacca, M., and Presta, M. (1999) Multiple interactions of HIV-I Tat protein with size-defined heparin oligosaccharides. *J Biol Chem* **274**(40):28198-28205.

Safaiyan, F., Lindahl, U., and Salmivirta, M. (1998) Selective reduction of 6-O-sulfation in heparan sulfate from transformed mammary epithelial cells. *Eur J Biochem* **252**(3):576-582.

Safaiyan, F., Kolset, S. O., Prydz, K., Gottfridsson, E., Lindahl, U., and Salmivirta, M. (1999) Selective effects of sodium chlorate treatment on the sulfation of heparan sulfate. *J Biol Chem* **274**:36267-36273.

Safi, J., Jr., DiPaula, A. F., Jr., Riccioni, T., Kajstura, J., Ambrosio, G., Becker, L. C., Anversa, P., and Capogrossi, M. C. (1999) Adenovirus-mediated acidic fibroblast growth factor gene transfer induces angiogenesis in the nonischemic rabbit heart. *Microvasc Res* **58**(3):238-249.

Salmivirta, M., Lidholt, K., and Lindahl, U. (1996) Heparan sulfate: a piece of information. *Faseb J* **10**(11):1270-1279.

Sanderson, R. D. (2001) Heparan sulfate proteoglycans in invasion and metastasis. *Semin Cell Dev Biol* **12**(2):89-98.

Sasisekharan, R., and Venkataraman, G. (2000) Heparin and heparan sulfate: biosynthesis, structure and function. *Curr Opin Chem Biol* **4**(6):626-631.

Sasisekharan, R., Ernst, S., and Venkataraman, G. (1997) On the Regulation of Fibroblast Growth Factor Activity by Heparin-Like Glycosaminoglycans. *Angiogenesis* **1**:45-54.

Sasisekharan, R., Bulmer, M., Moremen, K. W., Cooney, C. L., and Langer, R. (1993) Cloning and expression of heparinase I gene from *Flavobacterium heparinum*. *Proc Natl Acad Sci U S A* **90**:3660-3664.

Sasisekharan, R., Moses, M. A., Nugent, M. A., Cooney, C. L., and Langer, R. (1994) Heparinase inhibits neovascularization. *Proc Natl Acad Sci U S A* **91**(4):1524-1528.

Schlessinger, J., Lax, I., and Lemmon, M. (1995) Regulation of growth factor activation by proteoglycans: what is the role of the low affinity receptors? *Cell* **83**(3):357-360.

Schlessinger, J., Plotnikov, A. N., Ibrahimi, O. A., Eliseenkova, A. V., Yeh, B. K., Yayon, A., Linhardt, R. J., and Mohammadi, M. (2000) Crystal structure of a ternary FGF-FGFR-heparin complex reveals a dual role for heparin in FGFR binding and dimerization. *Mol Cell* **6**(3):743-750.

Schmidt, N. O., Westphal, M., Hagel, C., Ergun, S., Stavrou, D., Rosen, E. M., and Lamszus, K. (1999) Levels of vascular endothelial growth factor, hepatocyte growth factor/scatter factor and basic fibroblast growth factor in human gliomas and their relation to angiogenesis. *Int J Cancer* **84**(1):10-18.

Selleck, S. B. (1999) Overgrowth syndromes and the regulation of signaling complexes by proteoglycans. *Am J Hum Genet* **64**(2):372-377.

Sen, J., Goltz, J. S., Stevens, L., and Stein, D. (1998) Spatially restricted expression of pipe in the Drosophila egg chamber defines embryonic dorsal-ventral polarity. *Cell* **95**(4):471-481.

Senay, C., Lind, T., Muguruma, K., Tone, Y., Kitagawa, H., Sugahara, K., Lidholt, K., Lindahl, U., and Kusche-Gullberg, M. (2000) The EXT1/EXT2 tumor

suppressors: catalytic activities and role in heparan sulfate biosynthesis. *EMBO rep* **1**(3):282-286.

Shakibaei, M., and Frevert, U. (1996) Dual interaction of the malaria circumsporozoite protein with the low density lipoprotein receptor-related protein (LRP) and heparan sulfate proteoglycans. *J Exp Med* **184**(5):1699-1711.

Sharma, B., Handler, M., Eichstetter, I., Whitelock, J. M., Nugent, M. A., and Iozzo, R. V. (1998) Antisense targeting of perlecan blocks tumor growth and angiogenesis in vivo. *J Clin Invest* **102**(8):1599-1608.

Sher, I., Weizman, A., Lubinsky-Mink, S., Lang, T., Adir, N., Schomburg, D., and Ron, D. (1999) Mutations uncouple human fibroblast growth factor (FGF)-7 biological activity and receptor binding and support broad specificity in the secondary receptor binding site of FGFs. *J Biol Chem* **274**(49):35016-35022.

Shiang, R., Thompson, L. M., Zhu, Y. Z., Church, D. M., Fielder, T. J., Bocian, M., Winokur, S. T., and Wasmuth, J. J. (1994) Mutations in the transmembrane domain of FGFR3 cause the most common genetic form of dwarfism, achondroplasia. *Cell* **78**(2):335-342.

Shin, E. Y., Lee, B. H., Yang, J. H., Shin, K. S., Lee, G. K., Yun, H. Y., Song, Y. J., Park, S. C., and Kim, E. G. (2000) Up-regulation and co-expression of fibroblast growth factor receptors in human gastric cancer. *J Cancer Res Clin Oncol* **126**(9):519-528.

Shing, Y., Folkman, J., Sullivan, R., Butterfield, C., Murray, J., and Klagsbrun, M. (1984) Heparin affinity: purification of a tumor-derived capillary endothelial cell growth factor. *Science* **223**(4642):1296-1299.

Shriver, Z., Sundaram, M., Venkataraman, G., Fareed, J., Linhardt, R., Biemann, K., and Sasisekharan, R. (2000a) Cleavage of the antithrombin III binding site in heparin by heparinases and its implication in the generation of low molecular weight heparin. *Proc Natl Acad Sci U S A* **97**(19):10365-10370.

Shriver, Z., Raman, R., Venkataraman, G., Drummond, K., Turnbull, J., Toida, T., Linhardt, R., Biemann, K., and Sasisekharan, R. (2000b) Sequencing of 3-O sulfate containing heparin decasaccharides with a partial antithrombin III binding site. *Proc Natl Acad Sci U S A* **97**(19):10359-10364.

Shukla, D., Liu, J., Blaiklock, P., Shworak, N. W., Bai, X., Esko, J. D., Cohen, G. H., Eisenberg, R. J., Rosenberg, R. D., and Spear, P. G. (1999) A novel role for 3-O-sulfated heparan sulfate in herpes simplex virus 1 entry. *Cell* **99**(1):13-22.

Silver, P. J., Moreau, J.-P., Denholm, E., Lin, Y., Nguyen, L., Bennett, C., Recktenwald, A., DeBlois, D., Baker, S., and Ranger, S. (1998) Heparinase III limits rat arterial smooth muscle cell proliferation in vitro and in vivo. *Eur J Pharm* **351**:79-83.

Slavin, J. (1995) Fibroblast growth factors: at the heart of angiogenesis. *Cell Biol Int* **19**(5):431-444.

Sleeman, M., Fraser, J., McDonald, M., Yuan, S., White, D., Grandison, P., Kumble, K., Watson, J. D., and Murison, J. G. (2001) Identification of a new fibroblast growth factor receptor, FGFR5. *Gene* **271**(2):171-182.

Smith, K., Fox, S. B., Whitehouse, R., Taylor, M., Greenall, M., Clarke, J., and Harris, A. L. (1999) Upregulation of basic fibroblast growth factor in breast carcinoma and its relationship to vascular density, oestrogen receptor, epidermal growth factor receptor and survival. *Ann Oncol* **10**(6):707-713.

Smyth, P. G., Berman, S. A., and Bursztajn, S. (2002) Markers of apoptosis: methods for elucidating the mechanism of apoptotic cell death from the nervous system. *Biotechniques* **32**:648-665.

Sommer, A., and Rifkin, D. B. (1989) Interaction of heparin with human basic fibroblast growth factor: protection of the angiogenic protein from proteolytic degradation by a glycosaminoglycan. *J Cell Physiol* **138**(1):215-220.

Sorlie, T., Perou, C. M., Tibshirani, R., Aas, T., Geisler, S., Johnsen, H., Hastie, T., Eisen, M. B., van de Rijn, M., Jeffrey, S. S., Thorsen, T., Quist, H., Matese, J. C., Brown, P. O., Botstein, D., Eystein Lonning, P., and Borresen-Dale, A. L. (2001) Gene expression patterns of breast carcinomas distinguish tumor subclasses with clinical implications. *Proc Natl Acad Sci U S A* **98**(19):10869-10874.

Sperinde, G. V., and Nugent, M. A. (1998) Heparan sulfate proteoglycans control intracellular processing of bFGF in vascular smooth muscle cells. *Biochemistry* **37**(38):13153-13164.

Spivak-Kroizman, T., Lemmon, M. A., Dikic, I., Ladbury, J. E., Pinchasi, D., Huang, J., Jaye, M., Crumley, G., Schlessinger, J., and Lax, I. (1994) Heparin-induced oligomerization of FGF molecules is responsible for FGF receptor dimerization, activation, and cell proliferation. *Cell* **79**(6):1015-1024.

Springer, B. A., Pantoliano, M. W., Barbera, F. A., Gunyuzlu, P. L., Thompson, L. D., Herblin, W. F., Rosenfeld, S. A., and Book, G. W. (1994) Identification and concerted function of two receptor binding surfaces on basic fibroblast growth factor required for mitogenesis. *J Biol Chem* **269**(43):26879-26884.

Stauber, D. J., DiGabriele, A. D., and Hendrickson, W. A. (2000) Structural interactions of fibroblast growth factor receptor with its ligands. *Proc Natl Acad Sci U S A* **97**(1):49-54.

Su, H., Blain, F., Musil, R., Zimmermann, J., Gu, K., and Bennett, D. C. (1996) Isolation and expression in E.coli of hepB and hepC genes coding for the glycosaminoglycan-degrading enzymes heparinase II and heparinase III, respectively from *F. heparinum*. *Appl. Environ. Microbiol* **62**:2723-2734.

Sugimori, H., Speller, H., and Finklestein, S. P. (2001) Intravenous basic fibroblast growth factor produces a persistent reduction in infarct volume following permanent focal ischemia in rats. *Neurosci Lett* **300**(1):13-16.

Taguchi, T., Kishida, A., Sakamoto, N., and Akashi, M. (1998) Preparation of a novel functional hydrogel consisting of sulfated glucoside-bearing polymer: activation of basic fibroblast growth factor. *J Biomed Mater Res* **41**(3):386-391.

Taipale, J., and Keski-Oja, J. (1997) Growth factors in the extracellular matrix. *Faseb J* **11**(1):51-59.

Tamm, I., Kikuchi, T., and Zychlinsky, A. (1991) Acidic and basic fibroblast growth factors are survival factors with distinctive activity in quiescent BALB/c 3T3 murine fibroblasts. *Proc Natl Acad Sci U S A* **88**(8):3372-3376.

Tannheimer, S. L., Rehemtulla, A., and Ethier, S. P. (2000) Characterization of fibroblast growth factor receptor 2 overexpression in the human breast cancer cell line SUM-52PE. *Breast Cancer Res* **2**(4):311-320.

Tarantini, F., LaVallee, T., Jackson, A., Gamble, S., Carreira, C. M., Garfinkel, S., Burgess, W. H., and Maciag, T. (1998) The extravesicular domain of

synaptotagmin-1 is released with the latent fibroblast growth factor-1 homodimer in response to heat shock. *J Biol Chem* **273**(35):22209-22216.

Tepper, C. G., Jayadev, S., Liu, B., Bielawska, A., Wolff, R., Yonehara, S., Hannun, Y. A., and Seldin, M. F. (1995) Role for ceramide as an endogenous mediator of Fas-induced cytotoxicity. *Proc Natl Acad Sci U S A* **92**(18):8443-8447.

The, I., Bellaiche, Y., and Perrimon, N. (1999) Hedgehog movement is regulated through tout velu-dependent synthesis of a heparan sulfate proteoglycan. *Mol Cell* **4**(4):633-639.

Thornberry, N. A., and Lazebnik, Y. (1998) Caspases: enemies within. *Science* **281**(5381):1312-1316.

Tibell, L. A., Sethson, I., and Buevich, A. V. (1997) Characterization of the heparin-binding domain of human extracellular superoxide dismutase. *Biochim Biophys Acta* **1340**(1):21-32.

Toida, T., Yoshida, H., Toyoda, H., Koshiishi, I., Imanari, T., Hileman, R. E., Fromm, J. R., and Linhardt, R. J. (1997) Structural differences and the presence of unsubstituted amino groups in heparan sulphates from different tissues and species. *Biochem J* **322**(Pt 2):499-506.

Tumova, S., Woods, A., and Couchman, J. R. (2000) Heparan sulfate proteoglycans on the cell surface: versatile coordinators of cellular functions. *Int J Biochem Cell Biol* **32**(3):269-288.

Turnbull, J., Powell, A., and Guimond, S. (2001) Heparan sulfate: decoding a dynamic multifunctional cell regulator. *Trends Cell Biol* **11**(2):75-82.

Turnbull, J. E., Hopwood, J. J., and Gallagher, J. T. (1999) A strategy for rapid sequencing of heparan sulfate and heparin saccharides. *Proc Natl Acad Sci U S A* **96**(6):2698-2703.

Turnbull, J. E., Fernig, D. G., Ke, Y., Wilkinson, M. C., and Gallagher, J. T. (1992) Identification of the basic fibroblast growth factor binding sequence in fibroblast heparan sulfate. *J Biol Chem* **267**(15):10337-10341.

Uno, F., Fujiwara, T., Takata, Y., Ohtani, S., Katsuda, K., Takaoka, M., Ohkawa, T., Naomoto, Y., Nakajima, M., and Tanaka, N. (2001) Antisense-mediated suppression of human heparanase gene expression inhibits pleural dissemination of human cancer cells. *Cancer Res* **61**(21):7855-7860.

Utt, M., Danielsson, B., and Wadstrom, T. (2001) Helicobacter pylori vacuolating cytotoxin binding to a putative cell surface receptor, heparan sulfate, studied by surface plasmon resonance. *FEMS Immunol Med Microbiol* **30**(2):109-113.

van Neck, J. W., Medina, J. J., Onnekink, C., Schwartz, S. M., and Bloemers, H. P. (1995) Expression of basic fibroblast growth factor and fibroblast growth factor receptor genes in cultured rat aortic smooth muscle cells. *Biochim Biophys Acta* **1261**(2):210-214.

Veal, J. M., Merchant, K., and Rill, R. L. (1991) The influence of reducing agent and 1,10-phenanthroline concentration on DNA cleavage by phenanthroline + copper. *Nucleic Acids Res* **19**(12):3383-3388.

Venkataraman, G., Raman, R., Sasisekharan, V., and Sasisekharan, R. (1999a) Molecular characteristics of fibroblast growth factor-fibroblast growth factor receptor-heparin-like glycosaminoglycan complex. *Proc Natl Acad Sci U S A* **96**(7):3658-3663.

Venkataraman, G., Shriver, Z., Davis, J. C., and Sasisekharan, R. (1999b) Fibroblast growth factors 1 and 2 are distinct in oligomerization in the presence of heparin-like glycosaminoglycans. *Proc Natl Acad Sci U S A* **96**(5):1892-1897.

Venkataraman, G., Shriver, Z., Raman, R., and Sasisekharan, R. (1999c) Sequencing complex polysaccharides. *Science* **286**(5439):537-542.

Venkataraman, G., Sasisekharan, V., Herr, A. B., Ornitz, D. M., Waksman, G., Cooney, C. L., Langer, R., and Sasisekharan, R. (1996) Preferential self-association of basic fibroblast growth factor is stabilized by heparin during receptor dimerization and activation. *Proc Natl Acad Sci U S A* **93**(2):845-850.

Vives, R. R., Pye, D. A., Salmivirta, M., Hopwood, J. J., Lindahl, U., and Gallagher, J. T. (1999) Sequence analysis of heparan sulphate and heparin oligosaccharides. *Biochem J* **339**(Pt 3):767-773.

Vlodavsky, I., Fuks, Z., Bar-Ner, M., Ariav, Y., and Schirrmacher, V. (1983) Lymphoma cell-mediated degradation of sulfated proteoglycans in the subendothelial extracellular matrix: relationship to tumor cell metastasis. *Cancer Res* **43**(6):2704-2711.

Vlodavsky, I., Miao, H.-Q., Medalion, B., Danagher, P., and Ron, D. (1996) Involvement of heparan sulfate and related molecules in sequestration and growth promoting activity of fibroblast growth factor. *Cancer Metastasis Rev* **15**(2):177-186.

Vlodavsky, I., Fuks, Z., Ishai-Michaeli, R., Bashkin, P., Levi, E., Korner, G., Bar-Shavit, R., and Klagsbrun, M. (1991) Extracellular matrix-resident basic fibroblast growth factor: implication for the control of angiogenesis. *J Cell Biochem* **45**(2):167-176.

Vlodavsky, I., Friedmann, Y., Elkin, M., Aingorn, H., Atzmon, R., Ishai-Michaeli, R., Bitan, M., Pappo, O., Peretz, T., Michal, I., Spector, L., and Pecker, I. (1999) Mammalian heparanase: gene cloning, expression and function in tumor progression and metastasis. *Nat Med* **5**(7):793-802.

von Leoprechting, A., van der Bruggen, P., Pahl, H. L., Aruffo, A., and Simon, J. C. (1999) Stimulation of CD40 on immunogenic human malignant melanomas augments their cytotoxic T lymphocyte-mediated lysis and induces apoptosis. *Cancer Res* **59**(6):1287-1294.

Waksman, G., and Herr, A. B. (1998) New insights into heparin-induced FGF oligomerization. *Nat Struct Biol* **5**(7):527-530.

Walicke, P., Cowan, W. M., Ueno, N., Baird, A., and Guillemin, R. (1986) Fibroblast growth factor promotes survival of dissociated hippocampal neurons and enhances neurite extension. *Proc Natl Acad Sci U S A* **83**(9):3012-3016.

Walker, A., Turnbull, J. E., and Gallagher, J. T. (1994) Specific heparan sulfate saccharides mediate the activity of basic fibroblast growth factor. *J Biol Chem* **269**(2):931-935.

Wang, J. K., Gao, G., and Goldfarb, M. (1994) Fibroblast growth factor receptors have different signaling and mitogenic potentials. *Mol Cell Biol* **14**(1):181-188.

Wang, X., Gorospe, M., Huang, Y., and Holbrook, N. J. (1997) p27Kip1 overexpression causes apoptotic death of mammalian cells. *Oncogene* **15**(24):2991-2997.

Watanabe, H., Nakata, K., Kimata, K., Nakanishi, I., and Yamada, Y. (1997) Dwarfism and age-associated spinal degeneration of heterozygote cmd mice defective in aggrecan. *Proc Natl Acad Sci U S A* **94**(13):6943-6947.

Watowich, S. S., Hilton, D. J., and Lodish, H. F. (1994) Activation and inhibition of erythropoietin receptor function: role of receptor dimerization. *Mol Cell Biol* **14**(6):3535-3549.

Wei, G., Bai, X., Gabb, M. M., Bame, K. J., Koshy, T. I., Spear, P. G., and Esko, J. D. (2000) Location of the glucuronosyltransferase domain in the heparan sulfate copolymerase EXT1 by analysis of Chinese hamster ovary cell mutants. *J Biol Chem* **275**(36):27733-27740.

Weitz, J. I. (1997) Low-molecular-weight heparins. *N Engl J Med* **337**(10):688-698.

Werb, Z. (1997) ECM and cell surface proteolysis: regulating cellular ecology. *Cell* **91**(4):439-442.

Werner, S., Duan, D. S., de Vries, C., Peters, K. G., Johnson, D. E., and Williams, L. T. (1992) Differential splicing in the extracellular region of fibroblast growth factor receptor 1 generates receptor variants with different ligand-binding specificities. *Mol Cell Biol* **12**(1):82-88.

Whitelock, J. M., Murdoch, A. D., Iozzo, R. V., and Underwood, P. A. (1996) The degradation of human endothelial cell-derived perlecan and release of bound basic fibroblast growth factor by stromelysin, collagenase, plasmin, and heparanases. *J Biol Chem* **271**(17):10079-10086.

Wilkie, A. O., Morriss-Kay, G. M., Jones, E. Y., and Heath, J. K. (1995) Functions of fibroblast growth factors and their receptors. *Curr Biol* **5**(5):500-507.

Wong, P., and Burgess, W. H. (1998) FGF2-Heparin co-crystal complex-assisted design of mutants FGF1 and FGF7 with predictable heparin affinities. *J Biol Chem* **273**(29):18617-18622.

Wyllie, A. H., Morris, R. G., Smith, A. L., and Dunlop, D. (1984) Chromatin cleavage in apoptosis: association with condensed chromatin morphology and dependence on macromolecular synthesis. *J Pathol* **142**(1):67-77.

Yan, G., Fukabori, Y., McBride, G., Nikolaropolois, S., and McKeehan, W. L. (1993) Exon switching and activation of stromal and embryonic fibroblast growth factor (FGF)-FGF receptor genes in prostate epithelial cells accompany stromal independence and malignancy. *Mol Cell Biol* **13**:4513-4522.

Yang, C. F., Yasukawa, T., Kimura, H., Miyamoto, H., Honda, Y., Tabata, Y., Ikada, Y., and Ogura, Y. (2000) Experimental corneal neovascularization by basic fibroblast growth factor incorporated into gelatin hydrogel. *Ophthalmic Res* **32**(1):19-24.

Yayon, A., Klagsbrun, M., Esko, J. D., Leder, P., and Ornitz, D. M. (1991) Cell surface, heparin-like molecules are required for binding of basic fibroblast growth factor to its high affinity receptor. *Cell* **64**(4):841-848.

Ye, S., Luo, Y., Lu, W., Jones, R. B., Linhardt, R. J., Capila, I., Toida, T., Kan, M., Pelletier, H., and McKeehan, W. L. (2001) Structural basis for interaction of FGF-1, FGF-2, and FGF-7 with different heparan sulfate motifs. *Biochemistry* **40**(48):14429-14439.

Yoshida, T., Miyagawa, K., Odagiri, H., Sakamoto, H., Little, P. F., Terada, M., and Sugimura, T. (1987) Genomic sequence of hst, a transforming gene encoding a protein homologous to fibroblast growth factors and the int-2-encoded protein. *Proc Natl Acad Sci U S A* **84**(20):7305-7309.

Young, E., Wells, P., Holloway, S., Weitz, J., and Hirsh, J. (1994) Ex-vivo and in-vitro evidence that low molecular weight heparins exhibit less binding to plasma proteins than unfractionated heparin. *Thromb Haemost* **71**(3):300-304.

Yuan, J. (1997) Transducing signals of life and death. *Curr Opin Cell Biol* **9**(2):247-251.

Zhan, X., Bates, B., Hu, X. G., and Goldfarb, M. (1988) The human FGF-5 oncogene encodes a novel protein related to fibroblast growth factors. *Mol Cell Biol* **8**(8):3487-3495.

Zhang, J. D., Cousens, L. S., Barr, P. J., and Sprang, S. R. (1991) Three-dimensional structure of human basic fibroblast growth factor, a structural homolog of interleukin 1 beta. *Proc Natl Acad Sci U S A* **88**(8):3446-3450.

Zhou, M., Sutliff, R. L., Paul, R. J., Lorenz, J. H., Hoying, J. B., Haudenschild, C. C., Yin, M., Coffin, D., Kong, L., Kranias, E. G., Luo, W., Boivin, G., Duffy, J., Pawlowski, S. A., and Doetschman, T. (1998) Fibroblast growth factor 2 control of vascular tone. *Nat Med* **4**:201-207.

Zhu, X., Hsu, B. T., and Rees, D. C. (1993) Structural studies of the binding of the anti-ulcer drug sucrose octasulfate to acidic fibroblast growth factor. *Structure* **1**(1):27-34.

Zhu, X., Komiya, H., Chirino, A., Faham, S., Fox, G. M., Arakawa, T., Hsu, B. T., and Rees, D. C. (1991) Three-dimensional structures of acidic and basic fibroblast growth factors. *Science* **251**(4989):90-93.